



U.S. Department
of Transportation

Federal Railroad
Administration

Wheel Failure Mechanisms of Railroad Cars

Interim Report

Office of Research and
Development
Washington, D.C. 20590

CONTRACT NO. DTRF53-82-C-00282, TASK ORDER #6

ASSOCIATION OF AMERICAN RAILROADS

BRITTO R. RAJKUMAR
TRANSPORTATION TEST CENTER
PUEBLO, COLORADO

DANIEL H. STONE
AAR TECHNICAL CENTER
CHICAGO, ILLINOIS

GEORGE P. CARPENTER
AAR TECHNICAL CENTER
CHICAGO, ILLINOIS

and

GERALD J. MOYAR
MOYAR TECHNICAL SERVICES, INC.
DOWNERS GROVE, ILLINOIS

DOT/FRA/ORD-

This document is available to the
public through the National
Technical Information Service,
Springfield, Virginia 22161.

WHEEL FAILURE MECHANISMS OF RAILROAD CARS

INTERIM REPORT

TTC-040(FRA-IR85)

January 1986

NOTICE

The results in this report were obtained under test procedures and criteria established by the Federal Railroad Administration. The data or results do not imply an endorsement by the Association of American Railroads of the product tested nor the applicability of the results beyond those samples tested.

ACKNOWLEDGEMENTS

This work was conducted for the Federal Railroad Administration (FRA), by the Association of American Railroads (AAR) at the Transportation Test Center (TTC), Pueblo, and Technical Center, Chicago. The authors wish to express thanks and appreciation to Mr. Cliff Gannett, the FRA Technical Monitor, Mr. Gordon Stevens and Mr. Don Gray of the Federal Railroad Administration, who provided technical direction and guidance for the program.

The authors also wish to express thanks and appreciation to Mr. Bob Krick, Mr. George Way, and Mr. Scot Lovelace, members of the Technical Overview Committee for providing overall project direction.

The authors wish to thank the following who actively participated in the Wheel Failures Mechanisms Program: Michael Fec, Art Opinsky, Mike Joerms, and Dave Utrata of the AAR Technical Center in Chicago; Bob Swearingen, Wayne Cooksey, Jack Minor, and John Blackman of the Transportation Test Center in Pueblo.

The contributions of Dr. Milton Johnson and his staff of IITRI are deeply appreciated. Thanks also to Mr. Tom Guins of the AAR in Washington, D.C., for his contribution to National Study of Wheel Removal Guidelines. Thanks to Mr. Lynn Ballard and his staff of the Word Processing Section, TTC, for the timely production of the Interim Report and the Appendices.

FOREWORD

This Interim Report of the FRA sponsored Wheel Failure Mechanism Program was prepared in fulfillment of contractual requirements to provide a major mid-term technical progress report on the status of on-going research. It is not a final report, and although it does provide technical highlights and observations on many of the project tasks, it is not intended at this time to provide conclusions. One of the major purposes of this interim report is to solicit timely suggestions and critiques from our sponsors as well as interested parties in the railroad industry and technical community. Such comments are welcomed at the earliest opportunity so that they may be considered and possibly incorporated prior to scheduled completion of the current tasks by September 1986.

The overall purpose of this research program is to develop understanding of the mechanism of wheel failure. Specific technical tasks and objectives are required by the contract in support of this goal. At this time in the program, good progress is being made toward achieving many of the task objectives and several important observations and correlations are suggested in this report, although it is too early to offer complete conclusions.

Some of the technical highlights of the program to date are as follows:

1. Demonstration, by review of derailment data, of the superiority of low stress wheel designs in their resistance to fracture,
2. Use of cyclic plasticity data to predict levels of residual stress in wheels tested on the RDU,
3. Development of finite element techniques to predict residual stress fields from saw-cutting displacements,
4. Determination of the amount of heat lost at the wheel/rail interface, and
5. Formulation of fracture mechanisms for flange and back rim crack.

The project is approximately 2/3rds complete in terms of schedule and expenditures.

Several technical and planning issues remain to be resolved during the final stages of research, including brake thermal load variability between wheels on the same truck, benchmark testing needs for correlating results gathered at different facilities, and the difficulty of producing cracked wheels.

TABLE OF CONTENTS

1.0 Overview and Project Status

1.1 Objectives

- 1.1.1 Overview and Program Control (Subproject 1)
- 1.1.2 Failure Mechanisms, Verifications, Countermeasures (Subproject 2)
- 1.1.3 The State of Safety Risks Due to Overheated Wheels (Subproject 3)
- 1.1.4 Nondestructive Methods to Detect Damaged Wheels (Subproject 4)
- 1.1.5 Safety of Commuter Cars with Hollow Axles (Subproject 5)

1.2 History of Report

1.3 Progress Toward Subproject Objectives

1.4 Introduction to Following Task Summaries

2.0 National Study of Wheel Removal Guidelines (Task 1)

2.1 Current Statement of Work

2.2 Introduction

2.3 Data Sources

2.4 Trends

2.4.1 Car Maintenance Cost Data Base

2.4.2 The Car Repair Billing System Data Base

2.4.3 The AAR Wheel Failure Data Base

2.4.4 FRA Accident Data Base

3.0 Pilot Technology Survey (Task 2)

3.1 Current Statement of Work

3.2 Major Findings and Current Status

3.2.1 Definition and Progress of Technology Survey

3.2.2 Initial Survey

3.2.3 Computerized Information Retrieval System

3.2.4 Select Bibliography Criteria and Organization

3.2.5 Selection Criteria

3.2.6 Format Explanation

3.2.6.1 TTC Document Number

3.2.6.2 Standard Reference Detail

3.2.6.3 Special Classification Notes

3.2.6.4 Special Annotation

3.2.7 Other Selected References

3.2.8 Annotated Listings

3.2.9 Applications of Pilot Technology Survey to Wheel Failure Mechanisms Program

3.3 Work Remaining

3.4 Schedule

TABLE OF CONTENTS (Continued)

4.0 Pertinent Material Properties (Task 3)

4.1 Current Task Statement of Work

4.2 Major Findings/Current Status

4.2.1 Elevated Temperature Cyclic Behavior Task

4.2.2 Fracture Crack Arrest Tests

4.2.3 Thermal Cracking Test

4.2.3.1 Wheels

4.2.3.2 Apparatus and Instrumentation

4.2.3.3 Preliminary Results

4.2.3.4 Thermal Analysis

4.2.4 Effect of Slow Strain Rate

4.2.5 Wheel Saw-Cutting

4.2.5.1 Radial Saw-Cutting Procedure

4.2.5.2 Results and Discussion

4.2.6 Experimental Stress Analysis

4.2.6.1 Determination of Residual Stresses by the Hole Drilling Strain Gage Method

4.2.6.2 Experimental Stress Analysis Results

4.3 Work Remaining

4.3.1 Conventional Elevated Temperature Fatigue Tests

4.3.2 Crack Arrest Tests

4.3.3 Thermal Cracking

4.3.3.1 Infrared Thermal Video Test Plans

4.3.3.2 Thermomechanical Analysis

4.3.4 Advanced Slow Strain Rate Test

4.3.5 Saw-Cutting Work Remaining

4.4 Schedule

4.4.1 Cyclic Properties Test Schedule

4.4.2 Crack Arrest

4.4.3 Schedule for Thermal Cracking Tests

4.4.4 Advanced Slow Strain Rate Tests

4.4.5 Schedule for Saw-Cutting

5.0 Effect of Heat Transfer and Rail Loading (Task 4)

5.1 Current Task Statement of Work

5.2 Major Findings/Current Status

TABLE OF CONTENTS (Continued)

- 5.2.1 Brake Dynamometer Status
 - 5.2.1.1 Wheels
 - 5.2.1.2 Instrumentation
 - 5.2.1.3 Test Conditions
 - 5.2.1.4 Results
 - 5.2.1.5 Heat Transfer Analysis
 - 5.2.1.5.1 Convection Loss Estimate
 - 5.2.1.5.2 Effect of Rail Load on Heat Transfer
- 5.2.2 Roll Dynamics Unit Status
 - 5.2.2.1 Wheels
 - 5.2.2.2 Instrumentation
 - 5.2.2.3 Test Conditions
 - 5.2.2.4 Test Results
 - 5.2.2.5 Stress Analysis Results
 - 5.2.2.6 Heat Transfer Analysis
- 5.2.3 Induction Heating Test Status
 - 5.2.3.1 Wheels
 - 5.2.3.2 Instrumentation
 - 5.2.3.3 Test Conditions
 - 5.2.3.4 Test Results
- 5.3 Work Remaining in Task T4
 - 5.3.1 Work Remaining For Dynamometer
 - 5.3.2 Work Remaining for Roll Dynamics Unit
 - 5.3.3 Work Remaining for Induction Heating Test
- 5.4 Schedule
 - 5.4.1 Schedule for Dynamometer Tests
 - 5.4.2 Schedule for RDU Data Reduction Completion
 - 5.4.3 Schedule for Induction Heating Data Reduction
- 6.0 Monitor Wheel Temperatures and Strains During Braking in Track Tests (Task 7)
 - 6.1 Current Statement of Work
 - 6.2 Major Findings/Current Status
 - 6.3 Schedule
- 7.0 Determine the Effect of Wheel Design, Material and Operation on Residual Stress Development (Task 6)
 - 7.1 Current Task Statement of Work
 - 7.2 Major Findings/Current Status

TABLE OF CONTENTS (Continued)

- 7.2.1 Track Tests
- 7.2.2 Dynamometer Tests
- 7.3 Work Remaining
 - 7.3.1 Track Tests
 - 7.3.2 Dynamometer Tests
- 7.4 Schedule
 - 7.4.1 Track Tests
 - 7.4.2 Dynamometer Tests
- 8.0 Determine Brake Shoe Thermal Input and Behavior (Task 7)
 - 8.1 Current Task Statement of Work
 - 8.2 Major Findings/Current Status
 - 8.2.1 Track Tests
 - 8.2.2 Finite Element Analysis
 - 8.3 Work Remaining
 - 8.3.1 Track Tests
 - 8.3.2 Finite Element Analysis
 - 8.4 Schedule
 - 8.4.1 Track Tests
 - 8.4.2 Finite Element Analysis
- 9.0 Initiate Wheel Cracks in Dynamometer and TTC Track Tests (Task 8)
 - 9.1 Current Task Statement of Work
 - 9.2 Major Findings/Current Status
 - 9.3 Schedule
 - 9.3.1 Dynamometer Tests
 - 9.3.2 Track Tests
- 10.0 Determine the Effect of Wheel Slid Flats on Tread Shell Production (Task 9)
 - 10.1 Current Task Statement of Work
 - 10.2 Major Findings/Current Status
 - 10.3 Work Remaining
 - 10.4 Schedule
- 11.0 Develop a Comprehensive Failure Model (Task 10)
 - 11.1 Current Task Statement of Work
 - 11.2 Major Findings/Current Status

TABLE OF CONTENTS (Continued)

- 11.2.1 General Data Correlation and Statistical Analyses
- 11.2.2 Wheel Stress Analysis Programs
- 11.2.3 Applications
 - 11.2.3.1 Induction Heating Experiment, etc.
 - 11.2.3.2 Detailed Residual Stress
 - 11.2.3.3 Tread Crack Rig Design
 - 11.2.3.4 Wheel/Rail Heat Transfer
 - 11.2.3.5 Saw-Cut Opening Analysis
 - 11.2.3.6 Thermal Analysis of Brake Shoes
 - 11.2.3.7 Linear Elastic Fracture Mechanics
- 11.2.4 Cumulative Fatigue Damage Model
 - 11.2.4.1 Computer Simulation Approach
 - 11.2.4.2 Other Candidate Fatigue Models
 - 11.2.4.2.1 Thermomechanical Fatigue Survey and Recommendations
 - 11.2.4.2.2 Preliminary Evaluation of Back Face Rim Failures
- 11.2.5 Cyclic Path Dependence of Stress Change
 - 11.2.5.1 Successive Hole Drilling Method
 - 11.2.5.2 Computer Simulation Approach
 - 11.2.5.2.1 Uniaxial Plasticity Model
 - 11.2.5.2.2 Biaxial Plasticity Model
 - 11.2.5.2.3 Finite Element Cyclic Plasticity Analysis
- 11.2.6 Tread Cracking
 - 11.2.6.1 Martensite Cracking
 - 11.2.6.2 Hot Spot Cracking Thermal Fatigue
- 11.3 Work Remaining
 - 11.3.1 General Data Correlation
 - 11.3.2 Wheel Stress Analysis Programs
 - 11.3.3 Applications
 - 11.3.4 Cumulative Fatigue Damage Model
 - 11.3.5 Cyclic Path Dependence of Stress Change
 - 11.3.6 Tread Cracking Analysis
- 11.4 Schedule
- 12.0 Determine Residual Stress and Metallurgical Changes in Test Wheels (Task 11)
 - 12.1 Current Task 11 Statement of Work
 - 12.2 Major Findings/Current Status of Task 11

TABLE OF CONTENTS (Continued)

- 12.2.1 Residual Stress Estimation from Saw-Cutting Results
- 12.2.2 Associated Metallurgical/Macrostructural Evaluation
- 12.2.3 Detailed (Triaxial) Residual Stress Tests
- 12.3 Work Remaining in Task 11
 - 12.3.1 Saw-Cutting Work Remaining
 - 12.3.2 Macrostructural Work Remaining
 - 12.3.3 Detailed Residual Stress Work Remaining
- 12.4 Schedule for Completion of Task 11
 - 12.4.1 Saw-Cutting Schedule
 - 12.4.2 Macrostructural Evaluation Schedule
 - 12.4.3 Detailed Residual Stress Schedule
- 13.0 Furnish Suitable Brake Dynamometer (Task 12)
 - 13.1 Current Task Statement of Work
 - 13.2 Major Findings/Current Status
 - 13.3 Work Remaining
 - 13.4 Schedule
- 14.0 Modify TTC Roll Dynamics Unit (Task 13)
 - 14.1 Current Task Statement of Work
 - 14.2 Major Findings/Current Status
 - 14.3 Work Remaining
 - 14.4 Schedule
- 15.0 Evaluate NDT Techniques (Task 14)
 - 15.1 Current Task Statement of Work
 - 15.2 Major Findings/Current Status
 - 15.2.1 Selection Criteria
 - 15.2.2 Review of State-of-the-Art NDE Techniques
 - 15.2.2.1 Residual Stress Detection Methods
 - 15.2.2.2 Crack Detection Methods
 - 15.2.3 Screening Criteria
 - 15.2.3.1 Possible Locations for NDE System Use
 - 15.2.3.2 Performance Categories
 - 15.2.3.3 Performance Levels
 - 15.2.3.4 Screening Criteria for Stress & Crack
 - 15.2.3.5 Screening Criteria Evaluation

TABLE OF CONTENTS (Continued)

15.2.4 Selected Techniques

15.2.4.1 Hot Wheel Detection

15.2.5 Barkhausen Technique for Residual Stress Determination

15.3 Work Remaining (Under Review)

15.4 Schedule (Under Review)

16.0 Conduct RDU Tests of the M-2 Car Axle/Bearing Failure Mode (Task 15)

16.1 Current Task Statement of Work

16.2 Major Findings/Current Status

16.3 Work Remaining

16.4 Schedule

LIST OF APPENDICES

- 2.0 Wheel Failures for 1983
- 2.1 Wheel Failures for 1984
- 2.2 Wheel Failures for 1985 (January-June)
- 3.1 Description of VAX-11 DATATRIEVE Data Management Facility
- 3.2 Annotated Bibliography (Sorted by File Number)
- 3.3 Annotated Bibliography (Sorted by Subject)
- 4.1 Elevated Temperature Fatigue Behavior of Class B, C, and U Wheel Steels
- 4.2 Crack Arrest Testing of Class U and Class C Railroad Wheel Steels
- 4.3 Master Data Base of Saw-Cut Wheels
- 5.1 Tabulation of Brake Dynamometer Data
- 5.2 Adaptation of Solution for Moving Heat Source on a Half Space
- 5.3 Adaptation of Solution for Moving Heat Source on the Edge of a Semi-infinite Plate
- 5.4 Estimate of Wheel/Rail Heat Transfer Rate Based on Leading and Trailing Surface Temperatures
- 5.5 Analysis of Brake Dynamometer Unit Heat Transfer Data
- 5.6 Steps Involved in Determining Actual Strains
- 5.7 Preliminary RDU Heat Transfer Analysis
- 11.1 Review of Life Prediction Methods for Applications in Railroad Wheel Rim Failure Research
- 11.2 Description of STRESS6 Computer Program for Calculation of Wheel Stresses During RDU Testing
- 11.3 Special Non-Linear Creep/Kinematic Strain Hardening Model for Variable Temperature and Total Strain Input

1.0 OVERVIEW AND PROJECT STATUS

The life of a railroad wheel is determined by various factors such as wear, plastic flow, fatigue failure of the wheel plate, shelling and thermal cracking of the wheel tread, and wheel fracture. The incidence of heat related wheel failure, which is initiated by a thermal crack in the wheel rim, has become of great importance in the railroad industry. A relatively large number of wheels are removed from service on the basis of the discoloration of the wheel plate, caused, presumably, by severe thermal loads. The problem of removing a thermally abused wheel from service has become more complex. Research has shown that a similar percentage of both nondiscolored and discolored wheels contain high levels of residual tensile stress in the rim. These stress levels can propagate radial rim cracks and eventually lead to catastrophic wheel failures. Research has also indicated that the initial residual stresses in the rim are altered by the complex effect of thermal stresses due to severe modes of braking operation. Additionally, the effect of alternating stresses due to the mechanical loads at the wheel/rail interface are not well understood.

To improve the safety performance of railcar wheels, the FRA is supporting the Wheel Failure research project to understand fully all important wheel failure mechanisms, and to develop technically sound wheel removal criteria and guidelines for safe operation. This project encompasses 14 Technical Tasks ranging from a technology survey through a national study of wheel removal guidelines to individual technical problem-oriented tasks which include laboratory and track testing and analyses. Supporting these technical tasks are 12 Planning Tasks oriented toward test facilities and methodology. The AAR has completed

these individual task plans which are assembled into the following five sub-projects:

1. Overview and Program Control (Subproject 1, SP1)
2. Failure Mechanisms, Verifications, and Countermeasures (Subproject 2, SP2)
3. The State of Safety Risks Due to Overheated Wheels (Subproject 3, SP3)
4. Nondestructive Methods to Detect Overheated Wheels (Subproject 4, SP4)
5. Safety of Commuter Cars with Hollow Axles (Subproject 5, SP5)

These documents were approved by the FRA in June of 1984, at which time work began on the project.

The individual technical tasks of this project are grouped into major subprojects for purposes of management control and clarity of the specific areas of wheel safety investigation. This grouping is illustrated in Figure 1.1. The AAR office with primary responsibility for each subproject is indicated parenthetically under each title.

The requirements of each of the 14 Technical Tasks are given in the FRA Statement of Work (SOW). The plans for meeting these requirements are provided in the following sections of this document and the four original subproject documents.

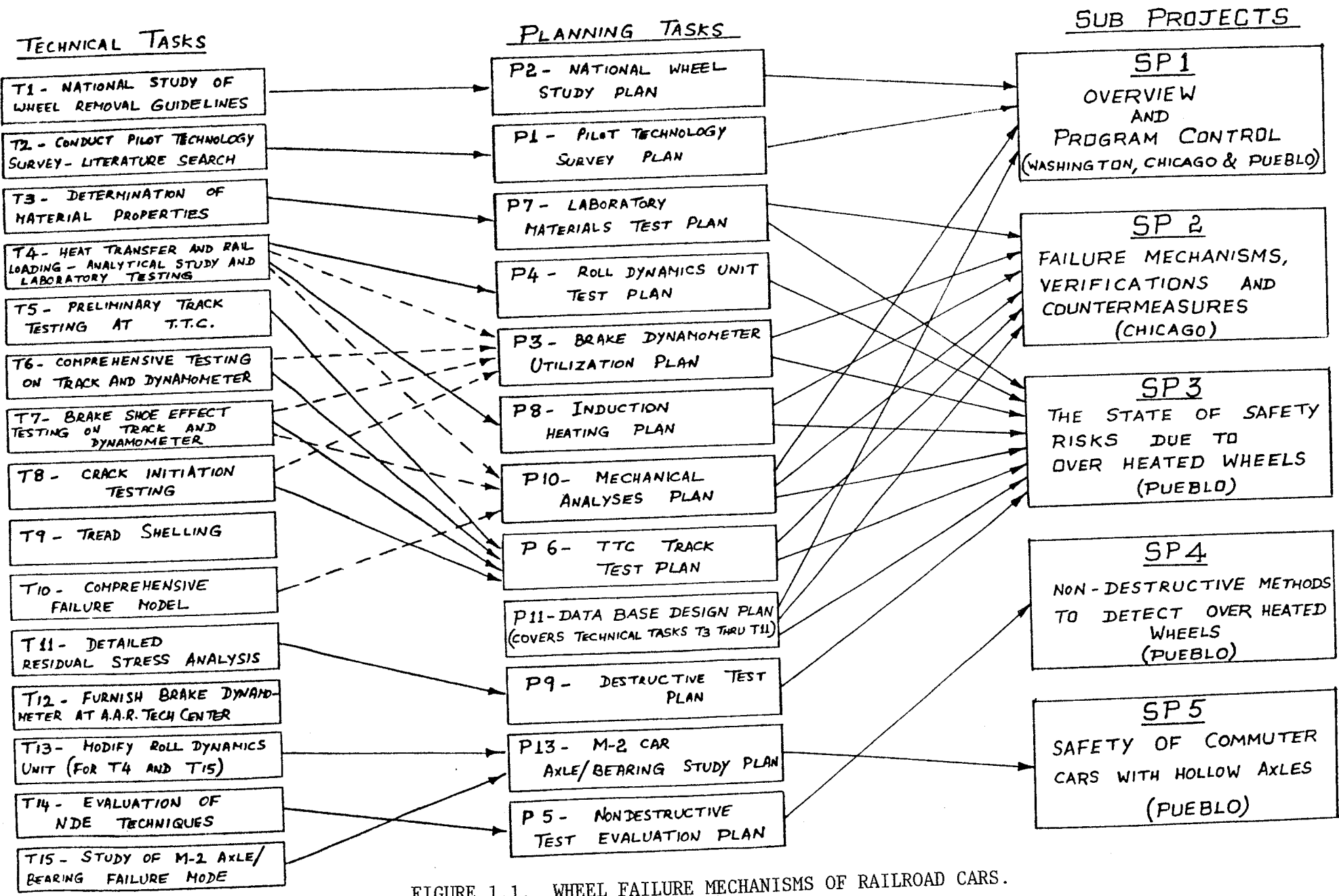


FIGURE 1.1. WHEEL FAILURE MECHANISMS OF RAILROAD CARS.

1.1 OBJECTIVES

1.1.1 Overview and Program Control (Subproject 1)

The purpose of this subproject is to provide overall safety guidelines for wheel removal based on a continuing review and evaluation of national wheel safety statistics. The data base and pertinent analysis techniques are developed and managed under this subproject. In addition, the research results developed within the other Technical Subprojects are monitored within this subproject. This subproject document will also include discussion of the current understanding of wheel failure modes and their relative safety significance.

1.1.2 Failure Mechanisms, Verifications and Countermeasures (Subproject 2)

The purpose of this subproject is to determine the mechanisms of wheel failure, demonstrate these mechanisms by causing a wheel failure under controlled conditions and to suggest methods for preventing wheel failure. Figure 1.1 shows the relationship of this subproject to the specific original tasks and plans. The requirements of each of the 14 Technical Tasks are given in the FRA Statement of Work (SOW).

1.1.3 The State of Safety Risks Due to Overheated Wheels (Subproject 3)

The purpose of this subproject is to determine the effects of wheel

design/material/size and brake application history on the development of residual stress. The state of residual stress in the overheated wheels due to severe modes of braking applications will be evaluated. Duration and force levels of braking application, and the sequence of reapplication required to accumulate critical levels of residual stress in the test wheels will be monitored.

Careful experimental study under controlled conditions in the laboratory and extensive track testing will be performed to meet the objective of this subproject. The data accumulated in these and other tasks will be analyzed and compiled into a final report on other subprojects.

1.1.4 Nondestructive Methods to Detect Damaged Wheels (Subproject 4)

This portion of the program will address the goal of developing technically sound wheel removal criteria. It includes the critical evaluation of nondestructive testing techniques, since they represent candidate methods of applying realistic wheel removal criteria developed during the course of the overall program.

1.1.5 Safety of Commuter Cars with Hollow Axles (Subproject 5)

The objective of this test program is to examine the thermal properties of bearings that have service worn grooves between the axle and roller bearing assembly, and to take static measurements of bearing cup and seal wear ring movement, and any wear which may

occur between the bearing cones and the axle. The dynamic performance of a "bent" solid axle with a straight hollow axle will also be compared.

The Roll Dynamics Unit (RDU) will be utilized to determine rates of fretting wear and thermal runaway on hollow axle/bearing/wheel assemblies of commuter railcars (M-2 Fleet). Test runs of up to 10,000 miles each, with an M-2 truck will be performed on the RDU and dynamic measurements of bearing temperature and bending strain will be monitored. Each test run will investigate two axle/bearing/wheel assemblies.

1.2 HISTORY OF PROJECT

The chronology of the project is as follows:

- October 13, 1982 - Task Request for Wheel Failure Mechanism of Railroad Cars Issued.
- December 21, 1982 - Task Proposal submitted to FRA.
- April 21, 1983 - Task Request for Addition of Pilot Technology and M-2 Axle/Bearing Failure Tasks.
- May 17, 1983 - Revised proposal submitted to FRA.
- September 9, 1983 - Task Order 6 authorized with thirteen planning tasks in support of fifteen technical tasks. The schedule and delivery of the planning tasks is shown in Table 1.1.
- October 5, 1983 - Master Work and Cost Schedule Plan delivered to FRA.
- May 7, 1984 - FRA reorganization of program into five subprojects.

- May 25, 1984 - Five subproject program technical plans submitted to FRA.
- June 7, 1984 - All technical task plans approved with the exception of Wheel Slid Flat/Shelling Project which was dropped from program.
- October 9, 1985 - Approval copy of Interim Report delivered to FRA.

It took almost nine months between the time of contract approval and permission to begin work on all of the technical tasks (with the exception of the M-2 bearing task).

TABLE 1.1. SCHEDULE AND DELIVERY OF PLANNING TASKS.

<u>Planning Task</u>	<u>Due</u>	<u>Delivered</u>	<u>Approved</u>
P-1 Pilot Technology Survey	10/09/83	10/24/83	01/17/84
P-2 National Wheel Study	12/09/83	12/06/83	06/07/84
P-3 Brake Dynamometer Utilization	02/09/84	01/10/84	06/07/84
P-4 RDU Modification	12/09/83	12/06/83	06/07/84
P-5 Nondestructive Test Evaluation	04/09/84	05/25/84	06/07/84
P-6 TTC Track Tests	01/09/84	02/03/84	06/07/84
P-7 Laboratory Materials Tests	11/09/83	11/04/83	01/17/84
P-8 Wheel Induction Heating	11/09/83	11/04/83	01/17/84
P-9 Destructive Testing	12/09/83	12/06/83	06/07/84
P-10 Mechanical Analysis	03/09/84	04/19/84	06/07/84
P-11 Data Base Design	11/09/83	11/04/83	01/17/84
P-12 Analysis of Slid Flats	02/09/84	02/03/84	*
P-13 M-2 Axle/Bearing Study	12/09/83	12/06/83	12/23/83

*Withdrawn from contract.

1.3 PROGRESS TOWARD SUBPROJECT OBJECTIVES

1.3.1 Subproject SP1 has three major tasks: the national study of wheel removal guidelines, the pilot technology survey, and the design of a data base for capturing all information gathered in the program. The schedule for these tasks is shown in Table 1.2, which presents the overall project schedule. All tasks in this project are completed or on schedule.

1.3.2 Subproject SP2 has the following tasks:

<u>Task</u>	<u>Status</u>
T3.1 Cyclic Properties	T3.1 work complete, work continues on time dependent properties.
T3.2 Thermal Cracking	Work underway with expected completion by February 1, 1986.
T3.3 Crack Arrest	Work complete.
T7.2 Track Test	Test underway with completion expected October 15, 1985.
T8.1 Track Tests	Tests scheduled to start February 1, 1986 and run eight weeks.
T8.2 Dynamometer Tests	Tests scheduled to begin May 1, 1986.
T11.2 Magnaflux Test	Will run concurrently with T8.1 and T8.2.
T7.1 FE/FD Analysis	Will run consecutively with T8.1 and T8.2. Should be finished on schedule.

1.3.3 Subproject SP3 has elements from five technical tasks. Each task's status is given below.

<u>Task</u>	<u>Status</u>
T4.1 Finite Element Analysis	Wheel analysis using the ANSYS system has been verified.
T4.2 Heat Transfer Analysis	Task complete.
T4.3 RDU Testing	Task complete.
T4.5 Induction Heating	Testing complete, analysis partially complete.
T5.1 Preliminary Track Test and	Tests underway, to be completed by October 15, 1985.
T5.2 Interim and Post NDE	Concurrent with 5.1
T5.3 Destructive Analysis	Will commence October 16, 1985.
T6.2-4 Track Test	Will commence November 1, 1985, for completion January 15, 1986.
T10 Failure Mode	Activity throughout entire program.
T11 Detailed Residual Stress	Work on first of four wheels underway.
T12 Dynamometer Procurement	Dynamometer installation completed April 1984.

13.4 Evaluation of Nondestructive Testing Methods has been completed and submitted. A proposal for rescoping this task as required by the COTR, was submitted July 2, 1985.

1.4 INTRODUCTION TO FOLLOWING TASK SUMMARIES

Each of the following sections is devoted to one of the fifteen subtasks. The current statement of work is given, and the major

results are presented and discussed. The remaining work is outlined and the schedule for completion is presented. An updated schedule for the entire project is shown in Table 1.2.

TABLE 1.2. OVERALL SCHEDULE FOR WHEEL FAILURE MECHANISMS PROJECT (CONTINUED).

SP - 2 Revision of 10/1/85
 WHEEL FAILURE MECHANISMS, VERIFICATIONS OF COUNTERMEASURES

The first column contains the Technical Task # from FRA Contract # DTFR53-82-C-00282.
 The second column contains the Sub-Project Plan paragraph reference that describes the action or SCHEDULE STEP.

		1983			1984			1985			1986																														
MONTHS SINCE AWARD >		1	2	3	4	5	6	7	8	9	10	11	12	13	14	15	16	17	18	19	20	21	22	23	24	25	26	27	28	29	30	31	32	33	34	35	36				
MONTH of YEAR >		O	D	N	D	I	J	F	M	A	M	J	J	A	S	O	N	D	I	J	F	M	A	M	J	J	A	S	O	N	D	I	J	F	M	A	M	J	J	A	S
SP2 PLAN APPROVAL				I						10+++0																															
SP2 INTERIM REPORT				I																					0++0																
SP2 FINAL REPORT				I																																				10+++++++0	
S.O.W. TECH. TASK	Sub-Project Plan Section/ *PLAN TASK SCHEDULE STEP			I																																					
T3 MAT'L PROPERTIES	Lab Mat'ls Test Plan			I																																					
T3.1 Cyclic	7.1 Cyclic Behavior Tests			I																																					
	7.1.1 Instrumentation & Equip.			I																																					
	*P7 PREPARE SPECIMENS			+++++++0																																					
	7.1.2 Testing			I																																					
	*P7 RN. TEMP. C			10+++0																																					
	*P7 HI TEMP. MOD.			0+++++++0																																					
	*P7 HI TEMP. B			10+++++++0																																					
	*P7 HI TEMP. C			I						10+++++++0																															
	*P7 HI TEMP. U			I									10+++++++0																												
	*P7 RATE AND TIME PROPS. (EXTRA)			I												10+++++++0																									
	*P7 REDUCE DATA			0++0						10+++0			10+++0																												
	*P7 PREPARE RPT.			I									10+++0																												
T3.2 Thera. Crack	7.2 Thermal Cracking Tests			I																																					
	7.2.1 Objective & Scope			I																																					
	7.2.2 Material			I																																					
	7.2.3 Apparatus			I																																					
	*P7 DESIGN APPARATUS			I									10++++0																												
	*P7 CONSTRUCT APPARATUS			I												10+++++++0																									
	7.2.4 Experimental Procedure			I																																					
	*P7 SET UP TEST			I																								10++++0													
	7.2.5 Data Collection			I																																					
	*P7 TEST			I																								10+++++++0													
	7.2.6 Results & Evaluation			I																																					
	12.7.3 Tread Crack Rig Design			I																																					
	12.11.1 Martensite Cracking			I																																					
	*P7 PREPARE REPORT			I																								10++++0													
T3.3 Crack Prop. & Arrest	7.3 Crack Arrest Testing			I																																					
	7.3.1 Objective			I																																					
	7.3.2 Equipment			I																																					
	*P7 TEST PREPARATION			I																																					
	7.3.3 Test Variables			I																																					
	*P7 TEST CLASS U			I																																					
	*P7 TEST CLASS C			I																																					
	7.3.5 Data Reduction & Analysis			I																																					
	*P7 REDUCE/ANALYZE CLASS U			I																																					
	*P7 REDUCE/ANALYZE CLASS C			I																																					
	*P7 PREPARE REPORT			I																																					
	12.7.6 L.E.F.M. Analysis			I																																					
	*P10 PREDICT CRACK GROWTH			I																																					

2.0 NATIONAL STUDY OF WHEEL REMOVAL GUIDELINES (TASK 1)

2.1 CURRENT STATEMENT OF WORK

The Association of American Railroad (AAR) shall assess the current status (1980-1983) of wheel discoloration removal, cracked wheel removal and catastrophic wheel failure. The AAR shall statistically correlate operational/traffic factors under latest wheel removal guidelines. The AAR shall monitor the impact of wheel removal modifications on operational wheel failures. This will be addressed by the monitoring of a national study to be conducted by AAR in conjunction with a partial change in FRA Rule 215.103(H) such that a major portion of the car fleet will be inspected on the basis of 4 inches of discoloration on the front and back of wheels. The AAR shall monitor the performance of these wheels by combining information from the AAR freight car repair data base and FRA accident reports on a large, statistically valid sample. AAR shall recommend a wheel failure "trigger mechanism" that will indicate the desirability of a change in wheel removal guidelines. The AAR shall attempt to develop technically sound wheel removal criteria which will likely reduce discolored wheel removal rates without interrupting the downward trend of wheel failure rates.

2.2 INTRODUCTION

The FRA/AAR Wheel Research Program continues to conduct a national study of the wheel removal guidelines. This provides the meth-

odology to evaluate potential changes in wheel removal criteria, including the definition of an overheated wheel from four inches of discoloration front or back to four inches of discoloration front and and back, and exempting wheels of "low" stress design from removal. This is being done by promulgation of waivers to existing rules which provides an evaluation of subsequent changes. In the meantime, the data is exercised to define existing conditions. The objective of this task is to provide a means of monitoring the impact of the rule change on wheel removal and failure patterns. Further, a trigger mechanism is being recommended that will indicate if the rule change is having a negative impact on safety.

The Association of American Railroads has agreed to monitor the removal and failure trends of railroad freight car wheels in conjunction with the FRA/AAR Wheel Research Program. Planning Task P2 established the methods to be used and the data sources of information chosen were:

1. The AAR Car Repair Billing System Data Base
2. The AAR Wheel Failure Report Data Base, and
3. The FRA Accident-Incident Reports Data Base
4. The AAR Car Maintenance Cost Data Base.

The method used to monitor the wheel removal and failure patterns is the control chart. The control charts have been established with control limits for one quarter, two consecutive quarters and three consecutive quarters. One control chart has been established for

each combination of data source and normalizing factor (car miles, active cars or ton miles). The control limits have been established to provide 95% confidence such that when the data source mean has shifted significantly, the limits have been exceeded.

The control limits will continue to change each quarter up to the time a waiver or rule modification is instituted. At this time the control limits will be fixed. In each subsequent quarter a new point will be plotted to indicate whether or not the process average has been changed by the waiver or rule modification.

This report contains the data sources chosen and the trends for each data source quarterly from 1980 to latest quarter for which information is available.

2.3

DATA SOURCES

Four sources of data have been identified which may be used to monitor the impact of a change in the definition of an overheated wheel. These are as follows:

1. The Car Repair Billing Exchange System Data (CRB) - These data contain foreign car repair billing on the majority of the North American freight car fleet. The job codes and why made codes in this system support the determination of the number of wheels removed due to thermal damage and/or discoloration.

Figure 2.1 contains a complete description of these data as it applies to wheels.

2. The AAR Mechanical Division Wheel Failure Report (or MD-115) - These forms are voluntarily completed and submitted to the AAR Mechanical Division for all cracked or broken plates, rims or flanges. The why made codes permit the number of wheel failures due to thermal damage to be determined. Figure 2.2 contains the reporting form used in this system.
3. The FRA Accident/Incident Reports - Railroad accidents (derailments/collisions) resulting in damage exceeding a minimal threshold (\$3,700 in 1984) must be reported to FRA. These reports permit the number of accidents caused by thermally damaged wheels to be estimated. Since the actual cause of a cracked or broken wheel can not be determined from these data, we assume all cracked or broken wheels are the result of thermal damage. The FRA Accident/ Incident reporting form is shown in Figure 2.3.
4. The Car Maintenance Cost Data Base - These data are maintained by the AAR Research and Test Department, and contains both system and foreign repairs to freight cars owned by eight participating roads. These railroads voluntarily submit this information for approximately 500,000 freight cars. The repair information in this data base is in a form consistent with the CRB system. Thus, the number of wheels removed due to thermal damage and discoloration can be determined.

FIGURE 2.1. CAR REPAIR BILLING EXCHANGE SYSTEM INFORMATION RULES.

RULE 112 - CAR REPAIR BILLING

A. BILLING REPAIR CARD REQUIREMENTS (MINIMUM)

1. Basic Common Information:

- a. Reporting Marks (Car Initials)
- b. Car Number
- *c. Kind of Car *This is not required for transportation yard repairs.
- d. Date repairs completed
- e. Repair point location
(Standard Point Location Code must be used on Billing Repair Card. Name may be used in addition to code.) If repairs are made on road, repair card must so indicate.
(Not required for repairs made in Mexico.)

2. See Section "F" of applicable Rule in Field Manual for requirements to be furnished for each repair made.

3. Charges and/or credits.

- a. Charge and/or credit for each respective repair or function performed will be shown.
- b. Items of repair where no charge is permitted, the words, "no charge", the letters "NC" or the numerals "\$.00" will be shown in column reserved for charges and/or credits.
- c. Billing Repair Card charges and/or credit will be totaled and sum shown on Billing Repair Card.
 - (1) If total for Billing Repair Card is zero, it will be shown "no charge", "NC" or "\$.00" in area reserved for total.
 - (2) Where repairs to a car at a same shopping require more than one Billing Repair Card, the total amount will reflect total of all items reported for that shopping of car.
 - (3) Items of repair that may be group billed.
 - (a) Single, multiple or combination of the following items of repairs only to the same car and where no other repairs are involved:

(1) Air Brake Hose.	(7) Angle Cock, Seal Ring or Ball Type.
(2) Brake Shoes.	(8) Air Hose Support Complete.
(3) Brake Shoe Keys.	(9) Air Hose Safety Chain "S" Hook.
(4) Cotter Keys.	(10) AB Valve Vent Protector.
(5) Journal Box Lids.	(11) Brake Connection Pin.
(6) Brake Head Wear Plates.	(12) Journal Box Lid Seal, Approved.
 - (b) See Section "F", Preparation of Bill Statement, for requirements of statement relative to group billed items.

RULE 112 - (Cont'd.)

4. Billing Repair Cards shall be 11" (width) x 8-1/2" (length) in size and shall be single pages.
5. Only information required in the Interchange Rules pertaining to car repairs shall be shown on Billing Repair Card.
6. The original Billing Repair Cards must be furnished to support charges in bill.

B. DEFECT CARD AND/OR JOINT INSPECTION CERTIFICATE HANDLING

1. Whenever a Defect Card is issued, a copy will be promptly forwarded to the Car Owner by mail.
2. Endorsement by company responsible for repairs is required, before Joint Inspection Certificate is negotiable.
3. Repairs to system cars repaired on authority of a Defect Card and/or endorsed Joint Inspection Certificate will be billed against party issuing Defect Card.
4. Repairs to foreign cars made on authority of a Defect Card and/or endorsed Joint Inspection Certificate will be billed against car owner. If an intermediate road is involved, see Rebuttal Charge Handling.
5. Billing Repair Card must always be issued when billing for repairs is covered by Defect Card and/or endorsed Joint Inspection Certificate.
6. Billing Repair Card reflecting repairs covered by Defect Card and/or endorsed Joint Inspection Certificate will show reference to name or initials of road issuing Defect Card and/or endorsed Joint Inspection Certificate.
7. Defect Card and/or endorsed Joint Inspection Certificate cannot be repudiated, unless time limit for handling has expired.
8. Defect Card and/or endorsed Joint Inspection Certificate must accompany Billing Repair Card to justify charges.

RULE 112 - (Cont'd.)

C. REBUTTAL CHARGE HANDLING

1. When repairs are made by an intermediate road and charges have been presented to the owner, a rebuttal charge by owner will be prepared and billed to responsible party to collect charges covered by Defect Card and/or endorsed Joint Inspection Certificate.
2. Only repairs covered by Defect Card and/or endorsed Joint Inspection Certificate are collectable from responsible party.
3. Defect Card and/or endorsed Joint Inspection Certificate must accompany Billing Repair Card to justify rebuttal charge.

D. COUNTER BILLING AUTHORITY

1. Counter Billing Authority will be used for the purpose of monetary adjustment for the parties concerned.
 - a. When adjustment is being made on the basis of a Counter Billing authority, such authority must accompany bill to justify charge.
 - b. All detail in Counter Billing Authority form must be properly filled out.

Name of Company _____	
Place _____	Date _____
This will authorize the _____ Co.	
to counterbill the _____ Co. \$ _____	
_____ dollars as	
(To bill number) _____	
adjustment (per letter) _____ file _____	
Signature of person issuing _____	
This authority must be attached to bill.	

ASSOCIATION OF AMERICAN RAILROADS COUNTER BILLING AUTHORITY

RULE 112 - SECTION E (Cont'd.)

E. TIME LIMITS FOR BILLING REPAIR CARDS, DEFECT CARDS, ETC.

1. Billing Repair Cards and bills for destroyed cars under Field Manual Rule 107 must be billed within twelve (12) months from date of repairs or date of acceptance for settlement of destroyed cars. Example: For repairs made in July, bill must be made and forwarded to the company against which bill is proper before August 1 of the following year.
2. Damage covered by Defect Card and/or endorsed Joint Inspection Certificate must be repaired within forty eight (48) months from date of Defect Card issuance. For cars retired under the provisions of Rules 102 and 103, Billing Repair Card must be issued within these time limits.
3. Rebuttal charges must be billed within seven (7) months from date of receipt from intermediate line. An additional three (3) months will be allowed in cases where bills covering repairs to leased cars involving offset bill subsequently rendered against lessor and such lessor takes exceptions to the charges.
4. Failure to bill within the limits prescribed above will result in forfeiting all claims. No charges may be rendered for repairs to cars after time limits have expired, even though previous attempts have been made to ascertain proper ownership.
5. Counter Billing Authority will be billed promptly.

F. PREPARATION OF BILL STATEMENT

1. Separate statements to be made as follows:
(Provisions of a and b below are optional with repairing line.)
 - a. When items shown in Section A.3.c.(3) are repaired in kind and Billing Repair Cards are group billed, the statement accompanying such Billing Repair Cards must contain the following:
 - (1) Job Code Number.
 - (2) Description.
 - (3) Number of Items.
 - (4) Price Each.
 - (5) Total amount for each item grouped.
 - (6) Total amount of statement.(It is not necessary to price Billing Repair Cards group billed.)

RULE 112 - SECTION F (Cont'd.)

- b. No Billing Repair Cards required for items shown in Section A.3.c.(3) if group billed and bill statement contains the following:
- (1) Car Initial.
 - (2) Car Number.
 - (3) Date repairs completed.
 - (4) Repair point location (SPLC code).
 - (5) Quantity.
 - (6) Condition Code.
 - (7) Job Code Applied.
 - (8) Description.
 - (9) Job Code Removed.
 - (10) Why Made Code.
 - (11) Price Each.
 - (12) Total amount of statement.
- c. For car repairs other than those covered by Defect Card, Joint Inspection Certificate or group billed, the following minimum information must be shown on bill statement:
- (1) Car Initial.
 - (2) Car Number.
 - (3) Total net charge or credit for all repairs made for that shopping. If total shown on Billing Repair Card is "No Charge", "NC" or "\$.00", such letters or numerals must be shown on bill statement.
- d. For computerized billing statements, the following information must be shown in addition to Paragraph c.:
- (1) Date repairs completed.
 - (2) Repair point location (SPLC).
- e. For Defect Card or Joint Inspection Certificate charges, the same information as that required in c. above must be shown on bill statement.
- f. For Rebuttal Charges the same information as that required in c. above must be shown on bill statement.
- g. Statements must be 11" (width) x 8-1/2" (length) in size and shall be single pages.
- h. Original copies of statements are to be furnished car owner.

RULE 112 - SECTION F (Cont'd.)

1. For Counter Billing Authority the following must be shown:

- (1) Billing company's bill number.
- (2) Total amount of Counter Billing Authority.

2. Entries on bill statements must be in same sequence as Billing Repair Cards, Defect Cards, etc., accompanying statement.

G. PREPARATION OF BILLS FOR CAR REPAIRS

1. Bill will identify each bill statement and total for each statement will be shown and recapped into one total, for total amount of bill.
2. No percentages shall be added to bills rendered under these rules.
3. Charges for repairs to cars after the time limits have expired must not be included in bill.
4. All charges for repairs, Defect Cards, rebuttals and Counter Billing Authorities shall be consolidated against any one company into one bill. This principle applies equally to railroads and to private car owners and specifically limits the number of car repair bills to one per month against any one company.
5. Bills will be rendered for whatever amount results in aggregate for car repairs against that company. In the event that the total against a particular company results in a credit or zero balance, the billing road will forward repair cards to car owner and issue a Counter Billing Authority if credit due.
6. Separate bills must be prepared for the following:
 - a. Settlement for cars destroyed.
 - b. Settlement for worn out cars, owner's responsibility.
 - c. Transfer or adjustment of loads.
7. In rendering bills, cars shall be treated as belonging to companies or individuals whose reporting marks it bears and that charges for repairs to all cars bearing like reporting marks will be billed against that one company or individual at one address and to one officer.

RULE 112 - SECTION G (Cont'd.)

8. The title and address of officer who will handle correspondence relating to exception to charges must appear on bill.
9. Freight and Passenger car repair bills, rendered between carriers, subject to draft settlement, as provided by Mandatory Disbursement Rule 23 of the AAR Accounting Division must be endorsed "Per AAR Disbursement Rule 23, subject to net draft settlement on(Show date)," and handled in accordance with the provisions of that rule.
10. All bills shall be rendered promptly. Where not otherwise specified by AAR Rule or by other agreement between parties, the rendering date specified by Disbursement Rule 23 will apply.

H. AUDITING REGULATIONS, BILL SETTLEMENT AND ADJUSTMENT OF CHARGES.

1. If entire bill is improperly rendered, it may be returned unpaid to the billing company for correction, giving proper explanation.
2. All bills shall be passed for payment unless net amount of errors or questionable charges (excluding incorrect car numbers or reporting marks) exceeds ten (10) percent of the total amount of bill, in which case the unpaid bill must be returned no later than 60 days from receipt of bill to the billing road. This provision does not apply to bills rendered between carriers, when subject to draft settlement, in accordance with Mandatory AAR Disbursement Rule 23.
3. Exceptions to paid car repair bills:
 - a. Must be brought to the attention of the billing company no later than seven (7) months after first receipt of bill:
 - (1) An additional three (3) months (or a total of ten (10) months) will be allowed after receipt of original bill when exceptions cover repairs to leased cars where offset bill is subsequently rendered against lessor and exceptions taken by lessor.
 - (2) For exceptions to repairs based on time limit guarantees per Rules 2, 3, 25, and 70, the provisions above apply to last bill received.
 - b. Undercharges shall be called to the attention of the billing company.
 - c. If exceptions (excluding incorrect car numbers or reporting marks) do not amount to \$5.00 in aggregate, no exception shall be taken.
 - d. All exceptions shall be taken at the same time. (Does not apply to exceptions covered by time limit guarantee).
 - e. Original Billing Repair Cards, or copy or facsimile thereof, returned for correction, or on account of exceptions, must not be defaced in any manner on the face of the card or copy. (When is necessary for billing road to make corrections, the incorrect information must be lined out and correct information furnished.)

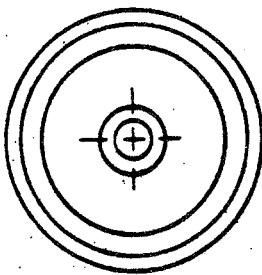

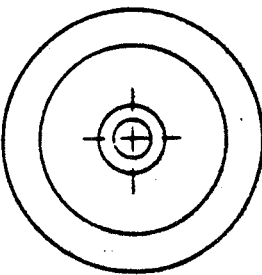
RULE 112 - SECTION H (Cont'd.)

- f. When exceptions are taken to a bill, all Billing Repair Cards and defect cards, except those in question, must be retained by the company against which bill has been rendered.
 - g. Exceptions taken must be fully detailed in letter form with reference given to bill number and date of bill or accounting month in which charges were included. Each exception will be supported by the original Billing Repair Card or a legible copy or facsimile thereof.
 - h. If it is alleged car was not on repairing road on date claimed, the car owner must show location of car on such date.
 - i. Billing road shall within ninety (90) days handle exceptions, make proper adjustment of charges and issue a Counter Billing Authority, if in order.
 - j. Billing road will notify car owner in detailed letter form of the disposition of each exception.
 - k. When original billing repair cards have been returned for correction or on account of exceptions, such original cards must be returned to the car owner. Copy or facsimile returned in lieu of the original need not be returned to the car owner.
4. In the event that car repair bill and attachments (Billing Repair Cards, Defect Cards, etc.) are lost or destroyed in transit, the billing road must arrange to furnish a copy of bill without supporting Billing Repair Cards. Car owner shall accept and pass bill for payment and may make claim for adjustments on the basis of the average percentage adjusted on the last three car repair bills presented by this same billing road. Billing road shall honor this claim and provide adjustment by issuing a Counter Billing Authority.

RULE 113 - DATA EXCHANGE PROCEDURES

- 1. All companies who participate in the Car Repair Billing data exchange procedures will submit data exchange, machine readable information in accordance with the specifications provided by the AAR Data Systems Division.

RULE 114 - 119 - VACANT

MD-115		REPORT OF DEFECTIVE LOCOMOTIVE, PASSENGER OR FREIGHT CAR WHEELS				Rev. 5/80
[INSTRUCTION: This report is to cover wheels which are removed for defects represented by the following WHY MADE Codes (See Rule 41F) 66, 68, 71, 74, and 83. All items should be completed. If illegible, draw a horizontal line through the box or boxes. Refer to back of form for further instructions.]						
DATE OF FAILURE		CAR INITIAL		KIND OF EQUIPMENT		WHEEL DIAMETER
Month Day Year <input type="text"/> <input type="text"/> <input type="text"/> <input type="text"/> <input type="text"/> <input type="text"/>		8 9 10 11 <input type="text"/> <input type="text"/> <input type="text"/> <input type="text"/>		B-Box P-Pass C-Cab. R-Refrig. F-Flat S-Stock G-Gon. T-Tank H-Hopper X-Loce. L-CovHop Q-Other		Enter Nominal Diameter If Not Listed 28 32 36 38 40
1 2 3 4 5 6		CAR NUMBER		<input type="text"/>		<input type="text"/>
12 13 14 15 16 17		18		19 20		
JOURNAL SIZE	FLANGE THICKNESS (Sixteenths)	RIM THICKNESS (Sixteenths)	TYPE DEFECT RULE 41F (WHY MADE CODE)	CLASS OF HEAT TREATMENT		
09 10 11 12 <input type="text"/> <input type="text"/>	<input type="text"/> <input type="text"/>	<input type="text"/> <input type="text"/>	<input type="text"/> <input type="text"/>	<input type="text"/> <input type="text"/>		
21 22	23 24	25 26	27 28	29 30		
WHEEL DESIGN DESIGNATION RULE 41E	WHEEL MFR	DATE MANUFACTURED	WHEEL SERIAL NUMBER		WHEEL OVERHEATED	
<input type="text"/> <input type="text"/> <input type="text"/> <input type="text"/>	<input type="text"/> <input type="text"/>	Month Year <input type="text"/> <input type="text"/> <input type="text"/> <input type="text"/>	<input type="text"/> <input type="text"/> <input type="text"/> <input type="text"/> <input type="text"/> <input type="text"/> <input type="text"/> <input type="text"/>		O-Old N-New R-Recent <input type="text"/>	
31 32 33 34	35 36	37 38 39 40	41 42 43 44 45 46 47 48		49	
REPORTING RAILROAD ACI NO.	FAILURE CAUSED DERAILMENT Y-YES N-NO	WHEEL TYPE	Brake Shoe Standard To Car		<input type="text"/>	
<input type="text"/> <input type="text"/> <input type="text"/> <input type="text"/>	<input type="text"/>	1W <input type="text"/> <input type="text"/> 2W W HW	57		<input type="text"/>	
50 51 52 53	54	55 56	58		58	
SHOW LOCATION OF DEFECT IN RED ON ALL THREE VIEWS ON SKETCHES BELOW						
			59 <input type="text"/> 60 <input type="text"/> 61 <input type="text"/> 62 <input type="text"/> DO NOT USE			
FRONT	Overheat in inches measured as shown <input type="text"/>	BACK				

Name of Reporting Road _____
 Repair Point _____ Date _____
 Chief Mechanical Officer _____

One Copy Of This Report, Completely Filled Out, Must Be Sent By The Chief Mechanical Officer To: Mr. B. C. Reber, Secretary, Mechanical Division, Association of American Railroads, American Railroads Building, Washington D.C. 20036.

FIGURE 2.2. MD-115 DEFECTIVE WHEEL REPORT.

RAIL EQUIPMENT ACCIDENT/INCIDENT REPORT

1. NAME OF REPORTING RAILROAD		1a. Alphabetical Code		1b. Railroad Accident/Incident No.	
2. NAME OF OTHER RAILROAD INVOLVED IN TRAIN ACCIDENT/INCIDENT		2a. Alphabetical Code		2b. Railroad Accident/Incident No.	
3. NAME OF RAILROAD RESPONSIBLE FOR TRACK MAINTENANCE (single entry)		3a. Alphabetical Code		3b. Railroad Accident/Incident No.	
4. U.S. DOT-ARR GRADE CROSSING IDENTIFICATION NUMBER		5. DATE OF ACCIDENT/INCIDENT month day year		6. TIME OF ACCIDENT/INCIDENT am <input type="checkbox"/> pm <input type="checkbox"/>	
7. TYPE OF ACCIDENT/INCIDENT (insert number in each box, single entry) 1. Derailment 3. Rear end collision 5. Rolling collision 7. Rail-Hwy crossing 9. Obstruction 11. Fire or violent rupture 12. Other (specify) 2. Head on collision 4. Side collision 6. Broken train collision 8. RR grade crossing 10. Explosion-Detonation					
HAZARDOUS MATERIALS (number of)					
8. CARS CARRYING		9. CARS DAMAGED OR DERAILED		10. CARS WHICH RELEASED HAZ. MAT.	
LOCATION					
12. DIVISION		13. NEAREST STATION		14. MILEPOST (no reserve mile)	
15. STATE (two letter code) CODE					
ENVIRONMENTAL CONDITIONS					
16. TEMPERATURE (specify if mixed) °F		17. VISIBILITY (single entry) 1. Dism 3. Dust 2. Day 4. Dark		18. WEATHER (single entry) 1. Clear 2. Cloudy 3. Rain 4. Fog 5. Sleet 6. Snow	
OPERATIONAL DATA					
19. METHOD (place X in appropriate box(es))					
1. <input type="checkbox"/> Manual block		4. <input type="checkbox"/> Automatic block		7. <input type="checkbox"/> Yard rules	
2. <input type="checkbox"/> Interlocking		5. <input type="checkbox"/> Traffic control		8. <input type="checkbox"/> Time table	
3. <input type="checkbox"/> Cab signal		6. <input type="checkbox"/> Auto. train stop		9. <input type="checkbox"/> Radio	
10. <input type="checkbox"/> Auto. train control		11. <input type="checkbox"/> Verbal permission		12. <input type="checkbox"/> Train orders	
13. <input type="checkbox"/> Other (specify)					
20. SPEED (recorded speed, if available) Est. MPH Recorded MPH		21. TRAIN NUMBER		22. TIME TABLE DIRECTION 1. North 2. South 3. East 4. West	
EQUIPMENT					
23. TRAILING TONS (gross weight, including power units)		24. TYPE OF EQUIPMENT CONSIST (single entry) 1. Freight train 3. Mixed train 2. Passenger train 4. Work train		25. WAS THE EQUIPMENT IDENTIFIED BY ITEM 24 UNATTENDED? 1. Yes 2. No	
26. TRACK NUMBER OR NAME		27. FRA TRACK CLASSIFICATION		28. ANNUAL TRACK DENSITY (gross tons in million)	
29. PRINCIPLE CAR/UNIT (1) First involved (derailed, struck, striking, etc.) (2) Causing (mechanical failures)		29a. Inroad end Number		29b. Position in Train	
30. LOCOMOTIVE UNITS (no. of)		30a. Head End		30b. Cars (no. of)	
		30c. Mid Train		30c. Labeled	
		30d. Rear End		30c. Empty	
		30e. Manual		30c. Freight	
		30f. Remote		30c. Pass.	
		30g. Manual		30c. Freight & Pass.	
		30h. Remote		30c. Caboose	
(1) Total in Train				(1) Total in Equipment Consist	
(2) Total Derailed				(2) Total Derailed	
PROPERTY DAMAGE (estimated cost, including labor, to repair or replace)					
31. EQUIPMENT DAMAGE (to be reported for this equipment consist only)			32. TRACK, SIGNAL, WAY AND STRUCTURE DAMAGE (to be reported by railroad in item 3 only)		
ACCIDENT/INCIDENT CAUSE CODE					
33. PRIMARY CAUSE		34. CONTRIBUTING CAUSE		37. If no code available, explain cause.	
CASUALTIES					
35. NUMBER OF PERSONS INJURED		36. ESTIMATED TOTAL DAYS OF ABILITY		38. NUMBER OF FATALITIES	
CREW (no. of)					
41. ENGINEER		43. CONDUCTOR		45. ENGINEER	
42. FIREMAN		44. BRAKEMAN		46. CONDUCTOR	
				Hrs: Min:	
47. TYPES NAME AND TITLE		48. SIGNATURE		49. DATE	
50. NARRATIVE DESCRIPTION - Describe the cause, nature and circumstances of accident/incident					

FIGURE 2.3. ACCIDENT/INCIDENT REPORT FORM.

The purpose of monitoring the impact of the proposed rule change on wheel removals, failures and accidents/incidents is primarily to detect significant increases in the number of thermally damaged wheels in service or the number of wheel thermal damage related accidents. This has been accomplished by the use of control charts for each variable of interest. The control chart is a plot of the data over the relevant period of time. Control limits are established to detect the occurrence of a significant change in process average. Control limits may be set for a variety of occurrences. For example, there may be limits for a single point, for two consecutive points, for three consecutive points, etc. The limits in this report are the 95% confidence intervals for one, two and three consecutive quarters.

2.4.1 Car Maintenance Cost Data Base

Figure 2.4 shows the the trend for the rate of wheel removals due to discoloration (why made code 89 from Field Manual of the AAR Interchange Rules) per 10,000 active cars (an active car is defined as a car which moved a minimum of 250 miles in the quarter). This average rate of removals is approximately 175 per 10,000 active cars per quarter. The rate went out of control during the first quarter of 1983 but has settled back into statistical control.

**RATE OF WHEEL REMOVALS DUE TO DISCOLORATION
FROM THE CAR MAINTENANCE COST DATA BASE - MAY, 1985
NUMBER OF WHEELS REMOVED 10,000 ACTIVE CARS**

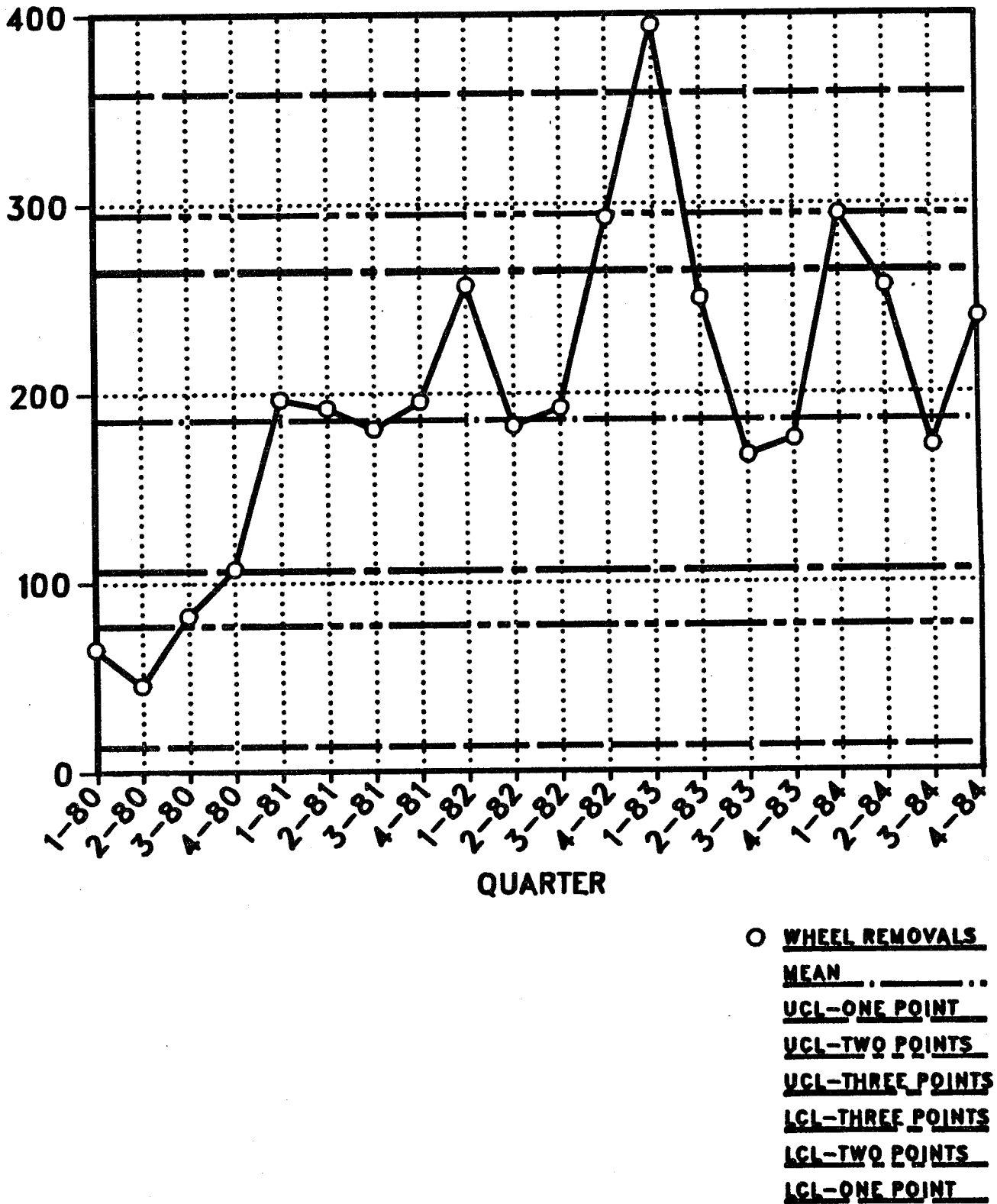


FIGURE 2.4. RATE OF WHEEL REMOVALS PER 10,000 CARS DUE TO DISCOLORATION.

The trend for the rate of wheel removals per million car miles due to discoloration is shown in Figure 2.5. The trend is very similar to the previous figure.

The rate of wheel removals per 10,000 active cars due to thermal damage is shown in Figure 2.6.

The why made codes from the Field Manual of the AAR Interchange Rules are:

- 66-flange cracked or broken,
- 68-rim cracked or broken,
- 69-thermal cracks with overheating,
- 74-thermal cracks, and
- 83-cracked or broken plate.

This chart indicates an average of approximately 22 wheels removed per 10,000 active cars per quarter due to thermal damage. The rate of wheel removals due to thermal damage has been quite low in the last four quarters.

The rate of wheel removals per million car miles due to thermal damage is shown in Figure 2.7. This chart is very similar in all respects to the previous figure.

**RATE OF WHEEL REMOVALS DUE TO DISCOLORATION
FROM THE CAR MAINTENANCE COST DATA BASE - MAY, 1985**
RATE OF WHEEL REMOVALS PER MILLION CAR MILES

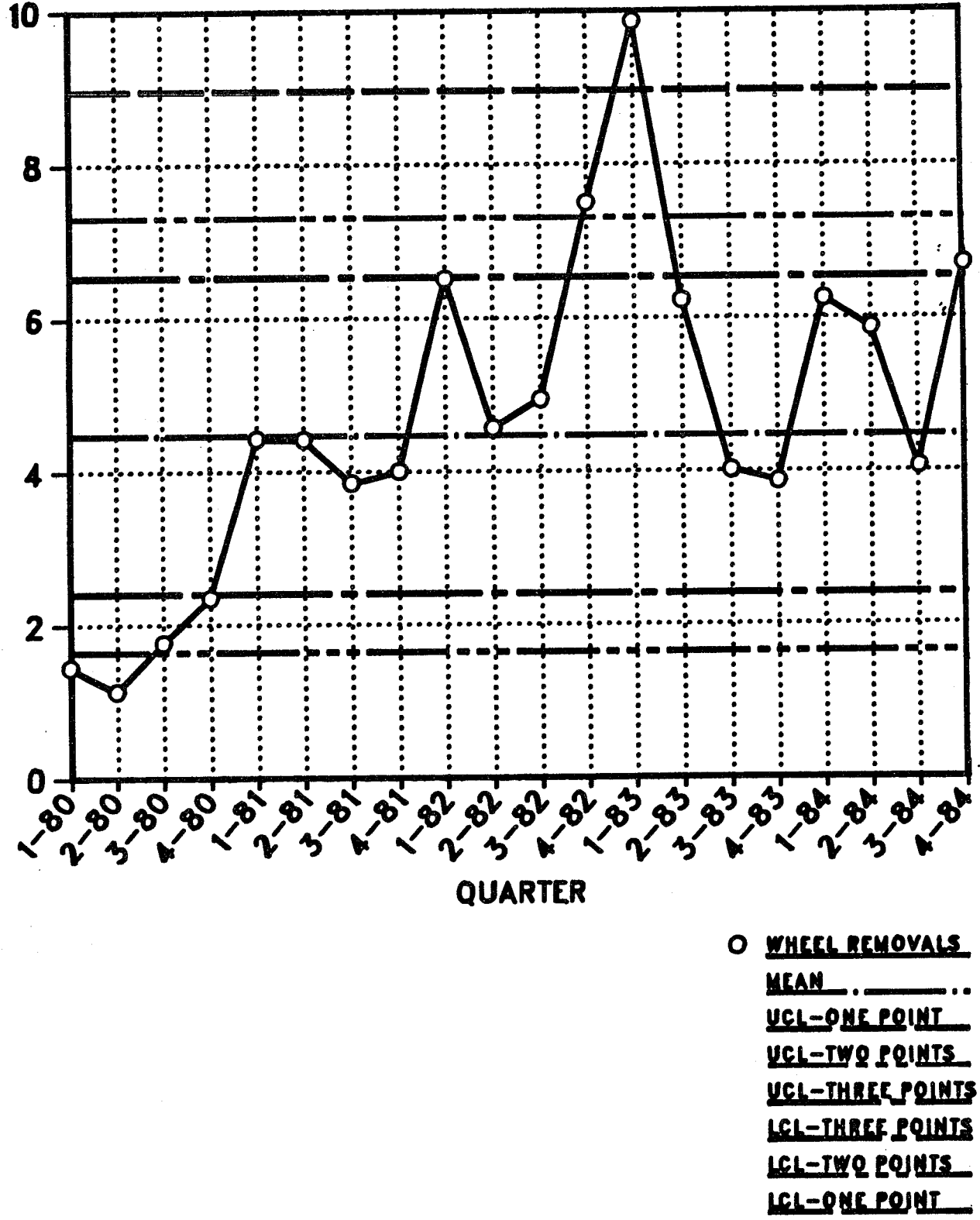


FIGURE 2.5. RATE OF WHEEL REMOVALS PER MILLION CARS DUE TO DISCOLORATION.

**RATE OF WHEEL REMOVALS DUE TO THERMAL DAMAGE
FROM THE CAR MAINTENANCE COST DATA BASE – MAY, 1985**

RATE OF WHEEL REMOVALS PER 10,000 ACTIVE CARS

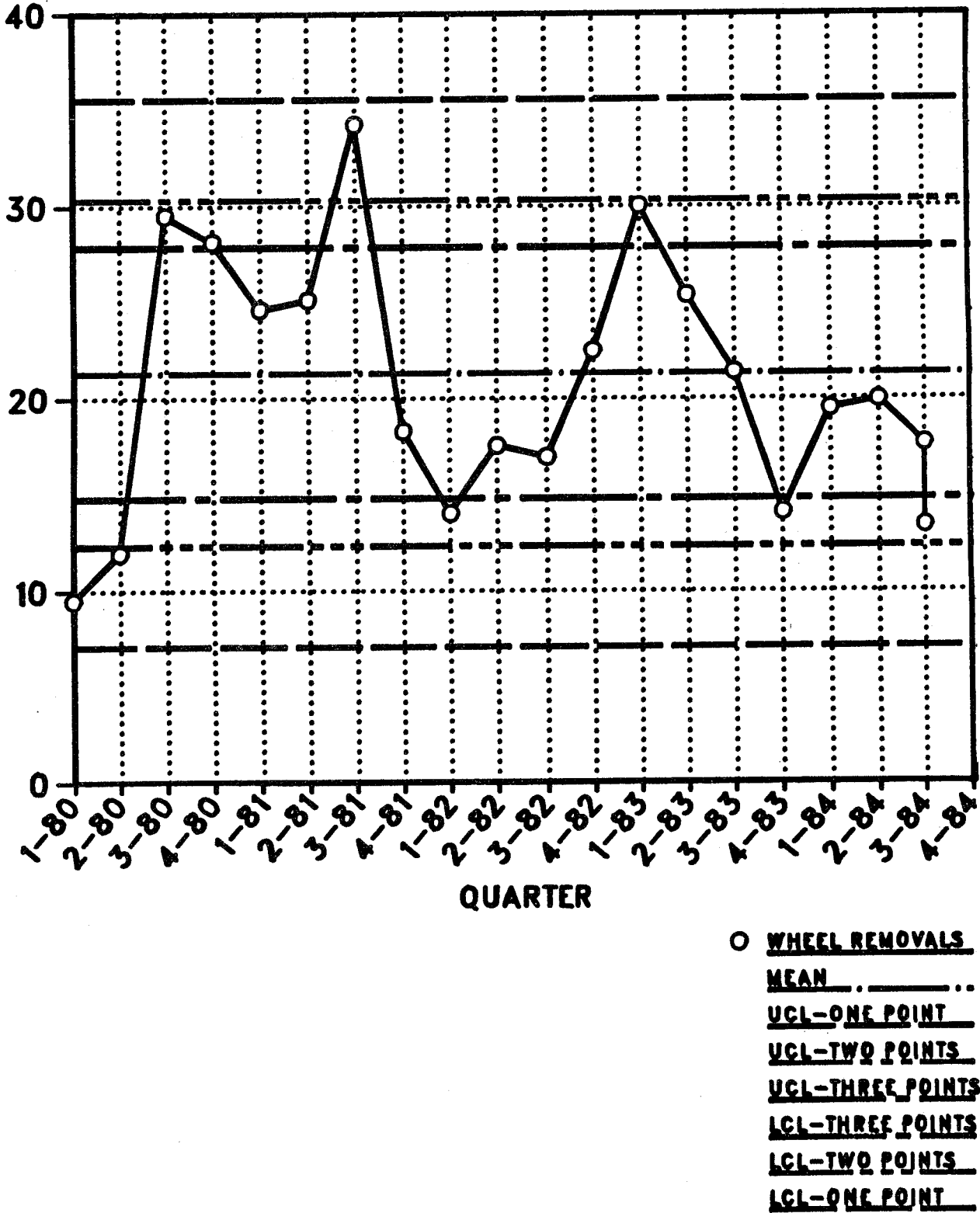


FIGURE 2.6. RATE OF WHEEL REMOVALS PER 10,000 CARS DUE TO THERMAL DAMAGES.

**RATE OF WHEEL REMOVALS DUE TO THERMAL DAMAGE
FROM THE CAR MAINTENANCE COST DATA BASE - MAY, 1985**

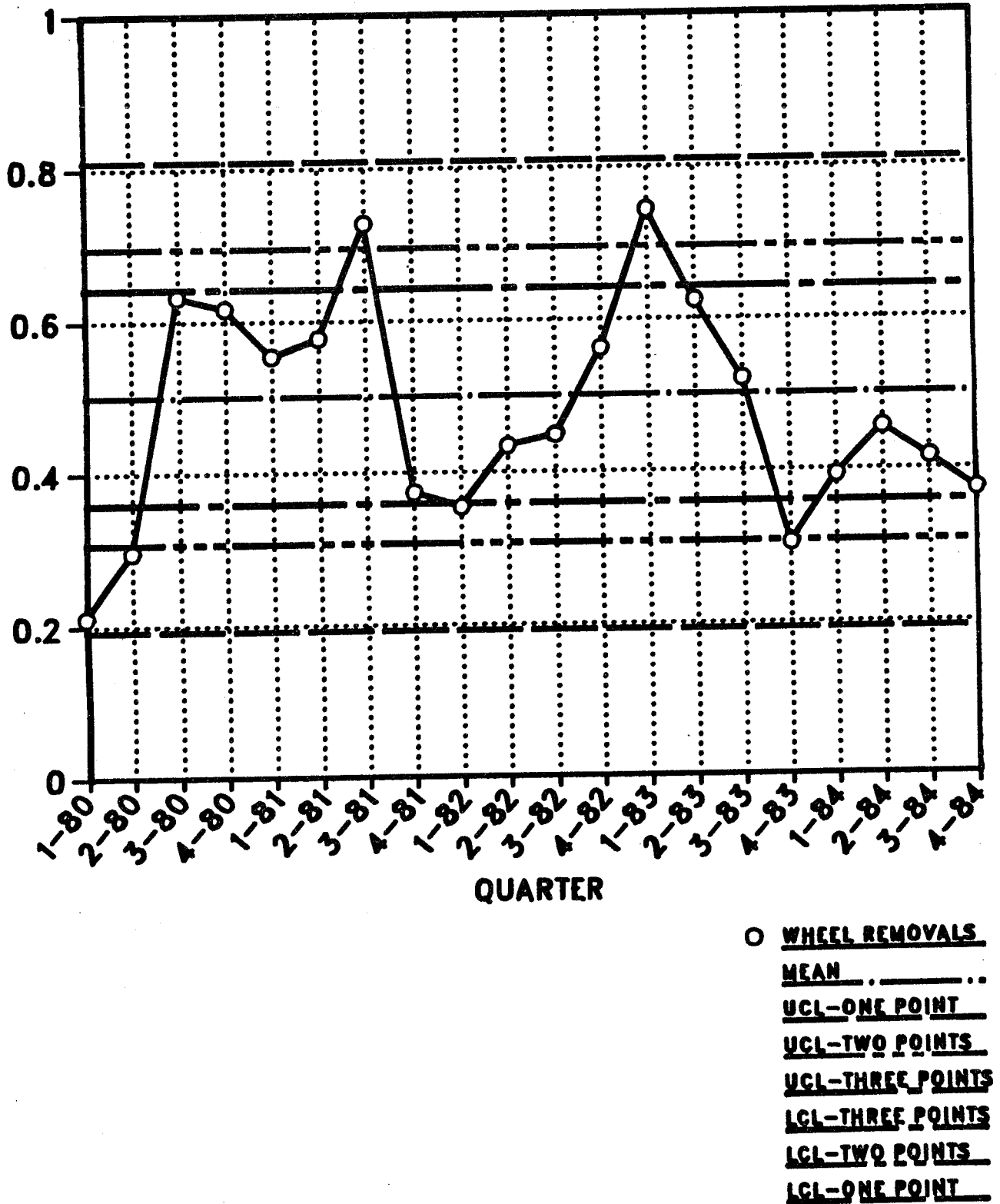


FIGURE 2.7. RATE OF WHEEL REMOVALS PER MILLION CARS DUE TO THERMAL DAMAGE.

2.4.2 The Car Repair Billing System Data Base

The rate of wheel removals per billion ton miles due to thermal damage is presented in Figure 2.8. This shows a very high rate of removals during the period from the first quarter of 1982 through the first quarter of 1983. The rate of removals for the last seven quarters suggests the rate of removals due to thermal damage has shifted dramatically. The reduction appears to be on the order of 2.5 wheels per billion ton-miles.

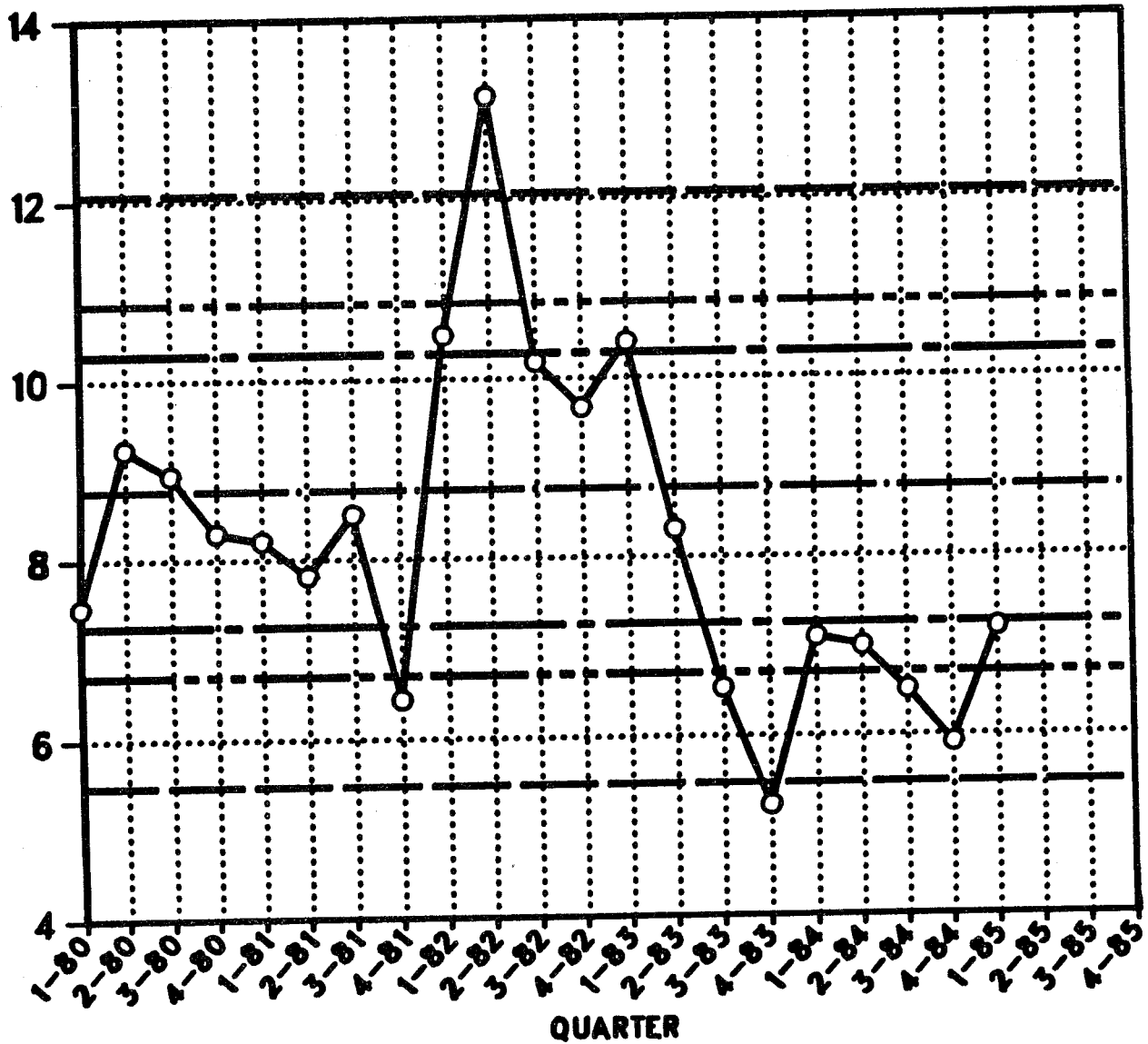
The rate of wheel removals per billion ton-miles due to discoloration is presented in Figure 2.9. This shows a very high rate of removals during the period from the first quarter of 1982 through the first quarter of 1983. The rate of removals then falls back into statistical control temporarily. However, the rate has been quite variable since. The average removal rate since the first quarter of 1981 is above 120 wheels per billion ton-miles.

2.4.3 The AAR Wheel Failure Data Base

The trend in the rate of wheel failure reports submitted to the AAR per billion ton-miles is shown in Figure 2.10. Only those failure reports which indicate an associated derailment are included. This figure shows a great deal of variation in these data. However, the rate has for the most part remained in statistical control. A large amount of the variation is due to the seasonality and the overall downward trend displayed by these data.

FOR THE RATE OF WHEEL REMOVALS DUE TO THERMAL DAMAGE
FROM THE CAR REPAIR BILLING DATA BASE - MAY, 1985

RATE OF WHEELS REMOVALS PER BILLION TON MILES



○ WHEEL REMOVALS
 MEAN
 UCL-ONE POINT ..
 UCL-TWO POINTS ..
 UCL-THREE POINTS ..
 LCL-THREE POINTS ..
 LCL-TWO POINTS ..
 LCL-ONE POINT ..

FIGURE 2.8. RATE OF WHEEL REMOVAL PER BILLION TON MILES DUE TO THERMAL DAMAGE.

FOR THE RATE OF WHEEL REMOVALS DUE TO DISCOLORATION
FROM THE CAR REPAIR BILLING DATA BASE - MAY, 1985

RATE OF WHEELS REMOVED PER BILLION TON MILES

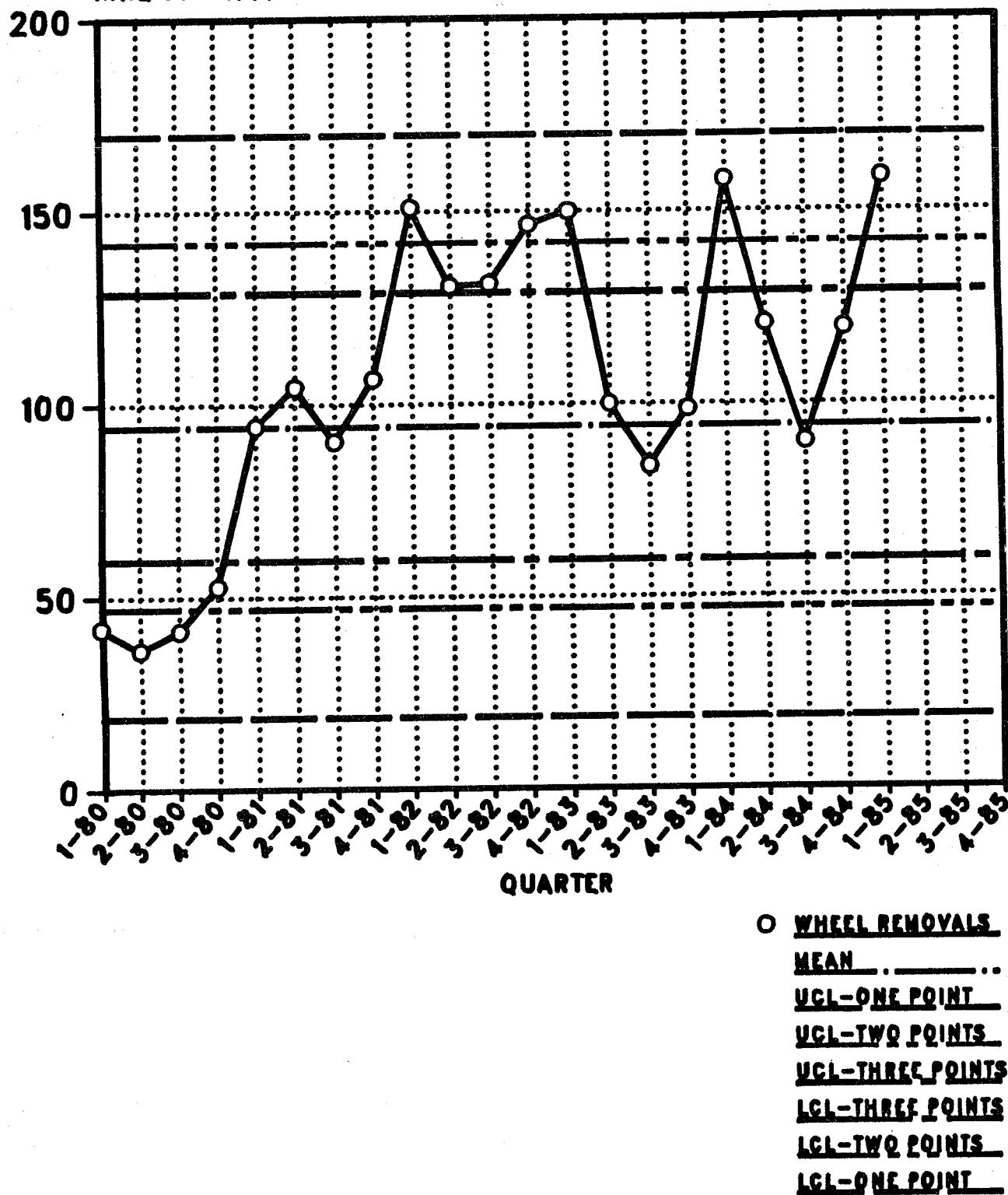


FIGURE 2.9. RATE OF WHEEL REMOVAL PER BILLION TON MILES DUE TO DISCOLORATION.

**FOR THE RATE OF WHEEL FAILURE REPORTS
DUE TO THERMAL DAMAGE CAUSING A DERAILMENT
FROM THE AAR WHEEL FAILURE DATA BASE - SEPTEMBER, 1985
RATE OF WHEEL FAILURES PER BILLION TON MILES**

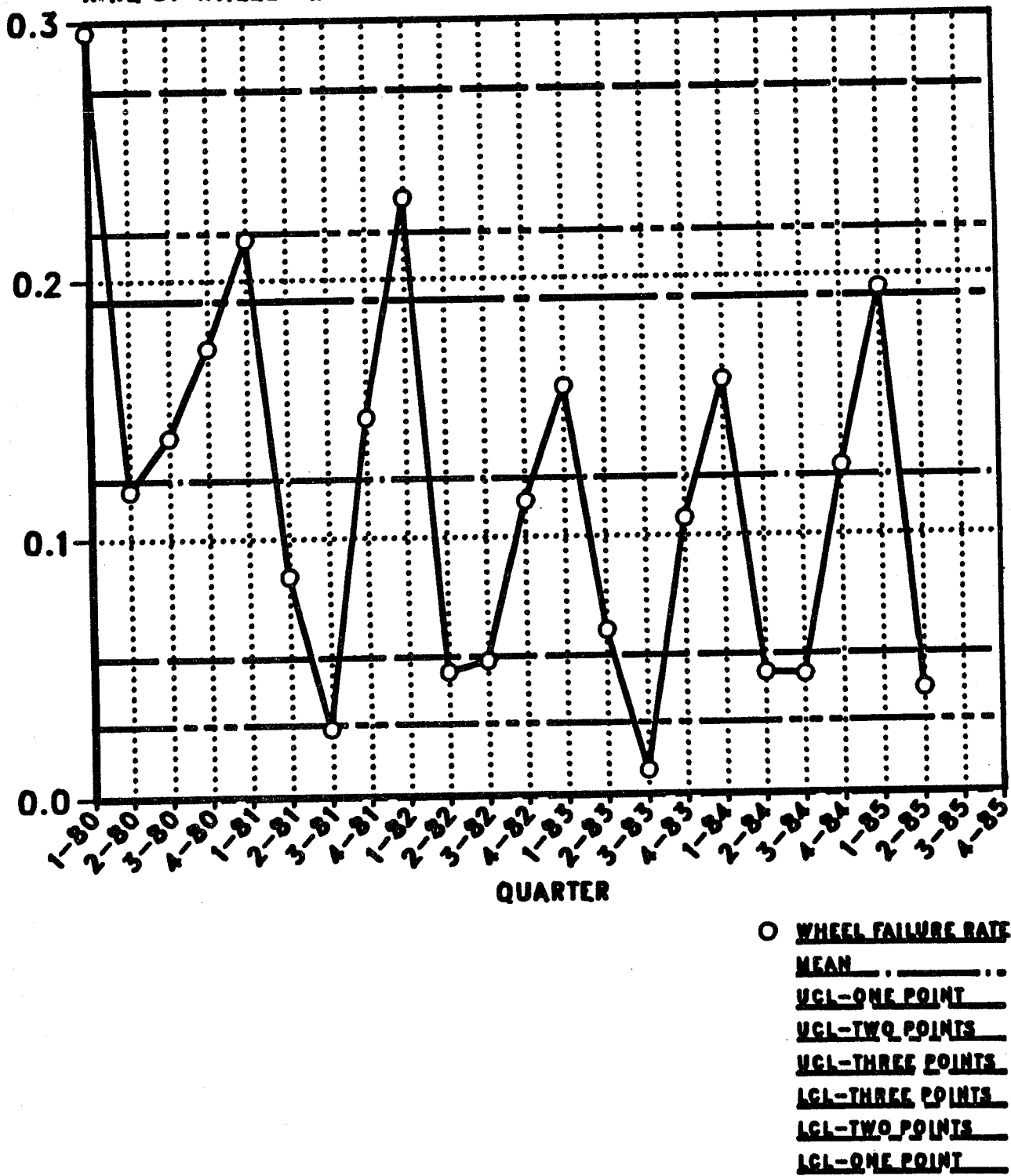


FIGURE 2.10. RATE OF DERAILMENT RELATED WHEEL FAILURE REPORTS PER BILLION TON MILES.

The monitoring of AAR Wheel Failure Reports (Form MD-115) has continued since the inception of Task Order 6. A full year's data have been gathered for 1984. During 1984, data were collected on 74 derailments in which 77 wheels fractured from thermal cracks. A tabulation of the 1984 data from Appendix 2.1, shows that 86 percent of the fractured wheels were of straight-plate design. Additionally, 58 percent of the wheels showed either no discoloration or less than 4-inches of discoloration at the time of failure. All of the data from AAR MD-115 forms to date are given in Appendices 2.0, 2.1, and 2.2 for 1983, 1984, and 1985 respectively.

M.R. Johnson has taken the data and attempted to normalize the failures per 100 billion ton miles. This analysis, shown in Figure 2.11 suggests the following:

1. The failure rate of nondiscolored curved plate wheels is an order of magnitude less than that of nondiscolored straight-plate wheels.
2. The failure rate of discolored curved plate wheels is less than, but of the same order of magnitude, as that of nondiscolored straight-plate wheels.
3. The failure rate of discolored straight-plate wheels is more than an order of magnitude greater than that of nondiscolored straight-plate wheels.

OVERVIEW OF DISCOLORED/NONDISCOLORED; HIGH STRESS/LOW STRESS
WHEEL FAILURE PROBLEM

Assumptions: 24.4 billion car miles per year (1983 data) implies 196 billion wheel miles per year

Wheel Failures 1/1/84 thru 3/31/85:
 11 curved plate nondiscolored
 4 curved plate discolored
 51 straight plate nondiscolored
 40 straight plate discolored

Terminology: Wheel failures/100 billion wheel miles

Total Failures 106/245

	<u>Curved Plate</u>	<u>Straight Plate</u>	
Assume 75% wheel miles curved plate, 25% straight plate:	15/184	91/61	
	<u>Nondiscolored</u>	<u>Discolored</u>	<u>Nondiscolored</u> <u>Discolored</u>
Assume 96% of wheel miles nondiscolored 4% discolored:	11/176.6	4/7.4	51/58 40/3
Failure rates per 100 billion wheel miles:	6.2/100B	54/100B	88/100B 1330/100B

FIGURE 2.11. OVERVIEW OF THE WHEEL FAILURE PROBLEMS.

2.4.4 FRA Accident Data Base

The trend in the rate of FRA reportable accidents caused by thermally damaged wheels is shown in Figure 2.12. The rate of accidents due to thermally damaged wheels has declined steadily since 1980. This trend has continued throughout 1984. The increase in the fourth quarter of 1984 follows the seasonal trend seen in these data since 1980.

The FRA causes codes which are considered to be related to thermal damage are the following:

- 460 - broken flange,
- 461 - broken rim,
- 462 - broken plate,
- 463 - broken hub, and
- 468 - thermal damage.

Any accidents involving locomotives are not included in these data.

To monitor the accident rate more closely, on a quarterly basis, the AAR must have access to the FRA Accident Data Base on a more frequent than annual basis. A mechanism needs to be established to provide this data to the AAR on a quarterly or monthly basis. This will permit the presentation of control charts in a more timely fashion.

FOR THE NUMBER OF ACCIDENTS CAUSED BY THERMALLY DAMAGED WHEELS FROM THE FRA ACCIDENT DATA BASE - MAY, 1985

RATE OF ACCIDENTS PER BILLION TON MILES

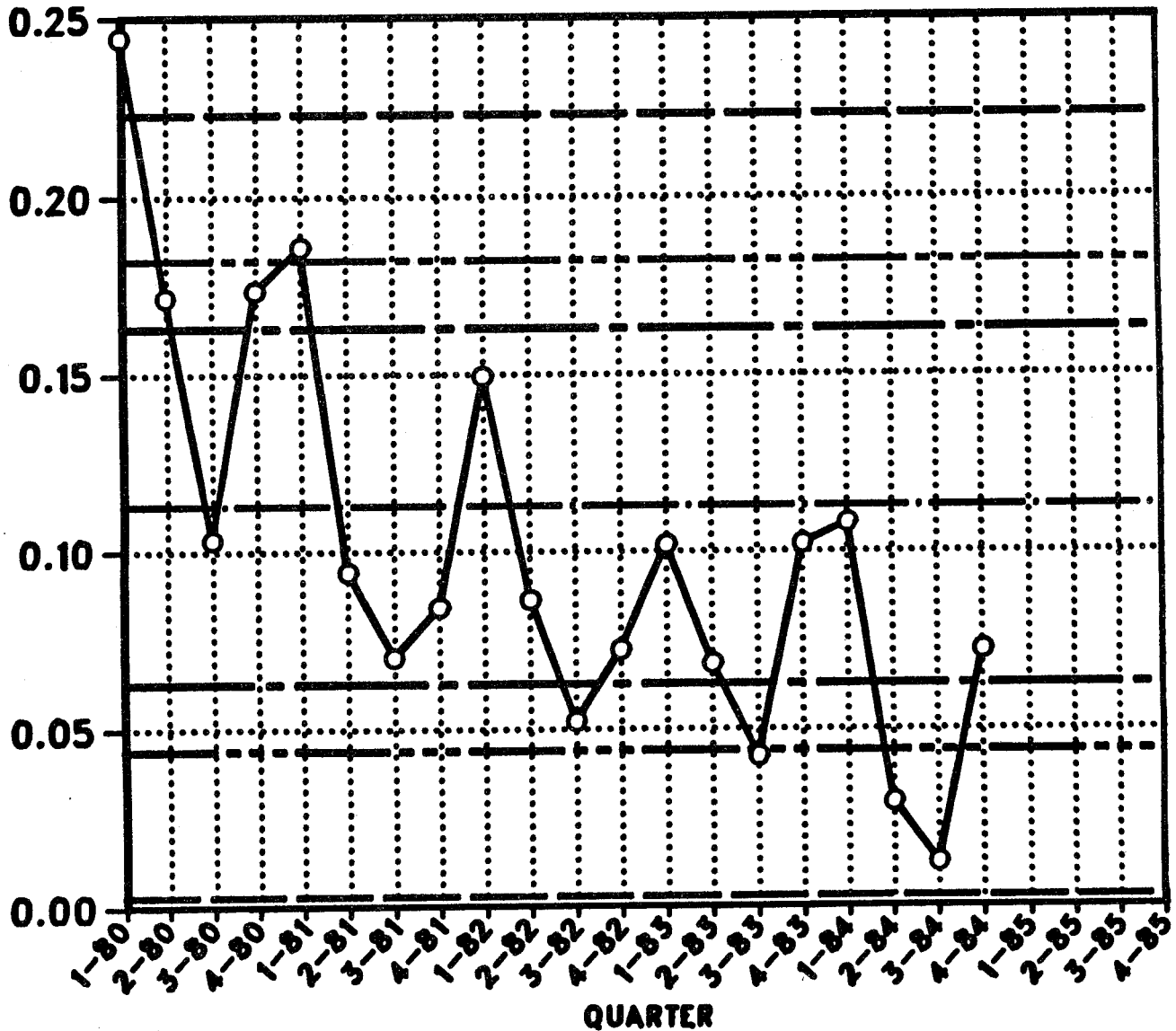


FIGURE 2.12. TREND IN THE RATE OF REPORTABLE ACCIDENTS CAUSED BY THERMALLY DAMAGED WHEELS.

3.0 PILOT TECHNOLOGY SURVEY (TASK 2)

3.1 CURRENT TASK STATEMENT OF WORK

1. Conduct a pilot technology search project to cover the subject areas of this work statement. It should be consistent with the general approach being proposed for all Transportation Test Center (TTC) projects. Since it may take some time to establish an automated data base for the literature search, consideration of using a previous data base such as the Railroad Research Information System or using manual means should be included. Reports and other documentation are only part of the sources that should be considered. Experts in the technology field should also be included.
2. Conduct a literature search, make contact with other experts to identify appropriate sources, and make a list of pertinent research reports or information sources that could support the research project.
3. Establish a small library of applicable documents for this particular project. Conduct a limited but comprehensive evaluation of the research.
4. Briefly, but concisely, document the results of that evaluation, noting which research will be used in the research project and why the other information could not be used.

5. Keep records of the time spent, the cost of conducting the literature search, and research result obtained for this pilot project. Prepare a short letter report on the effectiveness of the literature search, problems encountered, and recommendations for improvement. The report should also include estimates of cost savings on research that was not needed because of the use of prior research. Submit copies of the report to the Contracting Officer, Contracting Officer's Technical Representative, Acting Director of Research and Development, FRA and Senior Assistant Vice President, Research and Test Department, AAR.

3.2 MAJOR FINDINGS AND CURRENT STATUS

3.2.1 Definition and Purposes of Technology Survey

Technical Task 2 of this project is to conduct a survey of technological literature by (i) searching the available literature on this and related subjects, and (ii) contacting experts who have made or are currently making contributions in the field of wheel failure mechanisms. A small library of applicable documents for this particular project will be established at the Transportation Test Center. This small library will include a computerized information retrieval system with each listing accompanied by a special annotation prepared by the technical staff associated with the project. This will be performed after a comprehensive evaluation of the various documents compiled in the small library.

3.2.2 Initial Survey

A file search on Railroad Wheels has been acquired from the Railroad Research Information System. The following key phrases were used by the RRIS for this search:

wheel residual stresses	wheel thermal stress
crack propagation in wheel	finite element analysis of wheels
wheel fracture	plasticity in wheels
wheel designs	wheel metallurgy
mechanical properties of wheels	

The RRIS Field Search was then compared with the TTC Technical Library holdings to determine items that are currently on hand. Other items from the Field Search that seemed relevant and promising were identified for acquisition. These items were located and purchased, and gathered together into a separate library of research literature for this project.

The project personnel then conducted a limited, yet comprehensive evaluation of this "separate library" to decide which documents will be used. They also contacted appropriate experts in this technology field to become acquainted with on-going activity elsewhere. The rationale for their selection and organization of information is described in Section 3.2.4 below.

3.2.3 Computerized Information Retrieval System

The references, details, subject classification and special notations made by the project technical staff were then entered into the TTC Computerized Information Retrieval System so that research personnel could rapidly sort through this special "library" and locate references especially pertinent to their particular technical tasks.

The computer program used at the TTC to establish this Information Retrieval System is the DATATRIEVE Program. Selected capabilities of this system and user guidelines are provided in Appendix 2.1.

3.2.4 Select Bibliography Criteria and Organization

The criteria for selecting and organizing information from the preliminary technology survey follow.

3.2.4.1 Selection Criteria

The preliminary criteria for selecting a particular reference to include in this select bibliography was direct applicability to at least one of the technical tasks of the FRA Wheel Program. In addition, certain references of indirect applicability were selected if they contained good fundamental information or technology of general applicability to the research program.

3.2.5 Format Evaluation

The bibliographic reference details and special notations that appear in the listing are explained in the following.

3.2.5.1 TTC Document Number

The initial number or alphanumeric string is given in the upper left corner of each reference entry in the TTC Library assigned document number. This number serves as the "license plate" to identify a particular reference. Typical document numbers of various character types are: 100 000, 200 000, 300 000, FRA, etc.

3.2.5.2 Standard Reference Detail

Following the document number, a standard identification of the reference by article, title, author(s), volume or periodical name and number, publishing organization, date and page number is listed.

3.2.5.3 Special Classification Notes

Following the reference identification are selected subject categories and key words or phrases.

The first phrase listed is the primary subject group selected by the reviewing research personnel for classifying this particular reference. The ten primary subject groups established are:

1. Service Evaluations
2. Experimental Stress Studies
 - a. Nondestructive
 - b. Semidestructive
 - c. Destructive
3. Tread Contact Stress, Cracks or Hot Spots
4. Brake Shoe Studies
5. Material Properties
6. Crack Propagation
7. Finite Element Simulation
8. Laboratory Simulation
9. Track Tests
10. General Applicability

After the primary subject, the primary program technical task number to which the reference applies is listed. Then the specific wheel type(s) and class of steel (if available) are listed. If there are any secondary subjects to which the reference may apply, these are also listed in decreasing order of applicability. Closing out this group of key phrases are any pertinent ones listed on the standard library reference card.

3.2.5.4 Special Annotation

On some of the reference listings, a special abstract or annotation is provided by research personnel. This brief annotation focuses primarily on the purposes and conclusions of the particular refer-

ences that are especially applicable to the Wheel Failure Program. They sometimes contain an evaluation of the pertinence and quality of some aspect of work cited but generally do not attempt to abstract the entire document.

3.2.6 Other Selected References

The annotated bibliography is supplemented by the selected references that either have not been specially annotated or are judged to be secondary, but of general interest to the program.

3.2.7 Annotated Listings

Annotated listing of selected references according to the order of assigned numbering system is presented in Appendix 2.2.

Listings of annotated references retrieved using TTC's computerized information retrieval system under key words, "THERMAL", "STRESS", "CRACK", "FATIGUE", AND "BRAKING" are presented in Appendix 2.3.

3.2.8 Applications of Pilot Technology Survey to Wheel Failure Mechanisms Program

Because of the annotation processes the program's principal investigators were required to review each of the approximately 200 references, a review of the status of current technology more extensive than is normally undertaken. The benefits of the study are demon-

strated, however, in the fact that fracture toughness and fatigue crack growth investigations were, for example, deemed unnecessary since sufficient data existed in the literature.

3.3 WORK REMAINING

This task has been completed with the exception of new literature which is published or presented during the remainder of the program.

3.4 SCHEDULES

Task 2 is complete except for the addition of future sources.

4.0 PERTINENT MATERIAL PROPERTIES (TASK 3)

4.1 CURRENT TASK STATEMENT OF WORK

The AAR shall determine the cyclic behavior of Class B, C, and U wheels at elevated temperatures and for Class C wheels at ambient temperatures. AAR shall determine the effect of martensite on thermal cracking of the classes of wheels selected for this study. In order to make this determination, the AAR shall construct an appropriate test rig. Four wheels of each class shall be tested. AAR shall complete tests to characterize wheel materials in terms of their ability to arrest a running crack. A minimum of 12 specimens of each class shall be tested. The AAR, in order to make statistical distribution of dangerous wheels among non-discolored wheels in service, shall saw-cut a minimum of 100 wheels. Standardized test data from cooperating laboratories will also be analyzed.

A proposed modification (Stone to Gannett of 1/85) of the lab materials test plan was designed to enhance the applicability (to variable strain and temperature cycles) of elevated-temperature, mechanical property data, which is more representative of actual wheel braking cycles, particularly at slow strain rates.

4.2 MAJOR FINDINGS/CURRENT STATUS

Presently, material properties tests have been completed on the three wheel materials at the four temperatures of interest (using a

strain rate of 0.002 Sec⁻¹). The remainder of this section discusses the results of the testing.

4.2.1 Elevated Temperature Cyclic Behavior Task

The data gathered in the Cyclic Behavior Task is being used primarily in Tasks 4 and 10 to provide actual stress-strain curves for the temperatures of interest in the elastic/plastic finite element analyses.

Low cycle fatigue tests were conducted on Classes B, C, and U wheel materials at ambient and elevated temperatures. These tests have been completed and results were presented at the 1985 ASME spring annual Railroad Transportation meeting and a copy of this report is attached as Appendix 4.1.

It was generally observed that cyclic performance deteriorated with increasing temperature as shown in Table 4.1 and Figure 4.1. The heat-treated Classes B and C materials performed better than the nonheat-treated Class U material. The differences in carbon level had a noticeable effect on fatigue performance. Conclusions derived from these tests were that:

1. The cyclic fatigue lives at all temperatures tested converged at strains exceeding one percent.
2. At strains less than one percent, lives are considerably reduced as the test temperature is increased.

TABLE 4.1. FATIGUE PROPERTIES FOR CLASSES B, C, AND U WHEEL STEEL.

Wheel Steel	Temp. °C	σ_f' (ksi)	b	e_f'	c	K' (ksi)	n'
B	25	224	-0.106	0.631	-0.606	243	0.175
B	200	303	-0.156	0.257	-0.595	433	0.263
B	400	196	-0.114	2.590	-0.879	174	0.130
B	600	76	-0.093	0.918	-0.739	77	0.125
C	25	260	-0.111	1.850	-0.721	237	0.154
C	200	222	-0.092	0.147	-0.468	324	0.196
C	400	187	-0.096	8.700	-0.982	152	0.098
C	600	68	-0.075	1.921	-0.828	64	0.091
U	25	180	-0.101	0.528	-0.587	201	0.172
U	200	159	-0.102	0.147	-0.448	246	0.228
U	400	166	-0.118	1.685	-0.771	153	0.153
U	600	81	-0.104	0.762	-0.698	84	0.148

σ_f' -- Fatigue strength coefficient
 b -- Fatigue strength exponent
 e_f' -- Fatigue ductility coefficient
 c -- Fatigue ductility exponent
 K' -- Cyclic strength coefficient
 n' -- Cyclic strain hardening exponent

(1 ksi = 6.8948 MPa)

1. Steady state stress amplitude =

$$K^1 (\text{steady state plastic strain})^{n^1}$$

2. $\frac{\text{Strain range}}{2} = \frac{f^1}{E} (2N_f)^b + e_f^1 (2N_f)^c$

N_f = No. of cycles failures

3. $n^1 = \frac{b}{c}$

4. $k^1 = \frac{F^1}{(e_f^1)^{n^1}}$

FATIGUE LIFE vs TEMP FOR WHEEL STEELS

AT 0.2 % STRAIN AMPLITUDE

7-7

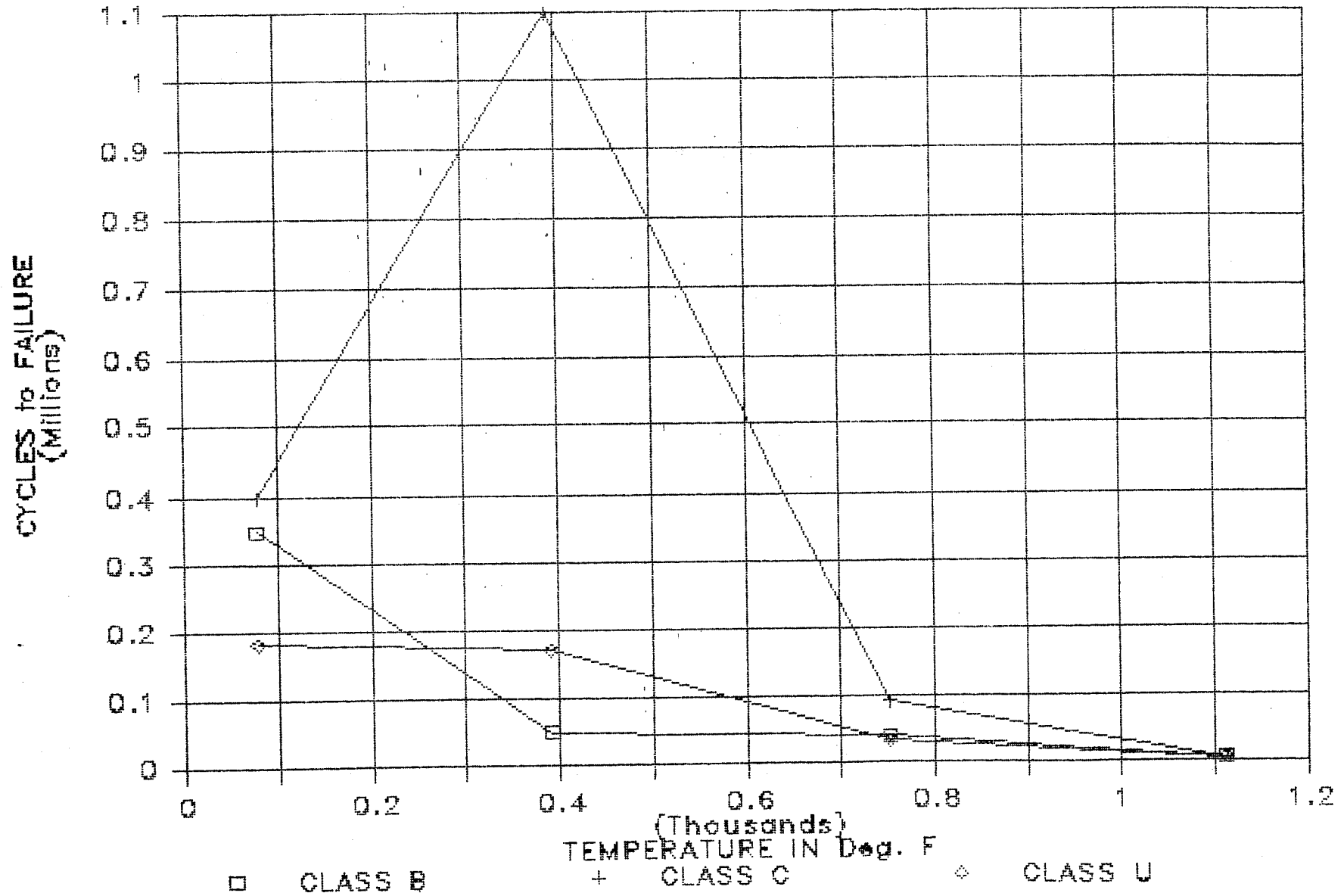


FIGURE 4.1. FATIGUE LIFE VERSUS TEMPERATURE FOR WHEEL STEELS.

3. Differences in material performance are more pronounced at longer lives (low strain amplitudes) than at shorter lives (high strain amplitudes).
4. The heat-treated wheel materials (C and B) exhibit a higher resistance to fatigue than the nonheat-treated U material.
5. The higher carbon C material shows better resistance to fatigue than the lower carbon B material.

4.2.2 Fracture Crack Arrest Tests

The crack arrest fracture toughness (K_{Ia}) properties of Class U and C wheel steels were examined.

The results of this study indicate that the crack arrest fracture toughness of heat-treated Class C wheel steel is somewhat higher than untreated Class U steel at room temperature, and that this difference increases with temperature.

A dependency of K_{Ia} values on test temperature was noted for Class C steel, while Class U steel appeared fairly insensitive to temperature. This difference appears to be related to the effect of inter-lamellar pearlite spacing on crack propagation in the steel.

Based solely on the K_{Ia} data, it may also be concluded that rim heat-treated wheels could arrest larger thermal cracks, prior to unstable propagation, than untreated wheels. The critical flaw size

tolerated would increase with temperature for the Class C wheels. This behavior would not appear in Class U wheels which are tested below 100°C.

A comparison of actual wheel failure data revealing critical flaw size prior to full failure showed fairly good agreement for Class U data, but suggested that predictions for critical flaw size tolerance for the Class C wheels based on K_{Ia} values were too large.

Considering that Class U wheels appear to fail more frequently than Class C wheels, and coupled with the fact that in all wheel classes, pronounced crack arrest is seemingly rare, it is suggested that crack arrest data be modified with some correction factor to more accurately reflect actual service lives. This factor could be based on the ratio of crack initiation fracture toughness to crack arrest fracture toughness.

A complete description of this sub-task and results is given in Appendix 4.2.

4.2.3 Thermal Cracking Test

The purpose of these tests is to develop a laboratory technique to produce thermal cracking in wheels and to evaluate the relative resistance to such cracking of Class B, C, and U wheels. The mechanism for the cracking being studied is the restrained contraction of untempered martensite, which is similar to the mechanism of quench cracking.

First, a localized portion of the wheel tread must be heated to a temperature exceeding 1333°F to obtain some transformation to austenite. Then this localized region must be cooled fast enough for the austenite to transform to martensite. The restraint provided by the unheated remainder of the wheel during subsequent cooling should produce sufficiently high stresses to crack the brittle martensitic region. Accordingly, in the initial portion of this program, an apparatus was constructed and trial runs were conducted with an instrumented wheel.

4.2.3.1 Wheels

All of the wheels for these tests are CJ33 with a parabolic plate. Four Class B, four Class C, and five Class U were designated for these tests. One of the Class U wheels was drilled for the placement of thermocouples in the rim. This wheel is being used for development of the test procedure.

4.2.3.2 Apparatus

A machine was constructed to support the wheel in a vertical position by the bore and to turn it at speeds of 1 rpm and slower. Further, an oxygen-acetylene burner was supported and clamped so that the distance from the torch tip could be adjusted. A steel pan, measuring 10-inches wide by 48 inches long by 11 inches deep, was fitted with a standpipe and drain and placed beneath the wheel so that the lower 9 inches of the wheel was submerged in water. The

make up water was provided by two low pressure nozzles directed at the wheel plate about 12 inches above the water level in the pan.

The trial wheel was fitted with eight 1/16-inch diameter sheathed thermocouples in holes drilled to the mid-tread positions from the back face of the rim. The 1/8-inch diameter holes were centered 1/4, 1/2, and one inch from the tread. After the thermocouples were placed in the holes, steel wool was packed around the thermocouples. The thermocouples were connected to a modified personal computer for data acquisition, storage and printout.

4.2.3.3 Preliminary Results

Several preliminary trials were conducted with about 1/4 of the wheel to determine the gas pressure, torch-tip/wheel proximity, and wheel speed that would result in the desired apparent surface temperature. After this was accomplished, additional preliminary trials were conducted to enhance the quenching of the heated spot. Subsequently, trials were conducted with full rotation of the wheel to determine if cracking would occur. The conditions for these trials were based on the results of the preliminary trials. They were as follows:

1. Rego tip TWP2579-56 - gas pressures of 20 psi oxygen and 10 psi acetylene to provide heat output of about 50,000 Btu/hr.
2. Torch tip to wheel tread distance - 1 inch.

3. Wheel speed about 1/20 rpm or 5 in/min.
4. Water sprays directed at wheel plate and water immersion of lower 9 inches of wheel.

After about 24 revolutions or cycles of heating and cooling, the wheel developed five cracks in the tread. Four of these cracks were in a radial/axial plane about 4 inches long and through and beyond the thermocouple holes. The fifth crack was generally in a radial plane oriented about 45° to the axis and through a one-inch diameter area that had been overheated during one of the preliminary trials. No other cracks were detected. Hardness tests of the of the surface heated by the torch indicated that martensite was probably not produced at the surface in these tests. Thereafter, one of the water sprays was directed at the tread about 3 inches beneath the center of the heated spot. Further trials showed that, with this arrangement, martensite was being produced at the surface. Infrared thermographs showed that the center of the heated spot attained a temperature of 915°C or 1679°F. After five additional heating/cooling cycles with this arrangement, three cracks were produced in areas of the tread not containing discontinuities. These cracks were oriented in the radial-axial plane and are from 1/2 to 1 inch long.

4.2.3.4 Thermal Analysis

For the purposes of selection of test conditions and interpretation

of results, available closed-form transient heat transfer analyses for a moving "hot spot" have been adapted to the Thermal Crack Test Rig conditions.

Figure 4.2 gives the relationships between temperature rise across the hot spot, torch power rating, and wheel rotational speed based on Archard's solution (ASME Wear Control Handbook, p. 135):

$$\Delta T = \frac{2\dot{Q}}{a} \sqrt{\frac{x}{\pi k p c V}}$$

where

\dot{Q} is the torch heating rate in [BTU/HR]

a is the hot spot radius in [FT] = 1/12'

k is the thermal conductivity in $[\frac{\text{BTU}}{\text{HR}\cdot\text{FT}\cdot^{\circ}\text{F}}] = 27.5$

p is steel density in $[\frac{\text{LB}}{\text{FT}^3}] = 489$

c is the thermal diffusivity in $[\frac{\text{BTU}}{\text{LB}\cdot^{\circ}\text{F}}] = 0.1072$

V is the surface velocity in [FT/HR] = $\pi \times 3' \times \text{RPM} \times 60$ M/HR

X is the distance from the leading edge of the hot spot () in the spot) in [FT] = $2a = 2/12'$
($x = 2a$ for ΔT_{MAX})

Perhaps the average temperature rise on the hot spot would be more realistic, but this solution has served as a preliminary guide in selecting torch tips and test specifications.

4.2.4 Effect of Slow Strain Rate

Almost all the monotonic and cycle mechanical property tests con-

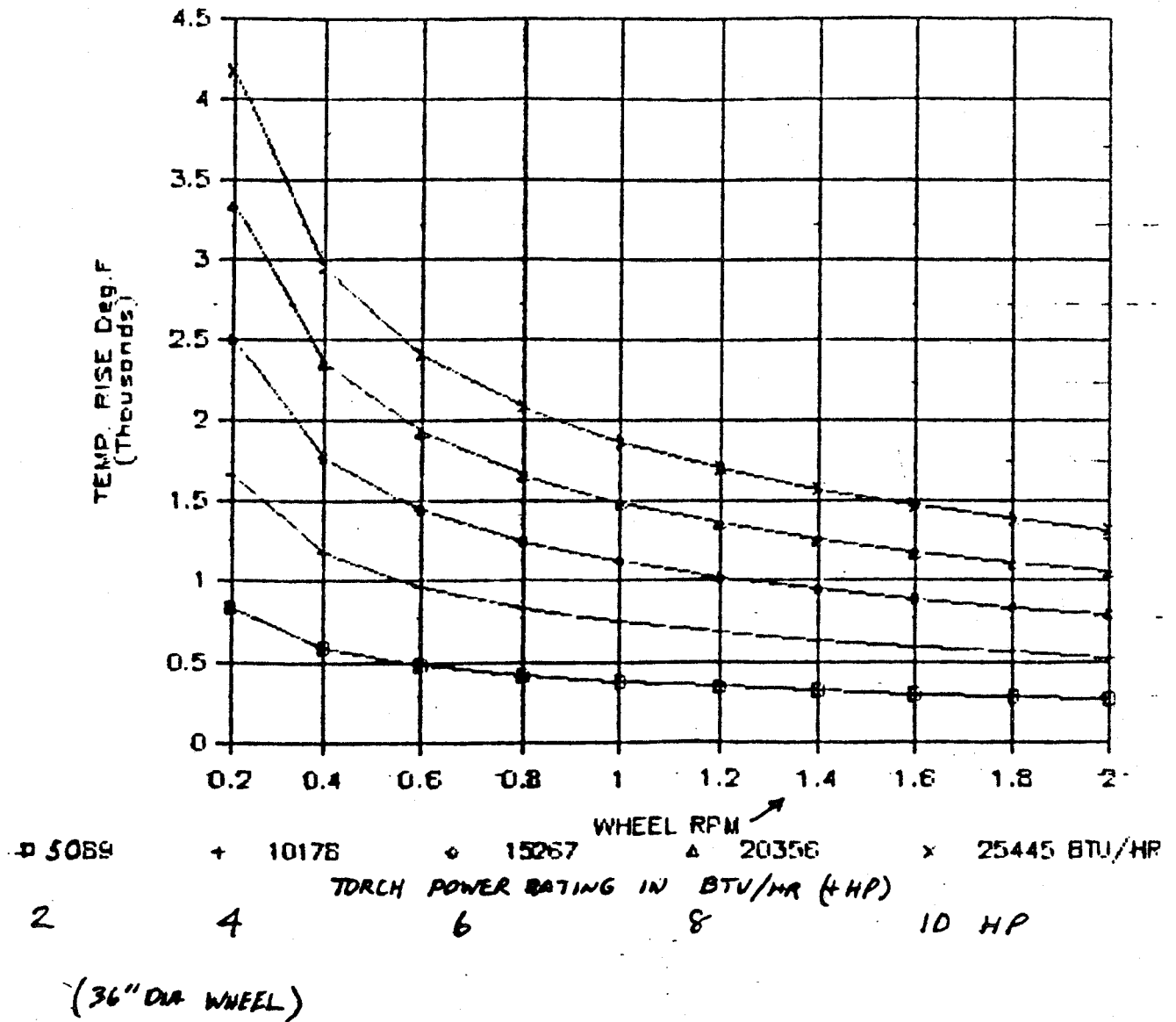


FIGURE 4.2. TEMPERATURE RISE ACROSS 2-INCH DIAMETER HOT SPOT.

ducted to date have been performed at a conventional strain rate of 0.002 Sec⁻¹. However, it has been observed that actual strain rates enforced on the hot rim steel of wheels subjected to prolonged drag braking are usually below 0.000002 Sec⁻¹ or some three orders of magnitude slower than conventional test rates. Therefore, test preparations have begun and more preliminary tests have been conducted to gain some insight into the possible rate sensitivity of wheel steel flow properties (cyclic and monotonic) at elevated temperature.

Preliminary results indicate that a three order of magnitude reduction in strain rate could cause a significant reduction in flow stress, that is, greater than 20% at 400°C (752°F). This indication is based on some cyclic property data obtained recently from Prof. Huseyin Sehitoglu at the University of Illinois and from a monotonic tensile test with step changes in strain rate conducted at AAR Chicago.

The effect of a one order reduction in strain rate on the cyclic 0.2% offset yield was tested by Prof. Sehitoglu at the University of Illinois. An 11% reduction in flow stress at 400°C was observed for a reduction in strain rate of one order of magnitude. No effect of strain rate was seen at 200°C.

The effect of step reduction and subsequent increases in strain rate over four orders of magnitude in a special tension test of Class U steel at 400°C is shown in Figure 4.3 after uniform strain hardening

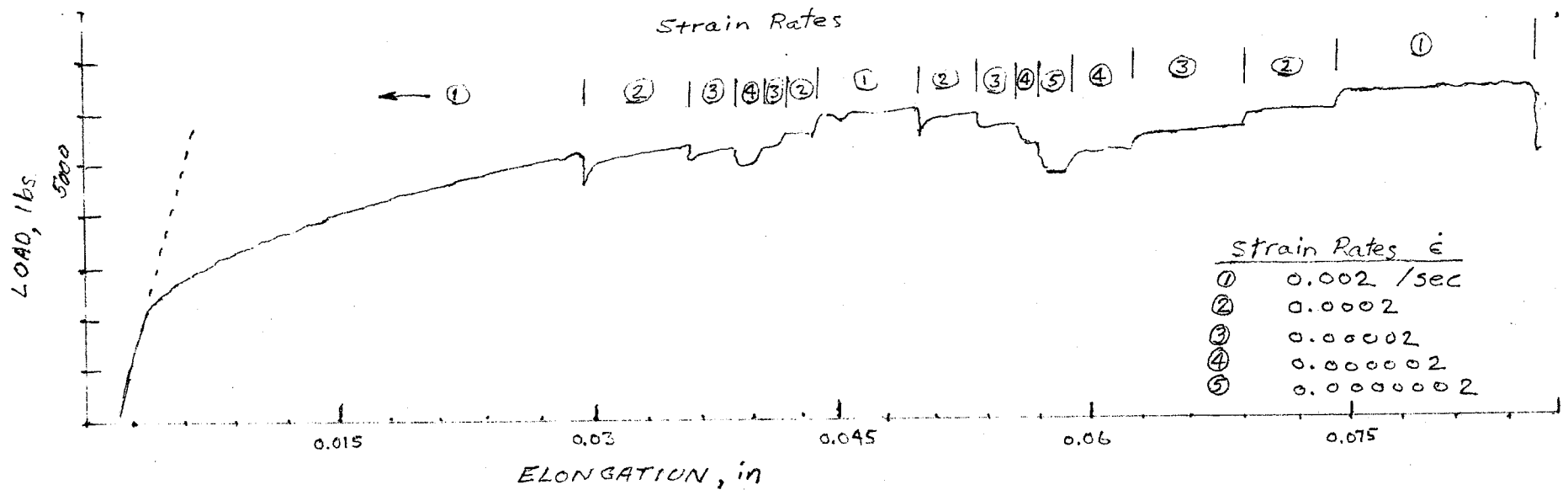


FIGURE 4.3. EFFECT OF STRAIN RATE ON FLOW CHARACTERISTICS OF CLASS U WHEEL STEEL AT 400°C (752°F).

was established at a strain of about 2.6%, the strain rate was abruptly reduced in steps from 0.002 Sec⁻¹ to 0.000002 Sec⁻¹ and subsequently increased back to 0.002 Sec⁻¹. This procedure was repeated but to a slower rate, 0.0000002 Sec⁻¹, at a higher strain in the same test. As seen in the figure, the drop in flow stress and subsequent rise are essentially identical for the same strain rate increment. A reduction of strain rate of two orders of magnitude to 0.00002 Sec⁻¹ causes a flow stress reduction of between 9.6 and 12.1%. At the slower rate of 0.000002 Sec⁻¹, the flow stress continues to relax during the period of straining but seems to reestablish at a flow stress level at least 21.6% below that for conventional rate. Even greater relaxation rate was indicated at the slowest rate of 0.000002 Sec⁻¹ but the test was too short to establish a steady flow stress.

From this preliminary test at 400°C a strain rate sensitivity, m , of at least 0.03 may be expected where the relation between flow stress and strain rate is given by:

$$\sigma = C (\dot{\epsilon})^m_{\epsilon, T}$$

This relationship was proposed originally by Zener and Hollaman in 1944. As Dieter (Mechanical Metallurgy, 1961) has observed, this parameter can be obtained from a test where the strain rate is rapidly changed from one value to another.

$$m = \frac{\log (\sigma_2 / \sigma_1)}{\log (\epsilon_2 / \epsilon_1)}$$

It is expected that the strain rate sensitivity will increase with temperature.

4.2.5 Wheel Saw-Cutting

The purpose of this sub-task is to estimate the number of unsafe wheels of various designs, at different levels of discoloration and usage.

The saw-cutting program undertaken resulted in a total of 160 freight car wheels cut by the end of April 1985. A data base has been compiled at the Transportation Test Center (TTC), Pueblo, which also comprises the saw-cut results of the Norfolk Southern, Union Pacific, and Santa Fe railroads produced at their respective research laboratories. The freight car wheels selected for this study include:

1. wheels taken out of service by visual inspection of wheel discoloration that extends 4 inches (102 mm) from the rim into the plate region on one side (AAR Why Made Code 89) and those subsequently taken out of service due to discoloration on both sides (there are 123 wheels in this data set),
2. wheels taken out of service due to thermal cracks (AAR Why Made Code 74),

3. those taken out of service due to reasons other than AAR Why Made Codes 89 and 74, and
4. 26 new wheels.

4.2.5.1 Radial Saw-Cutting Procedure

A Rockwell Model 28-345 Band Saw Unit has been modified at TTC, Pueblo, to facilitate radial saw-cutting of railroad wheels. This type of band saw has a movable table which is retrofitted with linear bearings, while the saw blade is mounted on a fixed column (Figure 4.4). A constant force feed is provided by a pulley and weight system. A wheel failure guard is fabricated around the saw unit to protect the saw in case a catastrophic wheel failure should occur.

Instrumentation for the radial saw-cutting unit consists of appropriate transducers, electronic signal conditioners, and data acquisition system. To monitor the movement of the table supporting the railroad wheel, a calibrated stringpot system is provided. An MTS clip gage with a range of 0.1" to 0.3" is used to measure the circumferential displacement that occurs at the flange tip during the radial cut. The clip gage is attached to knife edges that affix to the back of the wheel flange with the wheel mounted on the band saw table (Figure 4.5). An x-y plotter automatically records the MTS clip gage displacement vs the depth of cut during the cutting operation.

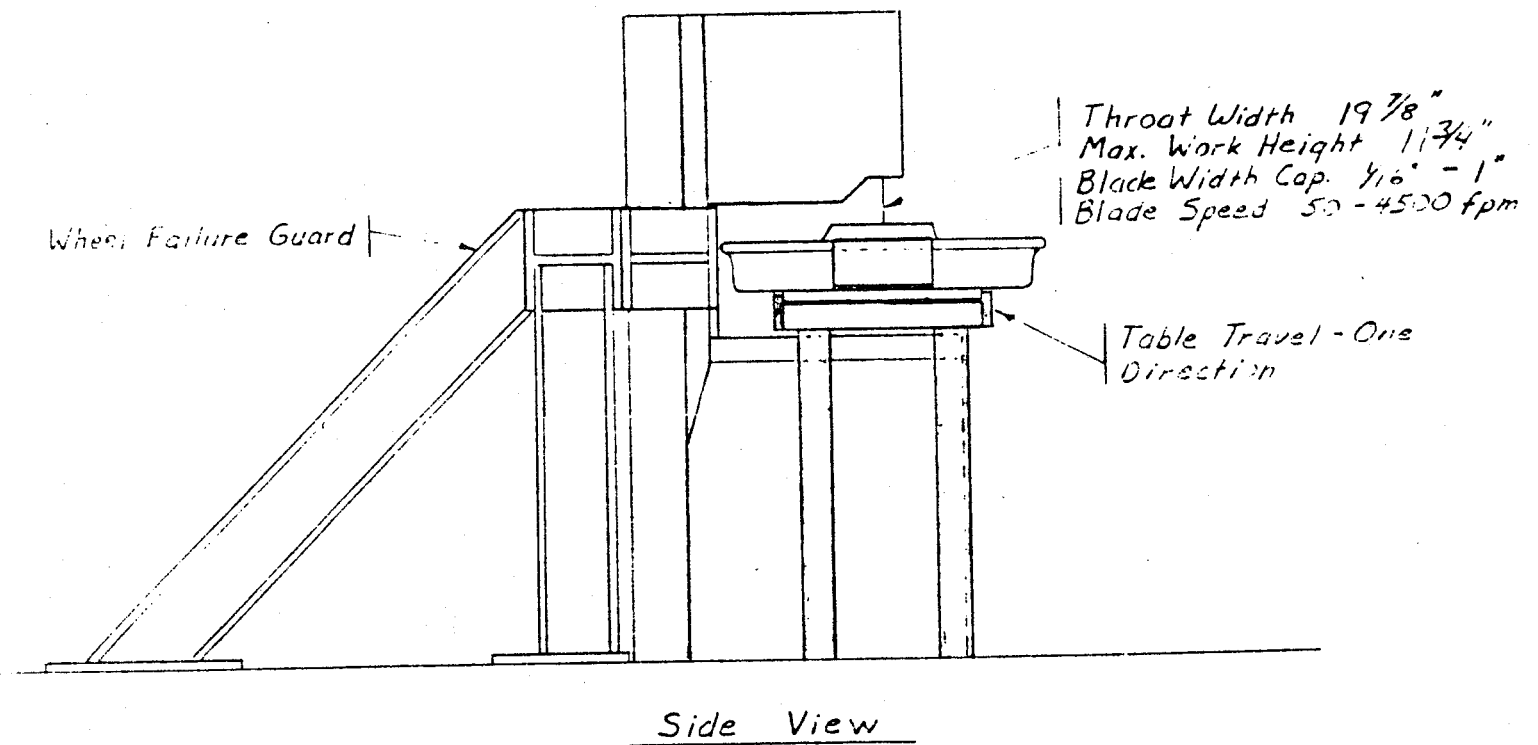
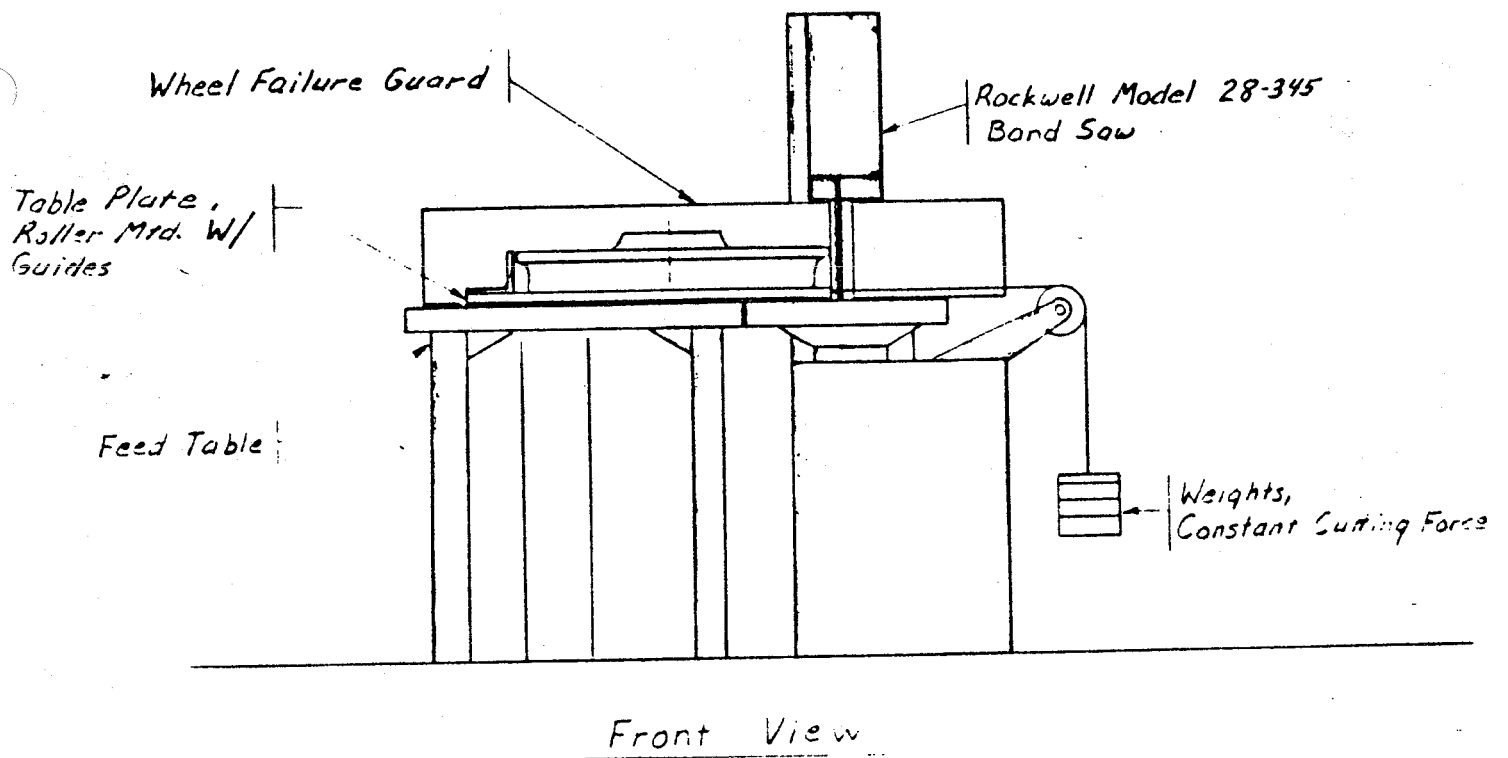


FIGURE 1. SCHEMATIC OF SAW-CUTTING UNIT AT PUEBLO.

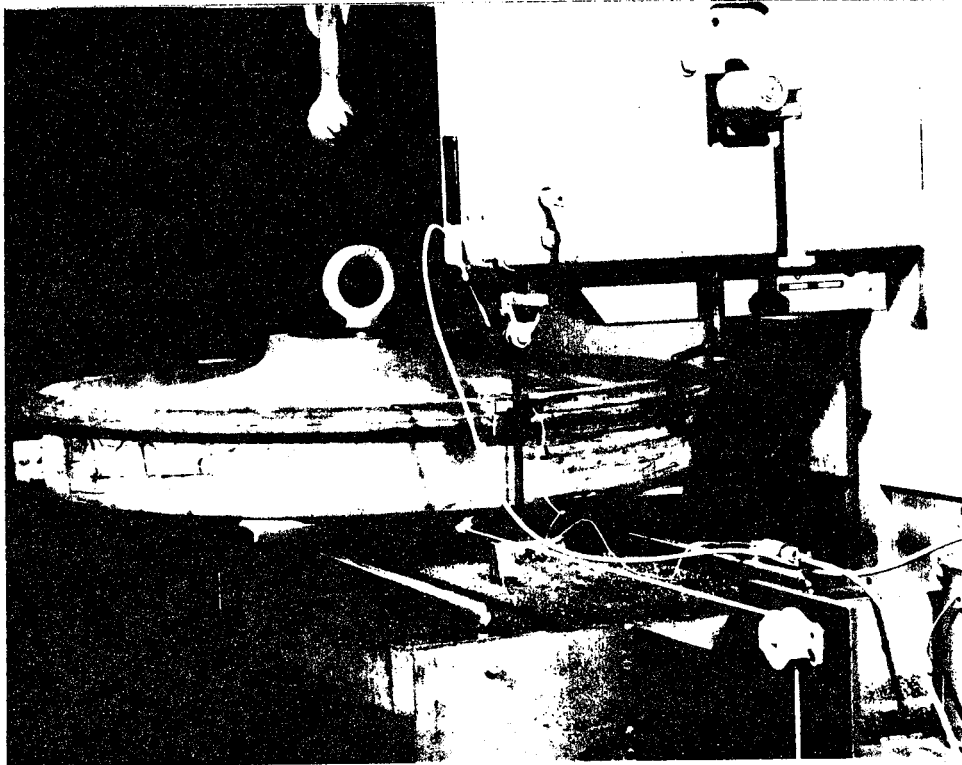


FIGURE 4.5. SAW-CUTTING UNIT WITH CLIP GAGE MOUNTED ON THE FLANGE TIP OF TEST WHEEL.

To prepare a wheel for cutting, the clip gage mount is attached to the back rim face. The wheel is placed flat on the band saw table and the blade is centered between the two knife edges. The band saw unit is started and the saw blade is allowed to cut through the knife edge support bracket until it just reaches the flange tip. At this point, the band saw unit is stopped and the clip gage is mounted on the knife edges around the cutting blade. The x-y plotter is initialized to zero displacement and zero depth of cut before the band saw unit is once again started to initiate the radial cut.

An informal standardization of the saw-cutting method was agreed upon by the AAR, Norfolk Southern, Union Pacific, Santa Fe, and the FRA to ensure ease of data interpretation between laboratories.

After the saw-cutting program at Pueblo was well underway, an additional saw-cut opening measurement capability was installed. Due to obvious differences in the opening/closing behavior of flange tip and tread surface (toward front face) for a number of test wheels, an extended arm clip-on displacement gage with a range of 0.5 inches to 1.0 inches (13 mm to 25 mm) was provided (Figure 4.6) with a special mounting bracket and knife edges. As saw-cutting progressed through the flange and the tread, the saw blade was allowed to cut through the mounting bracket of the extended arm clip gage, which was tack-welded to the tread position toward the front face, after which the saw unit was stopped and the second clip gage displacement on the x-y plot was initialized to zero.

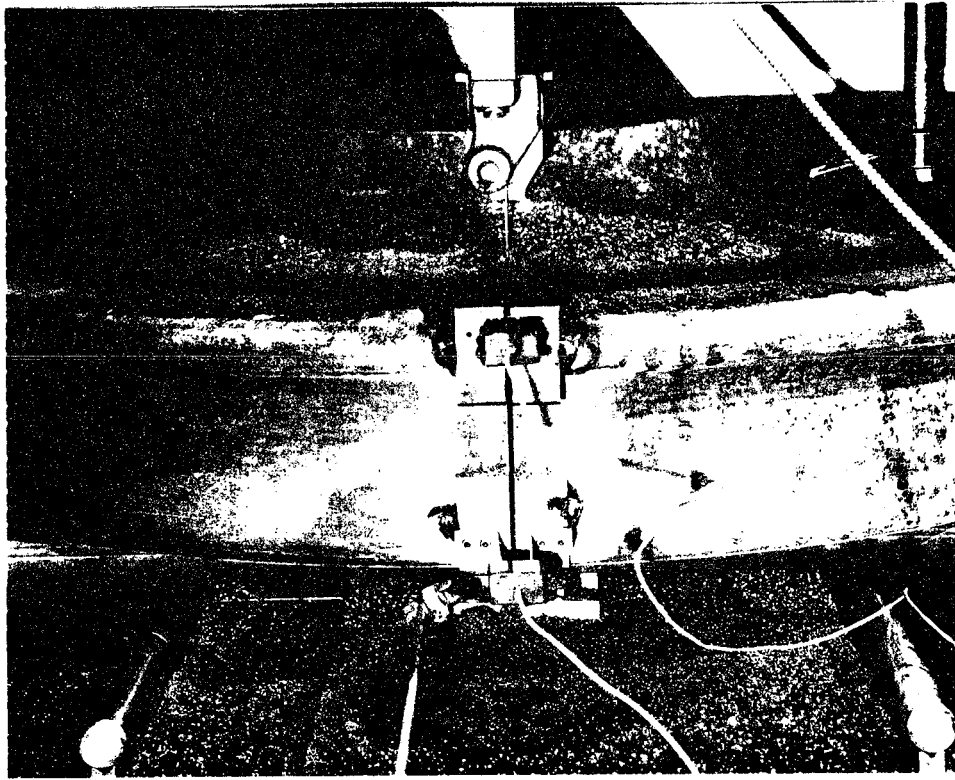


FIGURE 4.6. TWO CLIP GAGES MOUNTED ON THE TEST WHEEL TO MEASURE THE RESPONSES OF FLANGE TIP (BACK FACE) AND TREAD (FRONT FACE).

4.2.5.2 Results and Discussion

4.2.5.2.1 Saw-Cutting Results

If a rail car wheel is cut radially, one of three general types of behavior will usually be observed. A new or undamaged Class U wheel will show a relatively low saw-cut closing displacement as the cut proceeds into the rim. As the cut approaches the bottom of the rim, the circumferential displacement measured at the flange tip begins to increase in the positive direction as shown in Figure 4.7. A heat-treated wheel (Class B or C, new or undamaged) exhibits a continuously closing saw-cut displacement to a point approximately two inches into the plate where a constant saw-cut closing displacement is maintained, as shown in Figure 4.8.

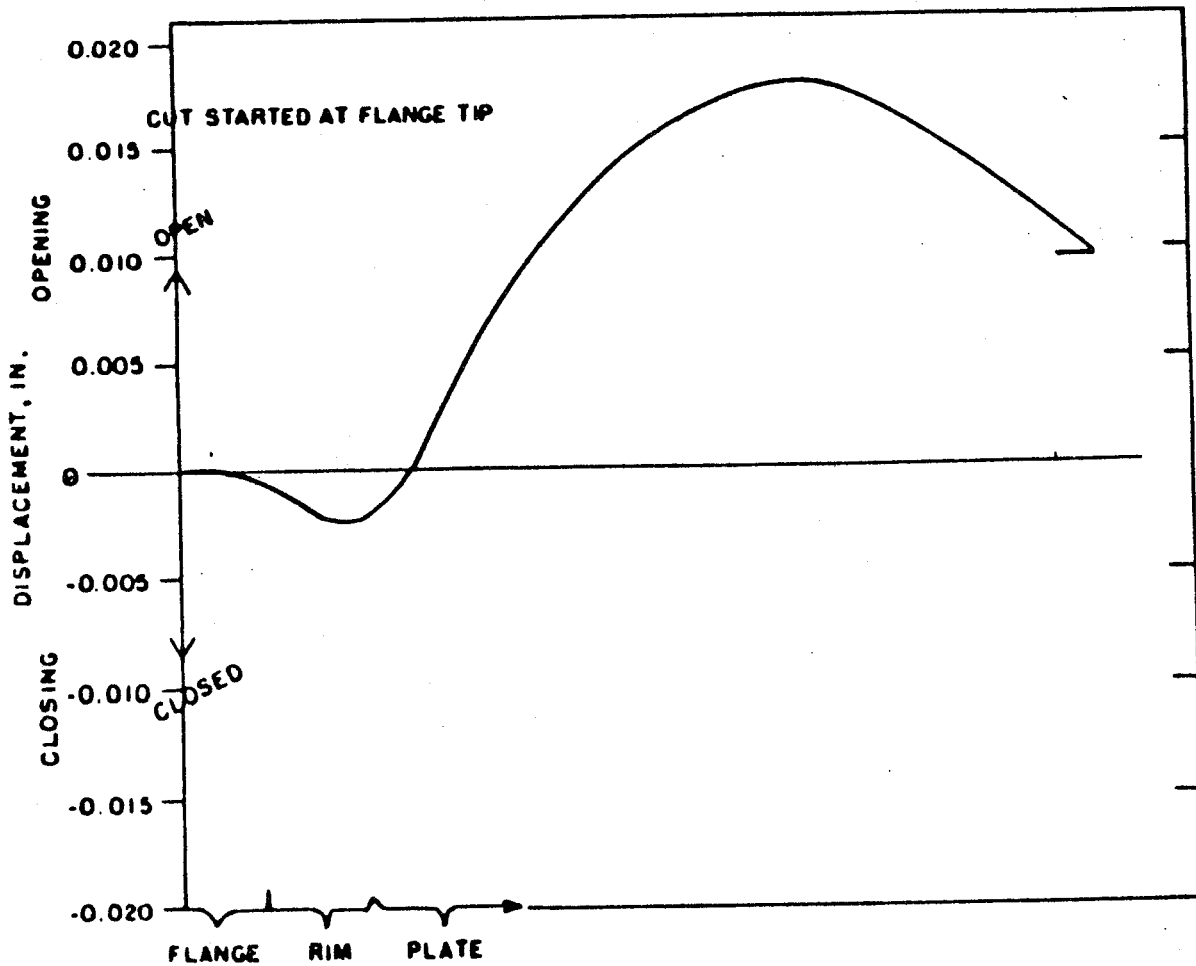


FIGURE 4.7. TYPICAL SAW-CUT DISPLACEMENT BEHAVIOR OF A NEW OR UNDAMAGED CLASS U WHEEL.

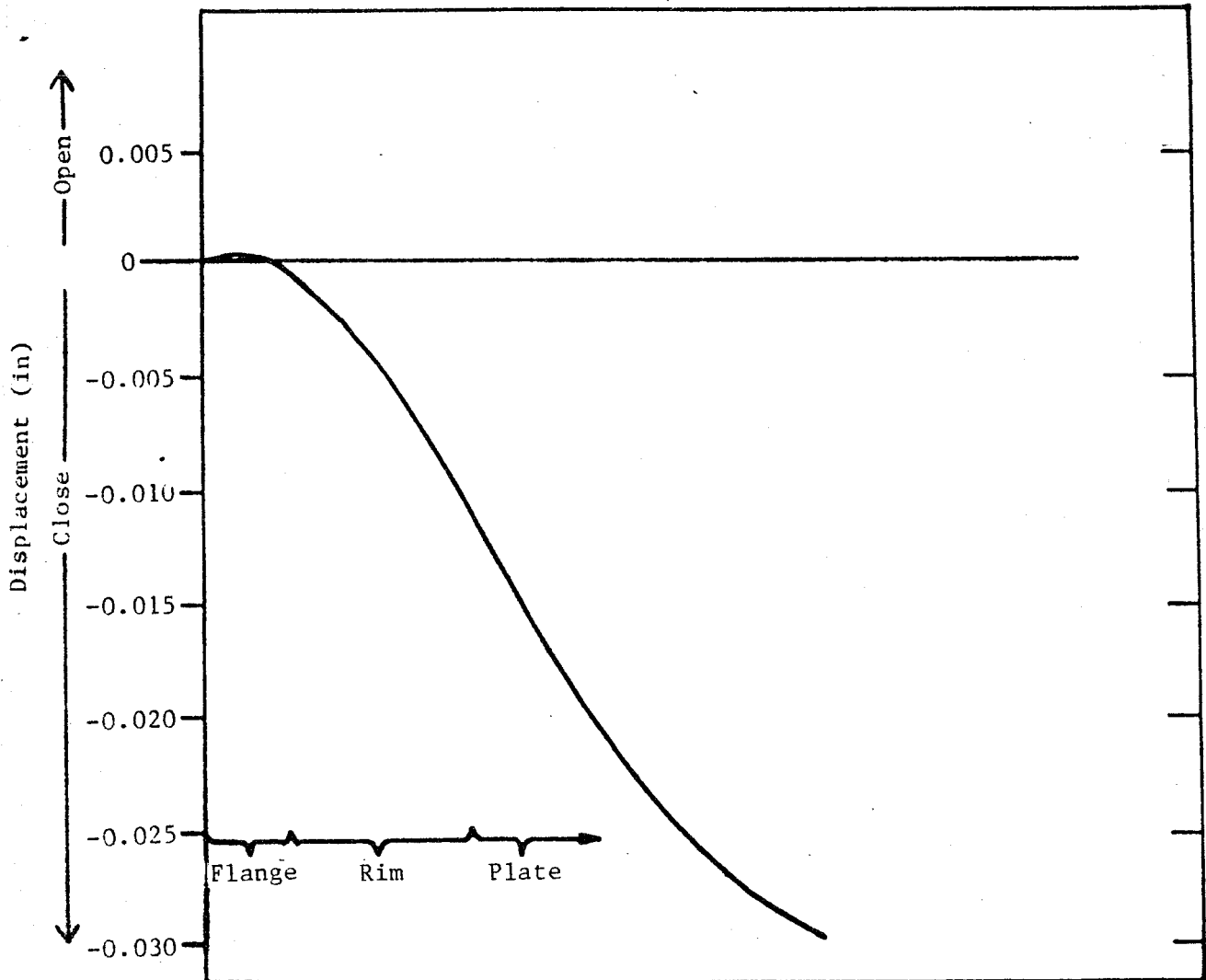


FIGURE 4.8. TYPICAL SAW-CUT DISPLACEMENT BEHAVIOR OF NEW OR UNDAMAGED CLASS B OR C WHEELS.

The presence of compressive residual stress around the circumference of the wheel is inferred from the behavior. A thermally damaged wheel, on the other hand, develops an increased level of opening at the flange tip as the cut proceeds inward, as shown in Figure 4.9 a crack located in this area of tensile stress would probably propagate with no possibility of arrest.

A tabulation of the results of saw-cutting of 348 wheels is given in Appendix 4.3. A wheel that closes is presumed to have a circumferential residual compressive stress, and a wheel that opens continually during saw-cutting contains a residual tensile stress. However, wheels that show mixed behavior (as illustrated in Figure 4.7) are more difficult to classify. Work on the finite element reconstruction of saw-cut wheels, as reported in paragraph 11.2.3.5, shows that a correlation may exist between maximum opening and maximum calculated residual stress in the wheel rim as shown in Figure 4.10, although additional confirmation is required. The data presented in Figure 4.10 consist of results from 8 curved plates and one straight plate wheel.*

The saw-cut opening can then be sorted, as shown in Table 4.2, and the percentages of various wheels at each increment of opening may be calculated. This data may then be used to estimate the distribution of wheel conditions in the car fleet.

*Additional data is being collected from straight plate wheel behavior to radial saw-cut as input to finite element analysis.

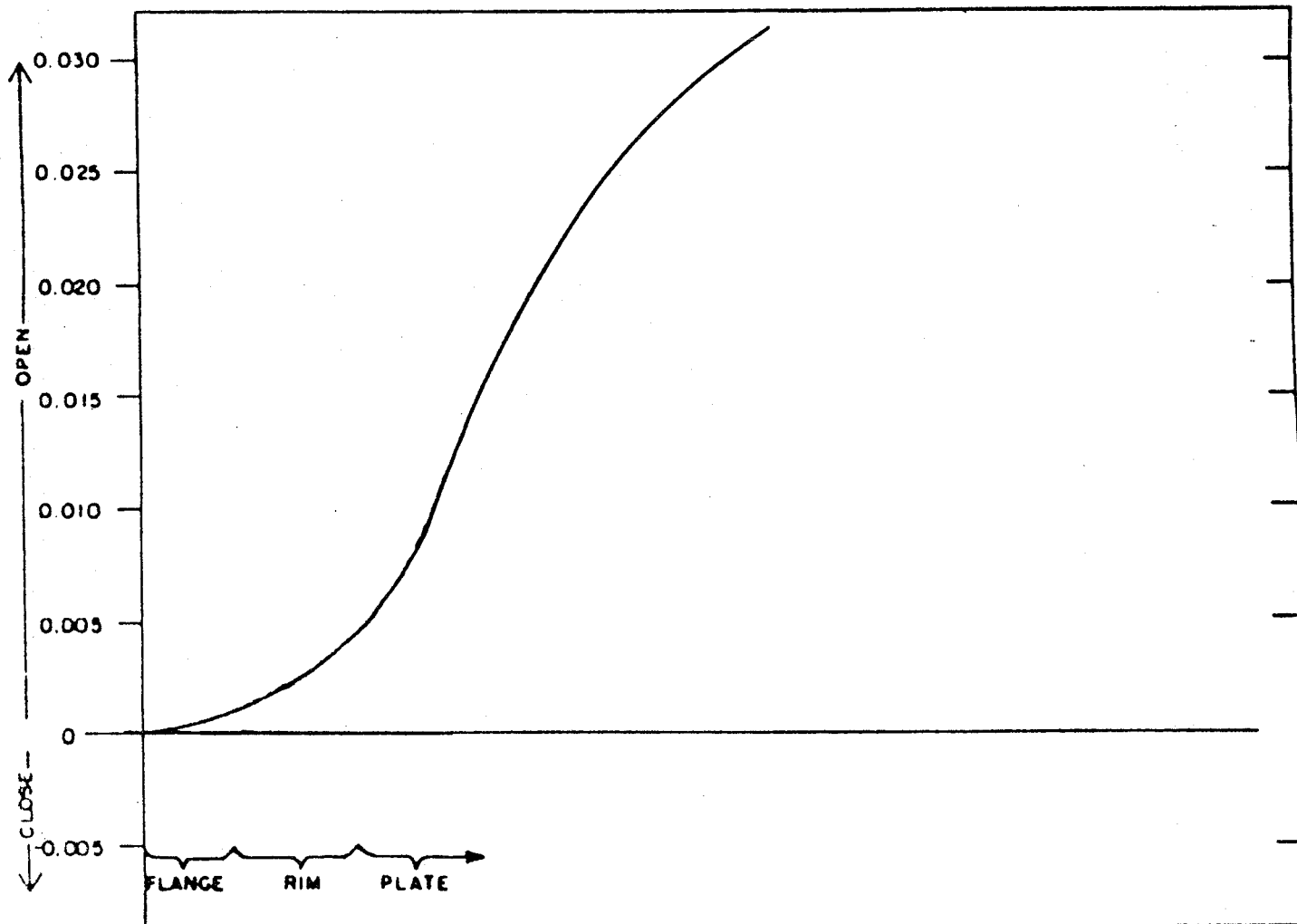
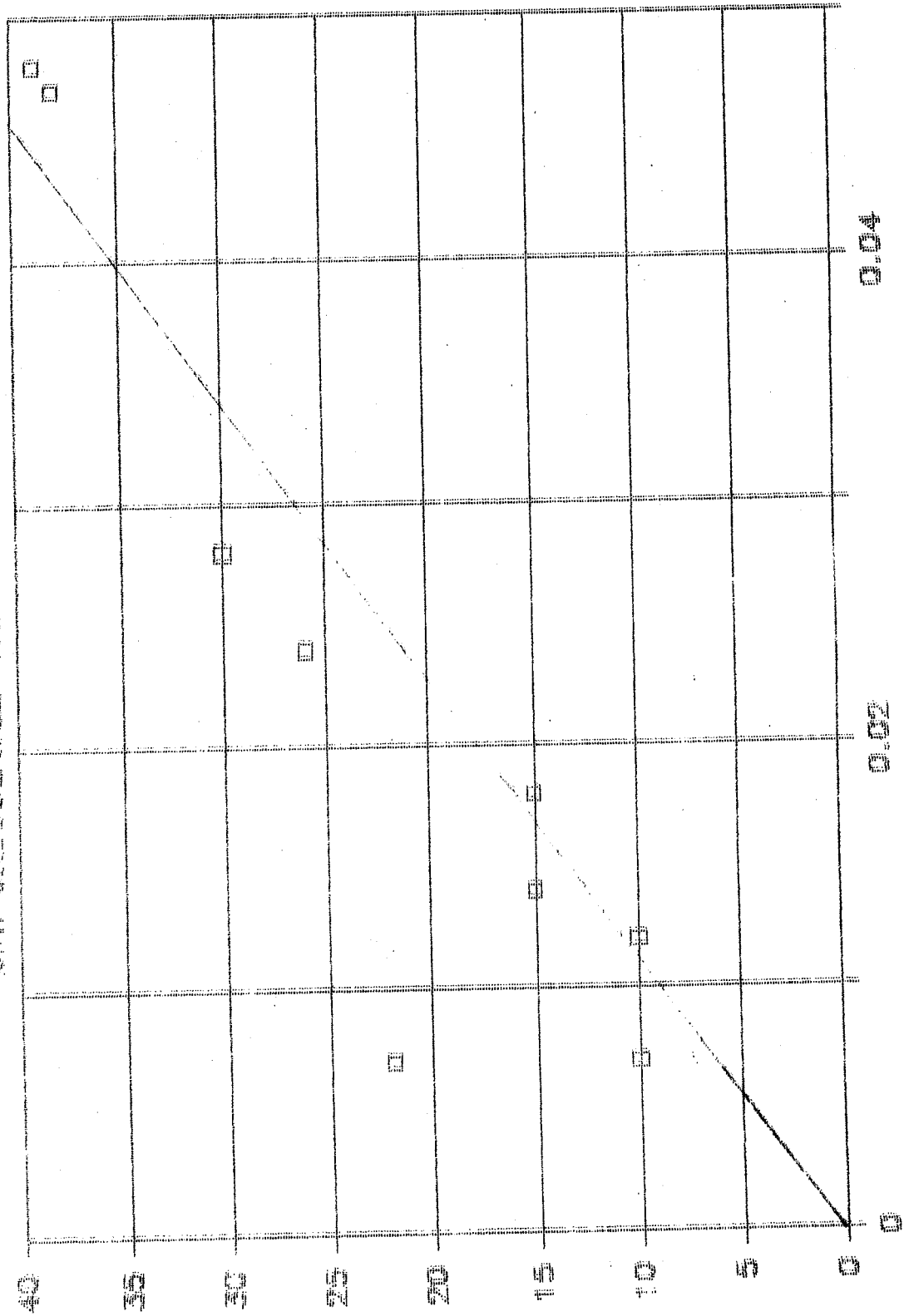


FIGURE 4.9. TYPICAL SAW-CUT DISPLACEMENT BEHAVIOR OF A THERMALLY DAMAGED WHEEL.

CORRELATION OF MAXIMUM SAW CUT OPENING
WITH CALCULATED MAX. RESIDUAL STRESS



(5) KSI

MAX. SAW CUT OPENING (INCHES)

FIGURE 4.10. SIZE OF OPENING VERSUS CALCULATED RESIDUAL STRESS.

TABLE 4.2. DISTRIBUTION OF MAXIMUM SAW-CUT OPENINGS.

Opening	Low-Non	Low-Disc	High-Non	High-Disc
<0.010	64.29%	56.44%	71.76%	20.00%
0.011-0.020	16.43%	9.90%	9.41%	15.00%
0.021-0.030	10.71%	11.88%	5.88%	15.00%
0.031-0.040	5.71%	7.92%	5.88%	20.00%
0.041-0.050	1.43%	9.90%	3.53%	10.00%
0.051-0.060	0.71%	0.99%	0.00%	0.00%
>0.060	0.71%	2.97%	3.53%	20.00%
Ratio	1.00	4.16	4.94	28.00

Opening	Low-Non	Low-Disc	High-Non	High-Disc
<0.010	64.29%	56.44%	71.76%	20.00%
0.011-0.020	16.43%	9.90%	9.41%	15.00%
0.021-0.030	10.71%	11.88%	5.88%	15.00%
0.031-0.040	5.71%	7.92%	5.88%	20.00%
0.041-0.050	1.43%	9.90%	3.53%	10.00%
>0.050	1.43%	3.96%	3.53%	20.00%
Ratio	1.00	2.77	2.47	14.00

Opening	Low-Non	Low-Disc	High-Non	High-Disc
<0.010	64.29%	56.44%	71.76%	20.00%
0.011-0.020	16.43%	9.90%	9.41%	15.00%
0.021-0.030	10.71%	11.88%	5.88%	15.00%
0.031-0.040	5.71%	7.92%	5.88%	20.00%
>0.040	2.86%	13.85%	7.06%	30.00%
Ratio	1.00	4.85	2.47	10.50

Nomenclature

Low → Low Stress (curved plate) wheel
 High → High Stress (straight plate) wheel

Low-Non → Low Stress, Nondiscolored
 Low-Disc → Low Stress, Discolored

High-Non → High Stress, Nondiscolored
 High-Disc → High Stress, Discolored

Ratio means the ratio of "low stress, nondiscolored" wheels to the rest of the varieties of wheels, which are saw-cut.

Most wheels purchased during the last five years have been of the low stress or curve plate designs. Virtually all wheels purchased today are of these designs. It is estimated that curved plate wheels make up about 60% of the population of the fleet.

Studies using finite element analysis techniques support the case for the use of the maximum opening as the criterion to identify thermally damaged wheels. It is our belief that an opening of 0.050 inches or more should be considered an indicator damage.

4.2.6 Experimental Stress Analysis

Ten wheels were selected for experimental stress analysis by the hole drilling strain-gage method before they were saw-cut. These wheels were taken out of service on account of discoloration (AAR Why Made Code 89) as well as for other reasons. Table 4.3 provides the general information about the test wheels.

4.2.6.1 Determination of Residual Stresses by the Hole Drilling Strain Gage Method

The hole drilling strain-gage method is a semidestructive method for measuring residual stresses near the surface of isotropic elastic material. The method involves placing a strain-gage rosette on the surface, drilling a hole in the vicinity of the gages to a depth greater than its diameter, and measuring the relaxation strains. The residual stresses in the area surrounding the drilled hole relax, and the relaxation is nearly complete when the depth of the drilled hole approaches 1.2 times the diameter.

TABLE 4.3. GENERAL INFORMATION ABOUT SELECTED TEST WHEELS
FOR EXPERIMENTAL STRESS ANALYSIS.

TTC ID	Mfg. Date	Serial No.	Class	Design	AAR Why Made Code	Discoloration
0009	78/02	42183	U	CH36	89	Yes
0010	78/02	45459	U	CH36	89	Yes
0011	80/03	61258	U	CH36	89	Yes
0031	82/02	24190	U	CH36	89	Yes
0046	76/10	4102	U	CH36	89	Yes
0047	82/03	61430	U	CH36	89	Yes
0051	75/10	51585	U	CH36	89	Yes
0054	75/10	51933	U	CH36	89	Yes
0070	64/09	18187	U	CJ36	--	No
0095	71/01	587204	C	CJ36	--	No

The measured strains are then related to relieved principal stresses through a series of equations.

The surface strains relieved are related to the relieved principal stresses by the following relationship:

$$\varepsilon_r = (A + B \cos 2\alpha)\sigma_x + (A - B \cos 2\alpha)\sigma_y \quad (1)$$

where

ε_r = radial strain relieved at point P,

$$A = -\frac{1+\mu}{2E} \times \frac{1}{r^2},$$

$$B = -\frac{1+\mu}{2E} \left(\frac{4}{1+\mu} \times \frac{1}{r^2} - \frac{3}{r^4} \right),$$

σ_x, σ_y = principal stresses present in the structure before drilling,

α = angle between the directions of ε_r and σ_x ,

E = Young's modulus,

μ = Poisson's ratio,

$r = \frac{D}{D_0}$ (see Figure 4.11)

D = diameter of gage circle, and

D_0 = diameter of drilled hole.

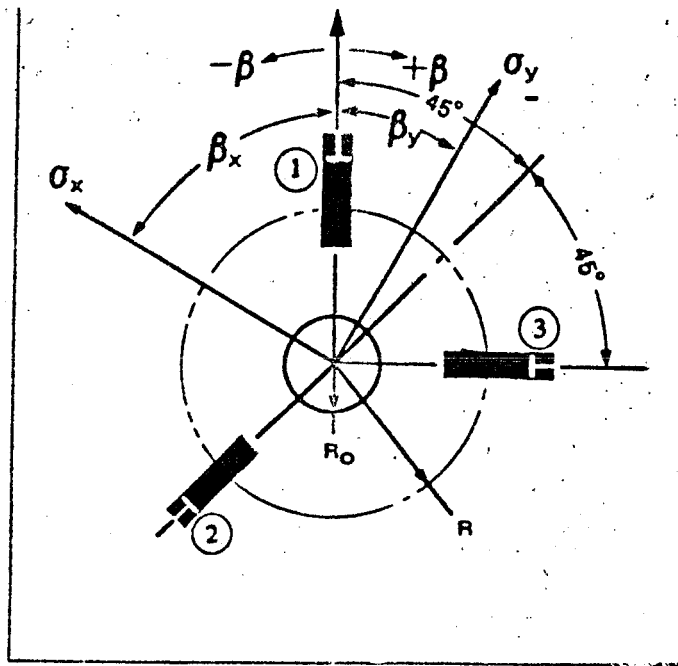


FIGURE 4.11. STRAIN GAGE ROSETTE ARRANGEMENT FOR DETERMINING RESIDUAL STRESSES.

Measuring the relieved radial strains ϵ_1 , ϵ_2 , and ϵ_3 provides sufficient information to calculate the principal stresses σ_x and σ_y and their orientation, β , with respect to an arbitrary selected reference.

Solving for principal stresses and direction yields:

$$\sigma_x = \frac{\epsilon_1 + \epsilon_3}{4\bar{A}} + \frac{\sqrt{2}}{4\bar{B}} \sqrt{(\epsilon_1 - \epsilon_2)^2 + (\epsilon_2 - \epsilon_3)^2} \quad (2)$$

$$\sigma_y = \frac{\epsilon_1 + \epsilon_3}{4\bar{A}} - \frac{\sqrt{2}}{4\bar{B}} \sqrt{(\epsilon_1 - \epsilon_2)^2 + (\epsilon_2 - \epsilon_3)^2} \quad (3)$$

$$\tan 2\beta = \frac{\epsilon_1 - 2\epsilon_2 + \epsilon_3}{\epsilon_3 - \epsilon_1}$$

where \bar{A} and \bar{B} (both of which are negative) are determined from Figure 4.12. Equations (2) and (3) define the maximum (σ_x) and minimum (σ_y) principal stresses. Direction angle β is referenced to gage 1 where clockwise is positive (+) direction and:

$$\beta = \beta_x \text{ if } (\epsilon_1 + \epsilon_3)/2 < \epsilon_1$$

$$\beta = \beta_y \text{ if } (\epsilon_1 + \epsilon_3)/2 > \epsilon_1$$

$$\beta = 45^\circ \text{ if } \epsilon_1 = \epsilon_3$$

$$\bar{A} = -\frac{1+\mu}{2E} \cdot \bar{a} \tag{4}$$

$$\bar{B} = -\frac{1}{2E} \cdot \bar{b} \tag{5}$$

The following graphs of Figure 4.12 are extracted from Technical Note TN-503-1 of Measurements Group Inc., Raleigh, North Carolina 27611.

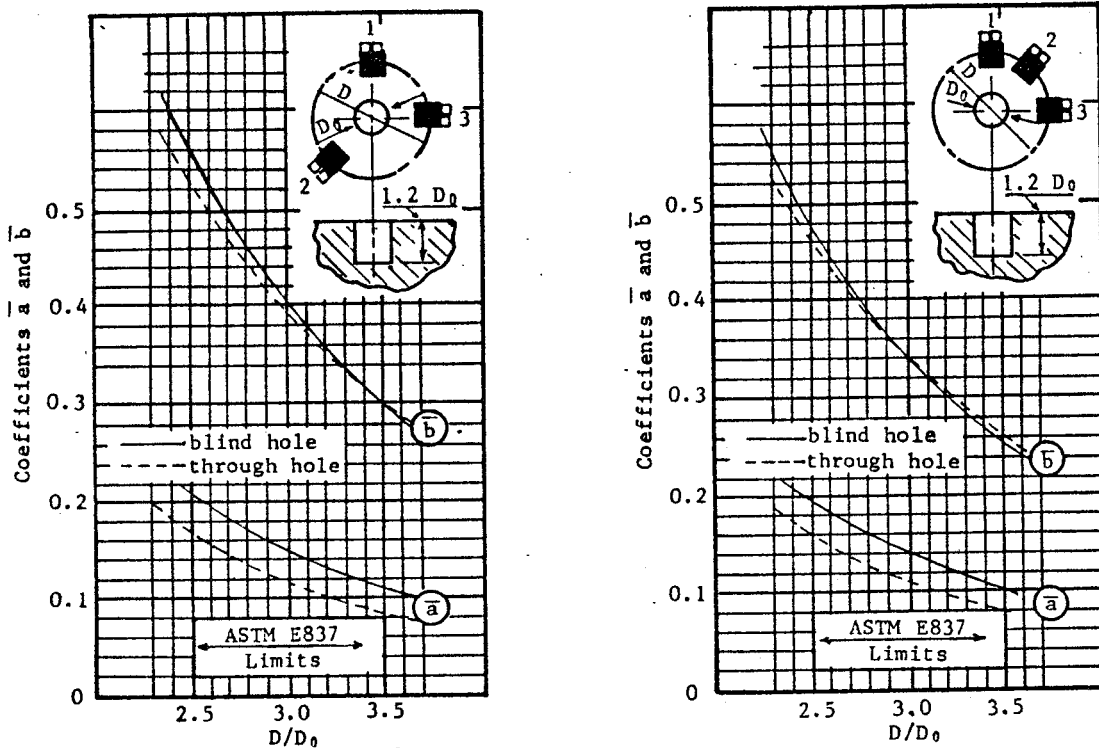


FIGURE 4.12. DATA REDUCTION COEFFICIENTS A AND B VS D/D₀. LEFT GRAPH FOR UM GAGE, RIGHT GRAPH FOR RE & RK⁰ GAGES.

A number of wheels were analyzed by the hole-drilling strain-gage method prior to saw-cutting. A few wheels were also analyzed after the saw-cut was made, since a study at Pueblo revealed that the saw-cut behavior of wheels is practically the same at 180° from the previous cut. Figures 4.13 and 4.14 show typical arrangements of the hole-drilling strain-gage method for railroad wheels.

4.2.6.2 Experimental Stress Analysis Results

Strain-gage rosettes with three radially-oriented gages were installed on the back face of the rim with their centers about 2.5 inches (64 mm) radially down from the flange tip (termed here the B1 location). Strain-indicating instrumentation consisted of a precision strain indicator augmented by a high quality switch-and-balance unit. A Micro Measurements RS-200 Milling Guide with a microscope provided visual alignment within ± 0.001 inch (± 0.025 mm) such that the position of the milling cutters was precisely in the center of the gage rosette. After the alignment with a microscope, a high-speed air turbine setup with carbide cutters was fitted in the RS-200 Milling Guide. Incremental drilling with the high-speed turbine device was carried out up to a total blind hole depth of 0.1 inch (2.54 mm). Relieved strains were monitored at every incremental depth of 0.01 inch (0.254 mm). After the completion of the drilling operation, the diameter of the hole (usually around 0.07 inch) was measured with the microscope. A data reduction procedure was set up with a Fortran program which computed the principal stresses (σ_x and σ_y) and their orientation (β) using equations (1) through (5) for every incremental drilling.

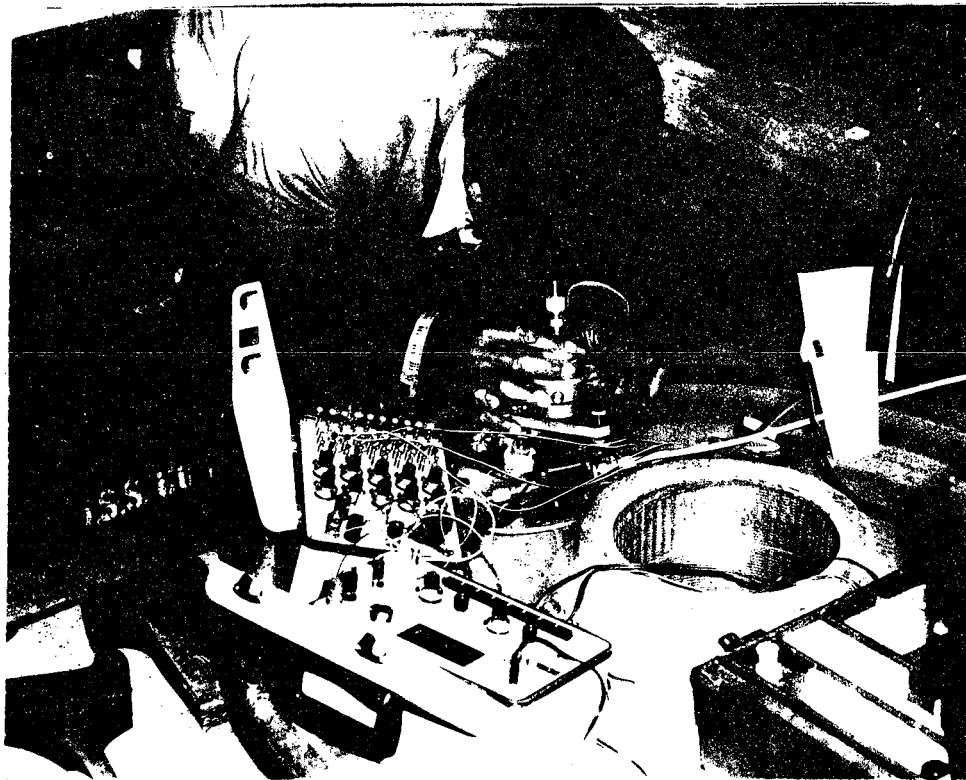


FIGURE 4.13. SETUP FOR HOLE DRILLING STRAIN GAGE METHOD TO EVALUATE RESIDUAL STRESSES IN RAILROAD WHEELS.

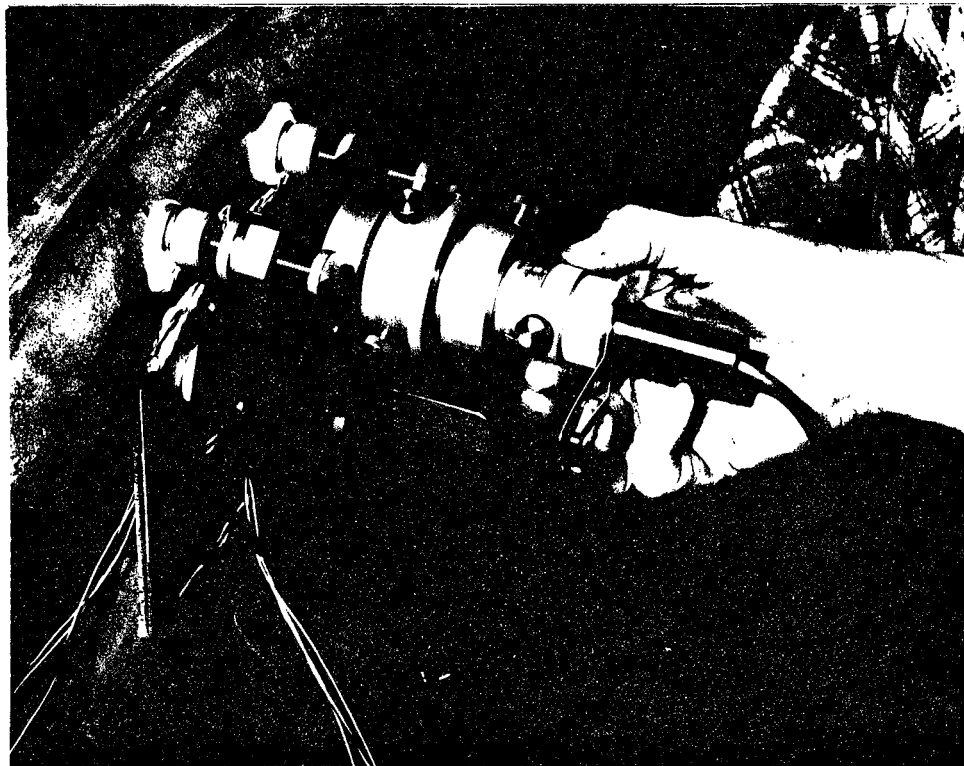


FIGURE 4.14. HOLE DRILLING UNIT SETUP ON BACK FACE RIM OF A WHEEL RESTING ON THE ROLL DYNAMICS UNIT AT PUEBLO.

It is determined experimentally that when the depth of the hole equals the diameter, 100% of the strain is relieved and, thereafter, the change in the relieved strain is minimal. For our analysis, the calculated principal stresses at the point where depth equals diameter are regarded as the residual stresses at location B1.

Once σ_x and σ_y are determined, σ_1 and σ_2 (which can be hoop or radial stresses, depending on the orientation of gage #1 on the wheel) can be calculated from the Mohr Circle relationships:

$$\sigma_{1, 2} = \frac{\sigma_x + \sigma_y}{2} \pm \frac{(\sigma_x - \sigma_y)}{2} \cos 2\beta \quad \text{if } \beta = \beta_x \quad (11)$$

$$\text{and } \sigma_{1, 2} = \frac{\sigma_x + \sigma_y}{2} \pm \frac{(\sigma_y - \sigma_x)}{2} \cos 2\beta \quad \text{if } \beta = \beta_y \quad (12)$$

The analysis of residual stresses on the back face of the rim (B1 location) revealed that the stress components in the hoop and radial directions were of the same order of magnitude resulting in a biaxial state of stress.

After the experimental stress analysis at the B1 locations of 10 wheels, the hole drilling strain-gaging method was applied to the test wheels at two other locations, viz., B2 and B4 locations. The B2 location was in the rim fillet region, 5.5 inches (140 mm) radially down from the flange tip. Analysis was performed at the B2 location for a set of six test wheels, with TTC ID numbers 0009, 0010, 0046, 0047, 0051, and 0052.

The B4 location was in the front face of the rim 2.5 inches (64 mm) radially down from the flange tip (exactly across from the B1 location which is on the back face of the rim). Analysis was performed at the B4 location for three test wheels, TTC ID numbers 0031, 0046, and 0070.

After completion of experimental stress analysis at B1, B2, and B4 locations, the selected test wheels were saw-cut and the individual wheel's response (in the hoop direction) to radial saw-cut was recorded with MTS clip gages as described under "Radial Saw-Cutting Procedure."

Analysis of flange tip displacement (in the hoop direction) to saw-cutting at various depths of cut was carried out, and it was seen that at a given depth of cut, the flange tip displacement exhibited a certain relationship with the bi-axial state of stress at B1, B2, and B4 locations.

At these locations, both the stress components (in hoop and radial directions) seem to have linear relationship with the flange tip displacement (in hoop direction) at a given depth of cut, as follows:

$$\sigma_{i_i} = A_i \sigma_{i_h} + B_i \sigma_r \quad (13)$$

where

i denotes the given depth-of-cut from flange tip,

and

σ_h and σ_r are stress components in hoop and radial directions.

In order to eliminate one of the independent variables, a new variable σ is chosen as

$$\sigma = \sigma_h - \mu\sigma_r$$

where μ is the Poisson's ratio.

which is compatible with equation (13), and the flange tip displacement is plotted versus σ . It is of interest to note that this relationship is linear for selected depths of cut as shown below.*

Figures 4.15 and 4.16 show the linear relationship between $\sigma = (\sigma_h - \mu\sigma_r)$ measured at the B1 location and flange tip displacement at 2 inches (51 mm) and 2.5 inches (64 mm) depth of cut, respectively.

In Figure 4.17 the average of σ values at B1 and B4 locations is plotted against the flange tip displacements at 2.5 inches (64 mm), 5.5 inches (140 mm), and 10 inches (254 mm) depth of cut for three test wheels. They also seem to hold a linear relationship.

Figure 4.18 presents the linear relationship between σ values measured at the B2 location, 5.5 inches (140 mm) radially down from flange tip for six test wheels and the corresponding flange tip displacement at 5.5 inches (140 mm) depth of cut. The same σ values are plotted against maximum flange tip opening during the saw-cutting operation in Figure 4.19 which is also a linear relationship.

*It may be noted that the value of $\sigma = \sigma_h - \mu\sigma_r$ is the equivalent unidirectional stress in the hoop direction. The expression $(1/\epsilon) (\sigma_h - \mu\sigma_r)$ gives ϵ_θ which is the maximum elastic strain in a biaxial state of stress.

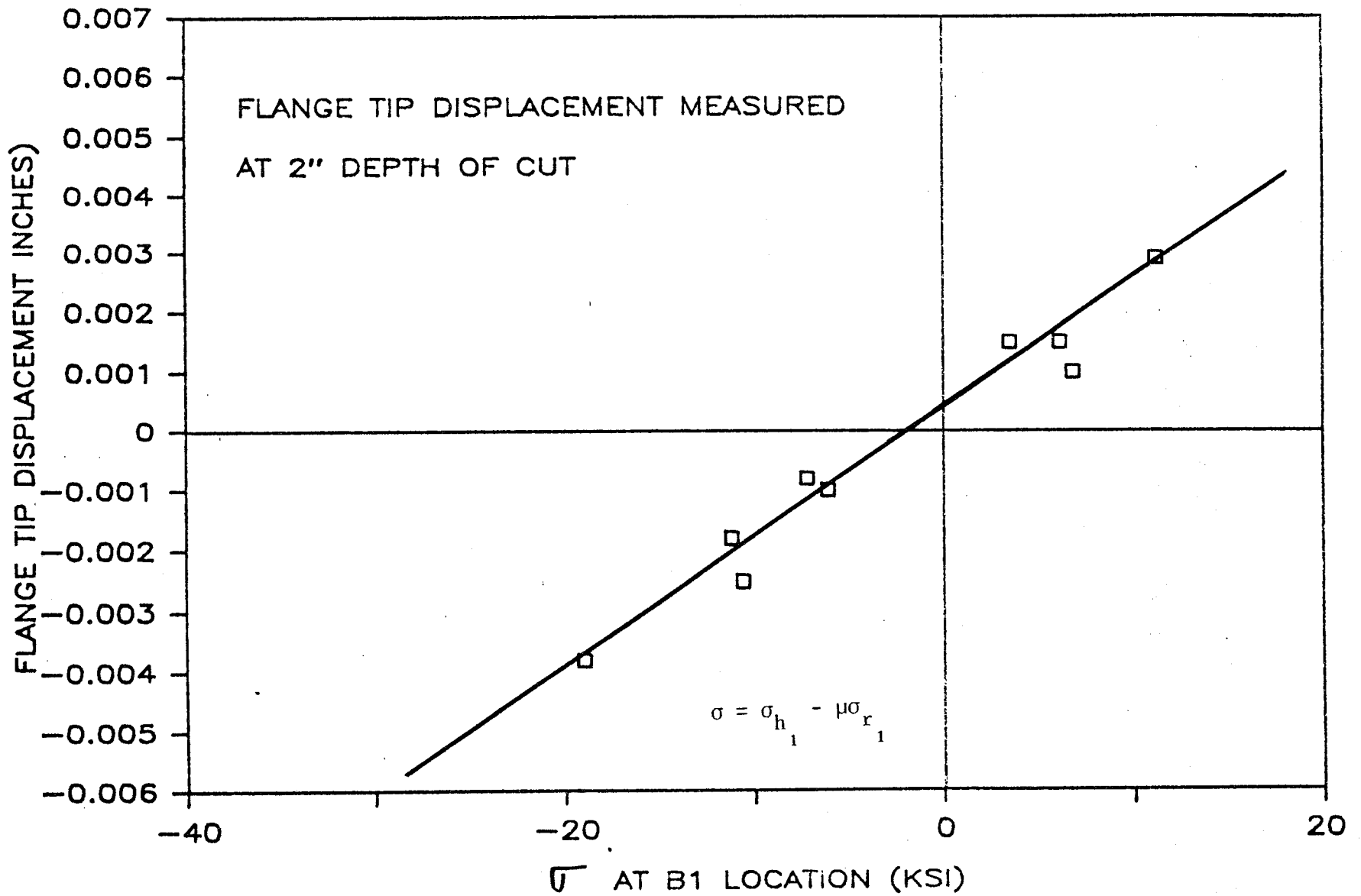


FIGURE 4.15. FLANGE TIP DISPLACEMENT AT 2 INCHES DEPTH OF CUT
VS σ AT B1 LOCATION ($\sigma = \sigma_{h_1} - \mu\sigma_{r_1}$).

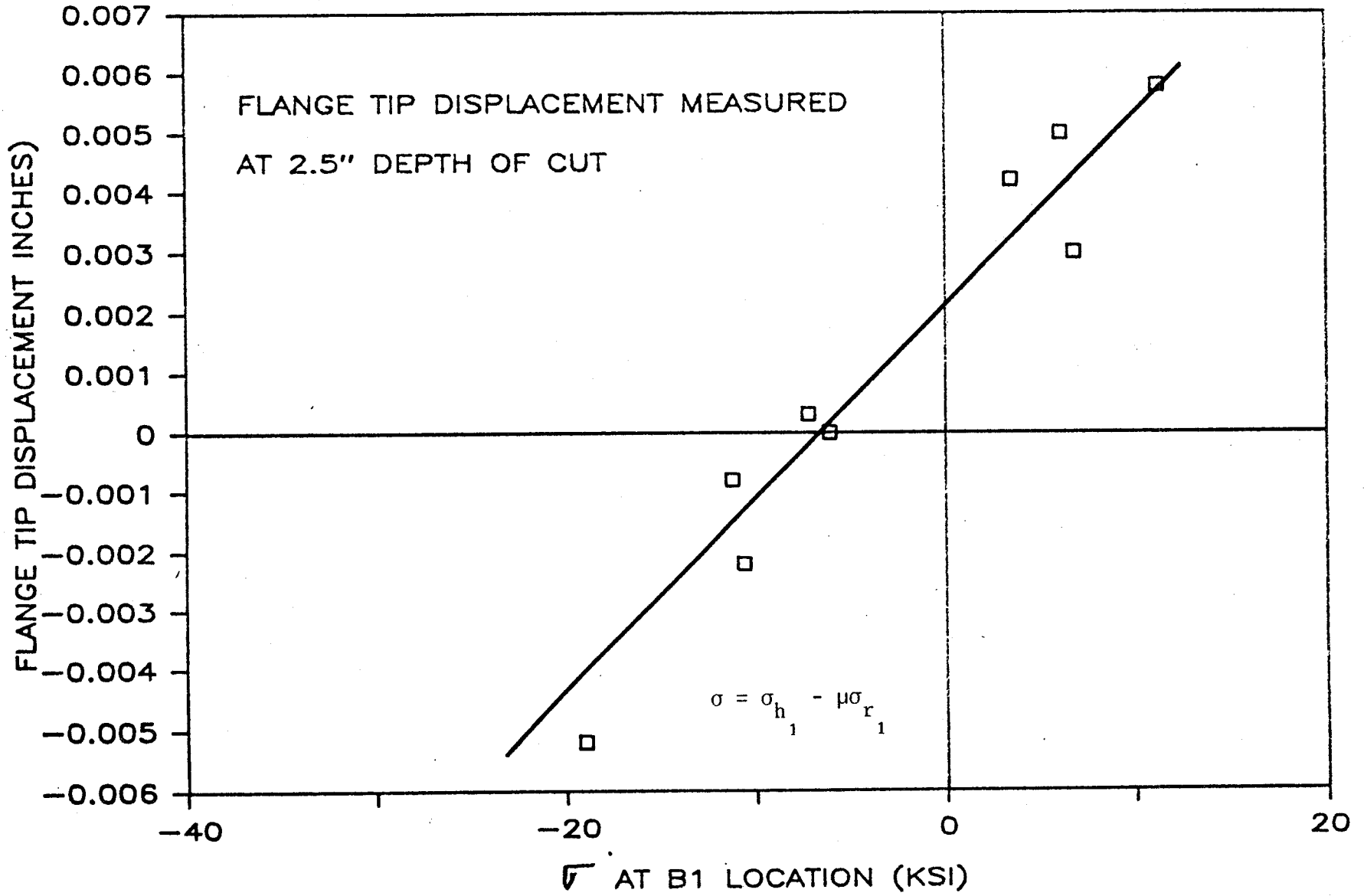


FIGURE 4.16. FLANGE TIP DISPLACEMENT AT 2.5 INCHES DEPTH OF CUT
VS σ AT B1 LOCATION ($\sigma = \sigma_{h_1} - \mu\sigma_{r_1}$).

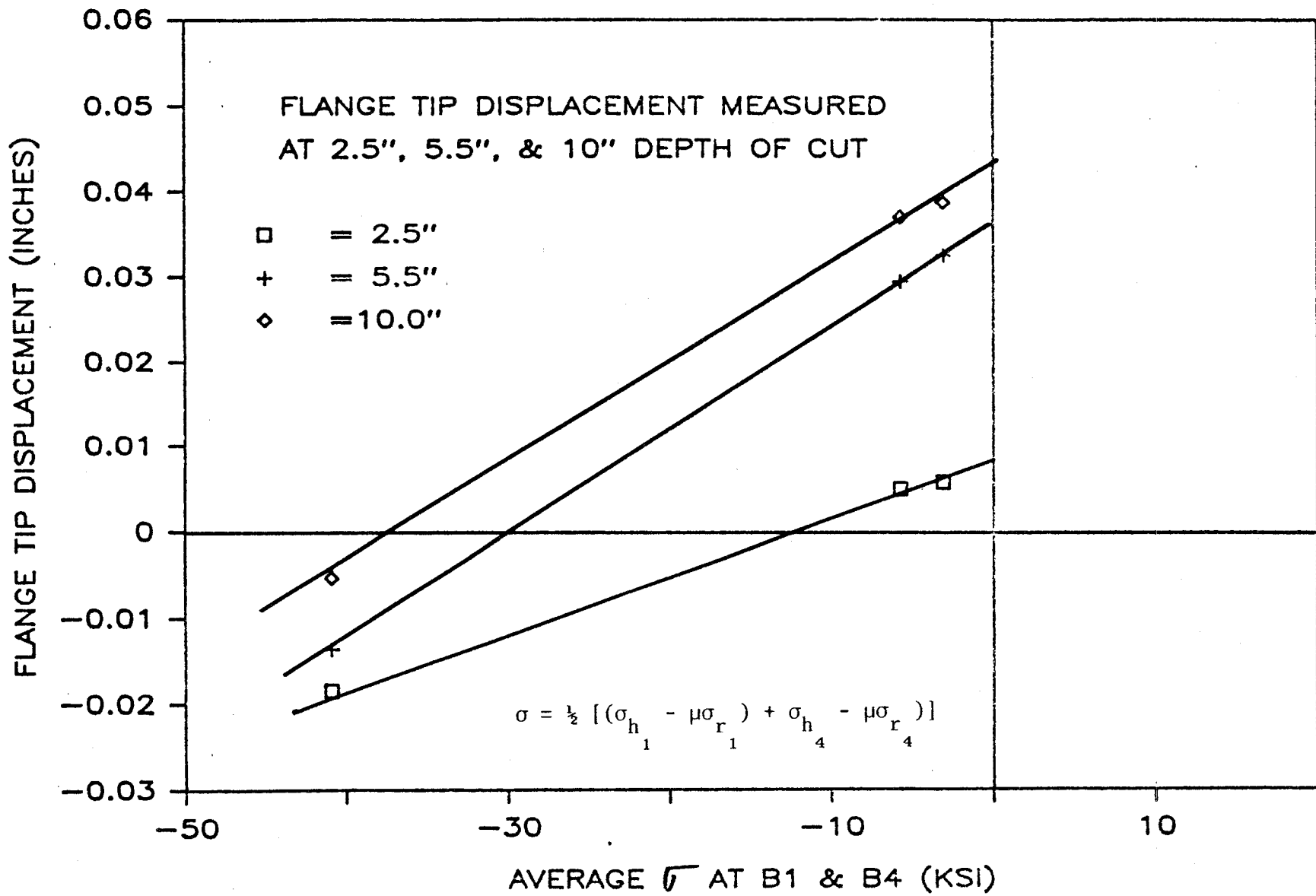


FIGURE 4.17. FLANGE TIP DISPLACEMENT AT 2.5 INCHES, 5.5 INCHES, AND 10 INCHES DEPTH OF CUT VERSUS AVERAGE OF σ VALUES AT B1 AND B4 LOCATIONS.

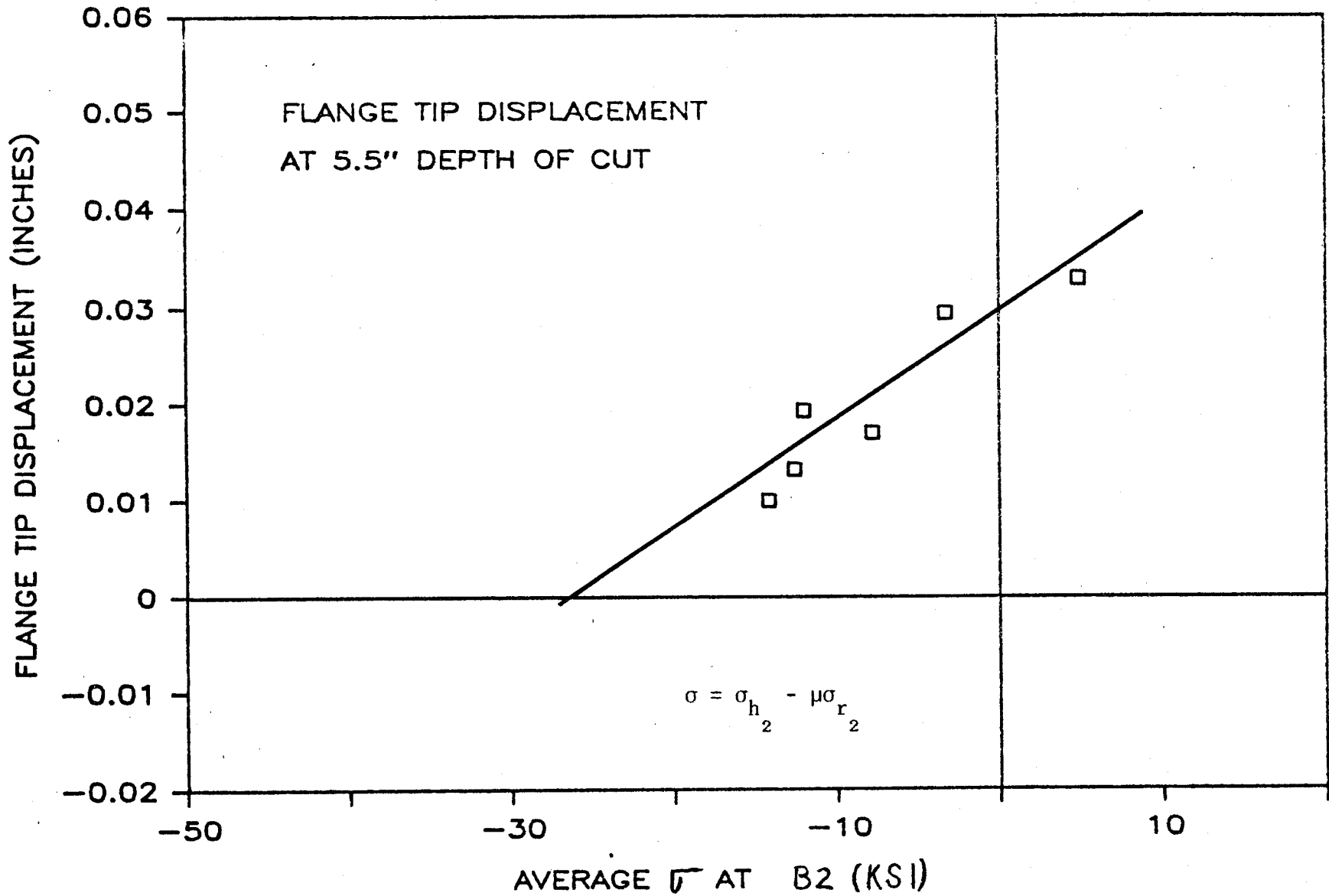


FIGURE 4.18. FLANGE TIP DISPLACEMENT AT 5.5 INCHES DEPTH OF CUT VS σ AT B2 LOCATION ($\sigma = \sigma_{h_2} - \mu\sigma_{r_2}$).

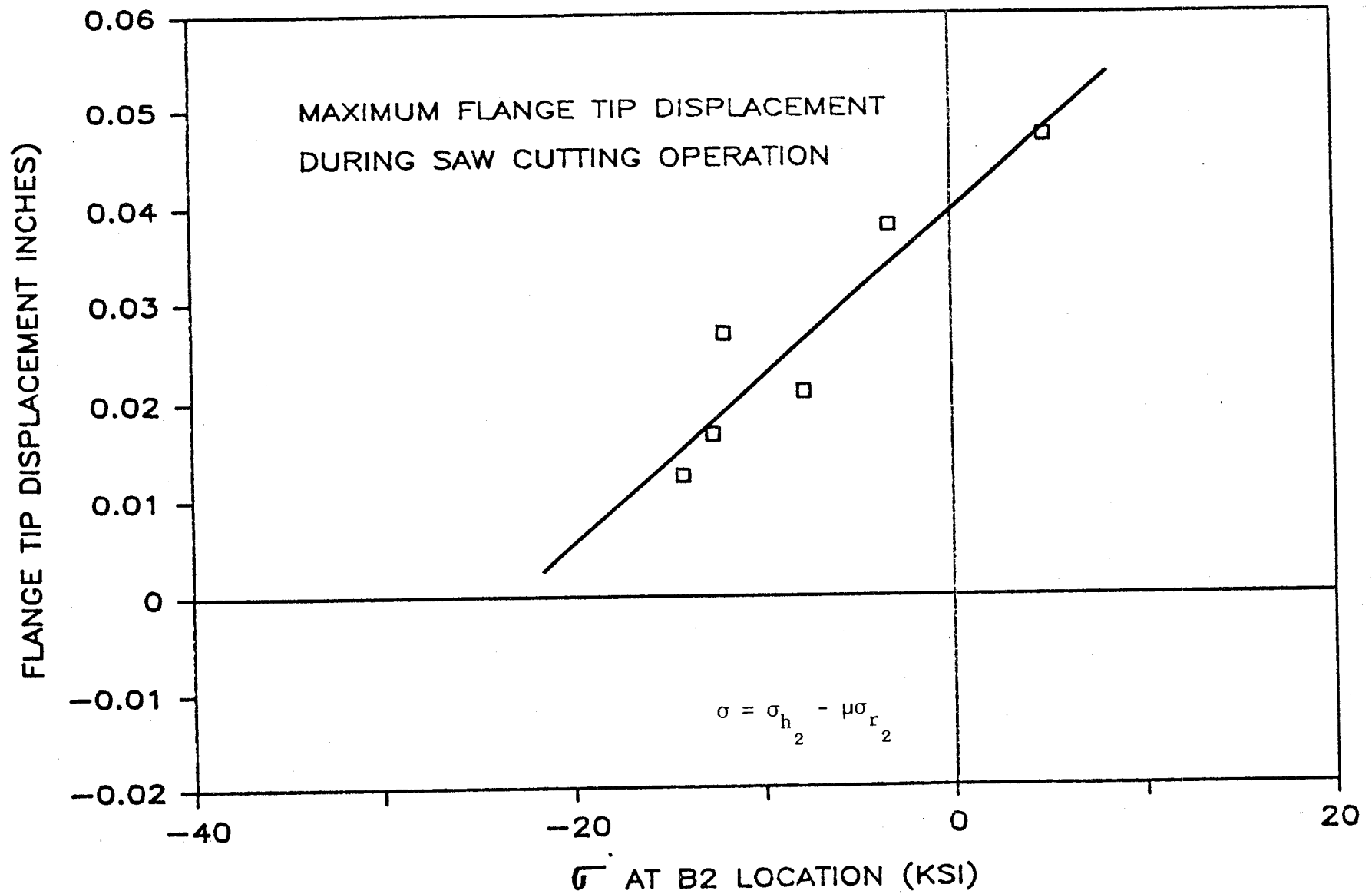


FIGURE 4.19. MAXIMUM FLANGE TIP DISPLACEMENT DURING SAW-CUTTING OPERATION VS σ AT B2 LOCATION ($\sigma = \sigma_{h_2} - \mu \sigma_{r_2}$).

4.3 WORK REMAINING

4.3.1 Conventional Elevated Temperature Fatigue Tests

The next phase of work includes duplicating the incremental step test at a strain rate of 0.00002 Sec⁻¹.

Relaxation and creep tests are scheduled following the completion of the incremental step tests.

4.3.2 Crack Arrest Tests

Task completed.

4.3.3 Thermal Cracking

We believe that we have established the test conditions necessary to produce cracking in Class U wheels by a mechanism similar to that of quench cracking. Therefore, testing of the twelve wheels (without thermocouples) will commence immediately. Thermography will be used to ascertain that adequate surface temperatures are being obtained. The criteria for evaluation of cracking will be based on inspections of the tread surface. Tentatively, the number of heating/cooling cycles required to produce the first cracking will be the criterion. However, testing of the wheels will be continued beyond detection of the first crack to determine if additional cracks form and if they grow in length. Other criteria can be selected based on these results.

Discussions at a review meeting indicated that the cracking behavior of wheels heated to a subcritical temperature (less than 1333°F) is also of some interest. In this case, martensite would not be formed and the cracks would initiate in a thermal-fatigue fashion in the normal ferrite-pearlite microstructure. If the program is changed to include this variable, half of the original wheels would be tested at the high temperature, and half would be tested at the lower temperature. Because of the different mechanics involved in the two types of cracking, the low temperature tests will require considerably longer testing times than the high temperature tests.

4.3.3.1 Infrared Thermal Video Test Plans

Infrared thermography will be used periodically during some of the tests to ascertain the distribution of temperature on the surface of the wheel in the vicinity of the heating torch.

4.3.3.2 Thermomechanical Analysis

The associated analytical task that remains is to estimate the magnitude of the thermomechanical strain cycle based on temperature measurements and thermal calculations.

4.3.4 Advanced Slow Strain Rate Tests

Incremental step cyclic strain tests with rates as slow as 0.000002 Sec⁻¹ and other tests, including some thermomechanical uniaxial

simulation realistic wheel strain and simultaneous temperature cycles (described in Stone to Gannett of 1/85) remain to be done.

4.3.5 Saw-Cutting Work Remaining

There are presently 117 wheels from the Burlington Northern Railroad and 14 test wheels (from RDU and Brake Dynamometer testing) awaiting saw-cutting.

4.4 SCHEDULE

4.4.1 Cyclic Properties Test Schedule

The incremental step tests are due for completion by mid September. Data reduction and reporting of the findings will be issued by mid October.

Scheduling for the relaxation and creep tests will be determined after results from initial tests are analyzed.

4.4.2 Crack Arrest

Work on this subtask is complete.

4.4.3 Schedule for Thermal Cracking Tests

If the original plan for testing 12 wheels by heating and cooling to

form martensite is used, the testing should be completed in about five months. However, if the plan is modified to incorporate testing of half the wheels by heating to subcritical temperatures, considerably longer testing time is anticipated because of the different mechanisms for producing cracking.

4.4.4 Advanced Slow Strain Rate Tests

These tests were initiated in October 1985 and are scheduled for completion in mid-December.

4.4.5 Schedule for Saw-Cutting

Saw-cutting will continue throughout the program in order to evaluate test wheels and strengthen the statistical confidence in service behavior predictions.

5.0 EFFECT OF HEAT TRANSFER AND RAIL LOADING (TASK 4)

5.1 CURRENT TASK STATEMENT OF WORK

The AAR shall determine the effect of heat transfer at the rail contact through careful experimental study under controlled conditions using the Roll Dynamics Unit (RDU), Brake Dynamometer (BDU), and the Induction Heating Facility. In support of the Induction Heating tests, the AAR shall develop finite element models for data analysis. Results of analysis and laboratory testing shall be compared with similar data (temperature and strains) from the Braking Tests (T5).

5.2 MAJOR FINDINGS/CURRENT STATUS

In keeping with this task objective to determine the effect of rail load and heat transfer on the development/alteration of wheel residual stresses and material damage generally, and to prepare for the evaluation and interpretation of in-track measurements, three laboratory experiments have been performed and are being analyzed. Status of these three tests (BDU, RDU and Induction Heating) follow.

5.2.1 Brake Dynamometer Status

The purpose of these studies is to determine the effects of wheel design, wheel heat treatment, speed, loading, and brake force on the alteration of residual stresses in wheels subjected to repetitive

drag braking on the AAR dynamometer. A secondary purpose is to determine the amount of heat transferred from the wheel to the reaction rail during some of these tests. Similar tests, but of other wheel designs, will be conducted in Task T6.

5.2.1.1 Wheels

The wheel design and heat treatments are listed in Table 5.1 along with the braking conditions. Included in the T4 portion of the study are new 33-inch diameter, one wear, parabolic and straight plate wheels with new rim profiles and with rims turned down to the reapplication limit. Heat treatments include Class U, Class U that have been reprocessed and designated as A in the table, and Class C. The chemical compositions of the wheels are essentially the same. The T6 study will be concerned with 33-inch diameter wheels and 36-inch diameter wheels with parabolic, S-shape, and straight plates. Wheels turned to the reapplication rim thickness and reheat-treated Class U wheels are not included in T6.

5.2.1.2 Instrumentation

Each wheel was instrumented with one strain gage on the front hub-plate fillet and three thermocouples: (1) a sliding type on the tread, (2) a washer type on the back-rim face, and (3) a washer type on the back rim fillet, as illustrated in Figure 5.1. The strain gage was monitored at the start and end of each heating cycle with a static strain indicator. The thermocouples were monitored continuously with a strip chart recorder.

TABLE 5.1. DYNAMOMETER TEST* FOR TASKS T4 AND T6 (WHEEL OR NUMBER TEST).

Section	Plate Type	Class**	Rim Type***	Low Speed (20 mph)			High Speed (40 mph)		
				HBF+	LBF+	UHB+	HBF	LBF	UHB
<u>TASK T4</u>									
CJ 33	Parabolic	A	N	--	--	--	3	-	-
			R	--	--	--	4	-	-
		U	N	5	--	6	7	-	-
			R	--	--	--	8	-	-
C	N	9	--	10	11	12	-		
J 33	Straight	A	N	--	--	--	13	-	-
			R	--	--	--	14	-	-
		U	N	15	--	16	17	18	-
			R	--	--	--	19	-	-
		C	N	20	--	21	22	-	-
								23++	-
C	N	--	--	--	24+++	-	-		
<u>TASK T6</u>									
J 33	S-Shape	U	N	--	--	--	25	-	-
			C	--	--	--	26	-	-
CH 36	Parabolic	U	N	--	--	--	27	-	-
			C	--	--	--	28	-	-
H 36	S-Shape	U	N	--	--	--	29	-	-
			C	--	--	--	30	-	-
H 36	Straight	U	N	31	--	32	33	34	-
			C	35	--	36	37	-	-

* Instrumentation consists of one metal strain gage on the front hub-plate fillet and thermocouple on the tread, back rim face, and front hub-plate fillet. Each wheel will be drag-brake tested for 25 heating/cooling cycles.

** A = Annealed Class U - not Class A

*** N = New, R = Reapplication Limit

+ HBF = High Brake Force, about 1,500 lbs
 LBF = Low Brake Force, about 750 lbs
 UHB = Unreleased Hand-brake force, about 3,000 lbs

++ With vertical and lateral loads

+++ Without loads

All numbers in the table represent wheel numbers.

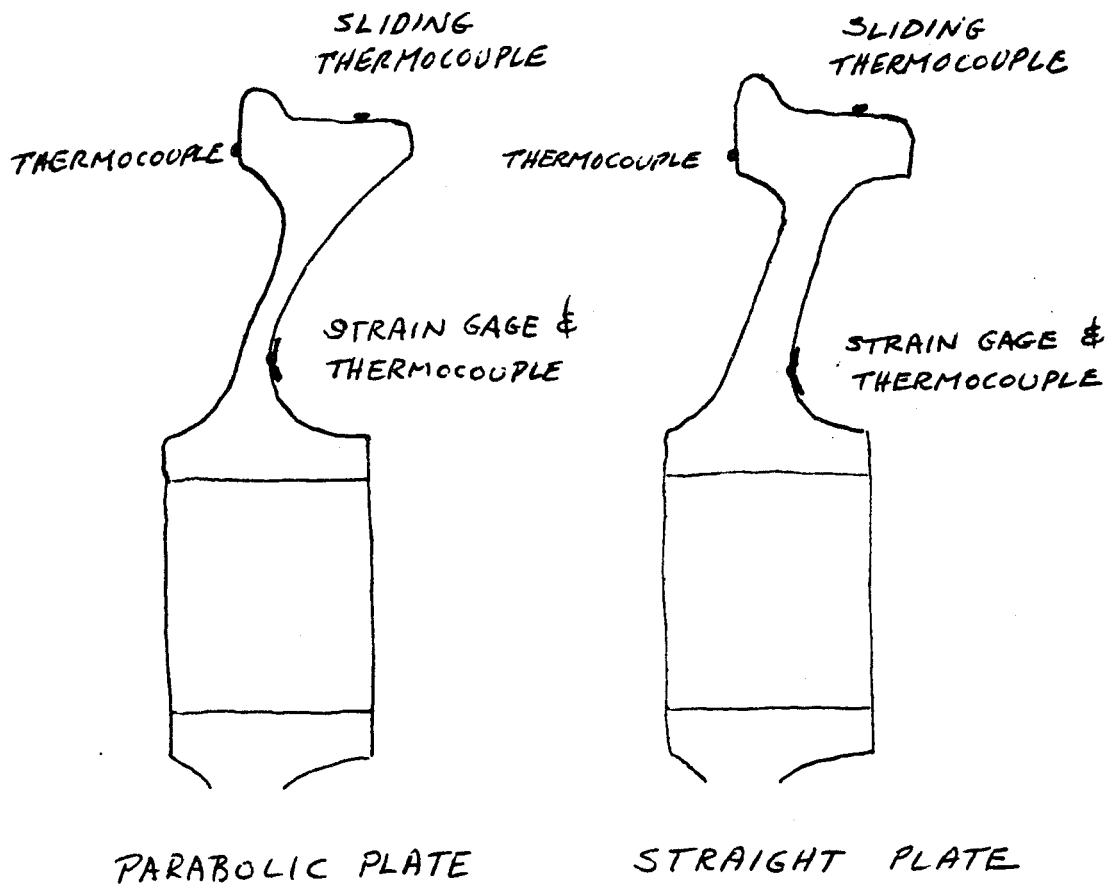


FIGURE 5.1. LOCATIONS OF THERMOCOUPLES AND STRAIN GAGES.

For the heat transfer portion of the study, additional sliding thermocouples were mounted on the reaction rail running surface and/or the wheel tread. An infrared pyrometer was also used for some tests.

5.2.1.3 Test Conditions

Table 5.1 shows the braking conditions for each wheel. The wheel speed was maintained constant while the brake (AAR M926) was applied for 45 minutes. The brake was released and the wheel speed was reduced to 20 rpm so that the wheel could be cooled to ambient temperature with water spray on the plate and rim. This cycle was repeated a total of 25 times for each wheel. During these tests, a vertical load was applied to the outboard or journal bearing to produce a vertical load of about 28,000 pounds on the wheel tread. All wheels had this load except wheels 5 and 24. Wheel 5 had a variable vertical load and wheel 24 had no vertical load.

5.2.1.4 Results

The ultimate objective of these tests is to determine the relationship of the wheel design and heat-treatment variables and drag-braking conditions on the alteration of residual stresses in the wheels. This cannot be done yet because the residual stress portion of the program will be done later. However, some observations can be made on the relationships of speed, brake shoe force, and vertical load (wheel 5) to wheel temperature, apparent strain at the front hub-plate fillet, and heat transfer to the reaction rail.

Appendix 5.1 lists the strain and temperature data obtained to date. These data are summarized in Table 5.2. Most of the heat transfer studies were conducted on wheel 5, Appendix 5.1, Table 1. Strain data were not obtained for this wheel. The temperature data show that it was not practical to use thermocouples on the rail surface to detect the incremental rise in temperature of the rail caused by contact with the heated wheel. The data showed inconsistencies of temperature differential of the two rail thermocouples located ahead and behind the contact zone. With regard to the increase in wheel and rail temperatures during the tests, it appears that both temperatures are markedly affected by the vertical load. For example, tests with a vertical load of about 27 kips produced average wheel tread and rail temperatures of 487 and 161°F, respectively. In contrast, tests with a vertical load of about 5 kips produced average wheel tread and rail temperatures of 528 and 106°F, respectively. Tests with a vertical load of 13.5 kips produced intermediate temperatures. Thus, increasing the wheel load decreased the wheel temperature and increased the rail temperature. This effect is probably caused by a corresponding increase in contact area.

The effects of wheel/rail contact on the strains and temperatures developed in the wheels from drag braking is further illustrated by the behavior of wheel 12 (Table 5.3 and Figures 5.2 and 5.3). This wheel was tested at 40 mph with a brake force of 750 lbs with the intended vertical load of 27 kips for the first six cycles, and then with no vertical load for the remaining 19 cycles. The change in loading was made because of excessive vibration in the outboard

TABLE 5.2. TEMPERATURE AND STRAIN RESULTS.

Wheel No.	Strain, $\mu\epsilon$	Temperature, °F							
		Cold	Hot	Tread		Rim		Plate	
				Cold	Hot	Cold	Hot	Cold	Hot
5	Max Min Avg			75	500				
6	Max Min Avg	+164 -303 - 41	+3242 +2276 +2556	100 65 83	845 500 573	- - -	- - -	95 65 81	220 160 191
7	Max Min Avg	+282 - 77 + 99	+2574 +2013 +2385	95 50 74	700 525 579	95 50 79	535 420 485	95 50 78	205 150 184
9	Max Min Avg	+143 - 43 + 47	+2440 +2180 +2259	100 60 76	590 530 565	100 55 76	490 430 446	100 60 82	195 155 184
10	Max Min Avg	+123 - 87 + 30	+2592 +2128 +2399	95 75 85	795 550 623	95 80 85	580 520 543	95 80 85	205 155 185
11	Max Min Avg	0 -129 - 66	+1786 +1215 +1381	100 75 84	610 370 525	85 75 81	470 400 422	85 75 80	180 150 162
12	See Table 5.3 and Figures 5.2 and 5.3								
15	Max Min Avg	-210 0 +127	+3222 +2342 +2839	120 70 93	790 545 628	110 65 85	505 420 467	100 65 73	210 170 196
16	Max Min Avg	+405 -500 -258	+3442 +1902 +2533	110 70 79	785 490 620	100 50 77	610 460 532	80 60 70	220 145 186
18	Max Min Avg	+ 56 -344 -127	+2760 +2071 +2400	100 75 80	595 405 527	80 75 78	515 385 446	85 75 77	170 145 151
17	Max Min Avg	+440 -205 - 15	+3605 +2184 +2816	115 60 87	725 450 573	110 50 83	545 390 467	110 50 82	205 140 174

$\mu\epsilon$ = Micro inch/inch

"Max" and "Min" are the extreme values of strains measured when wheel was cold and when wheel was hot, "Avg" represents the average of 25 strain values.

TABLE 5.3. DYNAMOMETER DATA FOR WHEEL #12 (7/31/85-8/6/85).

Test #	Gage-Cold $\mu\epsilon$	Gage-Hot $\mu\epsilon$	Wheel Load Kips	Ambient Temperature F	Tread Temperature F	Rim Temperature F	Comments
1	0		27	80	495	450	
2			27	85	495	420	
3	-164	1653	27	75	500	450	
4	-205	1662	27	90	510	430	
5	-303	1756	27	90	530	440	
6	-60	1951	27	75	530	425	
7	0	2740	0	80	675	515	Vert. load removed
8	-39	2922	0	95	720	550	
9	-124	2816	0	90	720	525	
10	5	2855	0	80	730	560	47.7 min. test
11	7		0	95	760	520	
12	-6	2794	0	80	750	525	47.39 min. test
13	-96	2754	0	95	770	540	
14	-134	2621	0	95	650	500	
15	98	1760	0	80	435	395	New shoe aft. 25 min.
16	0	2186	0	90	510	430	
17	195	2370	0	85	560	480	
18	47	2492	0	90	620	495	
19	75	2780	0	95	690	545	
20	137	3074	0	80	680	580	
21	13	3080	0	95	620	580	
22	94	3028	0	85	600	560	
23	11	2958	0	90	630	550	
24	50	2951	0	95	630	520	
25	3	2755	0	80	650	545	
Avg	1-6	-146.4	1775.5	27.0	82.5	510.0	435.8
Std	1-6	106.9	119.9	0.0	6.3	15.0	11.7
Avg	7-14	-48.4	2786.0	0.0	88.8	821.9	529.4
Std	7-14	56.4	88.3	0.0	7.0	38.7	18.3
Avg	15-25	65.7	2675.4	0.0	87.7	602.3	516.4
Std	15-25	59.0	406.9	0.0	5.8	71.6	57.8
Avg	7-25	17.7	2718.4	0.0	88.2	652.6	521.8
Std	7-25	80.8	327.3	0.0	6.3	84.2	46.0
Avg	1-25	-16.5	2543.3	6.5	86.8	618.4	501.2
Std	1-25	109.5	477.7	11.5	6.8	95.7	54.7

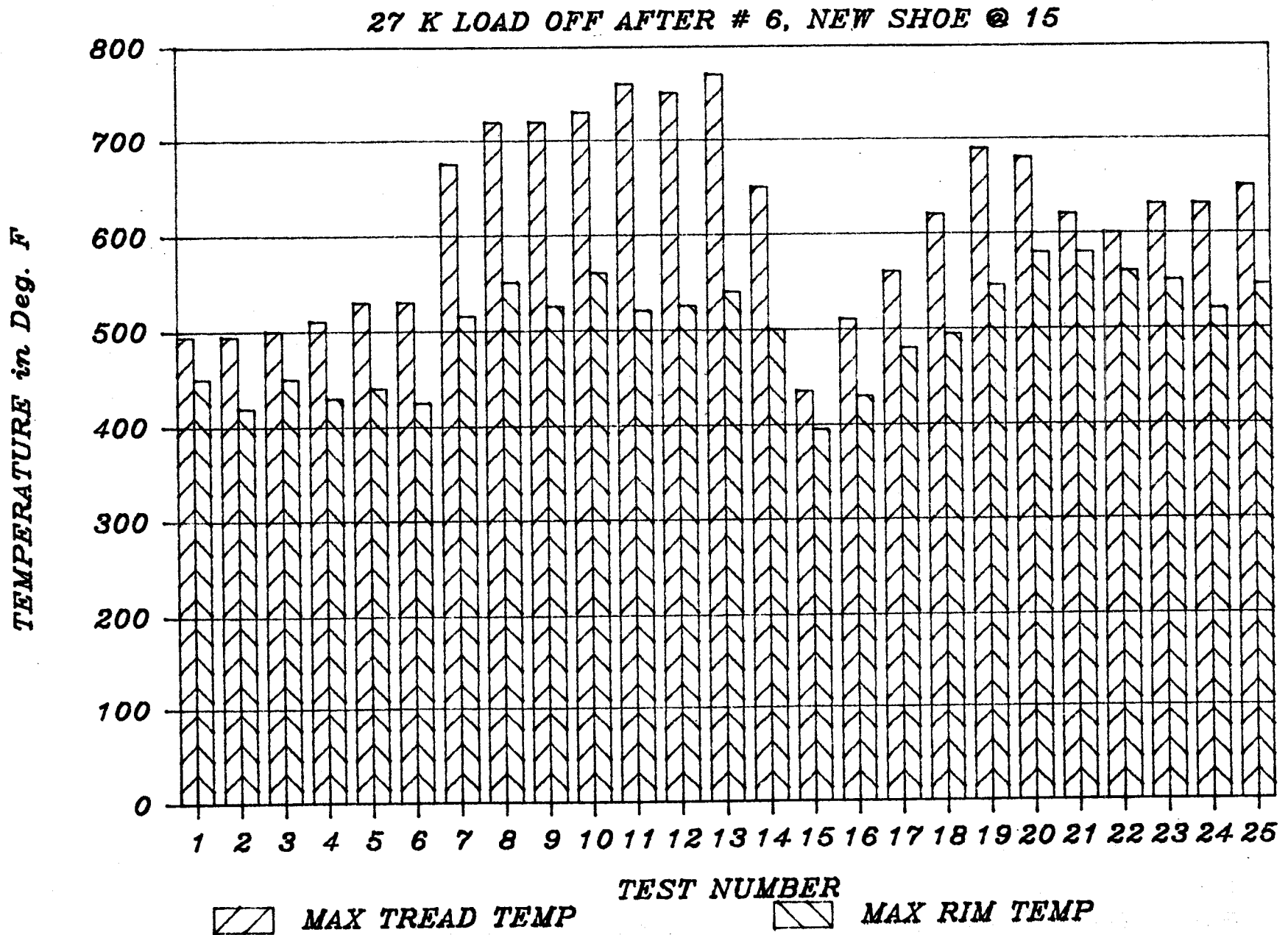


FIGURE 5.2. TEMPERATURE IN REPEAT DYNAMOMETER TESTS, CJ33 #12.

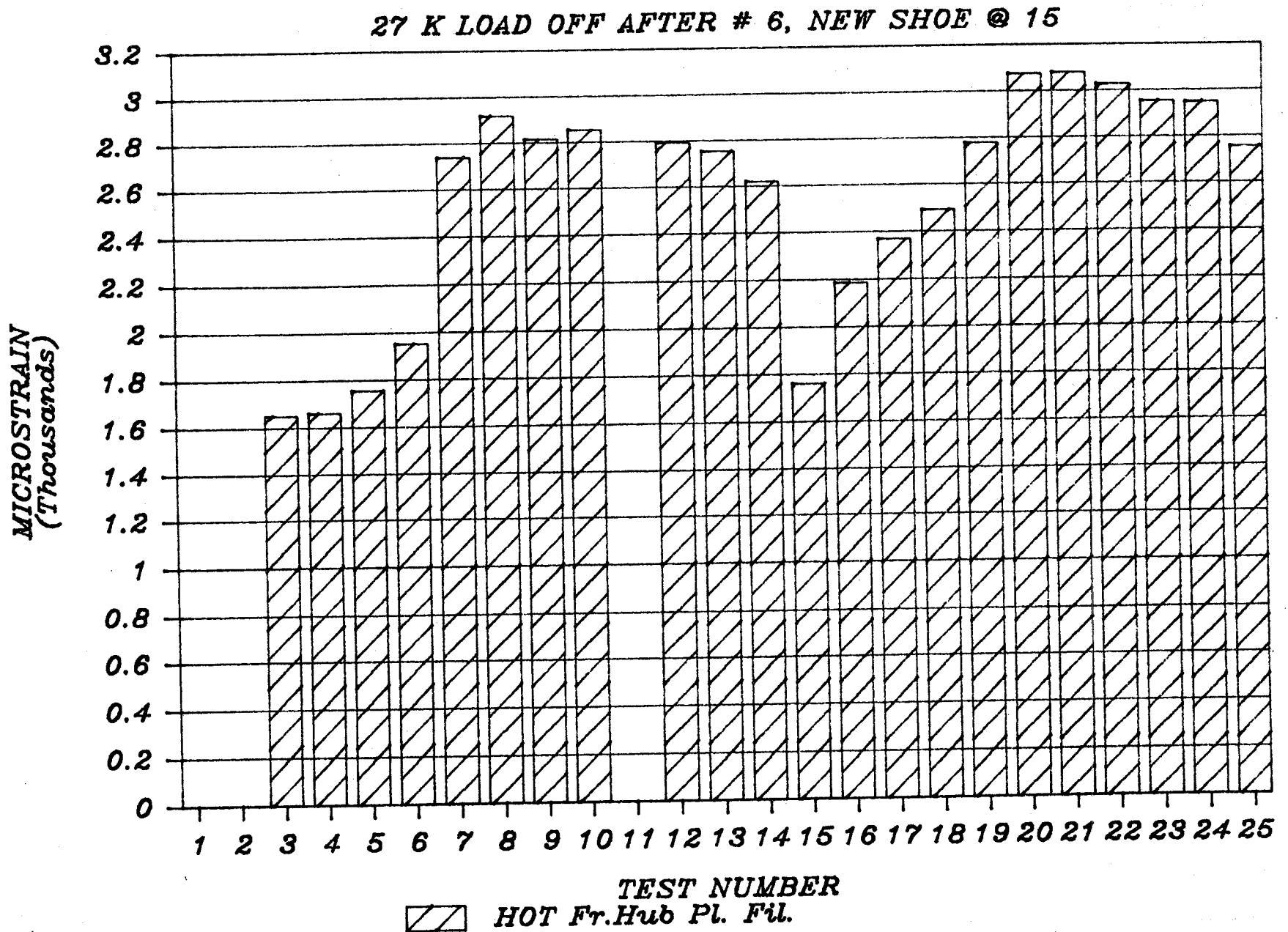


FIGURE 5.3. STRAIN IN REPEAT DYNAMOMETER TESTS CJ-33C #12.

bearing. Prior to this change, the wheel was being heated to about the same temperatures and strain values as the other wheel that had the same braking and loading conditions (wheel 18). Subsequently, with no vertical load, maximum temperatures increased by about 100°F on the tread and rim and the hot wheel strain increased by about 1000 $\mu\epsilon$, thus confirming that the rail wheel and the associated vertical load remove a substantial amount of heat from the test wheel.

Table 5.2 shows the representative samples of the maximum, minimum and average in the radial direction at the front hub-plate fillet as well as the temperatures for the tread, rim, and plate for the 25 tests. Values shown are for two points in time: (1) when the wheel was coldest and (2) when the wheel was hottest. The strain values of most importance are those measured when the wheel is coolest (minimum). Negative values indicate that the rim is smaller than it was originally, and is probably in a state of tensile residual hoop stress. The saw-cutting tests, to be conducted later, should confirm this. Strain values measured when the wheels are hottest indicate the relative expansion of the rim due to braking. Unusually high or low values of hot strain appear to be associated with unusually high or low tread temperatures. For example, the highest strain value for wheel 6, +3242 $\mu\epsilon$, was associated with the highest tread temperature, 845°F. Rim temperatures were about 120°F below those of the tread. Front hub-plate fillet temperatures were even lower, being generally around 200°F or less.

The power input to the 33-inch diameter wheel is related to the brake force and speed by the following:

$$\text{Power Input (BHP)} = \frac{\text{Brake Force (lbs)} \times \mu \times \text{Speed (mph)}}{375}$$

This equation gives power inputs of 24 and 48 BHP for the combinations of speed and brake force used in these tests when the coefficient of friction, μ , is assumed to be 0.3. However, the coefficient of friction of AAR M926 high-friction composition brake shoe is not constant, but decreases with increasing brake force, speed, and temperature of wheel and/or brake shoe. Other factors affecting μ are the contact area, wheel surface roughness and possible changes in the friction characteristics of the materials due to use. Therefore, when drag braking tests are conducted with a constant brake force, the horsepower changes (decreases) during the course of the 45 minute braking cycle and is consistent from cycle to cycle. Furthermore, because of the speed and force dependence of μ , doubling speed or brake force should not exactly double the horsepower. There is a considerable variation of heating among wheels exposed to essentially the same braking conditions. For example, wheels 7, 11 and 17 were exposed to 1,500 lbs brake force at 40 mph, but their average peak tread temperatures were 579°F, 525°F, and 573°F, respectively. Further, wheels 6, 10, and 16 were exposed to 3,000 lb brake force at 20 mph, and to corresponding average peak tread temperatures of 573°F, 623°F, and 620°F.

The variation of the coefficient of friction during a drag-brake heating cycle is illustrated by the torque curve shown in Figure 5.4. Torque for two of the wheels, 9 and 10, was measured with the strain gage torsion cell built into the axle. These torque values represent a combination of torque or retarding forces times radius, from two sources. These are brake shoe friction and traction or rolling resistance between the wheel and rail. Therefore, the values presented in Figure 5.4 do not reflect only the retarding forces due to braking. It is possible that the rolling resistance also changes during the test.

5.2.1.5 Heat Transfer Analysis

An important part of this task is to estimate the amount of heat transfer at the wheel/rail contact patch based on appropriate measurements. As described above, one approach was to measure the rail wheel temperature rise before and after passing through the hot wheel tread contact patch. It would then be theoretically possible, using transient thermal analyses such as those adapted to Brake Dynamometer Unit (BDU) application in Appendices 5.2 and 5.3, to estimate the "strength" of the heat source or power transmitted through contact. Although experimental difficulties with the sliding thermocouple were experienced that so far have prevented reliable application of this approach (see Figure 5.5), a review of Table 5.4 suggests that there is, on the average, a measurable increase in temperature from "lead-to-trail" position. It is significant to note that a temperature rise of only 15°F (measured 16

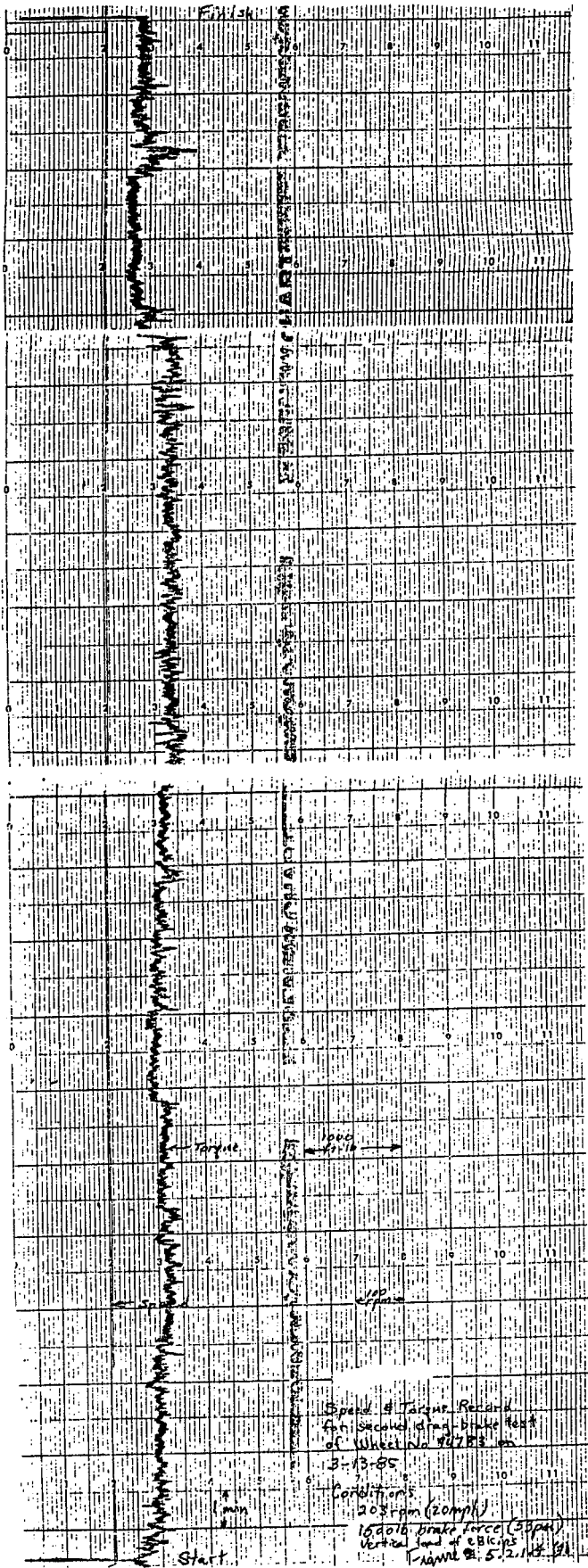


FIGURE 5.4. SPEED AND TORQUE RECORD FOR SECOND DRAG BRAKE TEST,
WHEEL #94783.

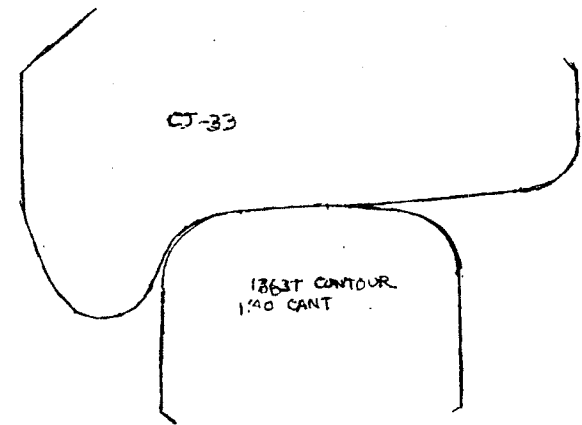
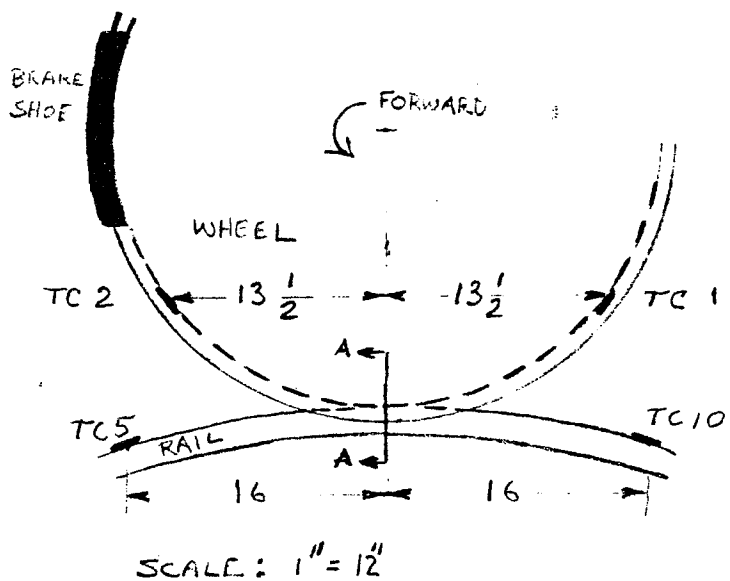


FIGURE 5.5. ARRANGEMENT OF WHEEL, RAIL, AND THERMOCOUPLES FOR HEAT TRANSFER TESTS OF WHEEL 5.

TABLE 5.5. HEAT TRANSFER ANALYSIS.

<u>Test</u>	<u>Direction</u>	<u>Test Conditions</u>				<u>Thermocouple Readings (°F)</u>			
		<u>Speed (mph)</u>	<u>Brake Shoe Force (lb)</u>	<u>Vertical Load (lb)</u>	<u>Time (Min)</u>	<u>TC2</u>	<u>TC1</u>	<u>TC5</u>	<u>TC10</u>
1		0	0	0	0	65	65	65	65
2	Forward	20	1200	26800	45	478	435	153	180
3*	Forward	20	0	26800	30	135	120	95	105
4**	Forward	20	0	26800	15	132	140	88	105
5	Reverse	20	0	26800	18	132	154	90	105
6	Reverse	20	1200	26800	45	***	***	145	130
7*	Reverse	30	0	26800	22	***	***	85	83
8	Reverse	30	1200	26800	20	***	***	150	135

 * After wheel was cooled with water
 ** Next day after one stop from 20 mph
 *** Thermocouple failure

inches trailing contact) would indicate a heat transfer rate of 7.75 HP for typical test conditions described and computed in Appendix 5.3.

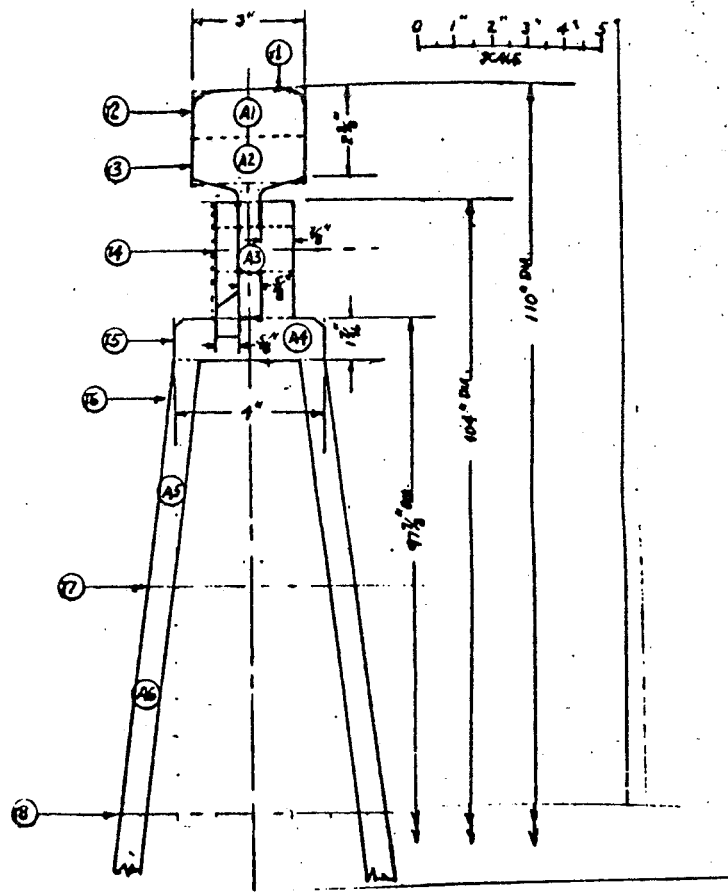
The other approach used to estimate the amount of heat transfer is to measure the slow rise in average rail temperature over time and use the first law of thermodynamics. This is illustrated in Appendix 5.4. A heat transfer rate of 7.3 HP was calculated based on measurements made (4/26/85) on a 40 mph nominal 50 BHP run.

Since convection heat losses were ignored this would be a lower estimate of at least 14.7% of the nominal power input at brake shoe.

5.2.1.5.1 Estimate of Convection Heat Loss

Measurements of the rate of cool-down of the rail wheel following a braking test while the wheel is still turning at test speed but under reduced (minimum) load have also been made in order to provide data for analysis of convection losses. Data are shown in Figure 5.6.

Although an analysis of these transient cool-down data is not complete, a rough estimate of the convection heat loss from the rail wheel as it heats up during the test may be obtained by using a nominal value of convection coefficient such as that given in AAR Standard S-660 -83 of 4 BTU/hr-sq ft-F. The basic equation for convection heat loss rate is:



BDU COOL DOWN*

40 MPH UNDER REDUCED LOAD (MIN)

** BRAKE OFF AT
10:31:30 AND
VERTICAL LOAD
REMOVED

CLOCK TIME**	Δ SEC	T1	$\frac{T2+T3}{2}$	T4	T5	T6 (F)
10:31:30	0	149	141	109	93	85
10:35:49	259	140	134	98	90	82
10:40:00	510	132	130	96	—	—
10:44:58	808	122	120	94	85	80
10:48:00	990	117	110	90	82	80

* DATA TAKEN FROM TAPE MADE BY
HUGHES AIRCRAFT CO. 'PROBEYE'
THERMAL VIDEO SYSTEM OF 4/26/85
TEST IN CHICAGO

FIGURE 5.6. COOL DOWN TIMES FOLLOWING BRAKE TEST.

$$q_c = hA\Delta T \text{ (BTU/HR)}$$

where

h is the convection coefficient area taken as 4 BTU/hr-sq ft-F

A is the rail head area

ΔT is the surface average temperature differential relative to ambient air in °F

If a simple linear temperature buildup during the test is assumed the rate equation above may be integrated for the following simple results:

$$Q_c = \frac{hA}{2} \Delta T_{\max} t$$

where ΔT_{\max} is the maximum temperature differential reached at the end of test period t hours. The average surface temperature of the rail wheel head at the end of test ($t = 0.766$ hours) is taken as the average of temperatures of the rail top surface, $T_1 = 160^\circ\text{F}$, and lower side, $T_3 = 146^\circ\text{F}$. Ambient air temperature was 75°F . The convection heat loss during the test is then calculated to be:

$$Q_c = \frac{4 \times 24}{2} \times \left[\frac{(160 + 146)}{2} - 75 \right] \times 0.766 = 2868 \text{ BTU}$$

The heat loss would require an additional average contact patch input: $2868 \text{ BTU} \div 0.766 \text{ HR} \div 2544.5 \text{ BTU/HR/HP} = 1.47 \text{ HP}$.

This calculation suggests that the 7.3 HP contact patch heat transfer rate estimate based on nonconvection losses is some 20% low. A "corrected" heat transfer rate of 8.8 HP is thus obtained. Since the nominal input brake HP for test was 50 BHP, the percentage loss

through rail/wheel contact would be about 18%. Perhaps an even higher percentage may be expected if the actual average BHP input was lower than 50 BHP due to reduction in brake shoe coefficient of friction below nominal.

5.2.1.5.2 Effect of Rail Load on Heat Transfer

The effect of rail load on the estimated heat transfer rate has also been estimated based on temperature measurements under three load levels. The results are shown in Figure 5.7. The calculated contact areas are also given below the graph for each test load. The rate of heat transfer appears to be roughly proportional to contact area.

5.2.2 Status of Testing on Roll Dynamic Unit

The objective of testing conducted on RDU is to investigate the effects of brake force and speed on the alteration of residual stresses in wheels for a given wheel design, heat treatment and wheel loading. The secondary purpose is to estimate the amount of heat transferred from the wheel to the roller during a few tests. The majority of tests were conducted in the drag braking mode for a sixty minute duration while the rest were executed under the stop braking mode.

The test wheels selected for testing on RDU were restricted to Class U, 33-inch diameter and parabolic plate design. All the wheels were brand new before instrumentation.

through rail/wheel contact would be about 18%. Perhaps an even higher percentage may be expected if the actual average BHP input were lower than 50 BHP due to reduction in brake shoe coefficient of friction below nominal.

5.2.1.5.2 Effect of Rail Load on Heat Transfer

The effect of rail load on the estimated heat transfer rate has also been estimated based on temperature measurements under three load levels. The results are shown in Figure 5.7. The calculated contact areas are also given below the graph for each test load. The rate of heat transfer appears to be roughly proportional to contact area.

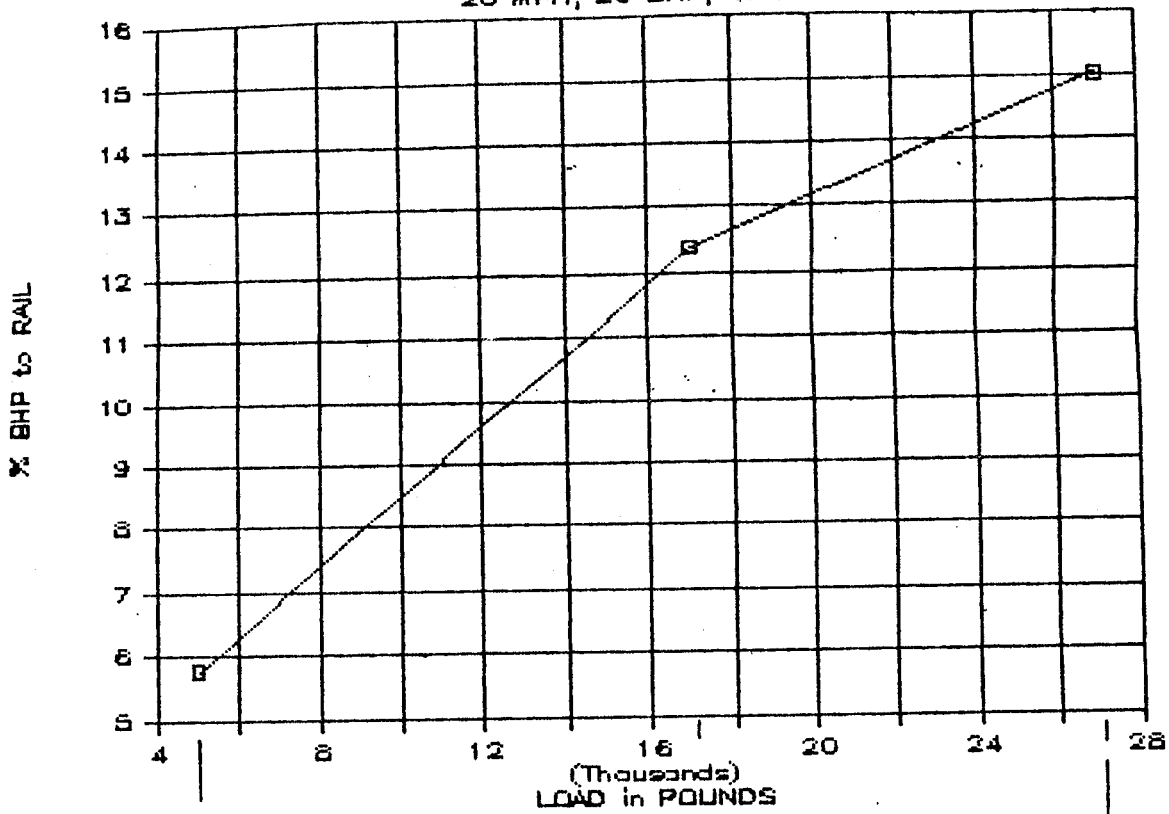
5.2.2 Status of Testing on Roll Dynamic Unit

The objective of testing conducted on RDU is to investigate the effects of brake force and speed on the alteration of residual stresses in wheels for a given wheel design, heat treatment and wheel loading. The secondary purpose is to estimate the amount of heat transferred from the wheel to the roller during a few tests. The majority of tests were conducted in the drag braking mode for a sixty minute duration while the rest were executed under the stop braking mode.

The test wheels selected for testing on RDU were restricted to Class U, 33-inch diameter and parabolic plate design. All the wheels were brand new before instrumentation.

EFFECT of LOAD on HEAT TRANS. to RAIL

20 MPH, 20 BHP, 45 MIN



$$A = 0.071 \text{ IN}^2$$

$$P_{AV} = 68 \text{ KSI}$$

①

$$\% \text{ BHP} = 5.8$$

$$\Delta T = 35^\circ \text{ F}$$

IN 45 MIN

$$A = 0.165$$

$$P_{AV} = 103 \text{ KSI}$$

②

$$A_2/A_1 = 2.32$$

$$P_2/P_1 = 1.51$$

$$\% \text{ BHP} = 12.4$$

$$\frac{\text{BHP}_2}{\text{BHP}_1} = 2.14$$

$$\Delta T = 75^\circ \text{ F}$$

IN 45 MIN

$$A = 0.225$$

$$P_{AV} = 120 \text{ KSI}$$

③

$$A_3/A_1 = 3.17$$

$$P_3/P_1 = 1.76$$

$$\% \text{ BHP} = 15.0$$

$$\frac{\text{BHP}_3}{\text{BHP}_1} = 2.59$$

$$\Delta T = 91^\circ \text{ F}$$

IN 45 MIN.

$\therefore \Delta \text{BHP} \propto A_{\text{CONTACT}}$

NOTE: NO MEAS. TEMP RISE TO TURN RAIL WHL.
 RAIL CONVECTION HT. LOSS TEST
 ... MEAS. OF $T_{\text{in}} - T_{\text{out}}$ ETC

FIGURE 5.7. EFFECT OF LOAD ON HEAT TRANSFER TO RAIL.

5.2.2.2 Instrumentation

Figure 5.8 presents the description of Test Trucks 1 and 2. Truck 1 was provided with limited instrumentation (only thermocouples), while Truck 2 was instrumented fully with high temperature strain gages and thermocouples.

Test Truck 1 was made ready with thermocoupled wheels, slip rings, and instrumented brake heads. The Static Golden Brake Shoe Test was performed for the validation of instrumented brake heads on the RDU. Brake rigging for Test Truck #1 on the RDU was retrofitted, similar to that of a 70-ton car truck.

The performance of various transducers, slip rings, signal conditioning equipment, and data collection were checked out during the first series of tests and the necessary remedial action for certain failures was taken.

Truck 2 was made ready with fully instrumented wheelsets with typical instrumentation layout as presented in Figures 5.9 and 5.10.

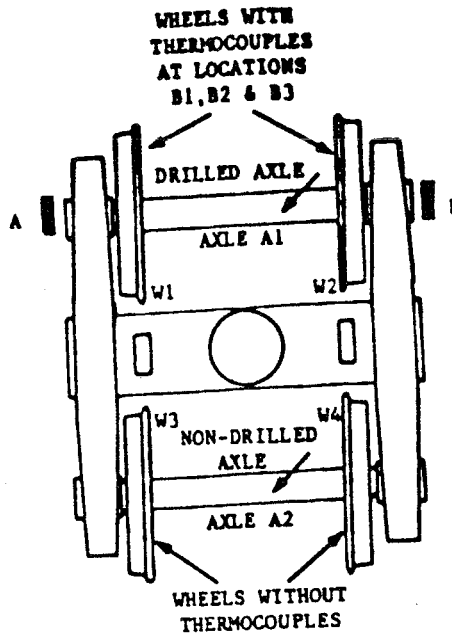
5.2.2.3 Test Conditions

Test Truck 1 was tested with a series of drag braking and stop braking cycles at different speeds and for different periods of time as per Table 5.5. A series of braking and stop braking tests were conducted on Truck 2 as per Table 5.6. Hole drilling strain gage method was used to estimate residual stresses at certain critical

WHEEL FAILURE MECHANISMS OF RAILROAD CARS TEST TRUCKS FOR RDU TESTING

(RDU) TEST TRUCK 1

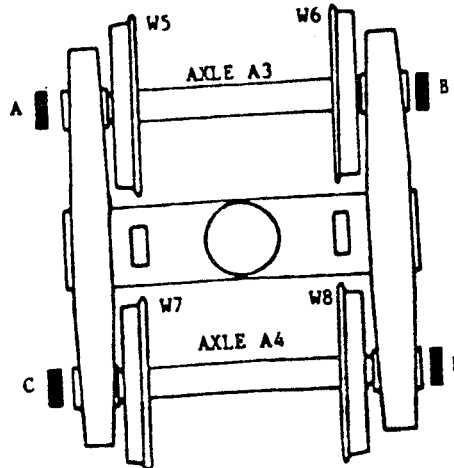
- 1) All Wheels: Class U, Parabolic Plate, New, Griffin CJ33
- 2) A&B - Slip Rings



WHEEL I.D.	SERIAL NO
W1	95554
W2	95551
W3	94552
W4	95528

(RDU) TEST TRUCK 2

- 1) All Wheels: Class U, Parabolic Plate, New, Griffin CJ33
- 2) A,B,C, & D - Slip Rings
- 3) Both Axles - Drilled
- 4) All Wheels Strain Gaged & Thermocoupled at Locations B1, B2, & B3.



WHEEL I.D.	SERIAL NO.
W5	94559
W6	94550
W7	94565
W8	94566

*BNA's theme
Nov 9, 1984*

FIGURE 5.8. WHEEL FAILURE MECHANISMS OF RAILROAD CARS TEST TRUCKS FOR RDU TESTING.

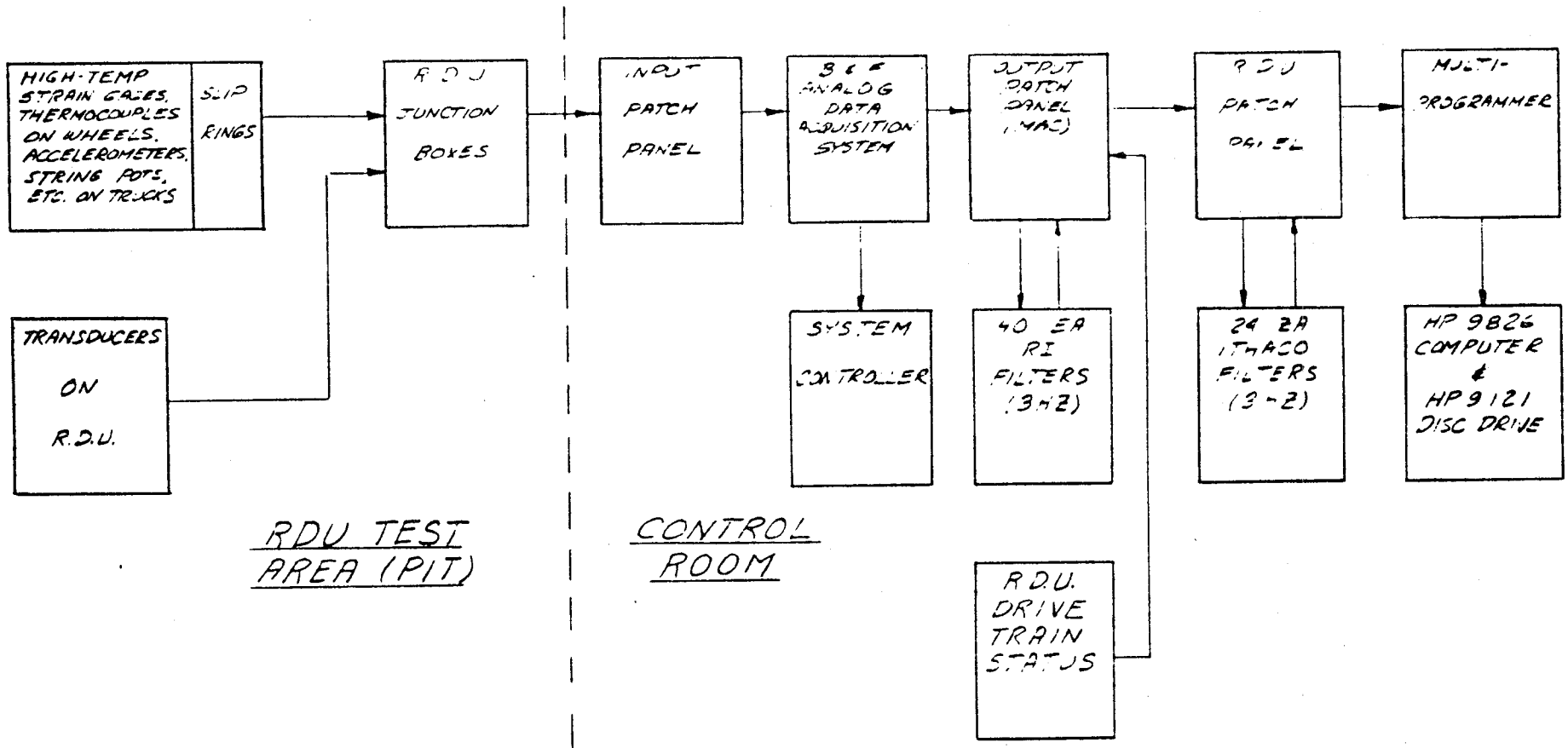


FIGURE 5.10. INSTRUMENTATION SCHEME FOR TEST SERIES #2.

TABLE 5.5. TESTING OF TRUCK #1 ON RDU (DRAG BRAKING).
 TASK ORDER #6
 WHEEL FAILURE MECHANISMS

<u>Date</u>	<u>Run No.</u>	<u>Brake Cylinder Pressure (psi)</u>	<u>Speed (mph)</u>	<u>Duration (minutes)</u>	<u>Direction</u>	<u>Axle Vertical Load (kips)</u>
02/25/85	2	30	30	60	West	44
02/26/85	3	30	30	60	East	44
02/27/85	4	40	40	30	West	52
02/28/85	5	40	40	40	East	52
03/01/85	6/7	40	45	30	West	52
03/04/85	8/9	45	40	30	East	52
03/05/85	10/11	50	30	60	West	52
03/06/85	12/13	50	30	60	East	52
03/07/85	14/15	60	20	60	West	52
03/08/85	16/17	50	40	60	East	52
03/18/85	18/19	45	40	60	West	52
03/18/85	20/21	50	35	60	East	52

<u>Brake Cylinder Pressure (psi)</u>	<u>Average Normal Force/Shoe (lbs)</u>
30	900
40	1400
50	1800
60	2200
45	1600

TABLE 5.5. TESTING OF TRUCK #1 ON RDU (STOP BRAKING CYCLES).
 TASK ORDER #6
 WHEEL FAILURE MECHANISMS

<u>Sl. No</u>	<u>Run.No.</u>	<u>Brake Cylinder Pressure (psi)</u>	<u>Initial Speed (mph)</u>	<u>Direction</u>	<u>Axle Vertical Load (Kips)</u>
1	22	50	30	West	52
2	23	60	30	West	52
3	24	50	35	East	52
4	25	60	35	East	52
5	26	50	40	West	52
6	27	60	40	West	52
7	28	50	50	East	52
8	29	60	50	East	52

TABLE 5.6. TESTING OF (INSTRUMENTED) TRUCK #2 ON RDU.
 TASK ORDER #6
 WHEEL FAILURE MECHANISMS

Average Vertical Load/Axle 52 Kips (Simulating Fully-Loaded 70-Ton Car)

Date	Run No.	Brake Cylinder Pressure (psi)	Speed (mph)	Duration (minutes)	Direction	Remarks
4/2/85	30/31	20/60				Static Brake Shoe Tests
4/2/85	32/33	10/20	20	80	West	Cleaning of new tread surfaces
4/3/85	34/35/36	30	30	60	West	Four video cameras in position for observing front & back of wheels #6 & #8
4/3/85	37/38	30	30	60	East	"
						(Hole Drilling Performed on Wheel #5 at B1, B2, B3 Locations)
4/4/85	39/40	40	30	60	West	"
4/4/85	41/42	40	30	60	East	"
						(Hole Drilling Performed on Wheel #6 at B1, B2, B3 Locations)
4/8/85	43/44	50	30	60	West	"
4/8/85	45/46	50	30	60	East	"
						(Hole Drilling Performed on Wheel #7 at B1, B2, B3 Locations)
4/9/85	47/48	50	25	60	West	"
4/9/85	49/50	50	25	60	East	"
						(Hole Drilling Performed on Wheel #5 at B1, B2, B3 Locations)
4/10/85	51/52	40	25	60	West	"
4/10/85	53/54	40	25	60	East	"
						(Hole Drilling Performed on Wheel #8 at B1, B2, B3 Locations)

TABLE 5.6. TESTING OF (INSTRUMENTED) TRUCK #2 ON RDU.
 TASK ORDER #6
 WHEEL FAILURE MECHANISMS

Average Vertical Load/Axle 52 Kips (Simulating Fully-Loaded 70-Ton Car)

Date	Run No.	Brake Cylinder Pressure (psi)	Speed (mph)	Duration (minutes)	Direction	Remarks
4/11/85	55/56	45/60	42/50	60	West	a) " b) Severe sustained drag braking to hold 50 BHP for at least first 30 minutes
4/11/85	57/58	45	42	30	East	a) 4 video cameras b) Sustained drag braking (after this test, all video cameras removed)
(Hole Drilling Performed on Wheels #8 at B1, B2, B3 Locations)						
4/12/85	59/60	40/50	38	40	West	Tried to maintain 40 BHP throughout the test
4/12/85	62/63	40/48	38	55	East	"
(Hole Drilling Performed on Wheel #5 at B1, B2, B3 Locations)						
4/13/85	64/65	50/53	33/28/30/ 32/37	65	West	a) Fan cooling with 2 fans in front 1 fan in rear b) Tried to maintain 40 BHP throughout the test
4/13/85	66/67	50	33/31/28/ 33/32/35	65	East	a) Fan cooling b) Maintain 40 BHP throughout the test
(Hole Drilling Performed on Wheel #6 at B1, B2, B3 Locations)						
4/15/85	68/69	50	30		West	Stop Braking Test
"	"	60	30		"	"
"	"	50	35		"	"

TABLE 5.6. TESTING OF (INSTRUMENTED) TRUCK #2 ON RDU.
 TASK ORDER #6
 WHEEL FAILURE MECHANISMS

Average Vertical Load/Axle 52 Kips (Simulating Fully-Loaded 70-Ton Car)

Date	Run No.	Brake Cylinder Pressure (psi)	Speed (mph)	Duration (minutes)	Direction	Remarks
"	"	60	35		"	"
"	"	50	40		"	"
"	"	60	40		"	"
"	"	50	45		"	"
"	"	60	45		"	"
"	"	50	50		"	"
"	"	60	50		"	"
"	"	50	55		"	"
"	"	60	55		"	"
"	"	50	60		"	"
"	"	60	60		"	"
4/15/85	70/71	40	40/42/45/ 49/51/53/ 55	60	West	a) Drag braking with fan cooling b) Maintained 40 BHP
(Hole Drilling Performed on Wheel #7 at B1, B2, B3 Locations)						
4/16/85	72/73	40/45	35/32/30/ 34/43/45	65	East	a) Fan cooling b) Maintained 40 BHP
4/16/85	74/75	45/50	40/46/50	55	West	a) Fan cooling b) Maintained 50 BHP throughout the test
(Hole Drilling Performed on Wheel #8 at B1, B2, B3 Locations)						
4/17/85	76/77	50	40		West	Stop Braking Test
"	"	60	40		"	"
"	"	50	45		"	"
"	"	60	45		"	"
"	"	50	50		"	"
"	"	60	50		"	"
"	"	50	55		"	"
"	"	60	55		"	"
"	"	50	60		"	"
"	"	60	60		"	"
"	"	50	40		East	"
"	"	60	40		"	"
"	"	50	45		"	"
"	"	60	45		"	"

TABLE 5.6. TESTING OF (INSTRUMENTED) TRUCK #2 ON RDU.
 TASK ORDER #6
 WHEEL FAILURE MECHANISMS

Average Vertical Load/Axle 52 Kips (Simulating Fully-Loaded 70-Ton Car)

Date	Run No.	Brake Cylinder Pressure (psi)	Speed (mph)	Duration (minutes)	Direction	Remarks
"	"	50	50		"	"
"	"	60	50		"	"
"	"	50	55		"	"
"	"	60	55		"	"
"	"	50	60		"	"
"	"	60	60		"	"

(Intermittent Drag Braking and Free Running - With Fan Cooling)

4/17/85	78/79	45	35	13	West	Drag braking (50 BHP)
"	"	0	35	8	"	Free running
"	"	45	35/40	15	"	Drag braking
"	"	0	40	9	"	Free running
"	"	45	40/45	14	"	Drag braking
"	"	0	45	12	"	Free running
"	"	55	45	16	"	Drag braking
"	"	0	45	5	"	Free running
"	"	55	45	10	"	Drag braking

(Hole Drilling Performed on Wheel #5 at B1 and B2 Locations Only)

4/18/85	80/81	45/50	40/45/50/ 55	65	East	Drag braking - with fan cooling - Maintained 50 BHP
---------	-------	-------	-----------------	----	------	---

(Hole Drilling Performed on Wheels #8, at B1, B2, B3 Locations)

-
- 1) It may be noted that some of the Runs are assigned two numbers (viz., 78/79). This is simply because two data acquisition disks (Computer HP 9826) were needed from the start until the completion of each of those Runs.
 - 2) " (Sign) under different Run numbers implies that, data for individual stop braking cycles was recorded on the same set of disks (Computer HP 9826).

locations of all the test wheels after few thermal cycles during both the test series.

Data were acquired on the HP9826 system with data reduction and analysis still continuing.

5.2.2.4 Preliminary Results

- o Satisfactory checkout of high temperature strain gages and thermocouples through slip rings and associated data collection software was achieved.
- o Preliminary estimates were made of braking cycle severity to cause wheel thermal damage, as measured by (positive) tensile stress field at the back face of the rim.
- o Wheel to wheel differences in temperatures and BHP were observed under controlled conditions.
- o Significant decay of the coefficient of brake shoe friction was observed with increasing temperature at the brake shoe/wheel interface.
- o Measurement of heat transfer at wheel/roller interface was consistent with similar observations at the Brake Dynamometer Unit.

- o Residual stress development in the test wheels as determined by hole drilling - strain gaging method showed a definite trend with increased braking cycle severity. The residual stress field at the back face of the rim changed from compressive to tensile and subsequently increased value of tensile stress.
- o Established the basis for comparison of residual stress estimates by hole drilling - strain gaging method and mechanical analysis of strain/temperature history.

The most important results of the RDU testing were the significant wheel to wheel variation in the thermal input, the changes with time in the coefficient of friction of the brake shoes, and the inability to hold a constant level of thermal input to the wheels.

During the drag braking tests, temperatures were monitored at three critical locations of the test wheels. The critical locations (B1, B2, and B3) were selected from previous finite element analysis, B1 being in the back rim region, B2 being in the back rim fillet region, and B3 being in the front hub fillet region. The coefficient of friction and B.H.P. levels at the brake shoe/wheel interface was computed from the strain gage data of the instrumented brake heads. Table 5.7 presents the differences in maximum temperatures attained by the test wheels as observed at B1, B2, and B3 locations during the drag braking episodes for a given brake cylinder pressure speed.

TABLE 5.7

WHEEL FAILURE MECHANISMS
TECHNICAL TASK T4
RDU TESTING (TRUCK #2)

Run #	Wheel #	Max. Temp. Attained (°F) at Locations			B.H.P. at Brake Shoe Wheel Interface		Coefficient of Friction	
		B1	B2	B3	Max	Min	Max	Min
32/33 20 mph 10/20 psi	5	263	228	---	3.5	3.1	.38	.36
	6	---	249	169	3.1	2.9	.31	.28
	7	238	197	135	---	---	.36	.32
	8	256	195	168	---	---	.45	.27
37/38 30 mph 30 psi	5	450	375	250	15.5	11	.28	.16
	6	390	350	230	12.5	9	.22	.15
	7	436	355	220	16	13	.28	.22
	8	390	345	236	16	10.5	.24	.16
39/40 30 mph 40 psi	5	433	377	---	31	20	.26	.18
	6	388	392	203	29.9	18.5	.24	.18
	7	468	369	209	20.7	13.9	.16	.12
	8	493	397	226	32	17	.24	.12
43/44 30 mph 50 psi	5	464	---	---	47	23.5	.30	.16
	6	---	397	198	44.5	23.3	.30	.19
	7	484	391	225	32.6	13.4	.26	.07
	8	461	234	219	45	18	.30	.11
49/50 25 mph 50 psi	5	512	415	250	26	15	.20	.10
	6	477	426	248	27.5	16.5	---	---
	7	455	424	228	27	20	.19	.16
	8	395	350	235	30	19	.22	.12
55/56 42/50 mph 45/60 psi	5	605	495	320	44	35	.22	.13
	6	496	480	270	57	25	.26	.15
	7	624	560	310	27	45	.18	.10
	8	705	520	350	30	95	.24	.11
57/58 42 mph 45 psi	5	550/600	445	255	50	---	---	---
	6	611	511	278	50	30	---	---
	7	490	460	245	62	40	.34	.25
	8	660	370	295	---	---	---	---

Details of changes in B.H.P., as well as the coefficient of friction levels are presented. Maximum level of coefficient of friction, and hence B.H.P., were attained during the start of the runs, and these values dropped down (with increase in temperature) toward the end of the braking cycle.

Figures 5.10(A) and 5.10(B) show the maximum and minimum B.H.P. levels (at the beginning and end of the different braking cycles) attained during Truck #1 testing on the RDU for wheels 1, 2, 3, and 4.

Figure 5.10(C) and 5.10(D) show the maximum and minimum levels of B.H.P. attained during Truck #2 testing on the RDU for wheels 5 and 7.

After every two significant thermal (drag braking) cycles, the residual stress at critical locations of the test wheels was determined by hole drilling strain-gaging method. The hole drilling strain-gaging method is fully described in Section 11.2.5 (Failure Model).

At B1 location, the hoop stress, σ_h , changed eventually from compressive to tensile stress of varying magnitudes for different test wheels as shown in Figures 5.11 and 5.12.

It was observed that the residual stress (σ_R) at B1 location became more compressive, making the equivalent uniaxial stress in the hoop direction ($\sigma_h - \mu\sigma_R$) more tensile.

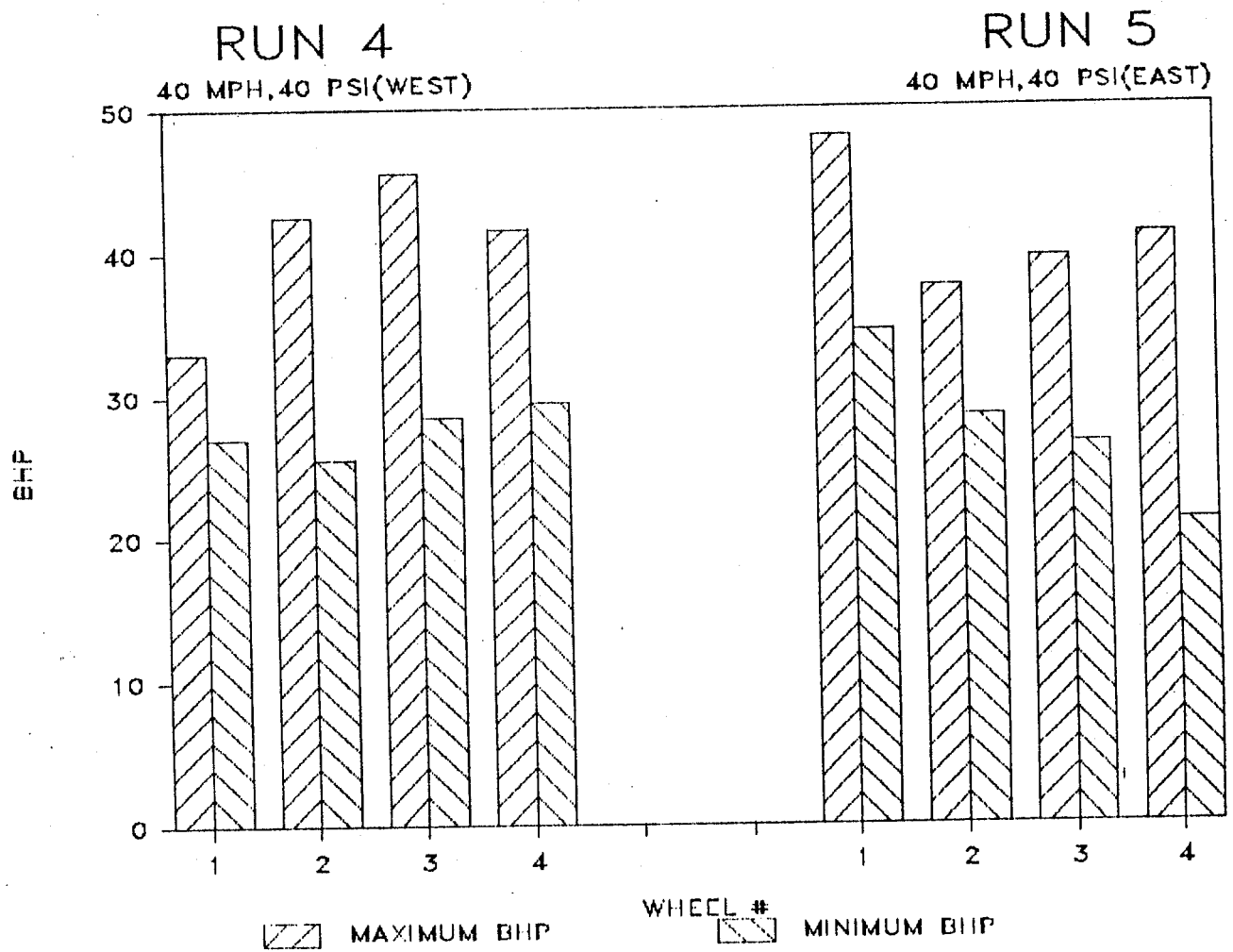


FIGURE 5.10(A). MAXIMUM VALUES OF BHP AT BRAKE SHOE/WHEEL INTERFACE FOR WHEEL # 1, 2, 3, AND 4 DURING DRAG BRAKING CYCLES.

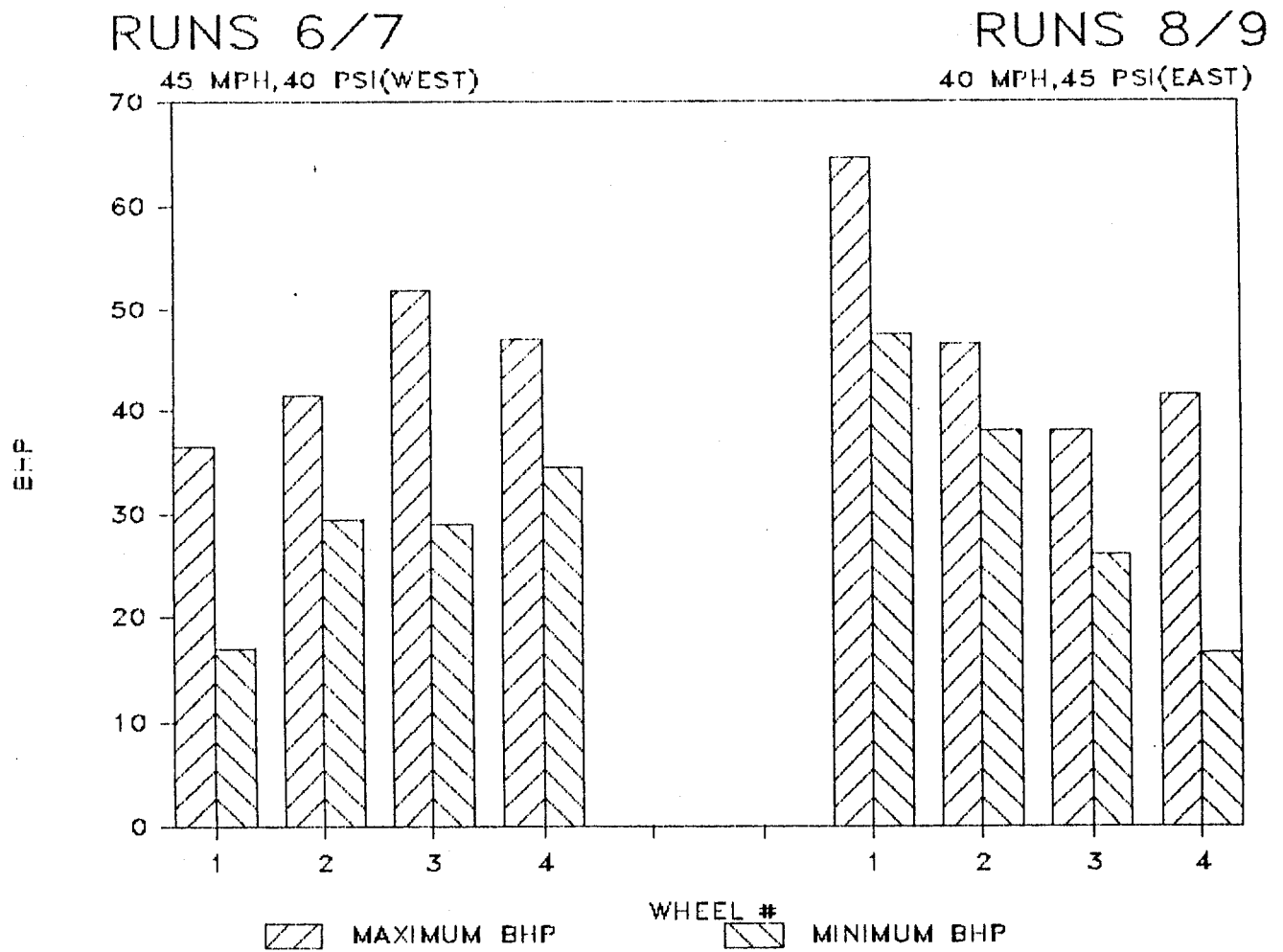


FIGURE 5.10(B). MAXIMUM AND MINIMUM VALUES OF BHP AT BRAKE SHOE/WHEEL INTERFACE FOR WHEEL # 1, 2, 3, AND 4 DURING DRAG BRAKING CYCLES.

RUNS 43/44
30 MPH, 50 PSI (WEST)

RUNS 45/46
30 MPH, 50 PSI (EAST)

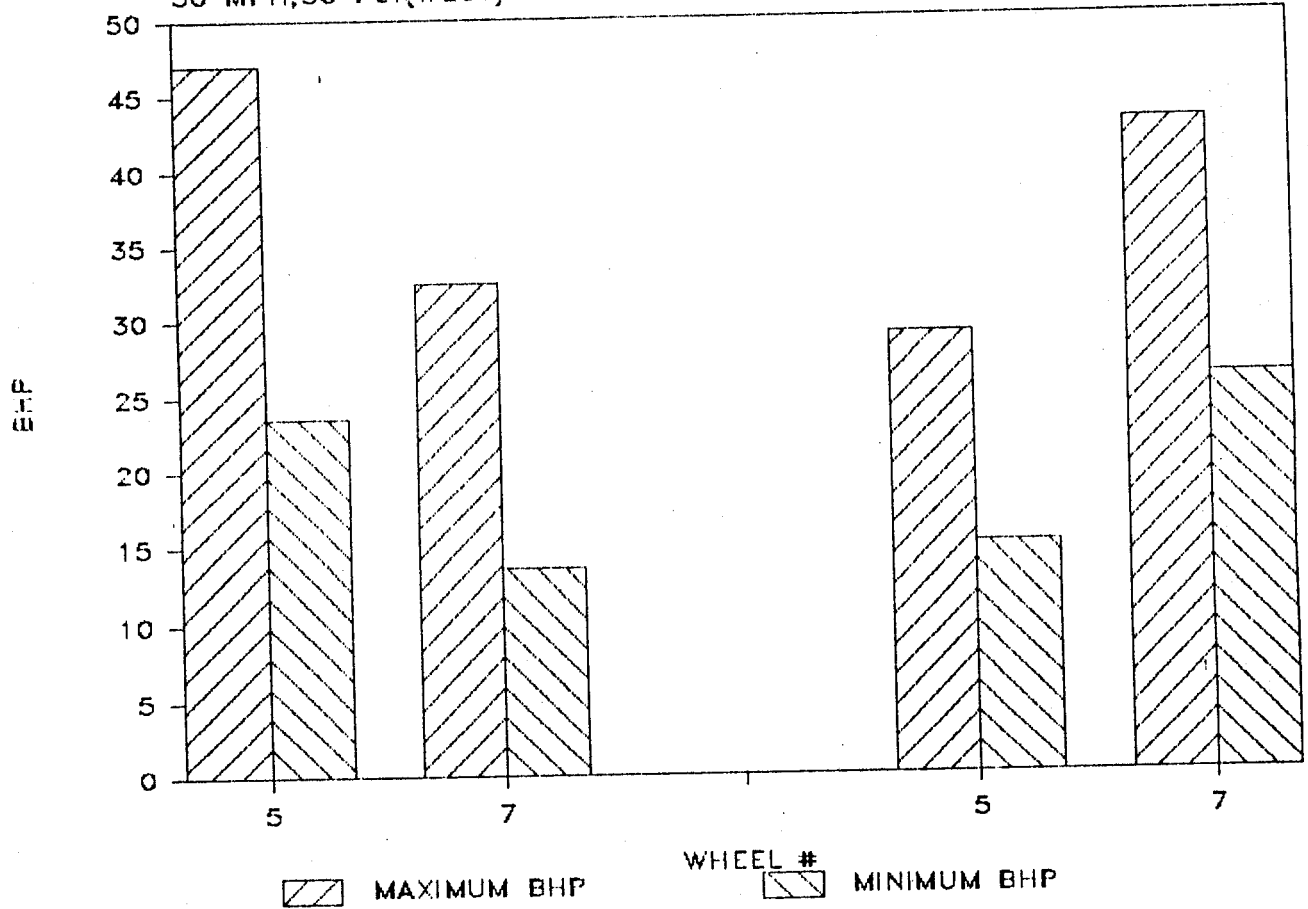


FIGURE 5.10(C). MAXIMUM AND MINIMUM VALUES OF BHP AT BRAKE SHOE/WHEEL INTERFACE FOR WHEEL # 5 AND 7 DURING DRAG BRAKING CYCLES.

RUNS 62/63
38 MPH, 40/48 PSI (EAST)

RUNS 64/65
28/37 MPH, 50/53 PSI (WEST)

RUNS 66/
28/35 MPH, 50 PSI

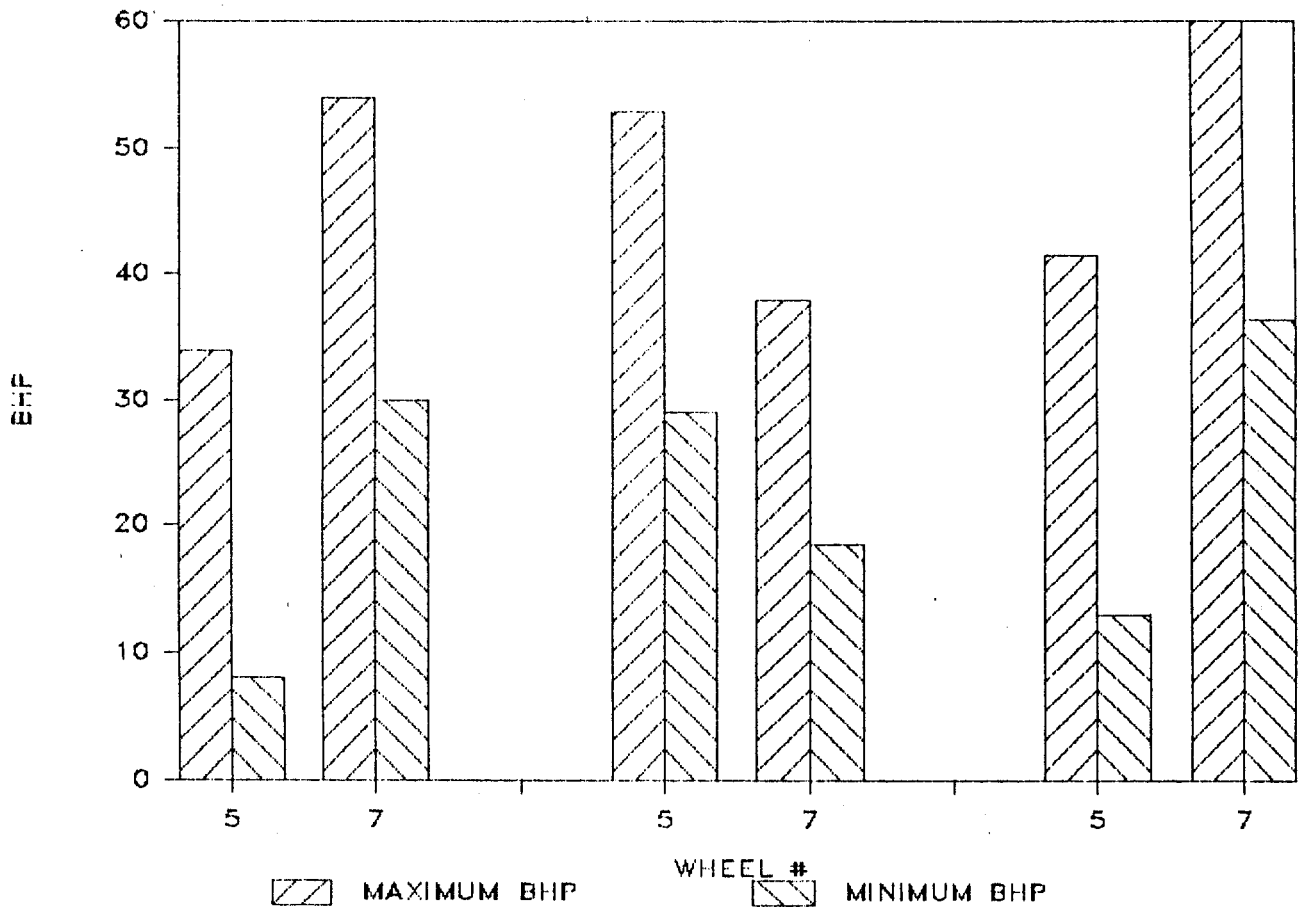


FIGURE 5.10(D). MAXIMUM AND MINIMUM VALUES OF BHP AT BRAKE SHOE/WHEEL INTER-
FACE FOR WHEEL # 5 AND 7 DURING DRAG BRAKING CYCLES.

WHEEL 8

LOCATION B1

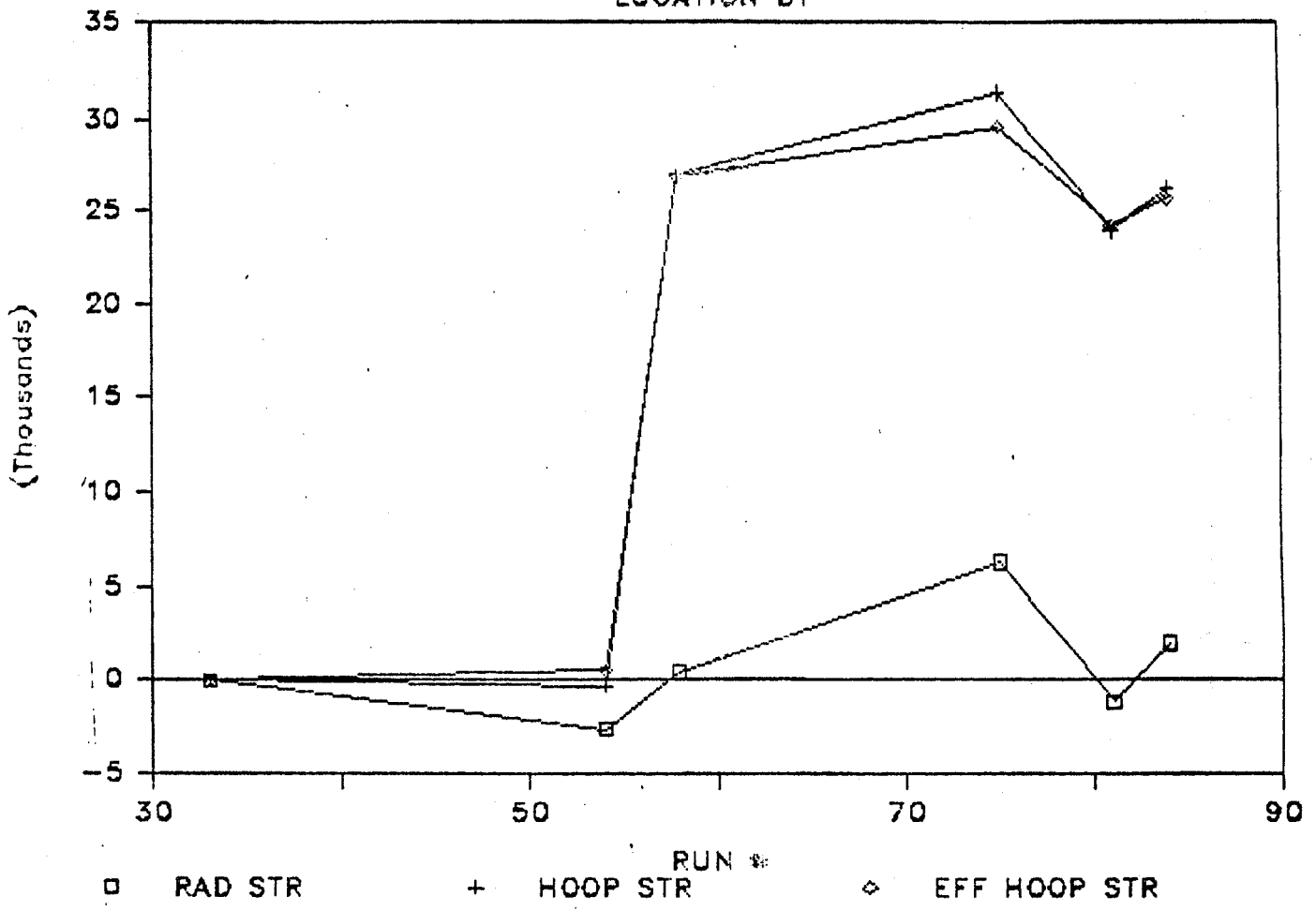


FIGURE 5.11. HOOP STRESS AT B1 LOCATION, WHEEL 8.

WHEEL 7

LOCATION B1

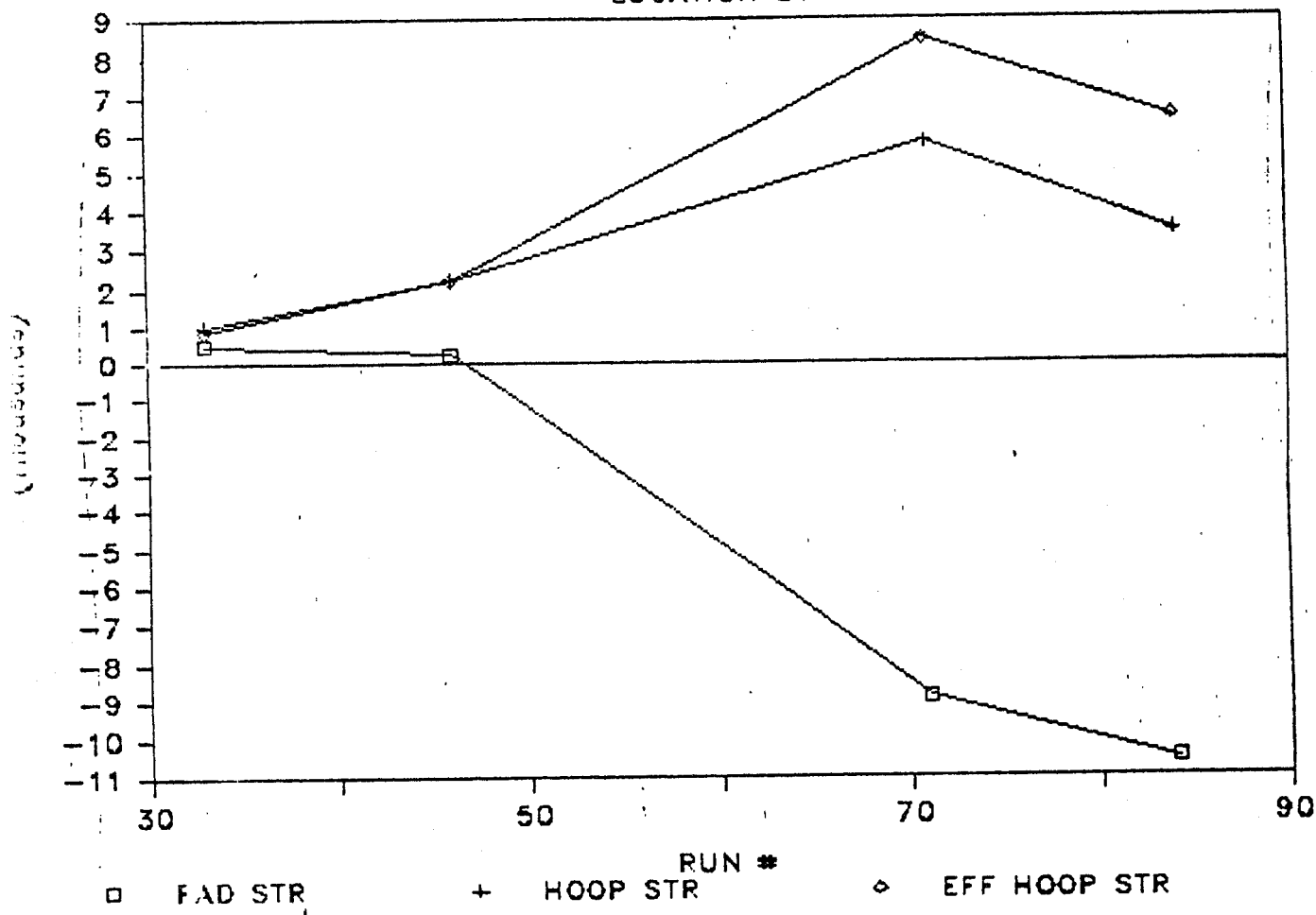


FIGURE 5.12. HOOP STRESS AT B1 LOCATION, WHEEL 7.

Similar trends were noticed at B2 and B3 locations except that the radial stress component (which is increased in the compressive direction) showed a more dominant effect resulting in an equivalent uniaxial stress in the hoop direction, pushed toward zero or the tensile direction (Figures 5.13 and 5.14).

5.2.2.5 Hot Stress Analysis Results

The strains monitored by high temperature strain gages at B1, B2 and B3 locations during the heating portions of drag braking cycles are converted into actual strains (mechanical components of strain) by applying the required corrections [Appendix 5.6]. At B1, strain is measured only in the tangential (hoop) direction. At B2 and B3, strains are measured in both tangential and radial directions. The information at B1 is treated as if it were a uniaxial stress situation and the elastic tangential stress is calculated from the corresponding actual strain. Locations B2 and B3 are treated as biaxial stress fields. The elastic stresses are calculated from:

$$\sigma_R^E = \frac{E}{(1-\mu^2)} (\epsilon_R + \nu\epsilon_T)$$

$$\sigma_T^E = \frac{E}{(1-\mu^2)} (\epsilon_T + \nu\epsilon_R)$$

From these, an elastic effective stress is calculated from:

$$\sigma_E = \sqrt{\sigma_T^2 + \sigma_R^2} - \sigma_T\sigma_R$$

WHEEL 5

LOCATION B2

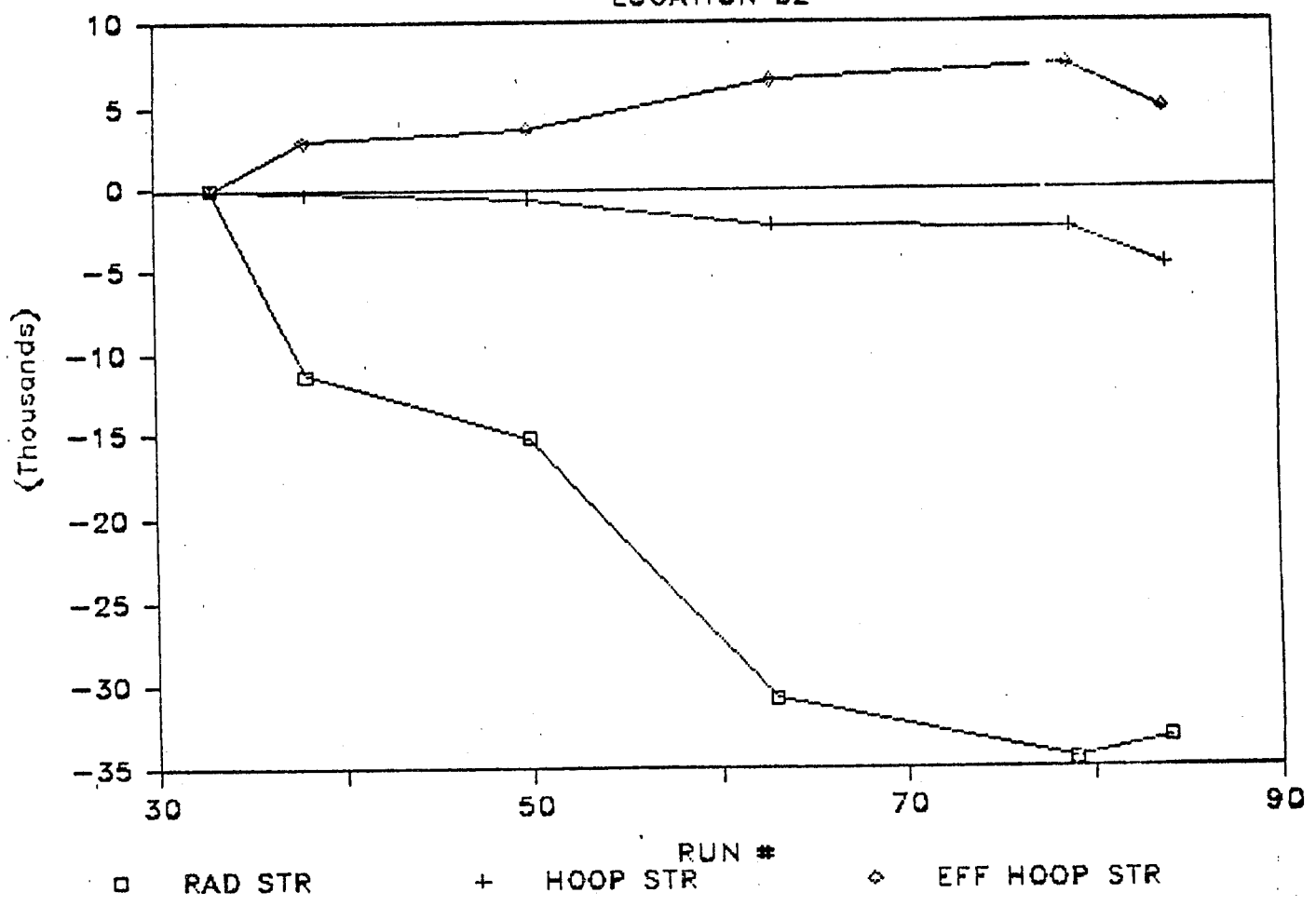


FIGURE 5.13. HOOP STRESSES AT B2 LOCATION, WHEEL 5.

WHEEL 6

LOCATION B2

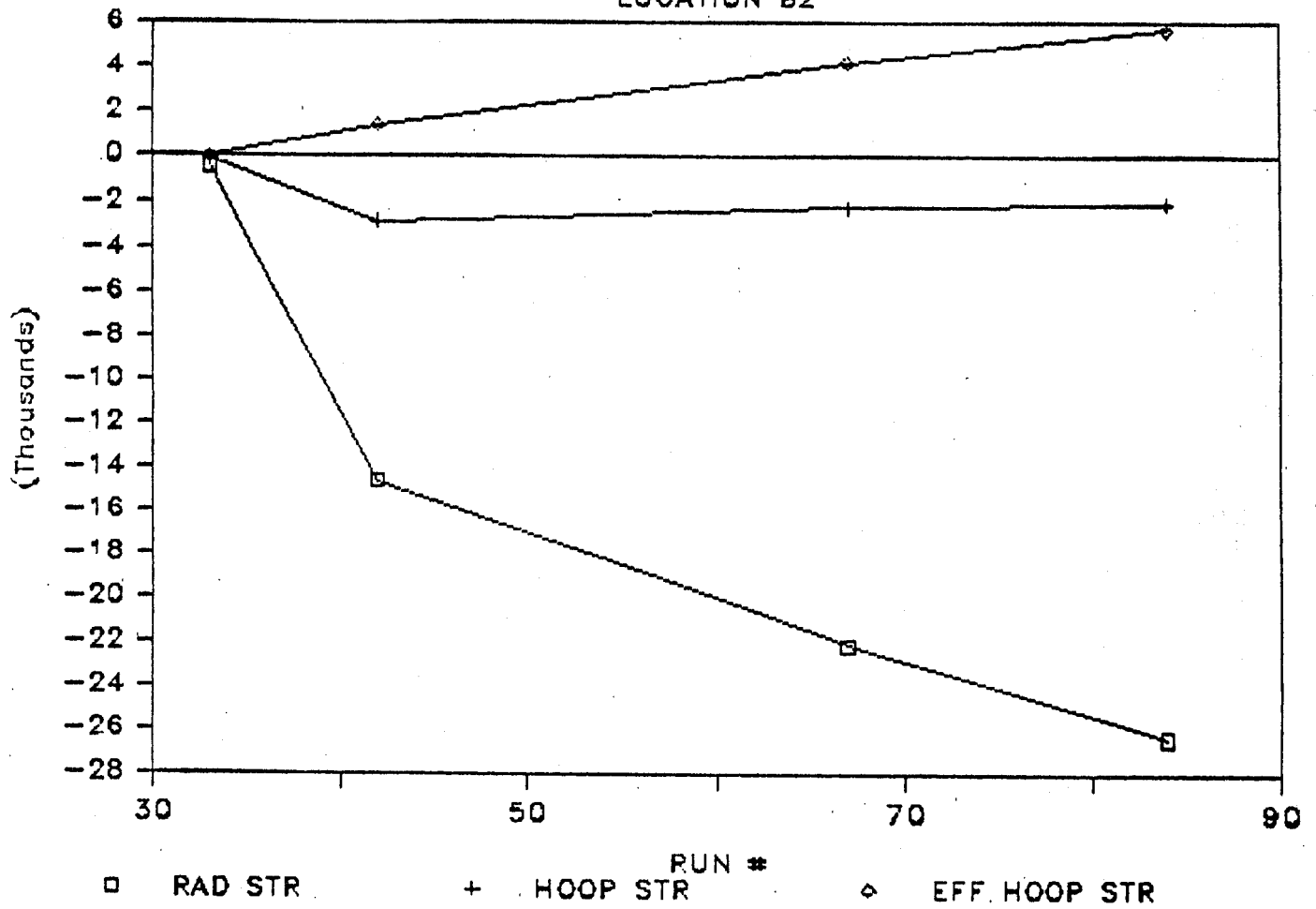


FIGURE 5.14. HOOP STRESSES AT B2 LOCATION, WHEEL 6.

The effective elastic stress is a measure of thermal severity to which the wheel has been subjected. This parameter is related to 1) average brake horsepower to which the wheel was subjected during each test run and, 2) maximum temperatures attained at various critical locations of test wheels (Figures 5.15 through 5.26). All these relationships are established for hot wheel conditions.

The inelastic analysis which takes into account the material yield is treated separately in Section 11.2.5.2.

5.2.2.6 Heat Transfer Analysis

An estimate of the wheel/heat transfer rate was made based on measurements of the average rise in temperature of the roller in a 40 mph, nominal 50 BHP test on the RDU, Test No. 56/57 and 58/59.

The calculations are given in Appendix 5.7. The result is a lower case estimate of at least 7.9 HP or about 16% of the nominal input braking horsepower.

5.2.3 Induction Heating Test Status

The induction heating test was developed to simulate brake thermal loading of wheels. While the test was not capable of simulating rail load and all brake shoe loading effects, it did provide an easily accessible and controlled facility to develop instrumentation, test optimum gage placement locations, test braking cycles, and explore residual stress measurement techniques.

WHEEL #8

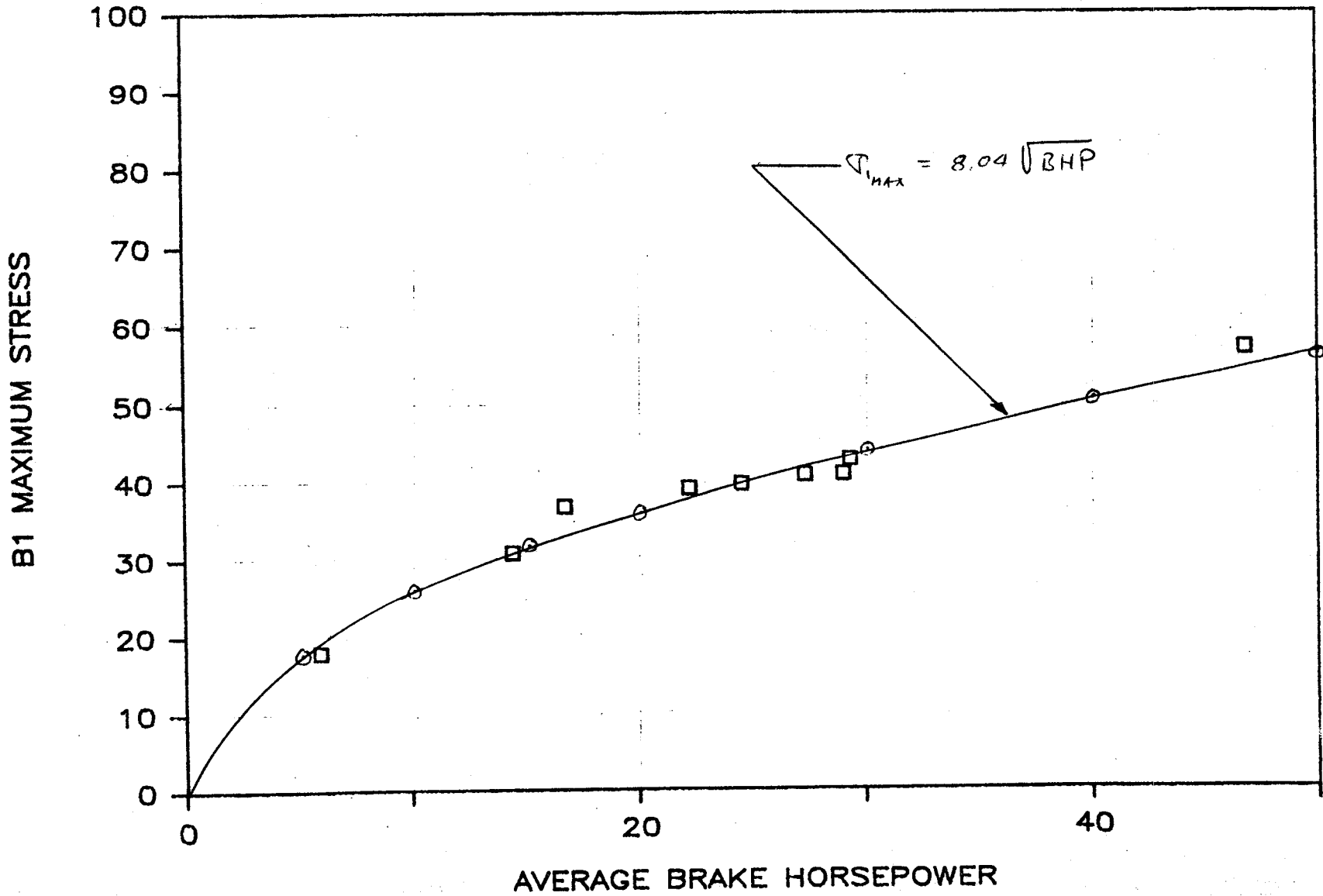


FIGURE 5.15. MAXIMUM ELASTIC STRESS VS AVERAGE BHP, WHEEL #8.

WHEEL #5

5-41

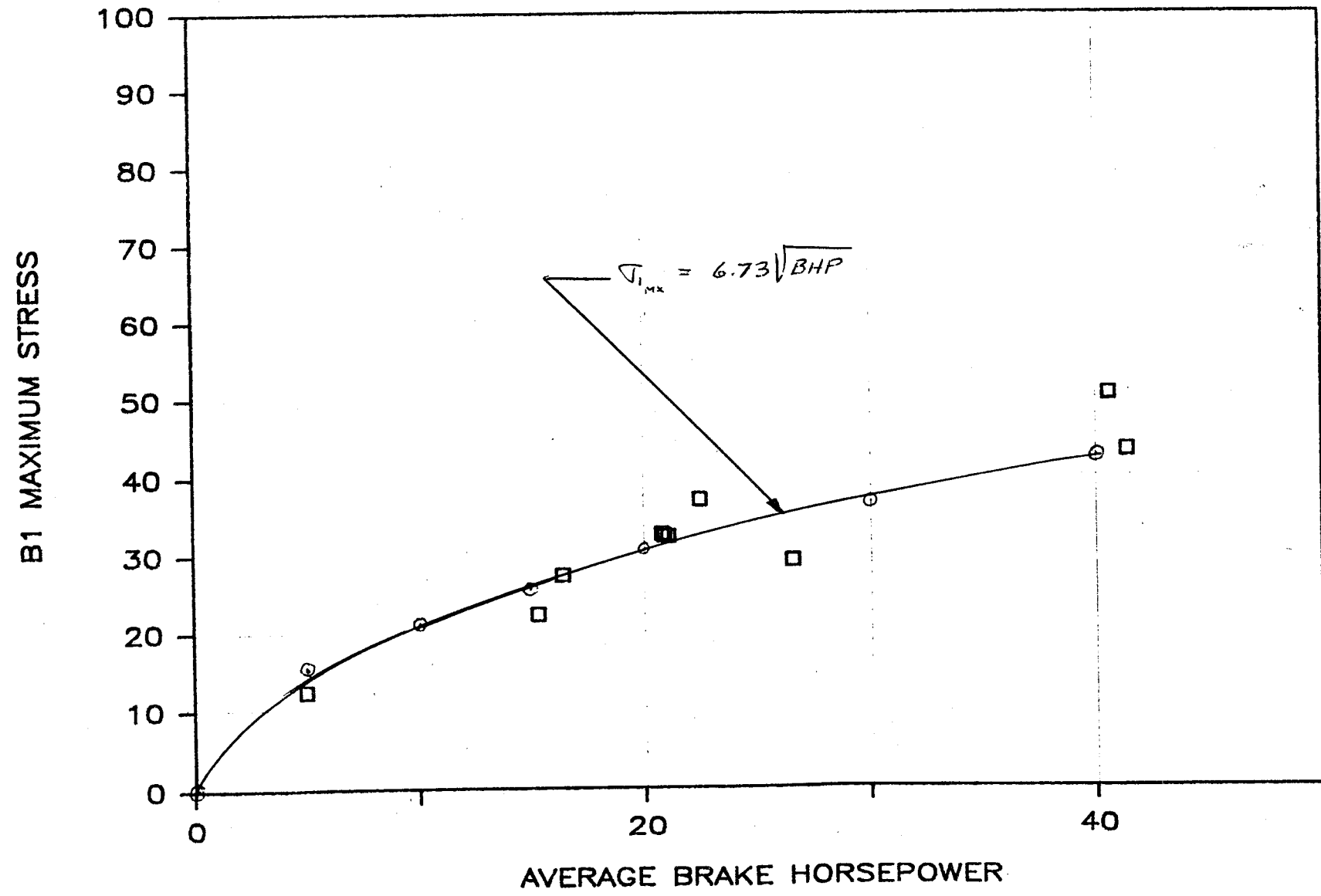
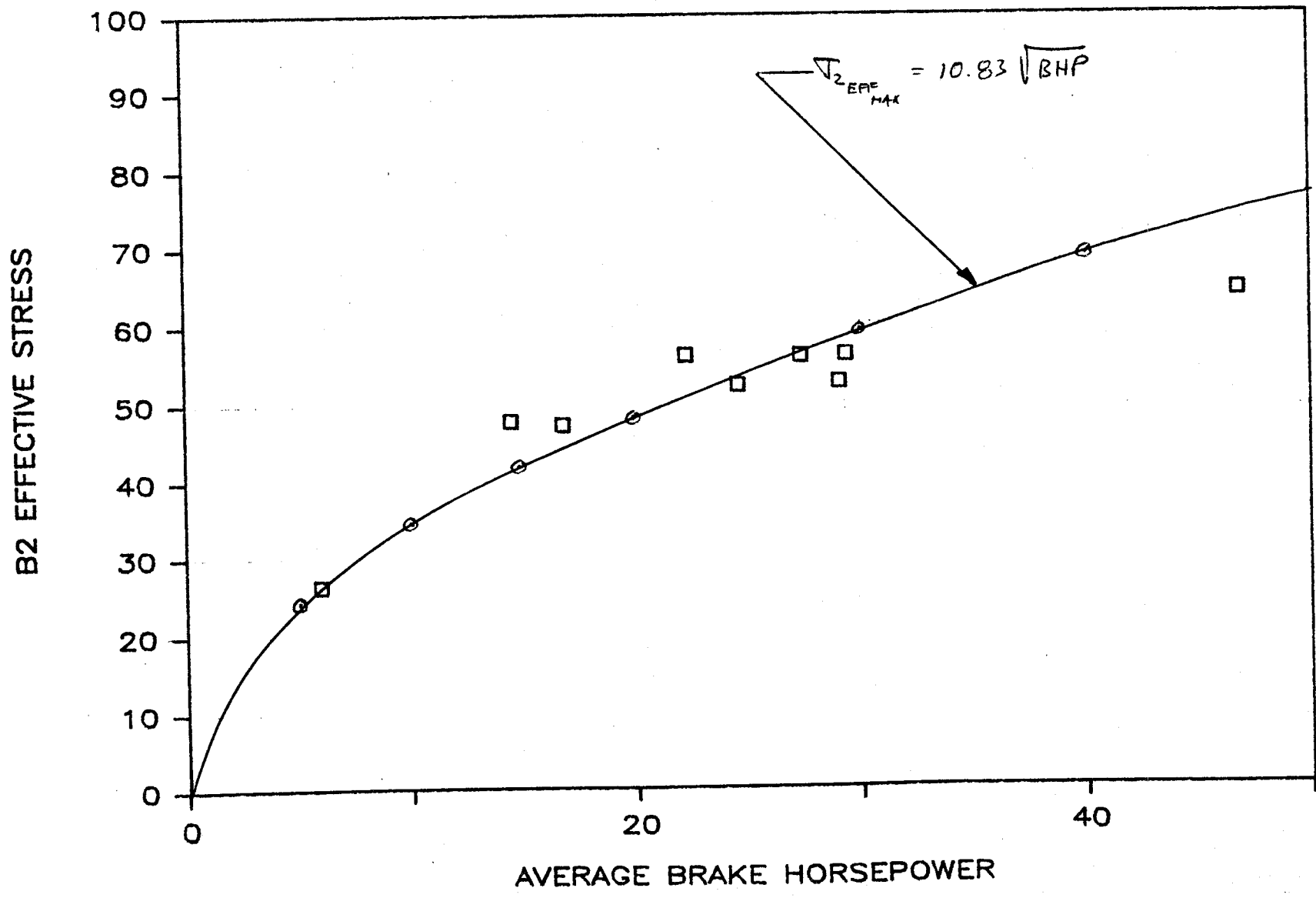


FIGURE 5.16. MAXIMUM, ELASTIC STRESS VS AVERAGE BHP, WHEEL #5.

WHEEL #8



5-42

FIGURE 5.17. EFFECTIVE ELASTIC STRESS VS AVERAGE BHP, WHEEL #8.

WHEEL #5

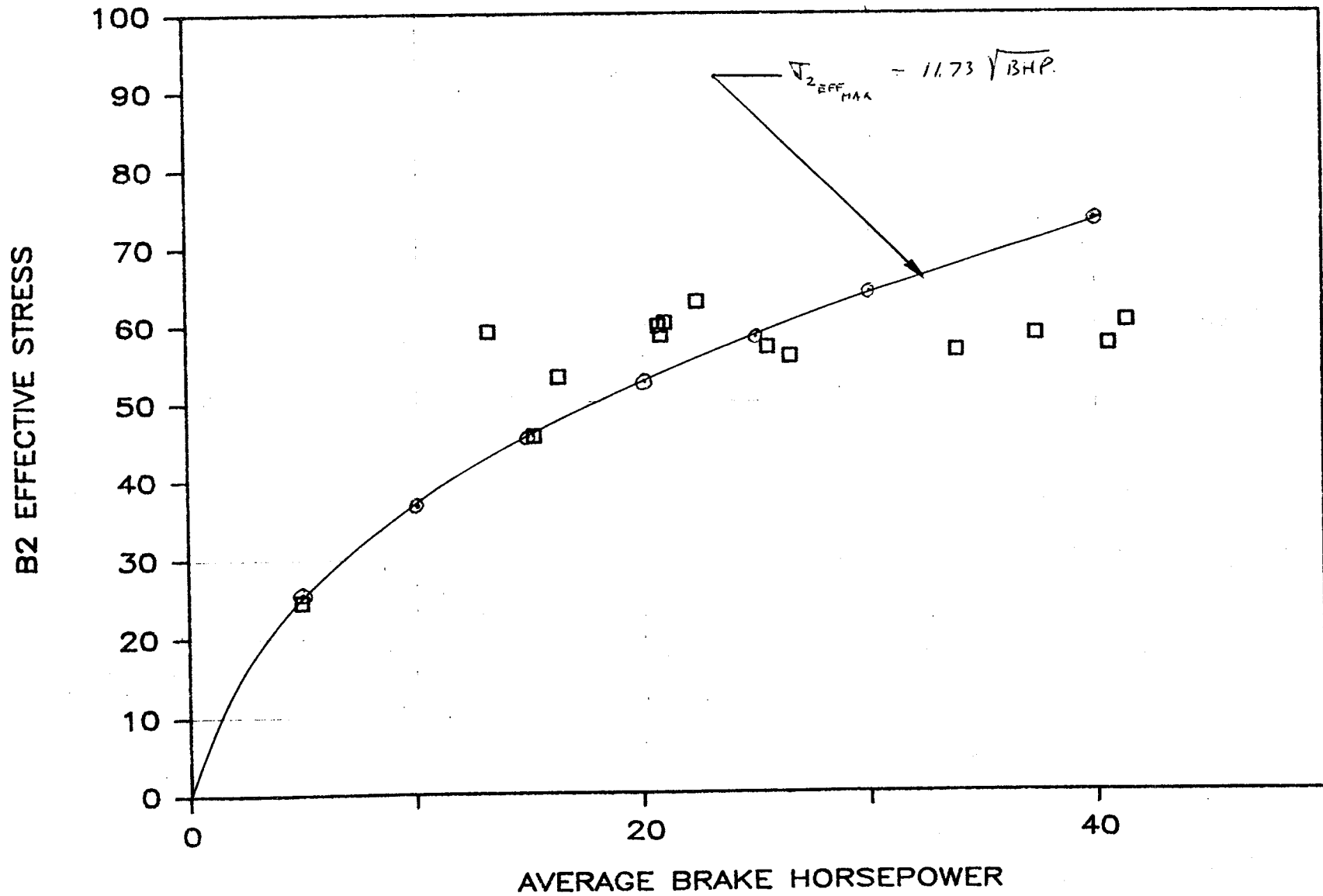


FIGURE 5.18. EFFECTIVE ELASTIC STRESS VS AVERAGE BHP, WHEEL #5.

WHEEL #8

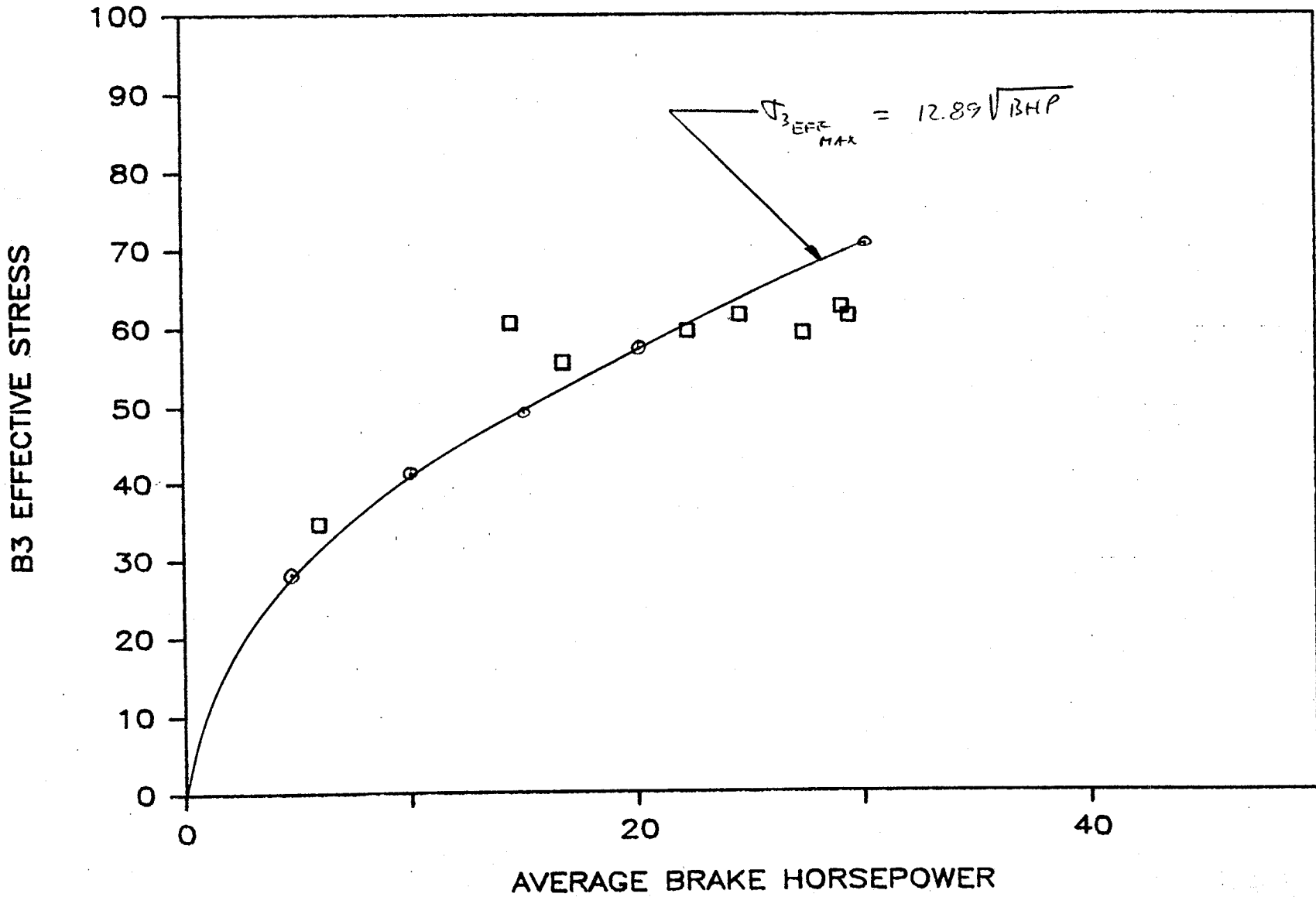


FIGURE 5.19. EFFECTIVE ELASTIC STRESS VS AVERAGE BHP, WHEEL #8.

WHEEL #7

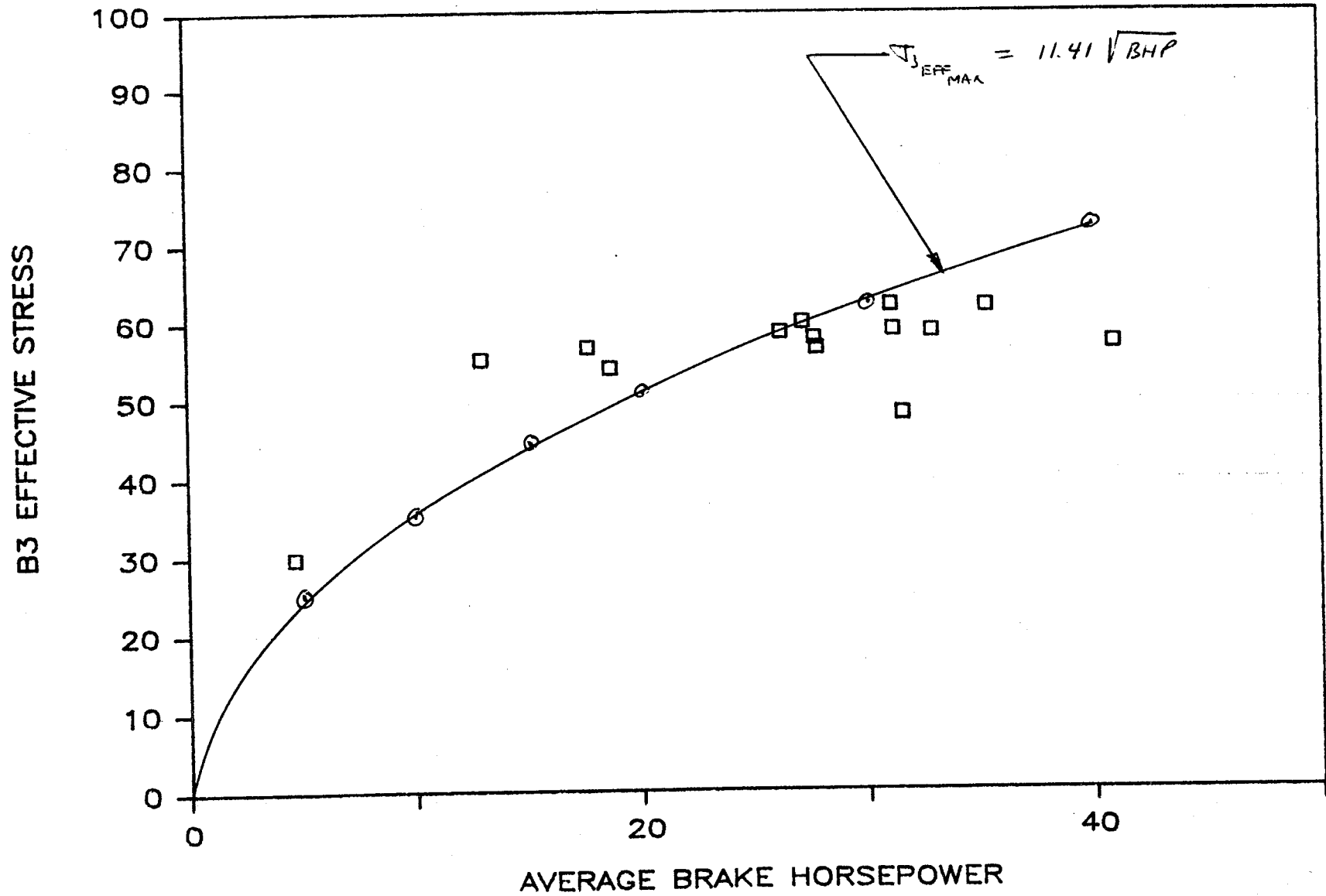


FIGURE 5.20. EFFECTIVE ELASTIC STRESS VS AVERAGE BHP, WHEEL #7.

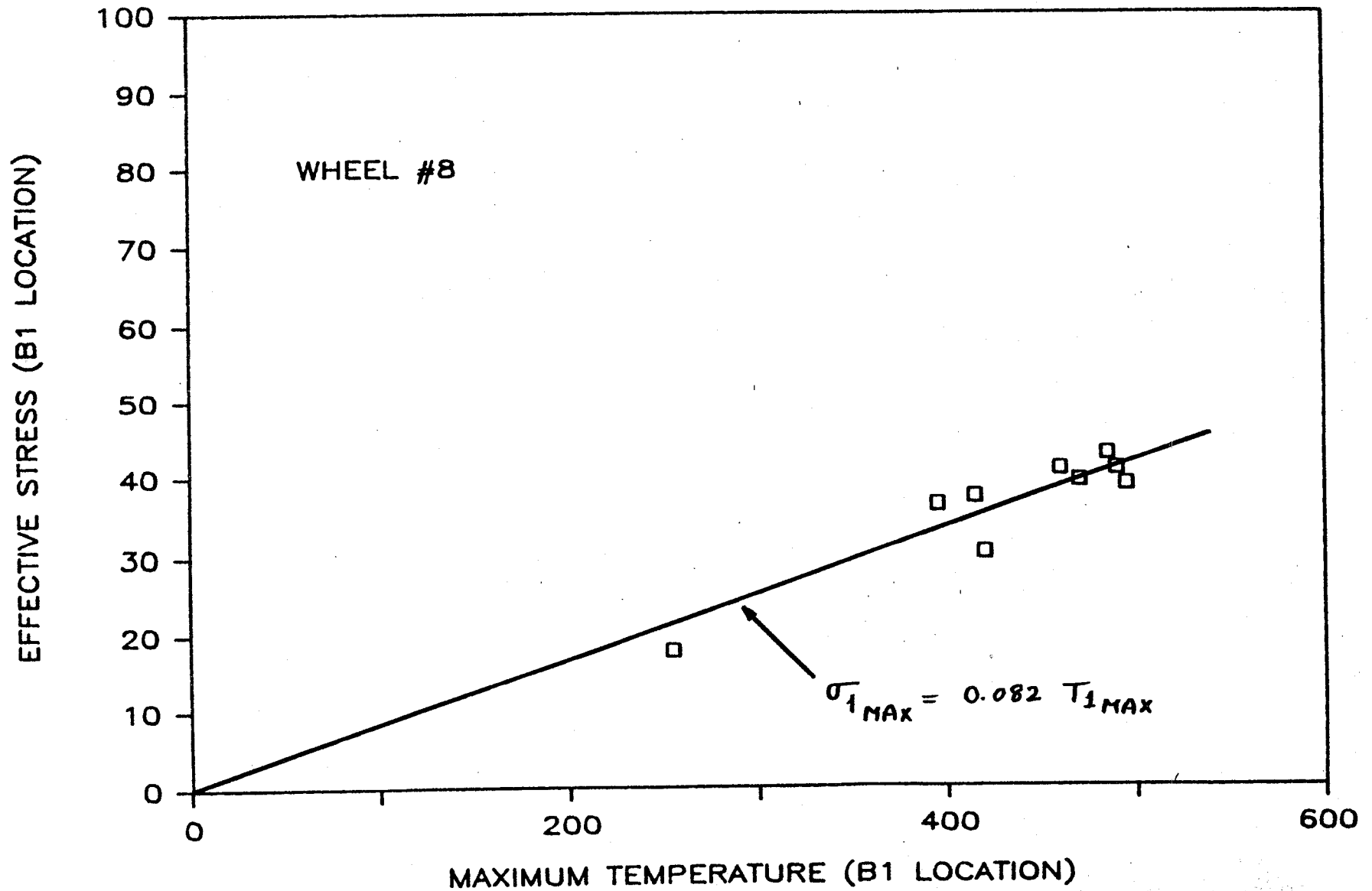


FIGURE 5.21. EFFECTIVE ELASTIC STRESS (B1) VS TEMPERATURE (B1), WHEEL #8.

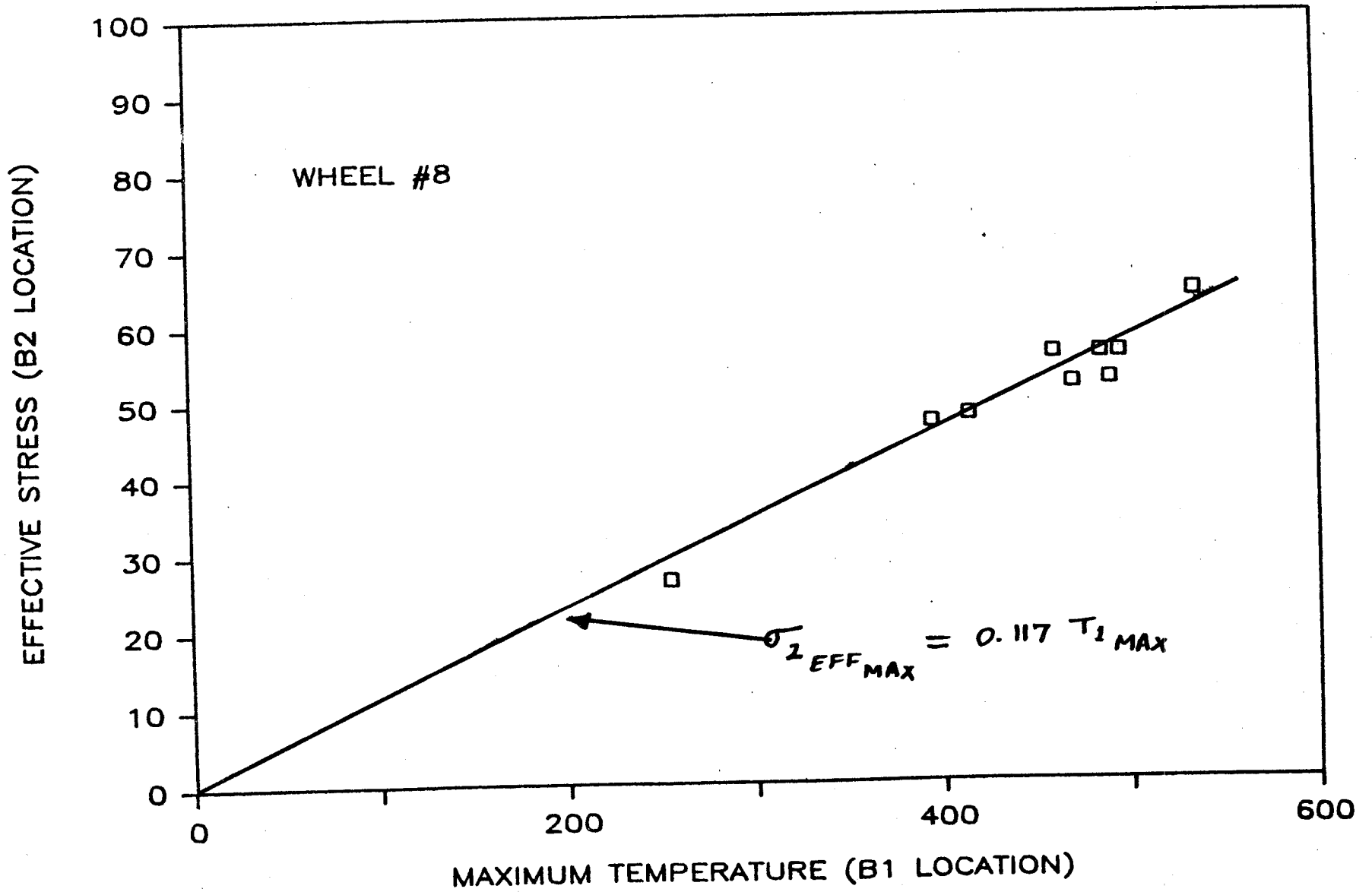


FIGURE 5.22. EFFECTIVE ELASTIC STRESS (B2) VS TEMPERATURE (B1), WHEEL #8.

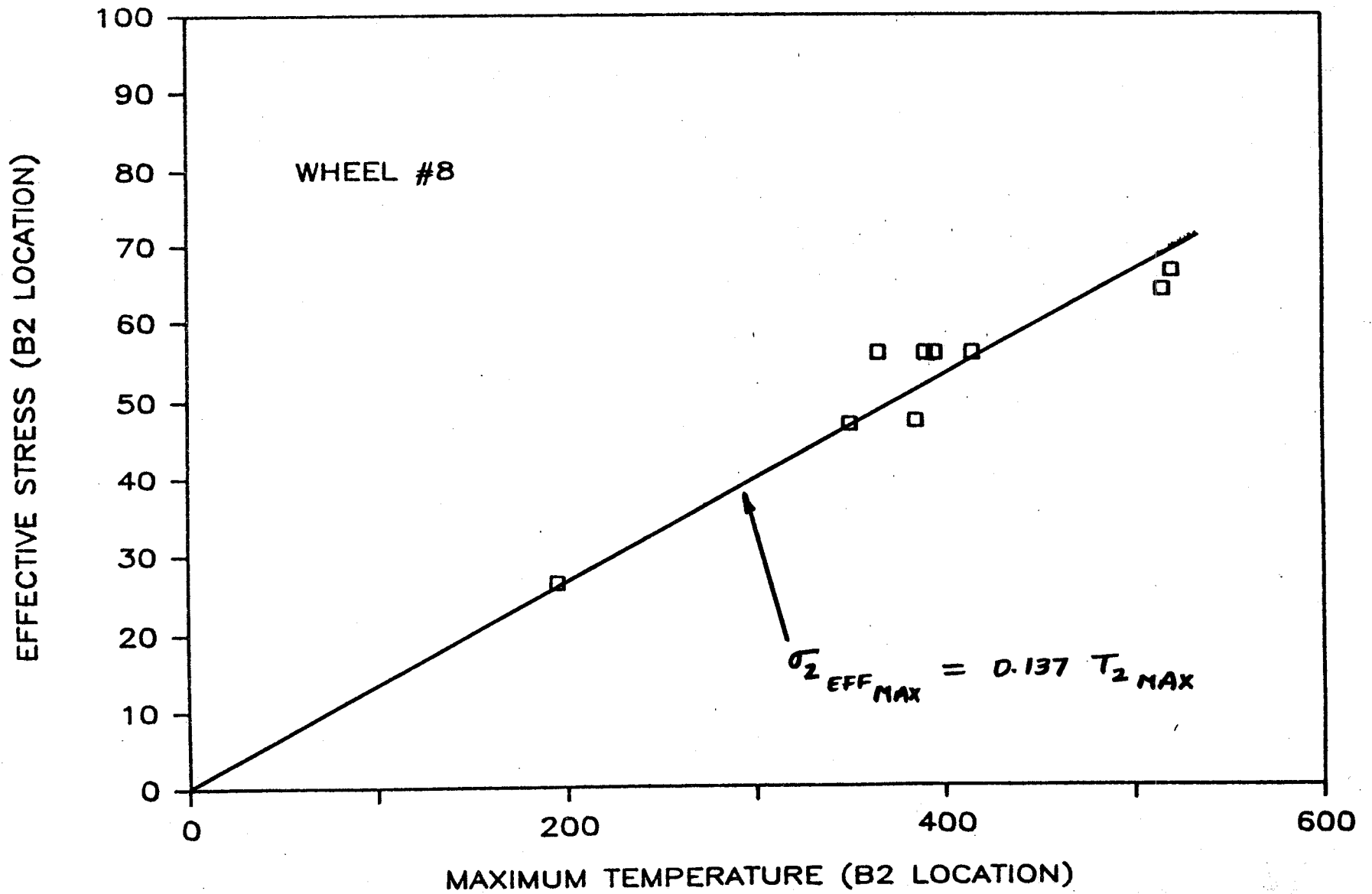


FIGURE 5.23. EFFECTIVE ELASTIC STRESS (B2) VS TEMPERATURE (B2), WHEEL #8.

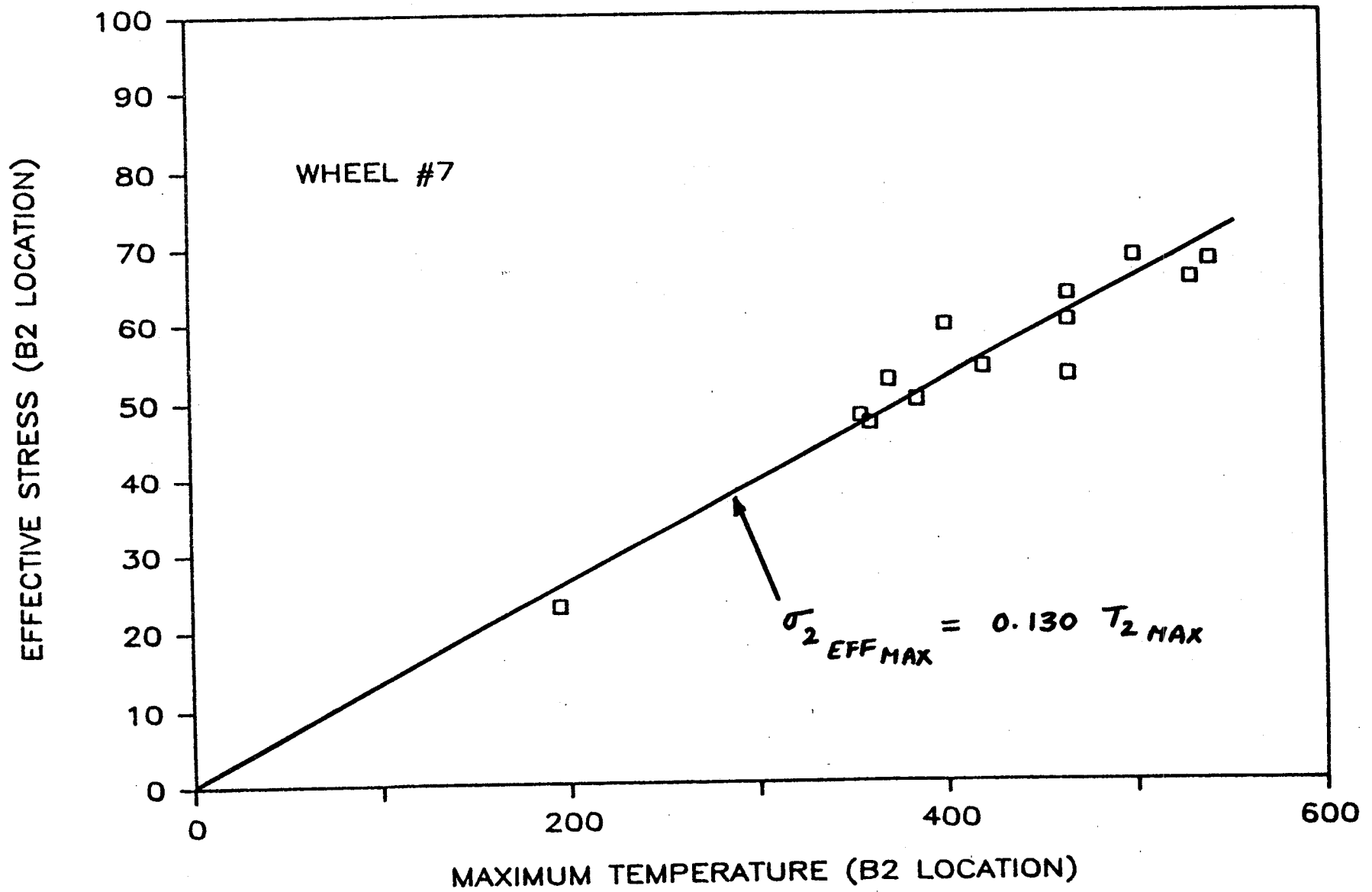


FIGURE 5.24. EFFECTIVE ELASTIC STRESS (B2) VS TEMPERATURE (B2), WHEEL #7.

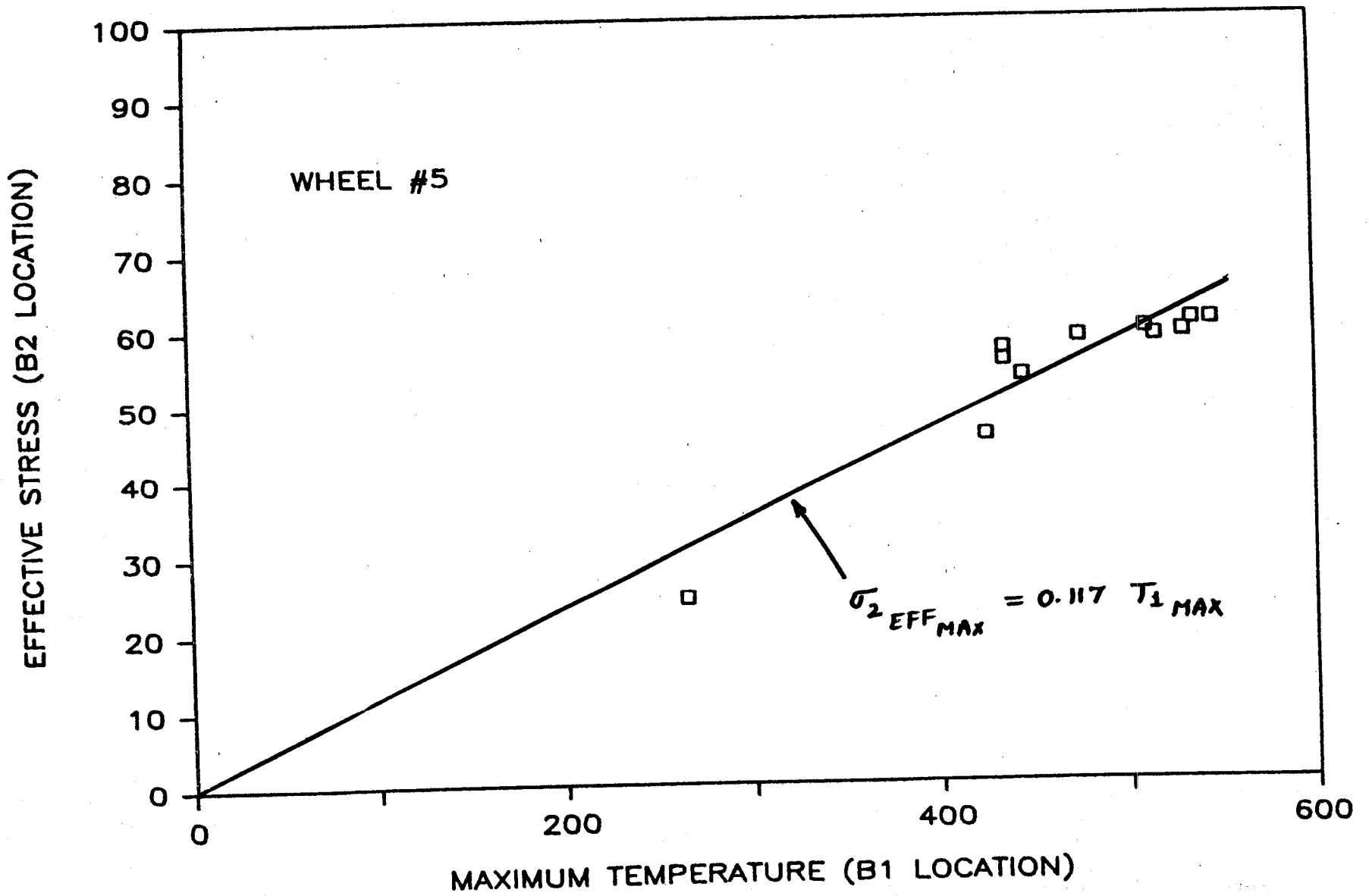


FIGURE 5.25. EFFECTIVE ELASTIC STRESS (B2) VS TEMPERATURE (B1), WHEEL #5.

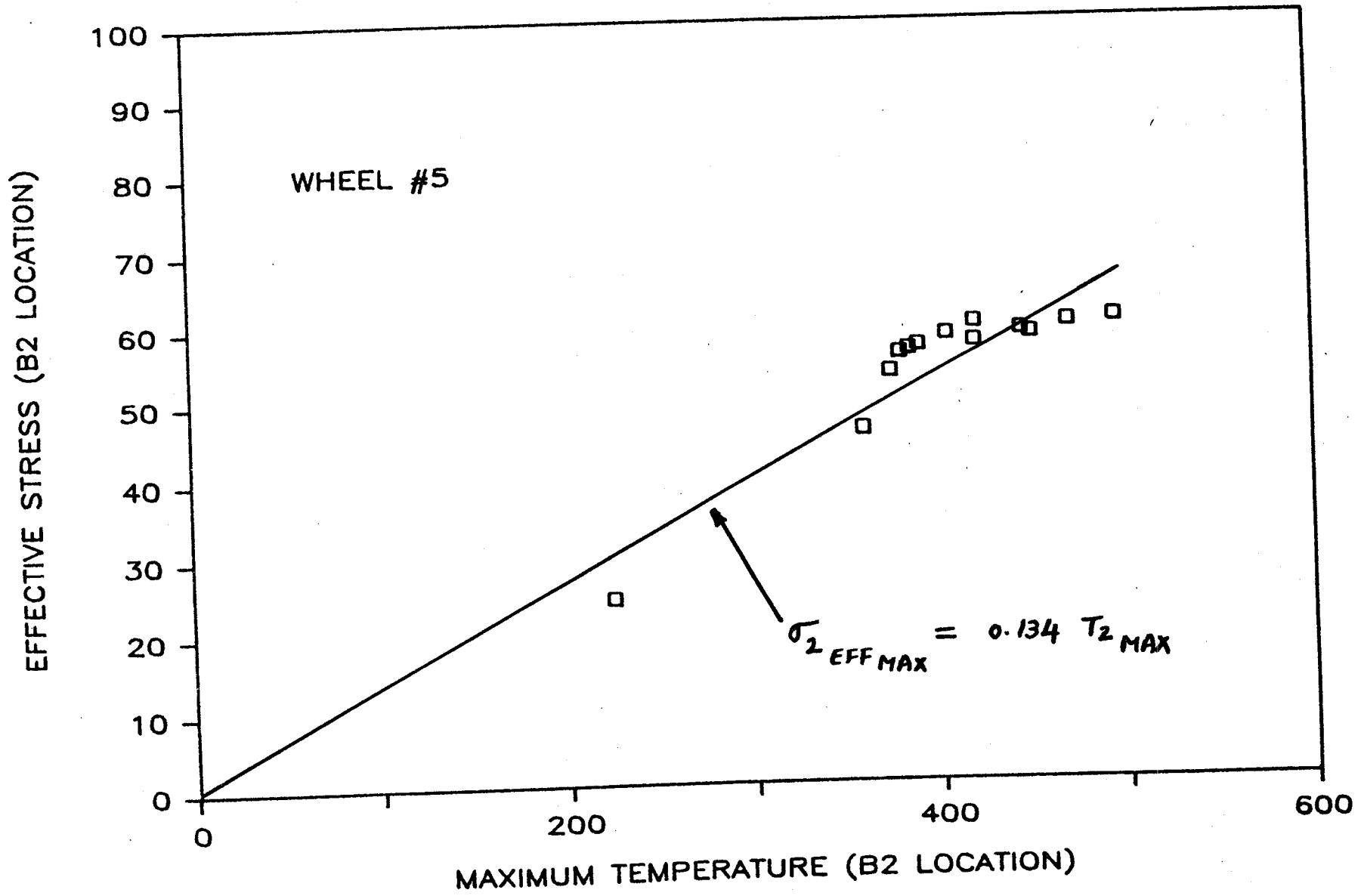


FIGURE 5.26. EFFECTIVE ELASTIC STRESS (B2) VS TEMPERATURE (B2), WHEEL #5.

Furthermore, such an induction heating test also provided a controlled source of heat to simulate brake application, for subsequent comparison to follow-on tests that included rail load and brake shoe effects. This comparison helped illuminate the issue of rail loading contribution to wheel failure mechanisms.

The uncertainty regarding the friction generated heat loss at the brake shoe/wheel interface was dealt with in preliminary thermal analyses, where assumptions were made consistent with those used by AAR in their wheel design evaluations, i.e., 70% of the heat generated by friction is conducted into the wheel. The ultimate aim was to contrast empirical results from the induction heating tests with the brake dynamometer results in order to infer the differences or explore the "equivalences".

The Induction Heating Program provided:

- o An instrumentation development phase for the measurement of strain and temperature at selected locations of the wheel under static conditions.
- o A confirmation phase for finite element analyses, which were used to obtain the understanding of the thermal problem of the freight car wheel.
- o A comparison phase, wherein the data generated during the induction heating was intended to be used in comparisons with data obtained from dynamometer and track tests.

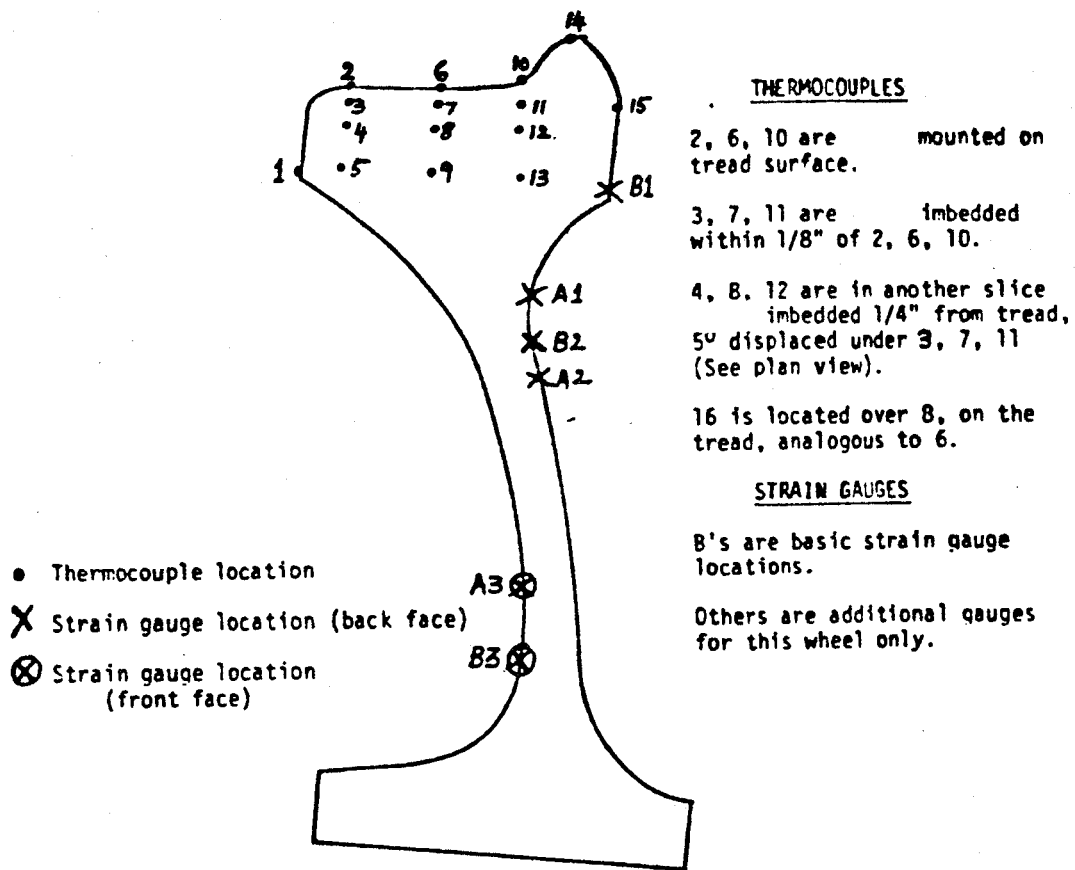
5.2.3.1 Wheels

Two one-wear 36-inch diameter wheel designs were studied under the induction heating plan. The first wheel was a CH-36, with curved-plate design, while the other was a wrought straight-plate wheel design with fairly sharp rim-plate fillets. Differences in development of residual strains in the two designs were investigated along with the relative temperature distributions. These wheels were in the stress-relieved state before instrumentation. Finite element calculations were made, using the best available estimate of the shape of the heating front, to yield a circumferential residual stress level at the bottom of the back rim face.

5.2.3.2 Instrumentation

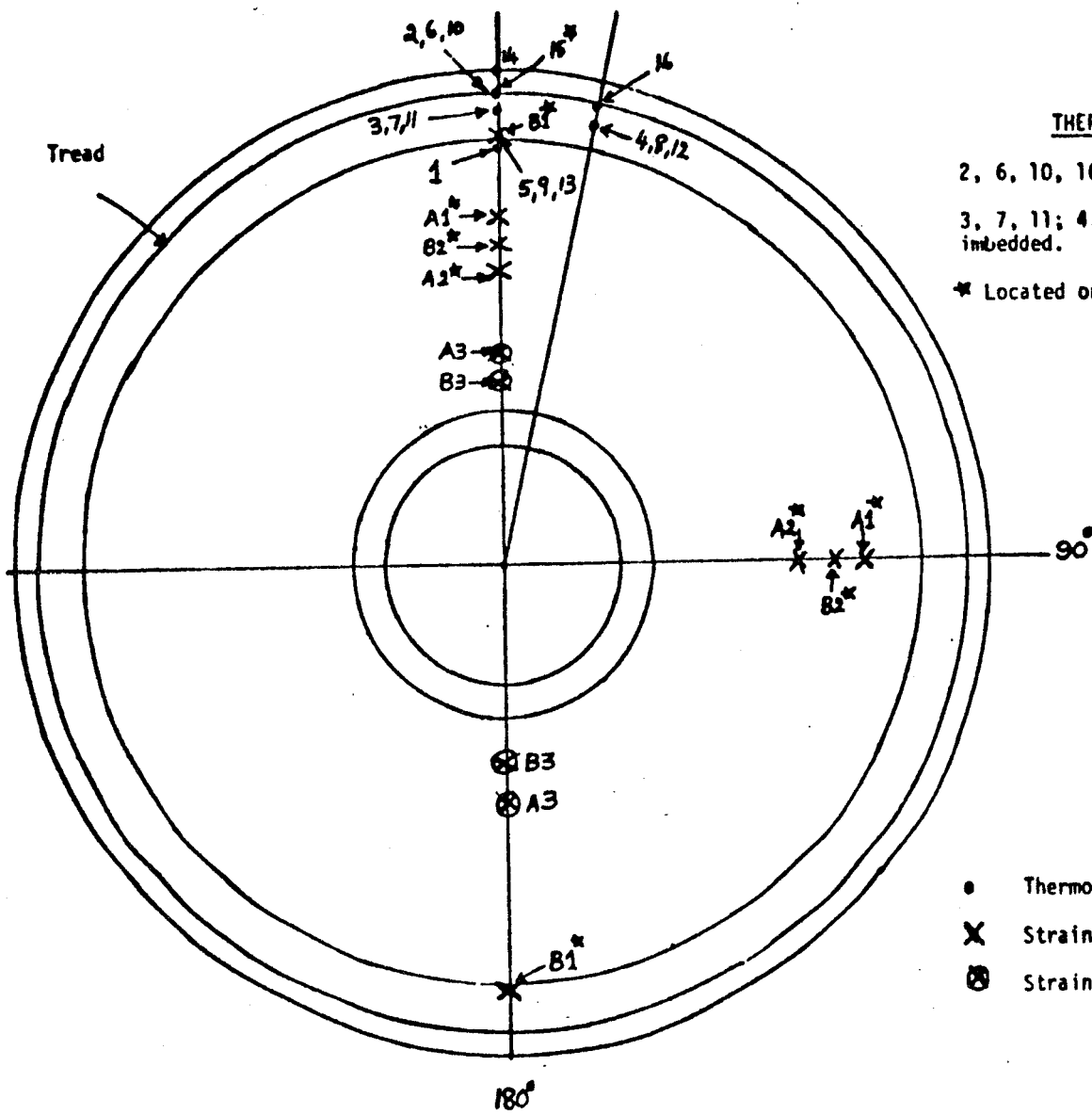
The typical instrumentation scheme for the first test wheel (CH36) is presented in Figures 5.27 and 5.28. For the second test (H36), the strain gages and thermocouples were installed at the base (B) locations.

Both the test wheels (Parabolic plate CH 36 and Straight Plate H 36) were sent to Ihly Industries in Denver, Colorado, for precise drilling of holes to install the subsurface thermocouples at the selected locations inside the rim compatible with the locations used in finite element calculations.



CH-36 WHEEL

FIGURE 5.27. INSTRUMENTED WHEEL FOR INDUCTION WHEEL TEST (FIRST WHEEL).



THERMOCOUPLES

2, 6, 10, 16 are mounted on surface.
 3, 7, 11; 4, 8, 12; and 5, 9, 13 are imbedded.
 * Located on back face.

- Thermocouple location
- X Strain gauge location (back face)
- ⊙ Strain gauge location (front face)

FIGURE 5.28. INSTRUMENTED WHEEL FOR INDUCTION WHEEL TEST (PLAN VIEW).

The test wheels were prepared for the installation of high temperature gages at the prescribed locations. Bridge completion networks consisting of temperature compensation and balance resistors were made ready for all the strain gages. During the installation of ALLTECH high temperature gages on both the test wheels, a data acquisition system with 42-channel capability was used. A Campbell Scientific CR7 data logger was made ready with new excitation and input cards for acquiring data during temperature cycling and induction heating.

Both the test wheels were transported to Maxcar Corporation at Colorado Springs and temperature cycled up to 1100°F to relieve welding stresses by holding at that temperature for 2 hours and subsequent uniform cooling to room temperature. The last cooling cycle was used to generate an actual apparent strain curve for each gage and was used to correct data acquired during the actual induction heating tests, (Appendix 5.6).

5.2.3.3 Test Conditions

After temperature cycling of both the test wheels, they were transported to AMSTED Research Laboratories, and induction heating experiments were performed during December 3 through December 12, 1984. The following heating cycles were completed on the test wheels, and data was acquired using CR7 Campbell Scientific data logger at the prescribed intervals during heating as well as cooling.

<u>Test No.</u>	<u>Test Wheel</u>	<u>Thermal Cycle (Drag Brake Simulation)</u>
1	CH36	30 KW, 12 minutes
2	CH36	40 KW, 15 minutes
3	CH36	30 KW, 25 minutes
4	CH36	40 KW, 30 minutes
5	CH36	40 KW, 30 minutes (Repeat)
6	H36	30 KW, 8 minutes
7	H36	30 KW, 16 minutes
8	H36	40 KW, 12 minutes
9	H36	40 KW, 24 minutes
10	H36	40 KW, 24 minutes (Repeat)

The heating facility consisted of a 100 kW induction coil and a high frequency generator (2500-2900 Hz) with 3/4 inch clearance between the surrounding coil and 36-inch wheel tread.

Locations of thermocouples and strain gages were across a wide band of temperature and stress distribution developed in the wheel as a result of a controlled source of heat to simulate a brake application. The exact locations of strain gages and thermocouples were determined after preliminary finite element calculations were completed, so that the observed strains and temperatures at strategic locations of the wheel could be compared with the calculated values. Strain gages used for this test were the Ailtech weldable type, SG 425-08-05-06S, a half-bridge configuration like the lower temperature range gages. However, this gage had a platinum-tungsten alloy designed for use in static measurements to 1200°F. The gage had a 5-foot stainless steel tube welded to it to protect the lead to 1500°F and required extension leads to signal conditioning.

The thermocouple (TC) wire used was 20-gage, ANSI type K premium gage. Each TC was welded to the wheel using the same welding unit

used for strain gages. The accuracy specifications for this premium gage wire was $\pm 2^{\circ}\text{F}$ or $+ .4\%$.

Data was collected utilizing a Campbell Scientific Model CR7 measurement system. This system's design represents a modular approach to combine precision measurement capability with multiple processors in a single battery-operated system. Some of the functions of the CR7 include data linearization, engineering unit conversion, programmed data processing, and data storage. The CR7 was configured to measure 24-four wire half bridges and 28 thermocouples for this test. The sample rate was set for 20 differential samples per second. The main advantages to the CR7 system are that it is portable, weighs approximately 30 pounds, is rugged, is expandable at a low per-channel cost, and requires no additional signal conditioning.

5.2.3.4 Test Results

The temperatures monitored during the induction heating program fitted fairly well with the predicted temperature distributions by Finite Element Analysis. The comparison of thermal residual strains between the induction heating experiments and finite element analysis is being completed.

The completed analysis of induction heating data is presented in Section 11.2.3.1.

5.3 WORK REMAINING IN TASK T4

5.3.1 Work Remaining for Dynamometer

To date, eleven of the planned thirty-five wheels involved in the dynamometer tests for Tasks T4 and T6 have been tested on the dynamometer; twenty-four wheels remain to be tested. In addition, all thirty-five wheels will be saw-cut at the Test Center for evaluation of residual stress.

5.3.2 Work Remaining for RDU Testing

Testing on RDU pertaining to Technical Task T4 has been completed in all respects.

5.4 SCHEDULE FOR COMPLETION OF TASK T4

5.4.1 Schedule for Dynamometer Tests

Dynamometer tests are continuing, one wheel at a time, at a current rate of about one per week. However, we have experienced considerable trouble recently with the outboard bearing assembly and the stub axles. We anticipate having an outage for an additional three to four weeks for an overhaul of this portion of the dynamometer. In addition, the dynamometer control and instrumentation system is going to be updated about the end of the year. This will provide vastly improved accuracy and precision of the brake-force system, as

well as modern data gathering capability. However, an outage of four to six weeks is anticipated for installation and testing of the system. Further, the dynamometer is also used for tests not covered in the FRA contract. Therefore, it is projected that it will be difficult, if not impossible, to complete the planned dynamometer tests on schedule.

5.4.2 Schedule for RDU Data Reduction Completion

Data reduction and analysis pertaining to RDU testing is continuing. Even though it was originally intended that the real time data collected by HP9826 computer would be transferred to TTC's VAX System electronically, difficulties were experienced in getting the suitable hardware. In view of this, the collected data (in engineering units) was edited and transformed to VAX System manually and further processed for analysis.

Several programs were written for analyzing the data and the major findings and results were reported in Section 5.2.2.5 and Section 11.2.5.2.

The data analysis (of RDU testing) will be formally completed by January 1986.



6.0 MONITOR WHEEL TEMPERATURES AND STRAIN DURING BRAKING
IN TRACK TESTS (TASK 5)

6.1 CURRENT TASK STATEMENT OF WORK

1. Monitor the development and/or shakedown of wheel strains during drag braking. Monitor the residual strain field after cooling.
2. Monitor the development of wheel plate temperatures during these braking tests.

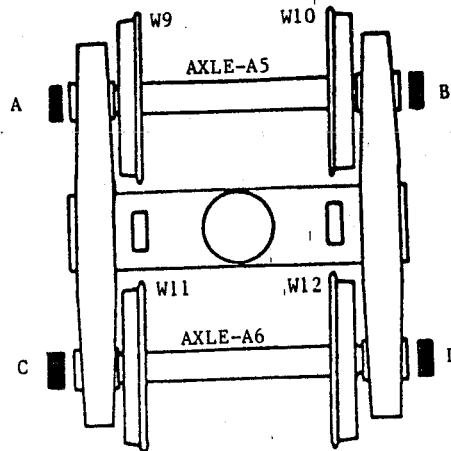
6.2 MAJOR FINDINGS/CURRENT STATUS

Preliminary track testing (T5) included measurement of wheel temperatures and strains during prescribed braking tests on railcar wheels of the same size, shape, and metallurgy, while keeping the wheel-related variables to a minimum. The test wheels selected for preliminary track testing were of Class U, 33-inch diameter as shown in Figure 6.1. Truck #1 was fully instrumented with high temperature strain gages, thermocouples and slip rings (exactly like the trucks tested on RDU as described in Section 5.0). A series of braking cycles was conducted on Truck #1 and residual stresses at strategic locations were estimated after each cycle to ascertain the stress buildup. Typical drag/stop braking cycles were selected from the test data already acquired during RDU testing in order to introduce significant stress reversals in the wheel.

WHEEL FAILURE MECHANISMS OF RAILROAD CARS PRELIMINARY TRACK TESTING

(TRACK) TEST TRUCK 1
(Instrumented Wheelsets with Slip Rings)

- 1) All Wheels: Class U, Parabolic Plate, New, Griffin CJ33
- 2) A,B,C, & D- Slip Rings
- 3) Both Axles-Drilled
- 4) All Wheels Strain Gaged and Thermocoupled at Locations B1, B2 & B3

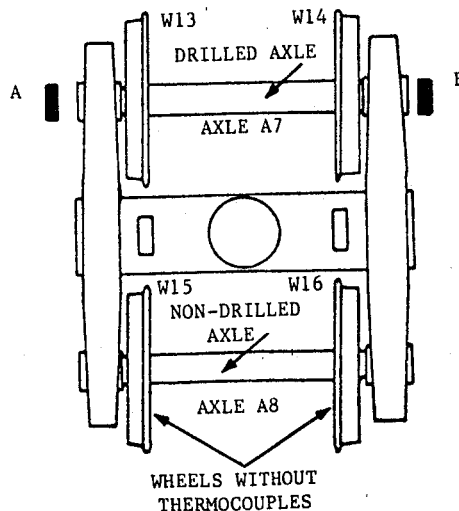


WHEEL I.D.	SERIAL NO.
W-9	94551
W-10	94554
W-11	94545
W-12	94562

NOTE: Truck 1 and Truck 2 are tested separately under two series of tests. These tests will be conducted in conjunction with thermocoupled composition brake shoes to study brake shoe thermal input effects covered under Technical Task T7.

(TRACK) TEST TRUCK 2
(With Limited Instrumentation)

- 1) All Wheels: Class U, Parabolic Plate, New, Griffin CJ33
- 2) A&B - Slip Rings



WHEEL I.D.	SERIAL NO.
W-13	95543
W-14	95531
W-15	95536
W-16	95553

FIGURE 6.1. TEST WHEELS FOR PRELIMINARY TRACK TESTS COVERED UNDER TECHNICAL TASK T5.

Apart from the estimation of residual stresses by the hole drilling technique, the test wheels with significant residual stress buildup will also be subjected to saw-cutting tests to provide the wheel data base with a known thermal history.

The test consist essentially consisted of a locomotive followed by an instrumentation car and test car. All the preliminary track tests were carried out on the Transit Test Track (TTT) at the TTC. The typical braking arrangement for the test truck is presented in Figure 6.2. The instrumentation car (211) brake reservoir was tapped into to provide the compressed air supply for the test truck brake cylinder. The test truck was also provided with instrumented brake heads to monitor the normal and tangential forces at each brake shoe/tread interface on a continuous basis.

The first phase of preliminary track testing has been completed and the data reduction/analysis is underway. During the second phase Truck #2 will be placed at the "A" end of the test car while retaining Truck #1 at the "B" end, and a second series of thermal cycles will be conducted.

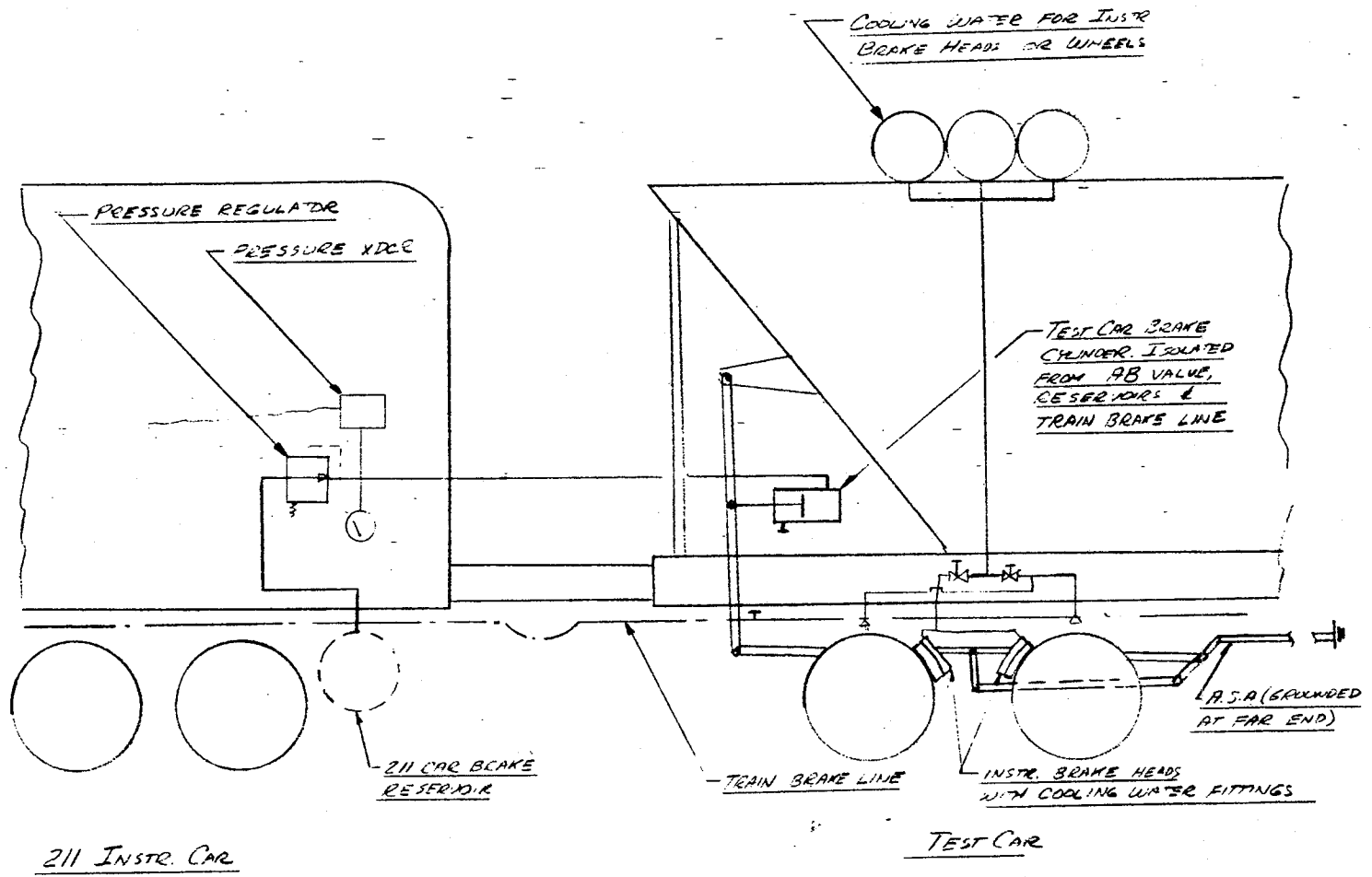


FIGURE 6.2. SCHEMATIC BRAKING ARRANGEMENT.

6.3

WORK REMAINING

Track testing with instrumented wheelsets and thermocoupled brake shoes is continuing. The tests are expected to be completed by the end of October 1985. Thermal analysis of brake shoes covered under Task 7 is also included in the above series of track tests.

6.4

SCHEDULE

Drag braking and stop braking (track) tests with instrumented wheelsets (with reapplication limit rim thickness) - October 7 through 31, 1985.





7.0 DETERMINE THE EFFECT OF WHEEL DESIGN, MATERIAL AND
OPERATION ON RESIDUAL STRESS DEVELOPMENT (TASK 6)

7.1 CURRENT TASK STATEMENT OF WORK

The AAR shall determine the effects of wheel design/material/size and brake application history on the development and/or shakedown of residual stress.

Making use of the demonstrated methodology established in Task 5, the AAR shall operate test consists, containing various types of wheels, applied with reduced instrumentation with various braking loads on TTC tracks.

Laboratory tests shall be confined to brake dynamometer, and the type of tests will be similar to those defined under Task 4, with additional wheel designs and sizes included in the testing program. The AAR shall determine the effect of the braking load on the amount of residual stress accumulated in the wheels in terms of duration and force levels of braking application and duration of cooling and reapplication.

7.2 MAJOR FINDINGS/CURRENT STATUS

7.2.1 Track Tests

Tests not started.

7.2.2 Dynamometer Tests

Tests not started.

7.3 WORK REMAINING

7.3.1 Track Tests

Table 7.1 lists the wheel types and braking conditions for the track tests.

7.3.2 Dynamometer Tests

See Table 7.2 for list of wheel types and braking conditions for the dynamometer tests.

7.4 SCHEDULE

7.4.1 Track Tests

These tests will start after the Task 5 track tests are completed.

7.4.2 Dynamometer Tests

These tests will start after the Task 4 dynamometer tests are completed.

TABLE 7.1. TECHNICAL TASK 6 - TRACK TESTING - MATRIX OF TEST WHEELS.

Size	Wheel Plate Design	Class	Brake Application				Moderate Speed				
			Low Speed		Unreleased Hand Brake	High Brake Force				Low Brake Force	
			High Brake Force	Low Brake Force			High Brake Force	High Brake Force	High Brake Force		High Brake Force
33"	Curved	U	PN	SN	PN	PN	PN	SN	PR	SR	PN
		C	PN	SN	PN	PN	PN	SN	PR	SR	PN
	Straight	U	N	N	N	N	N	R	N	N	
		C	N	N	N	N	N	R	N	N	
36"	Curved	U	SN		SN	SN	SR				
		C	PN		PN	PN	PR				
	Straight	U	N	N	N	N	N	R	N	N	
		C	N	N	N	N	N	R	N	N	

P - Parabolic
 S - Shape
 N - New
 R - Application Limit

TABLE 7.2. DYNAMOMETER TEST* FOR TASK T6.

Section	Plate Type	Class**	Rim Type***	Low Speed (20 mph)			High Speed (40 mph)		
				HBF+	LBF+	UHB+	HBF	LBF	UHB
<u>TASK T6</u>									
J 33	S-Shape	U	N	--	--	--	25	-	-
		C	N	--	--	--	26	-	-
CH 36	Parabolic	U	N	--	--	--	27	-	-
		C	N	--	--	--	28	-	-
H 36	S-Shape	U	N	--	--	--	29	-	-
		C	N	--	--	--	30	-	-
H 36	Straight	U	N	31	--	32	33	34	-
		C	N	35	--	36	37	-	-

* Instrumentation consists of one metal strain gage on the front hub-plate fillet and thermocouple on the tread, back-rim face, and front hub-plate fillet. Each wheel will be drag-brake tested for 25 heating/cooling cycles. All tests except 23 and 24 to be conducted with vertical load.

** A = Annealed Class U - not Class A

*** N = New, R = Reapplication Limit

+ HBF = High Brake Force, about 1,500 lbs

LBF = Low Brake Force, about 750 lbs

UHB = Unreleased Hand-brake force, about 3,000 lbs

All numbers in the table represent wheel numbers.

8.0 DETERMINE BRAKE SHOE THERMAL INPUT AND BEHAVIOR (TASK 7)

8.1 CURRENT TASK STATEMENT OF WORK

The AAR shall determine the thermal input to wheels from composition brake shoes. These data shall be obtained from preliminary runs of the test consist at TTC using instrumented wheelsets and thermocoupled composition brake shoes. Temperature data shall then be used in the finite element analysis at Chicago to quantify the heat input at the brake shoe/wheel interface.

8.2 MAJOR FINDINGS/CURRENT STATUS

8.2.1 Track Tests

These tests with instrumented wheelsets and brake shoes are currently in progress. Thermocouples are provided at different depths from the contacting face of brake shoes to monitor the temperature distribution within the brake shoe during drag braking tests.

8.2.2 Finite Element Analysis

These studies have not been started.

8.3 WORK REMAINING

8.3.1 Track Tests

These tests should be completed in October 1985. The temperature data will then be furnished to AAR Chicago for finite element analysis.

8.3.2 Finite Element Analysis

All of the finite element analysis work for the quantification of the heat input to the brake shoe/wheel interface remains.

8.4 SCHEDULE

8.4.1 Track Tests

These tests should be completed in October 1985.

8.4.2 Finite Element Analysis

These studies will start when the temperature data from the track tests are available. This analysis should be completed by May 1986.



9.0 INITIATE WHEEL CRACKS IN DYNAMOMETER AND TTC TRACK TESTS (TASK 8)

9.1 CURRENT TASK STATEMENT OF WORK

The AAR shall determine conditions necessary for crack initiation or growth. Data and results from Tasks 3 through 7 will be used to produce initiation or growth of thermal cracks in three to five wheels on a dynamometer.

Crack growth under selected thermal and mechanical inputs shall be monitored using a quantitative ultrasonic technique developed for measuring the size of rail flaws.

The wheels shall be sectioned after the crack has grown to approximately a half-inch depth to verify the ultrasonic crack size measurement, to determine the state of residual stress, and to analyze metallurgical changes and fracture modes.

Results from Tasks 3 through 7 and the results from the crack growth task on the dynamometer shall be used to produce initiation or growth of thermal cracks on at least 8 wheels of a representative wheel type and class in a test consist operating at two speeds at the TTC. The thermal cycles may constitute a combination of drag and stop braking efforts.

9.2 MAJOR FINDINGS/CURRENT STATUS

Testing not yet begun.

9.3 SCHEDULE

9.3.1 Dynamometer Tests

These tests will begin after the tests covered in Task 6 are completed.

9.3.2 Track Tests

These tests will begin after the above dynamometer tests are completed, probably in spring/summer 1986.



10.0 DETERMINE THE EFFECT OF WHEEL SLID FLATS
ON TREAD SHELL PRODUCTION (TASK 9)

10.1 CURRENT TASK STATEMENT OF WORK

Slid Flats and Tread Shelling Studies were originally intended as a preliminary and limited approach in modeling and testing efforts to investigate the overall tread shelling problem. In view of its limited effort in addressing a complex problem like tread shelling, Technical Task 9 has been eliminated (TTC as well as Chicago efforts) in the reduced scope of the Wheel Failure Mechanisms Program.

10.2 MAJOR FINDINGS/CURRENT STATUS

Not applicable.

10.3 WORK REMAINING

Not applicable.

10.4 SCHEDULE

Not applicable.



11.0 DEVELOP A COMPREHENSIVE FAILURE MODEL (TASK 10)

The overall objective of the program is to develop technically sound wheel removal criteria and guidelines for safe design and operation. To help achieve this objective, a comprehensive analytical effort is required to ensure thorough interpretation of data from various experimental tasks and to support the specific objectives of several other tasks. Therefore, Program Task 10 was created with the following statement of work.

11.1 CURRENT TASK STATEMENT OF WORK

The AAR shall complete an analysis of all data accumulated and results of previous tasks and the following, Task 11. The AAR shall isolate the combination of brake shoe force, time, and velocity which will produce critical levels of residual stress in combinations of the various wheel designs, heat treatments, and brake shoes. The data shall be presented graphically for selected sets of wheel design, heat treatment, and brake shoes. The methodology of producing the graphic results (either a three-dimensional plot or nomograph with velocity, brake force, and time inputs) shall be sufficiently documented so that plots can be constructed using any combination of design, heat treatment, and shoe type of interest. The AAR shall attempt to determine the path dependence of thermally induced stress change caused by more than one braking cycle. The AAR shall also develop a cumulative damage low-cycle fatigue model for calculating crack initiation, using data obtained in Tasks 3 through 9. Crack initiation from martensite will be presented in a statistical manner.

11.2

MAJOR FINDINGS/CURRENT STATUS

Interim progress on this task will be reported in the same topical outline as used in the task planning document, P-10, submitted to FRA in April 1983. The representation of subproject plans in May 1984 did not materially alter the original task plans, but rather emphasized the statistical and crack analyses aspects in SP2 (Wheel Failure Mechanisms, Verification, and Countermeasures) and the residual stress related analyses in SP3 (Safety Risks Due to Overheated Wheels). Both subproject plans contained many of the same elements for the Mechanical Analysis Task 10, and will be reported in consolidated form in the following.

11.2.1

General Data Correlation and Statistical Analyses

The primary goal of this subtask is to isolate combinations of wheel designs and operation that result in critical levels of residual stress. At this time in the overall program, the data base contains or is being updated with pertinent data from the wheel saw-cutting, RDU, and brake dynamometer test programs. Residual stress estimates based on hole drilling are available for some of these test wheels. Although there is insufficient data accumulation at this time for application of the statistical methods planned, some efforts to correlate indices of braking severity with residual stress changes have been undertaken.

11.2.1.1 Analyses

During braking tests on RDU, apart from the evaluation of residual stresses by hole drilling strain gaging method after regular intervals, the thermal and residual strains monitored by high temperature strain gages on a continuous basis during and after testing were reduced for further stress analysis. Fortran programs have been written to determine the hoop, radial, and effective stresses including plastic strains during RDU braking (heating) tests. The brake shoe/wheel interface forces were continuously monitored and the BHP for each wheel was computed and acquired. The temperature levels attained by different locations of the test wheels were monitored so that the actual strains, temperatures, and BHPs could be interrelated.

The data were analyzed assuming the indices of braking severity to be parameters such as average BHP dissipated at the brake shoe/wheel interface, and elastic effective stresses computed at various critical locations of the wheel. These indices were correlated with the maximum temperatures attained at different critical locations of the wheel.

Typical correlations between elastic effective stress and maximum temperatures attained at a given location are presented in Figures 11.1 and 11.2. Correlations between elastic effective stress computed at a given critical location and average BHP at the corresponding wheel/brake shoe interface are presented in Figures 11.3 through 11.5.

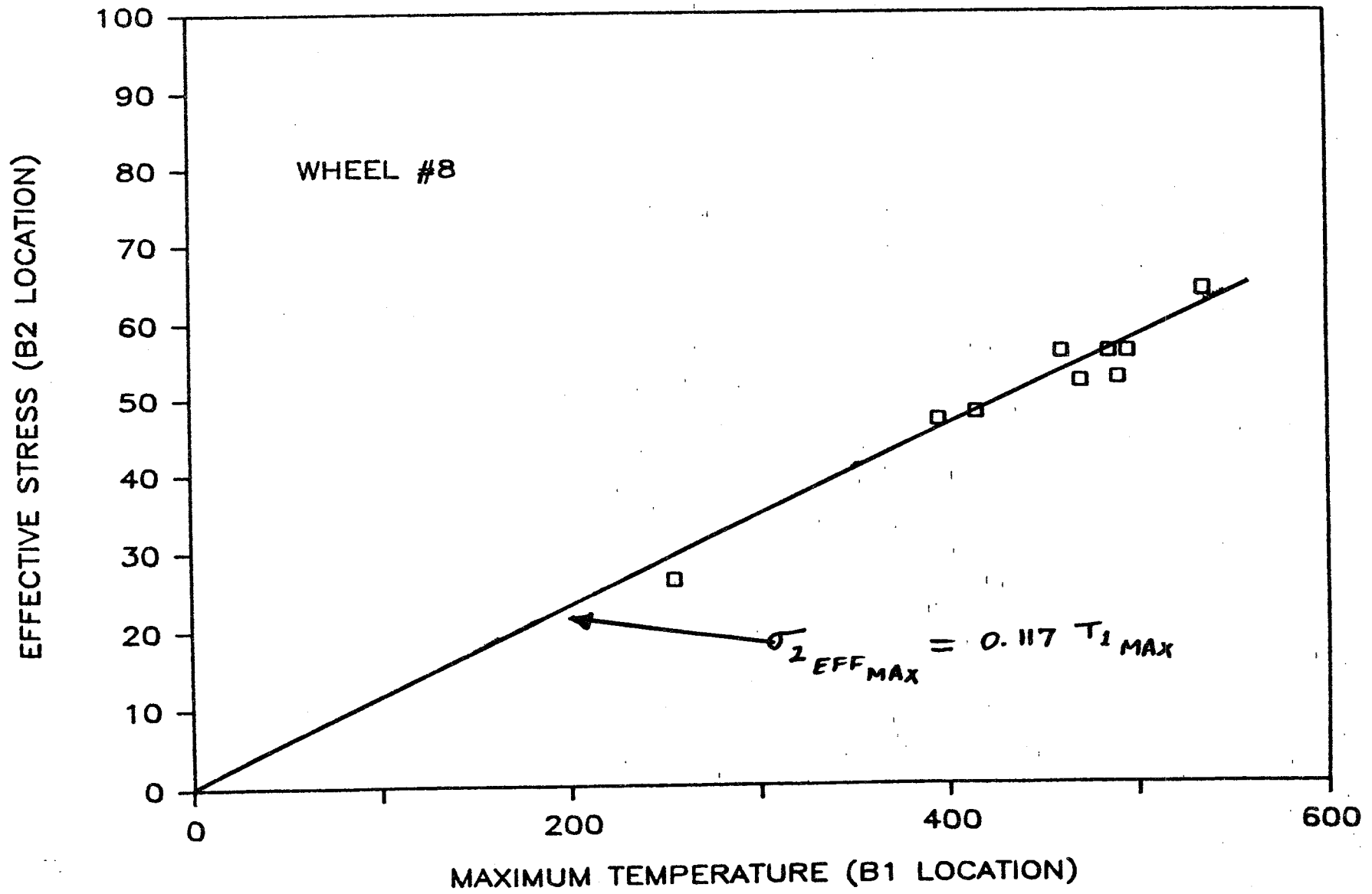


FIGURE 11.1. ELASTIC EFFECTIVE STRESS (B2) VS TEMPERATURE (B1), WHEEL #8.

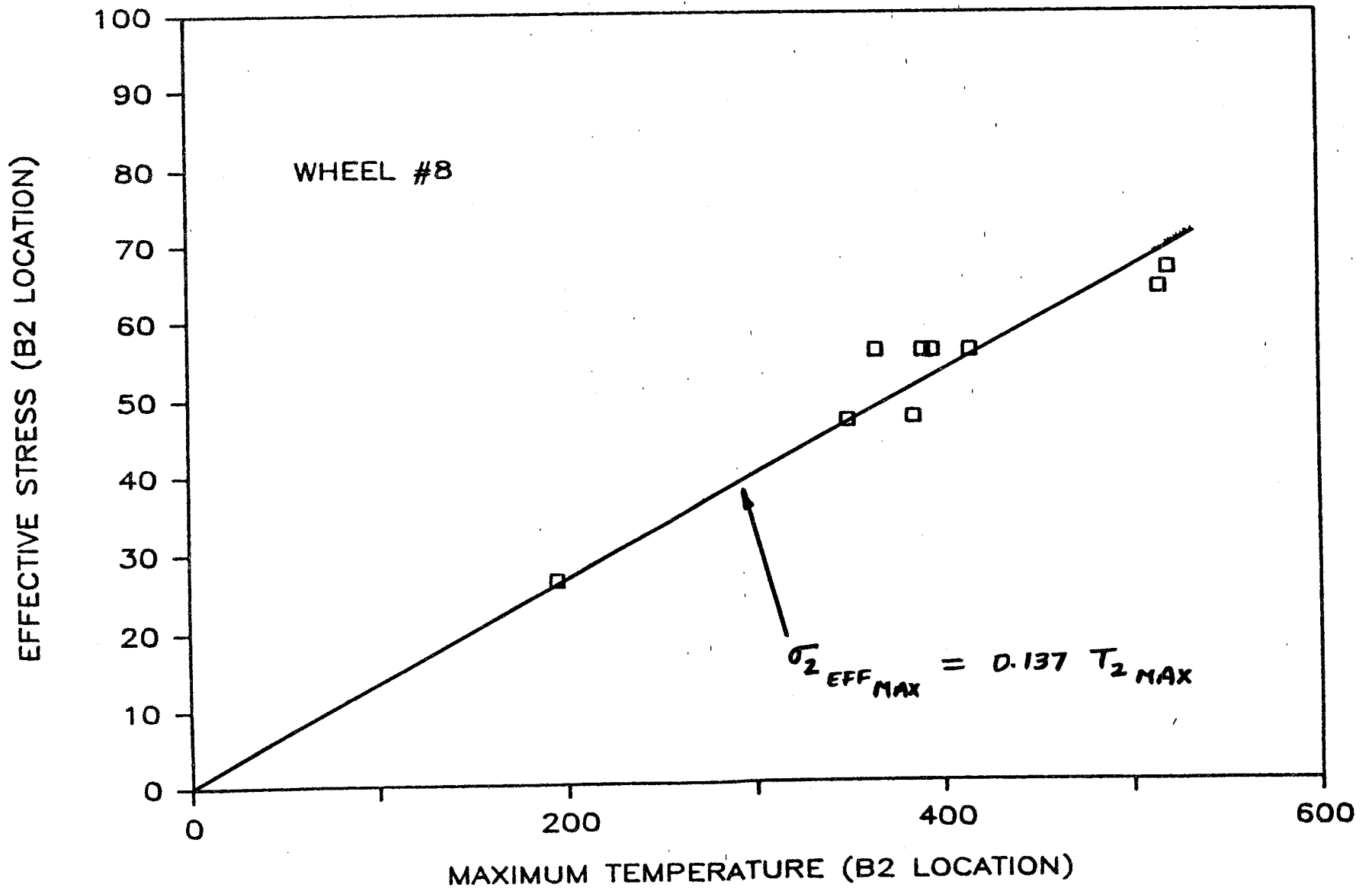
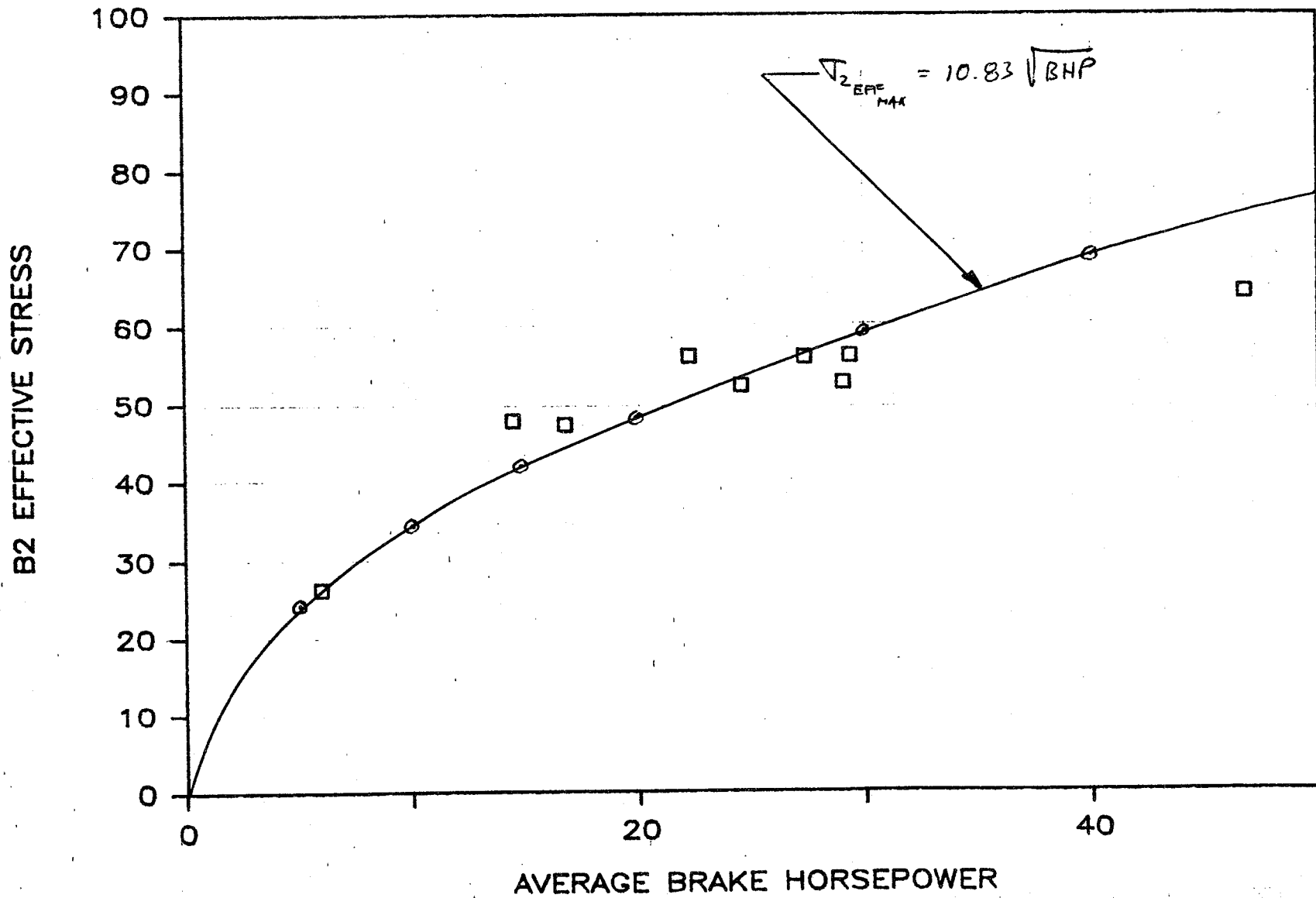


FIGURE 11.2. ELASTIC EFFECTIVE STRESS (B2) VS TEMPERATURE (B2), WHEEL #8.

WHEEL #8



11-6

FIGURE 11.3. ELASTIC EFFECTIVE STRESS (B2) VS AVERAGE BHP, WHEEL #8.

WHEEL #8

11-11

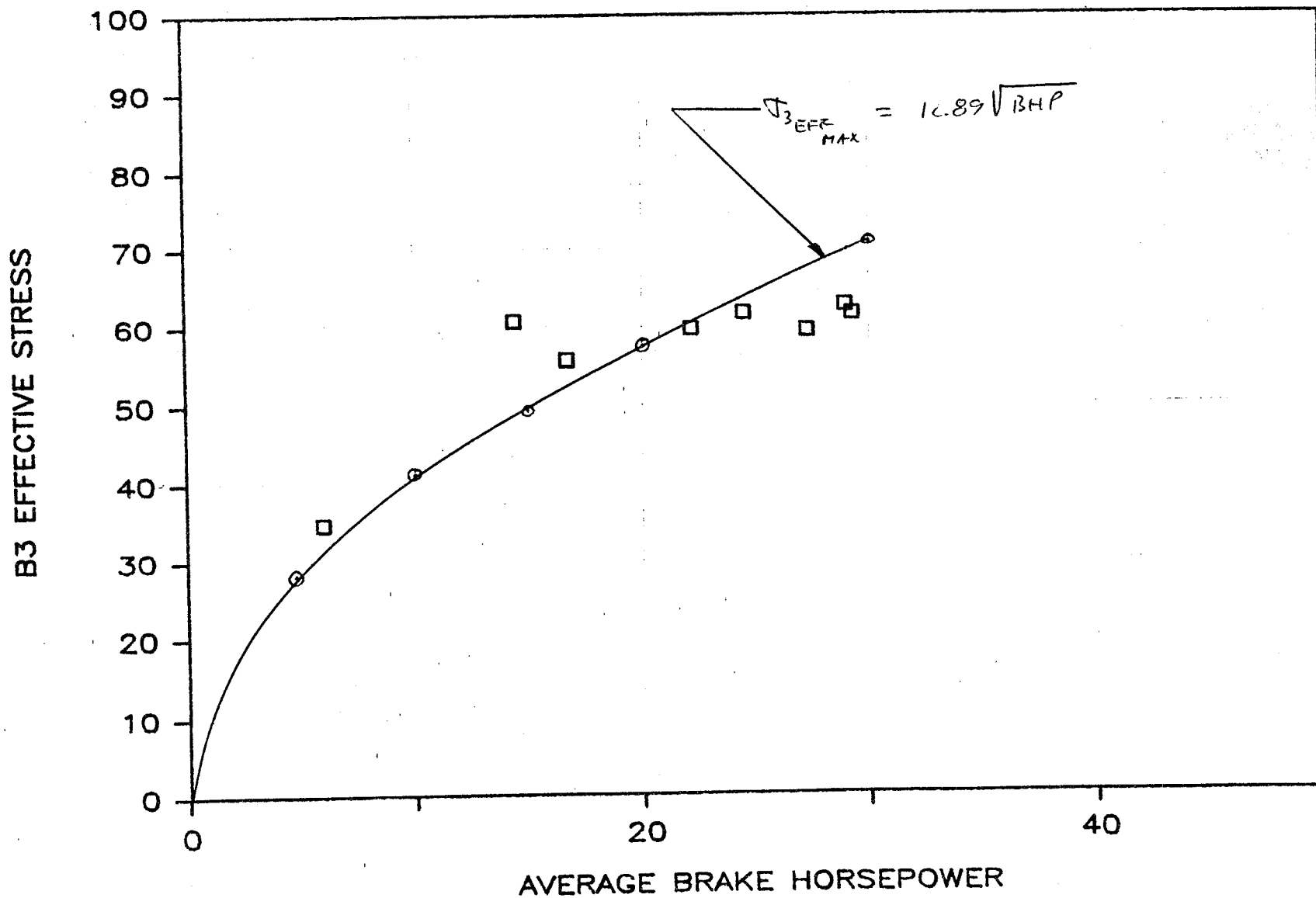


FIGURE 11.4. ELASTIC EFFECTIVE STRESS (B3) VS AVERAGE BHP, WHEEL #8.

WHEEL #7

11-8

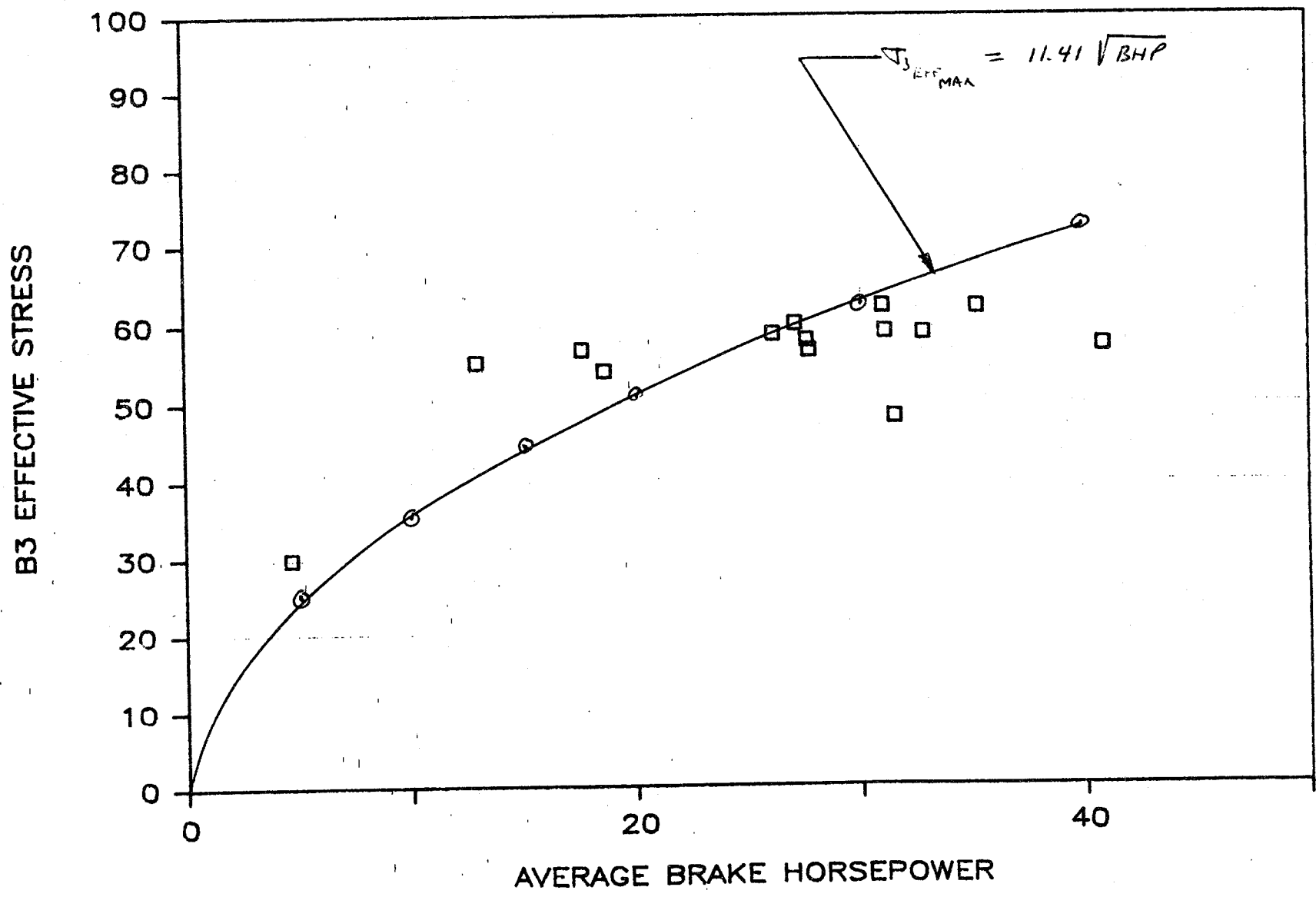


FIGURE 11.5.. ELASTIC EFFECTIVE STRESS (B3) VS AVERAGE BHP, WHEEL #7.

11.2.2 Wheel Stress Analysis Programs

The main program selected to perform finite element stress analysis (ANSYS) in support of wheel failure analysis work and other tasks has been qualified and some applications in the programs have been made. A brief summary of the thermal, elastic and inelastic analyses completed or attempted is presented below.

11.2.2.1 Wheel Temperature Correlation Attempts With ANSYS

The ANSYS computer program is a large-scale, general purpose computer program for the solution of several classes of engineering analyses. Analysis capabilities include static and dynamic; elastic, plastic, creep and swelling; buckling; small transfer, fluid and current flow. It is a well established, commercially available computer program that has been leased and used by AAR.

Since reliable wheel temperature predictions are an important precondition for obtaining good stress results, considerable effort was applied early in the program to a selection and refinement of thermal properties and boundary conditions to give a satisfactory match to prior temperature data from induction heating experiments. These attempts are described in the application Sections 11.2.3.1 on induction heating experiment.

11.2.2.2 Elastic Analysis

The ANSYS programs have been used routinely at AAR for Thermo-elastic wheel stress analyses in support of AAR Wheel Specification S.660. At present, the elastic option is being used in this research program to estimate the wheel rim stress cycles caused by lateral and vertical rail loading on both new and worn wheel profiles. Finally, ANSYS elastic analyses have been made to estimate the residual stresses revealed by saw-cut opening displacement measurements. This application is discussed in Section 11.2.3.5 below.

11.2.2.3 Inelastic Analyses

The initial effort with ANSYS in this program to account for inelastic behavior of wheel steel was the attempt, described in 11.2.3.1, to predict the total and residual strains observed in the most severely thermally loaded induction heating experiments. Time or rate independent plastic behavior with the ANSYS kinematic option to account for Bauschinger type unloading was used. The plastic properties were specified as functions of temperature.

In addition to these ANSYS plasticity analyses, some exploratory or "bench mark" studies have been made of the creep or rate sensitive material options in order to support the cyclic stress change material simulation effort described under Section 11.2.5.2. Simple uniaxial simulations of hypothetical strain and temperature cycles

were conducted and compared to the stress cycle predictions of an independent closed form solution for a special case of kinematic hardening with second degree non-linear creep and temperature dependent properties. The two solutions, illustrated in Section 11.2.5.2.1, were essentially identical, as had been hoped, which encourages further use of the ANSYS material options with more realistic cyclic and rate dependent steel behavior. The ANSYS solution for the stress/strain loops corresponding to the hypothetical uniaxial strain and temperature cycles is illustrated in Figure 11.6.

11.2.3 Applications

In addition to the overall analytical correlation effort (above) and the inherent task elements relating to cumulative damage modeling and cyclic path dependence of residual stress changes (reported later), specific analyses are required, and have been undertaken, to support other technical tasks in the program. Progress on these supporting mechanical analysis tasks is summarized below. In some cases, reference is made to these analyses reported as part of another task.

11.2.3.1 Induction Heating Experiments, etc.

Work in this subtask has supported the proper placement of gages on test wheels in the induction heating, RDU, brake dynamometer, and track tests (Tasks 4 and 5).

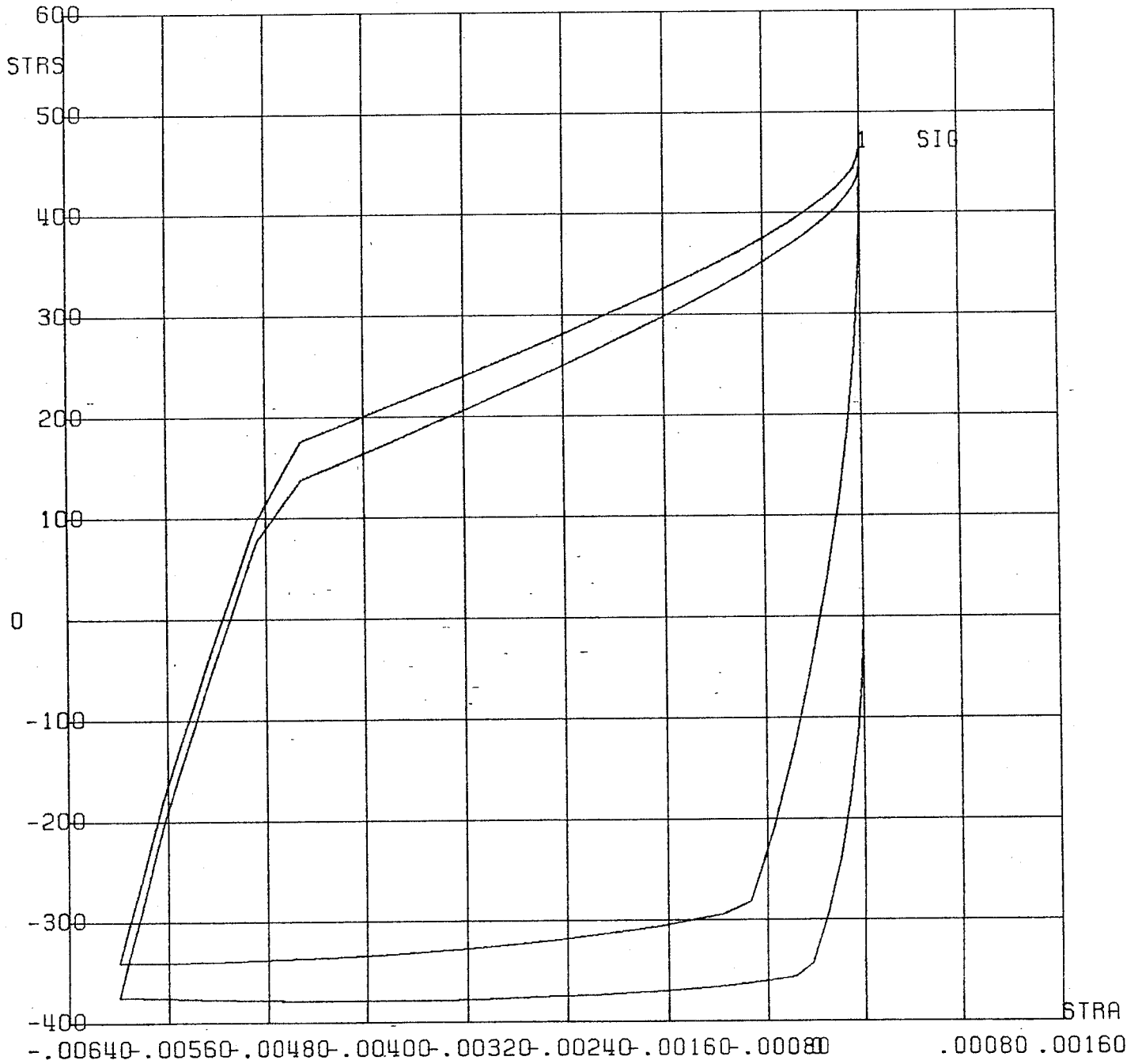


FIGURE 11.6. DEMONSTRATION ANSYS SOLUTION FOR STRESS/STRAIN LOOPS WITH RATE DEPENDENT INELASTIC MATERIAL OPTION.

Use of the AAR S-660 properties [1] with a heat input approximating 30 kW, except with a convection coefficient 30% of that listed in S-660, and radiation with an emissivity of 0.8 (there is no provision for radiation loss in S-660), yields a fairly good fit of the CH36 curved plate wheel data at 12 and 25 minutes, assuming an efficiency of 91% and deleting data from three rim thermocouples. Table 11.1 presents the observed and calculated temperature data and the deviation of the calculated from the observed. The H36 straight plate wheel data fit fairly well at 8 and 16 minutes with the assumption of 91% efficiency, except that we have to delete data from one of the two plate thermocouples in addition to one tread thermocouple. The data are given in Table 11.2.

The calculation of strains is awaiting a remeasurement of actual strain gage locations.

11.2.3.2 Detailed Residual Stress

Plans for the support of detailed residual stress measurements to be made in Task 11 are being made. In this regard, Wiss, Janney, Elstner and Associates have been hired to assist in both the experimental and analytical portion of Task 11.

11.2.3.3 Tread Crack Rig Design

Support for the design of the thermal cracking rig, part of Task 3, has been provided in the form of a transient thermal analysis of a

TABLE 11.1. INDUCTION HEATING CURVED PLATE CH36 WHEEL,
30 KW FOR 12 AND 25 MINUTES.

25 Minutes, $\eta = .91$

<u>T/C No.</u>	<u>Observed Temperature</u>	<u>Calculated Temperature</u>	<u>Deviation</u>
1	637	636	1
2	735	716	19
3	670	704	-34
4	653	685	-32
5	649	633	16
6	714	696	18
7	672	677	- 5
8	673	658	15
9	607	596	11
10	634	641	- 7
11	615	624	- 9
12	604	611	- 7
13	559	564	- 5
14	598	612	-14
15	528	575	-47
16	710	696	14
17	553	549	-16
18	416	417	- 1
19	180	178	2

12 Minutes, $\eta = .91$

<u>T/C No.</u>	<u>Observed Temperature</u>	<u>Calculated Temperature</u>	<u>Deviation</u>
1	428	398	30
2	511	474	37
3	438	462	-24
4	424	443	-19
5	423	394	29
6	477	453	24
7	433	436	- 3
8	435	417	18
9	373	359	14
10	401	402	- 1
11	379	385	- 6
12	367	373	- 6
13	325	330	- 5
14	374	375	- 1
15	313	340	-27
16	472	453	19
17	312	316	- 4
18	218	219	- 1
19	95	98	- 3

TABLE 11.2. INDUCTION HEATING OF STRAIGHT PLATE H36 WHEEL,
30 KW FOR 8 AND 16 MINUTES.

8 Minutes, $\eta = .91$

<u>T/C No.</u>	<u>Observed Temperature</u>	<u>Calculated Temperature</u>	<u>Deviation</u>
1	358	349	9
2	274	425	
3	407	416	- 9
4	401	401	0
5	359	348	11
6	378	390	-12
7	369	377	- 8
8	358	358	0
9	300	298	2
10	325	339	-14
11	307	317	-10
12	303	308	- 5
13	264	268	- 4
14	297	276	21
15	266	261	5
16	390	390	0
17	251	250	1
18	143	185	-42
19	72	78	- 6

16 Minutes, $\eta = .91$

<u>T/C No.</u>	<u>Observed Temperature</u>	<u>Calculated Temperature</u>	<u>Deviation</u>
1	532	540	- 8
2	457	620	
3	599	610	-11
4	592	594	- 2
5	544	539	5
6	576	581	- 5
7	562	568	- 6
8	551	549	2
9	487	484	3
10	517	528	-11
11	500	505	- 5
12	494	496	- 2
13	451	453	- 2
14	473	462	11
15	429	447	-18
16	587	581	6
17	427	434	- 7
18	272	333	-61
19	101	103	- 2

moving heat source (reported under Task 3). This analysis was based on an adaptation of Archard's solution (ASME Wear Control Handbook, p. 135) for a temperature rise across a moving hot spot of a given "strength" and speed. It facilitated a preliminary selection of torch thermal ratings and wheel rotation speeds to produce temperatures high enough to produce transformation to austenite. Austenite is required for transformation to martensite on cooling. Cracking initiates in martensite during further restrained cooling.

11.2.3.4 Wheel/Rail Heat Transfer

The amount of heat transfer at the wheel/rail contact in Task 4 has been estimated based on measurements of the increase of heat content of the "rail" wheel in both the RDU and the brake dynamometer as well as the leading to trailing rail surface temperature measurements reported in Task 4.

The first method assumes all the heat transferred through wheel/rail contact raises the internal energy or heat content of the rail-wheel or roller, which is calculated from the temperature rise measured at several radial locations at the end of the braking test. The energy increase in any "ring" region of the rail-wheel is simply the following product:

Ring volume x Steel density x Specific heat of steel x Average temperature increase in ring = I (BTU).

The heat transferred, Q (BTU), during the test period, t (HRS), may be expressed in terms of equivalent horsepower, HP, as:

$$Q = 2544.5 \times \text{HP} \times t$$

The heat transfer rate in horsepower may then be obtained by equating the heat transferred and the internal energy increase during the test period.

$$\text{HP} = I \text{ [BTU]} / (2544.5 \times t \text{ [HRS]})$$

This value is a lower bound estimate since convection losses are ignored. Even so, values as high as 8 HP are obtained for nominal 50 BHP braking tests under full vertical load.

The other method of estimating heat transfer rate is based on the adaptation of closed form solutions by Rosenthal (Trans. ASME, Vol. 68, 1946, pp 849-866). Solutions for the leading and trailing surface temperatures surrounding a moving point and line heat source are described in Appendices 5.2 and 5.3. Applications of this theory are discussed under Task 4 in Section 5.2.1.5. Although consistently reliable surface temperature measurements have not yet been achieved, preliminary indications are that temperature differentials of 15°F measured at 16 inches from the contact would be expected theoretically for a heat transfer rate of about 8 HP. Such a temperature differential is within the experimental scatter of the preliminary measurement attempts.

These applications of theoretical heat transfer analysis, including estimated convection heat loss and the effect of contact area, are discussed under Task 4.

11.2.3.5 Saw-Cut Openings Analysis

The interpretation of wheel "saw-cut opening" behavior has been considerably clarified through application of non-axisymmetric ANSYS analysis to calculate the residual stresses required to "close" the saw-cut displacements.

Typical saw-cut opening displacement curves are shown in Figures 11.7 through 11.9. These patterns are representative of those obtained by the saw-cutting procedure. Figure 11.7 shows closing the saw-cut. When this behavior is observed, it is assumed that there is a state of compressive residual hoop stress within the rim of the wheel. This would be representative of a safe condition within the wheel: one that would inhibit crack growth and subsequent unstable propagation.

Figure 11.8 illustrates opening of the saw-cut as the saw moves into the wheel. This behavior is interpreted as an indication of a potentially dangerous state of residual stress in the wheel: one where there are high tensile circumferential stresses that would promote the development, growth, and unstable propagation of radial thermal cracks.

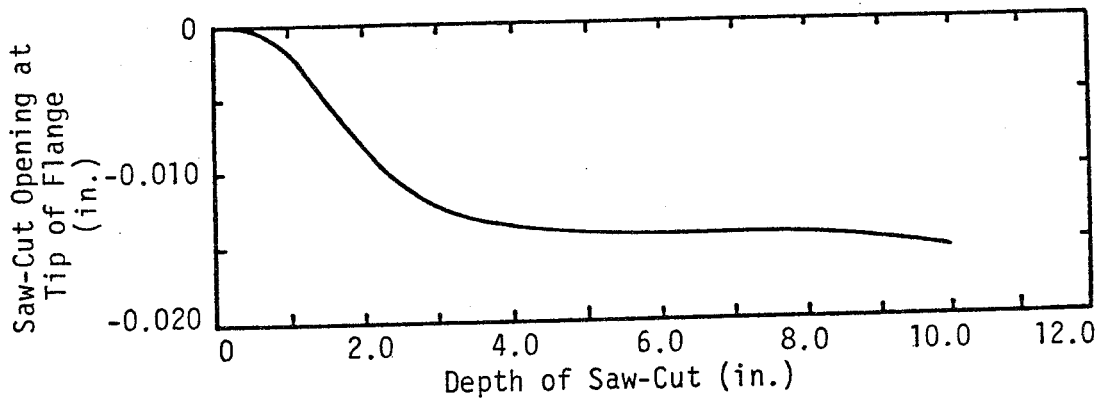


FIGURE 11.7. SAW-CUT OPENING AT TIP OF FLANGE AS FUNCTION OF DEPTH OF SAW-CUT, EXAMPLE OF SAW-CUT CLOSING (NEGATIVE DISPLACEMENT VALUES).

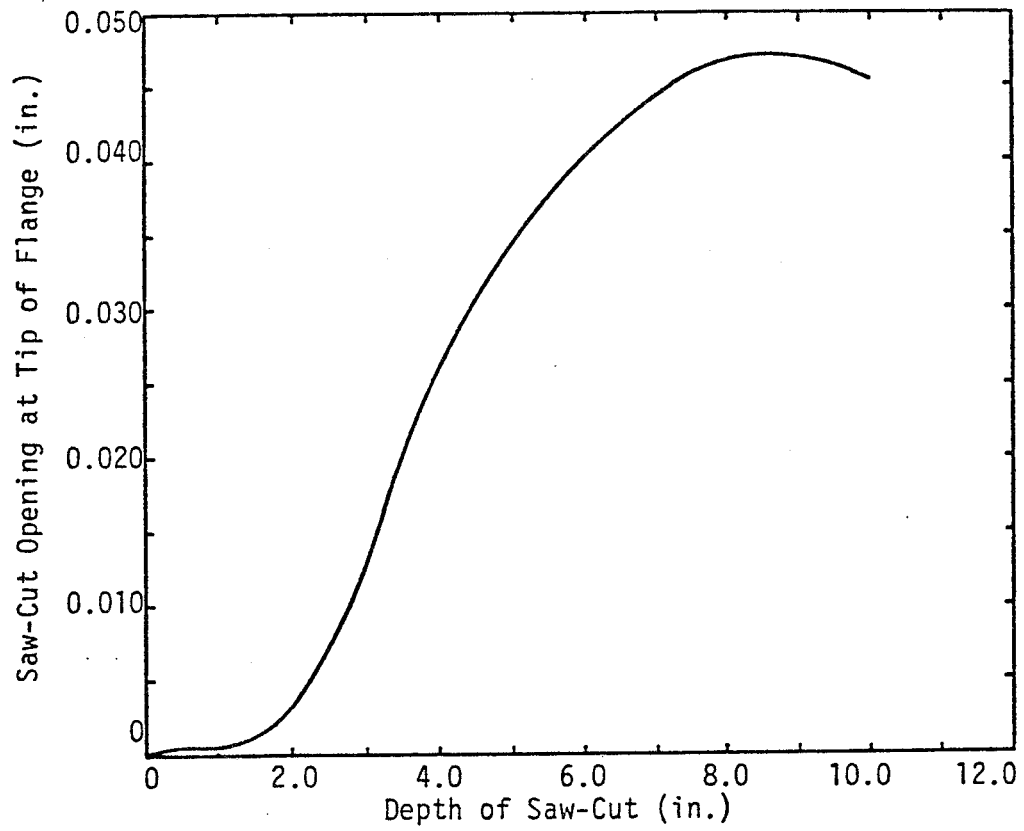


FIGURE 11.8. SAW-CUT OPENING AT TIP OF FLANGE AS FUNCTION OF DEPTH OF SAW-CUT, 36-INCH DIAMETER CURVED-PLATE WHEEL.

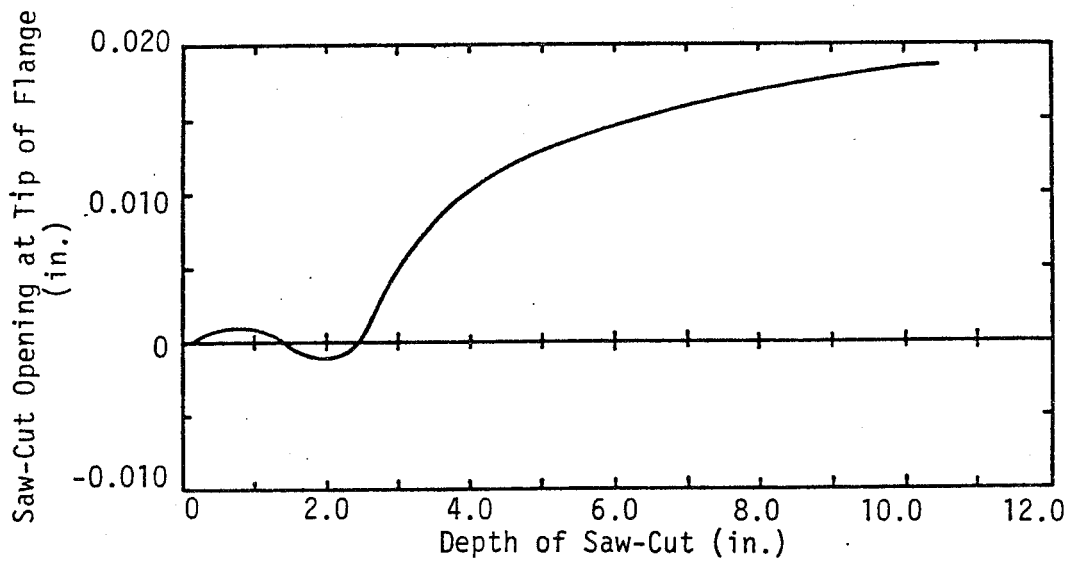


FIGURE 11.9. SAW-CUT OPENING AT TIP OF FLANGE AS FUNCTION OF DEPTH OF SAW-CUT, 36-INCH DIAMETER STRAIGHT-PLATE WHEEL.

Figure 11.9 illustrates an initial small opening and closing of the saw-cut, but then, as the cut becomes deeper, it opens. The most obvious interpretation of this type of curve is that there are compressive hoop stresses on the periphery of the wheel, but residual tensile stresses deeper in the rim and plate.

11.2.3.5.1 Analytical Procedures

The data obtained by saw-cutting can be analyzed to obtain an indication of the magnitude and distribution of the residual stresses within a wheel. The saw-cut opening-displacement curve by itself will not yield a good indication of the distribution of the residual stresses in the wheel. However, additional data, easily obtained, can lead to a much better indication of the magnitude and distribution of the residual stresses within the wheel.

The problem can be approached in the following way. The saw-cut opening displacement is measured on both sides of the wheel along the entire length of a cut that has not severed the hub. Then a three-dimensional finite element analysis is performed to determine the stresses that result when the cut is closed (as a result of circumferential displacement loading on the free surface). The radial and transverse displacements, which occur along with the circumferential displacements when the saw-cut is made, are not presently included in the displacement loading, assuming the symmetry of the problem. The stresses that are calculated for the plane of the cut are then an indication of the stresses that existed before the wheel was cut.

A number of factors must be considered when this type of analysis is performed. First, since a three-dimensional analysis is employed, a large number of elements is required, which results in a substantial amount of computational time. It is desired to use the minimum number of elements that will give acceptable convergence of the solution.

Several analyses have been done to determine the minimum number of elements that are required for an acceptable solution. The number of angle planes in the mesh is an important factor in determining the number of elements. It has been found that the optimum mesh configuration is one where the spacing of the angle planes is small in the vicinity of the cut and increased as one moves away from the cut. It has also been found that the angle planes need not go beyond 90° from the saw-cut.

The boundary conditions must also be considered. Little difference was found between calculations that utilized a model that spanned 180° and one that was fixed at 90° . The nodes at the bottom of the cut and the 90° boundaries were fixed circumferentially, but allowed to move radially.

Ideally, displacements should be measured on the inside surface of the rim that is generated by the cut. It is assumed for the present analysis that the interior surfaces are planar. No higher order approximation can be made with the present method of separation (saw-cutting).

11.2.3.5.2 Results from the Analysis of Saw-Cut Data

Three examples from the analysis of saw-cut data are presented. The primary objective of these analyses was to predict the residual circumferential stresses in the rim of the wheel before the wheel was cut.

Thirty-six-Inch Diameter Curved-Plate Wheel. The first example is for a 36-inch diameter curved-plate cast wheel which gave indications of being overheated by plate discoloration. The saw-cut opening at the tip of the flange versus saw-cut depth curve is shown in Figure 11.8 for a 10-inch saw-cut in the wheel. The total opening is rather large. Figure 11.10 shows the net opening displacement of the 10-inch saw cut as a function of depth into the wheel. There are data for both the inside and outside surfaces of the wheel. Note that there is a significant difference between the two in the rim of the wheel.

Calculations have been made using two different finite element codes: SAP IV(5) and ANSYS (6). The results were essentially the same. Figure 11.11 shows the circumferential residual stress that are calculated. The circumferential tensile residual stress on the back rim face is predicted to be approximately 35 ksi. The distribution of the residual stresses in the rim is quite similar to that predicted by inelastic finite element techniques for severe brake heating on the tread of the wheel [1,2,3].

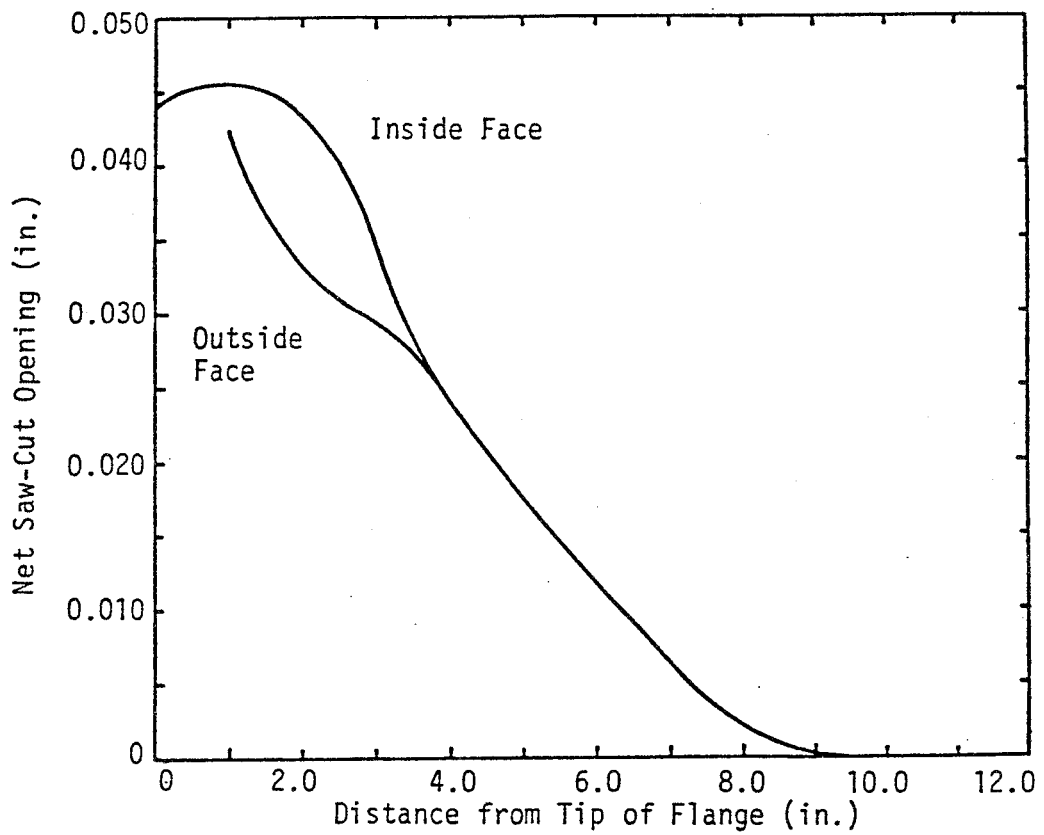


FIGURE 11.10. NET SAW-CUT AS FUNCTION OF DEPTH OF CUT INTO WHEEL, 36-INCH DIAMETER CURVED-PLATE WHEEL.

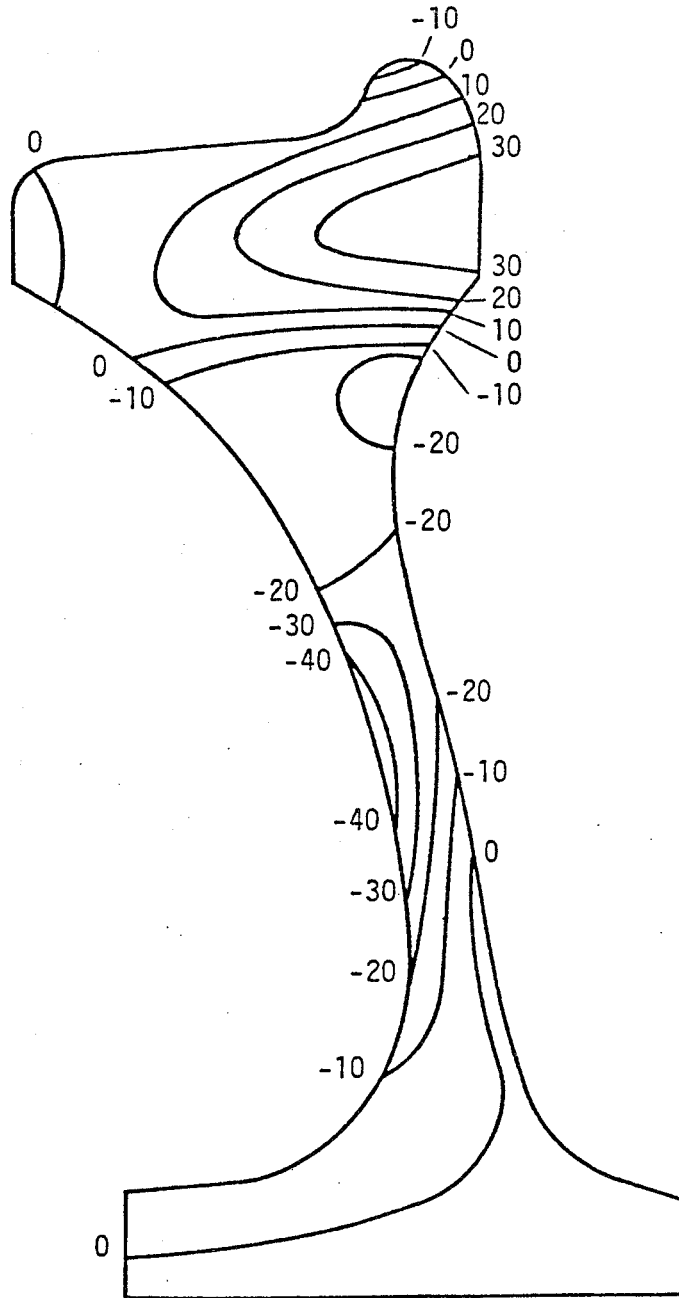


FIGURE 11.11. RESIDUAL CIRCUMFERENTIAL STRESS DISTRIBUTION PREDICTED FOR 36-INCH DIAMETER CURVED-PLATE WHEEL FROM SAW-CUT DISPLACEMENT DATA (STRESSES IN KSI).

Thirty-six-Inch Diameter Straight-Plate Wheel. Figure 11.9 shows the saw-cut opening at the tip of the flange versus saw-cut depth for a 10.5-inch saw-cut into a 36-inch diameter straight-plate wheel. This wheel also gave evidence of being overheated (plate discoloration). The saw-cut opening for this wheel is less than that shown for the curved-plate wheel in Figure 11.8. Figure 11.12 shows the net opening displacement of the saw-cut as a function of depth of the 10.5-inch saw-cut into the wheel. Note that there is again a significant difference in the displacement data for the opposite sides of the rim of the wheel.

Results from the finite element calculation for closing the cut are shown in Figure 11.13. This figure shows the predicted circumferential residual stresses. The distribution in the rim is similar to that shown in Figure 11.11 except that the magnitudes are lower. The maximum stress is again on the back rim face and is predicted to be approximately 19 ksi.

Thirty-three-Inch Diameter Curved-Plate Wheel. Figure 11.14 shows the saw-cut opening at the tip of the flange versus the saw-cut depth for an 8.5-inch saw-cut into a 33-inch diameter curve-plate wheel. This wheel was subjected to controlled braking cycles in tests conducted on the Roll Dynamics Unit at the Transportation Test Center in Pueblo, Colorado. The wheel was subjected to over 25 simulated drag braking cycles of approximately 60 minutes each at power levels from 25 to 50 BHP. Figure 11.15 shows the net opening displacement of the 8.5-inch saw-cut as a function of depth into the

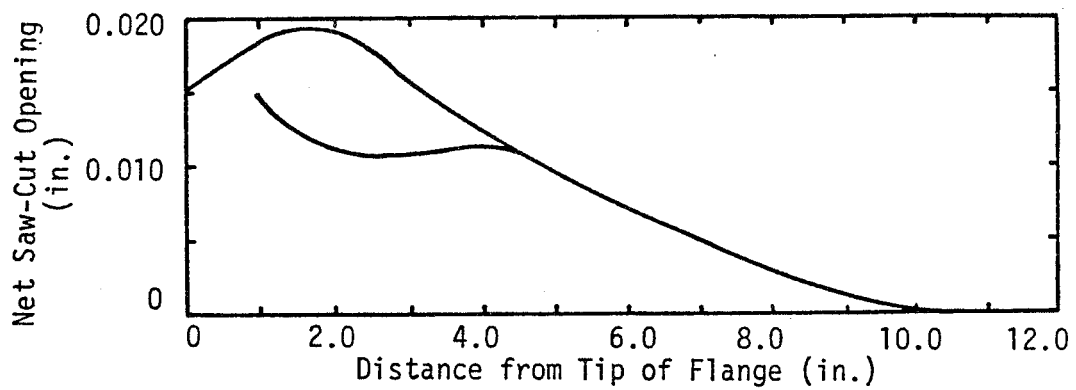


FIGURE 11.12. NET SAW-CUT OPENING AS FUNCTION OF DEPTH OF CUT INTO WHEEL, 36-INCH DIAMETER STRAIGHT-PLATE WHEEL.

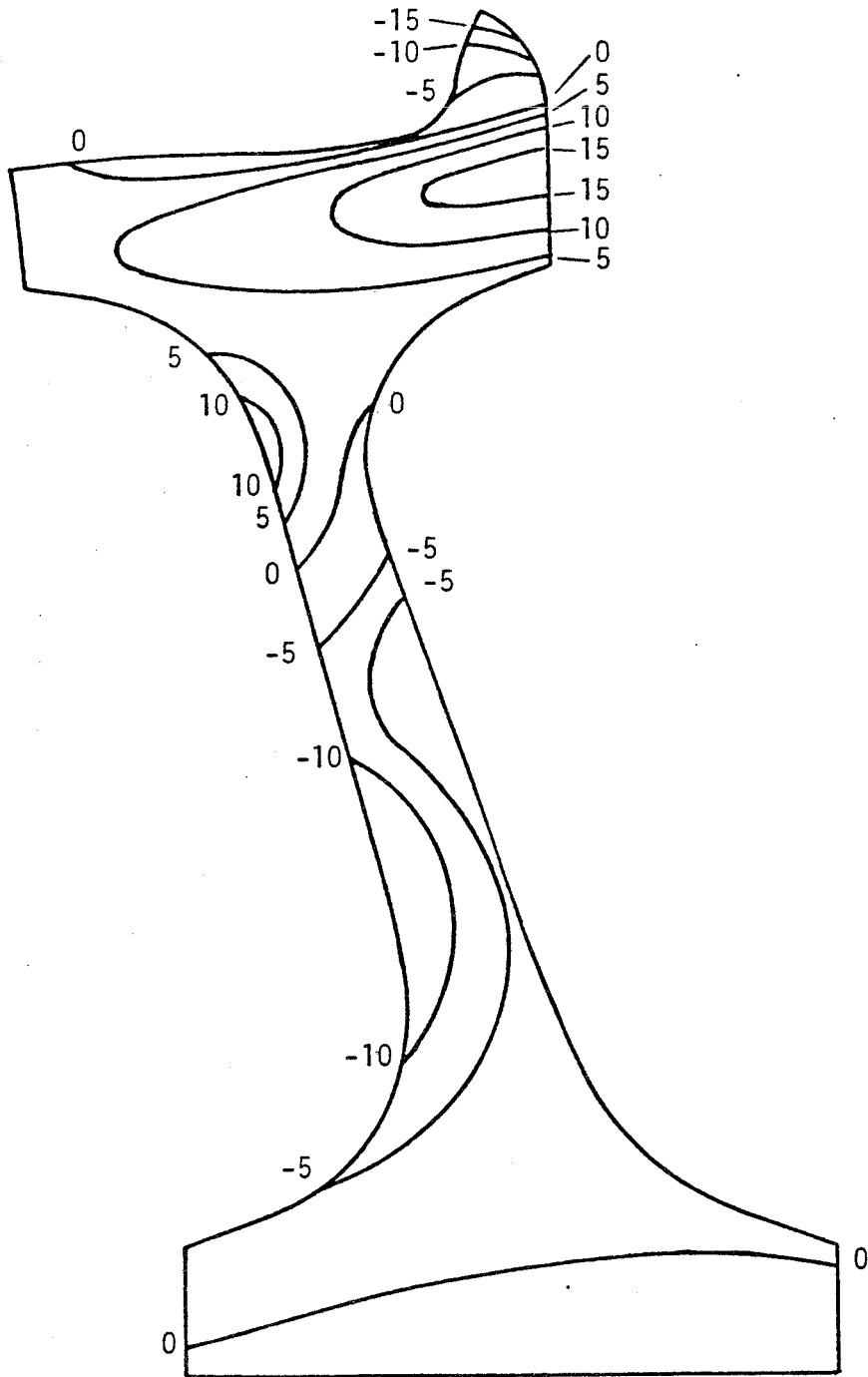


FIGURE 11.13. RESIDUAL CIRCUMFERENTIAL STRESS DISTRIBUTION PREDICTED FOR 36-INCH DIAMETER STRAIGHT-PLATE WHEEL FROM SAW-CUT DISPLACEMENT DATA (STRESSES IN KSI).

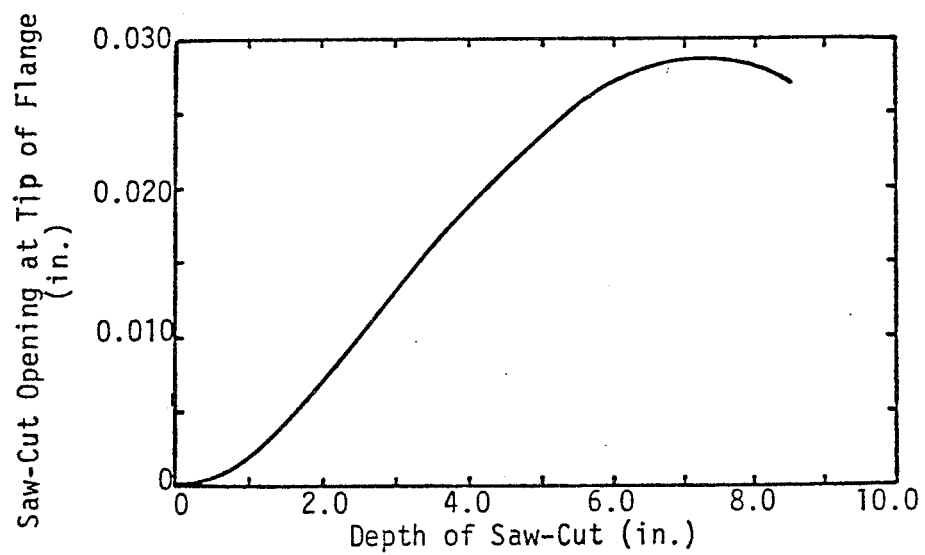


FIGURE 11.14. SAW-CUT OPENING AT TIP OF FLANGE AS FUNCTION OF DEPTH OF SAW-CUT, 33-INCH DIAMETER CURVED-PLATE WHEEL.

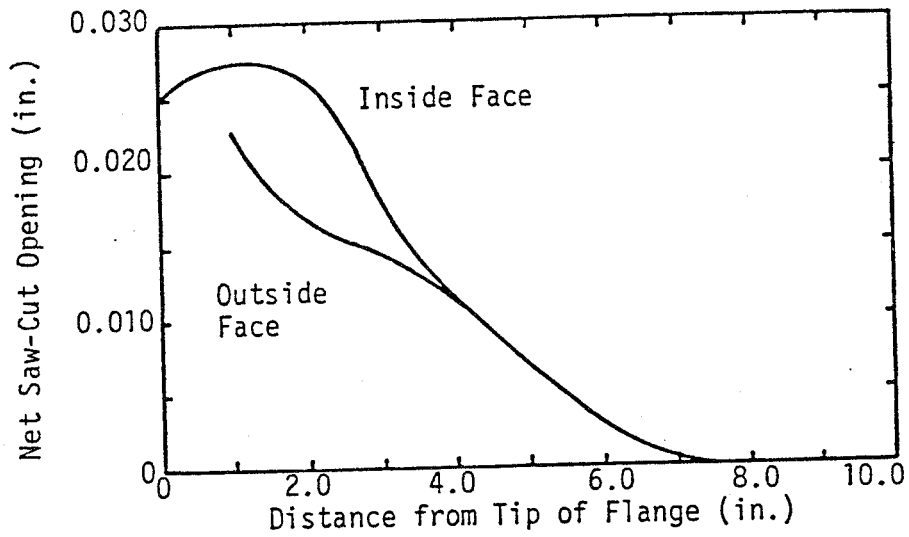


FIGURE 11.15. NET SAW-CUT OPENING AS FUNCTION OF DEPTH OF CUT INTO WHEEL, 36-INCH DIAMETER CURVED-PLATE WHEEL.

wheel. Note again that there is a significant difference in the displacement data for the opposite sides of the rim of the wheel.

Figure 11.16 shows the circumferential stresses that are predicted when the cut is closed. The stress distribution pattern in the rim is similar to those shown for the other wheels. The maximum circumferential residual stress predicted for the back rim face is approximately 30 ksi.

11.2.3.5.3 Conclusions

The following conclusions are presented for this work:

1. The technique shows great promise for calculating the state of residual stress in a wheel using saw-cut data.
2. Better cutting techniques are needed to allow a determination of residual stresses when the cut closes.
3. More accurate displacement measurement techniques are needed, especially within the rim, to improve the calculation.

11.2.3.5.4 References

1. Johnson, M.R., Welch R.E., and Yeung, K.S., "Analysis of Thermal Stresses and Residual Stress Changes in Railroad Wheels Caused by Severe Drag Braking," JOURNAL OF ENGINEERING FOR INDUSTRY (ASME) 99 (1), Series B. February 1977, pp 18-23.

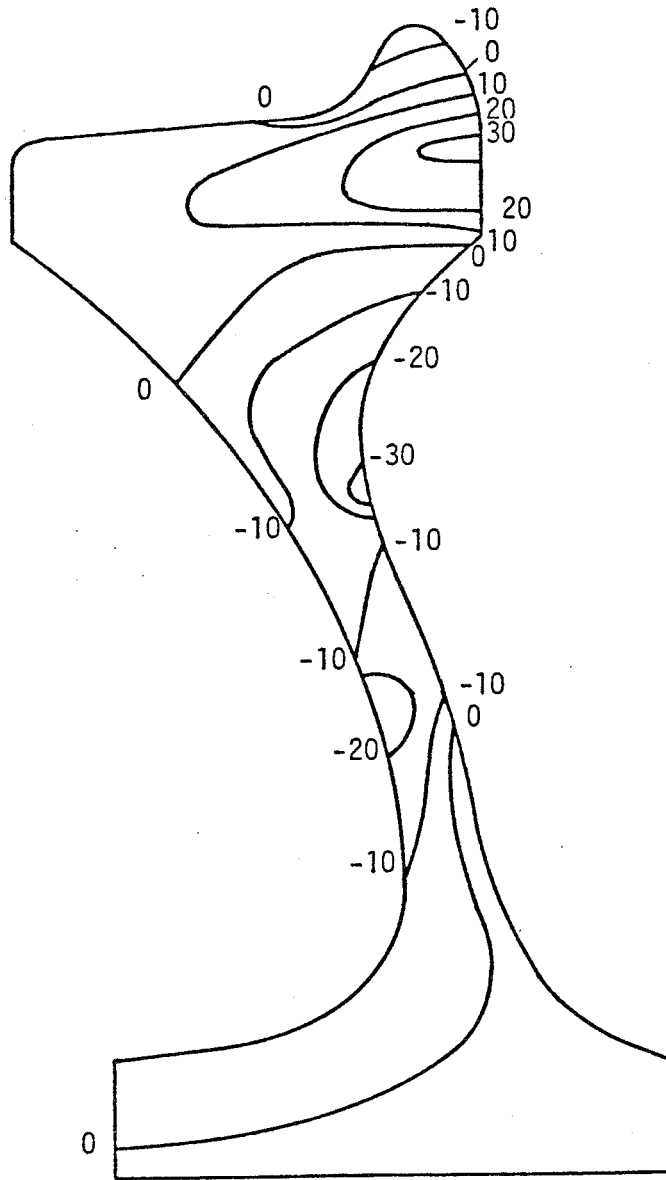


FIGURE 11.16. RESIDUAL CIRCUMFERENTIAL STRESS DISTRIBUTION PREDICTED FOR 33-INCH DIAMETER CURVED-PLATE WHEEL FROM SAW-CUT DISPLACEMENT DATA (STRESSES IN KSI).

2. Johnson, M.R., Robinson, R.R., Opinsky, A.J., and Stone, D.H., "Residual Stress Calculations on 33-Inch (838 mm) Diameter One-Wear Freight Car Wheels Under Simulated Unreleased Hand Brake Conditions," ASME Paper 82-WA/RT-11.
3. Wetenkamp, H.R., and Kipp, R.M., "Safe Thermal Loads," The Sixth International Wheelset Congress, Colorado Springs, Colorado, October 1978.
4. Jones, H.N. III, "The Characterization of the Residual Stress State of Railroad Wheels by the Saw-Cut Method," ASME RAIL TRANSPORTATION SPRING CONFERENCE PROCEEDINGS, April 1985, pp 15-19.
5. Bathe, K.J., Wilson, E.L., and Peterson, F.E., "SAP IV, A Structural Analysis Program for Static and Dynamic Response of Linear Systems," University of California (Berkeley, CA), Report No. EERC73-11, June 1973.
6. ANSYS Engineering System, Swanson Analysis Systems, Inc., Houston, PA 15432.

11.2.3.6 Thermal Analysis of Brake Shoes

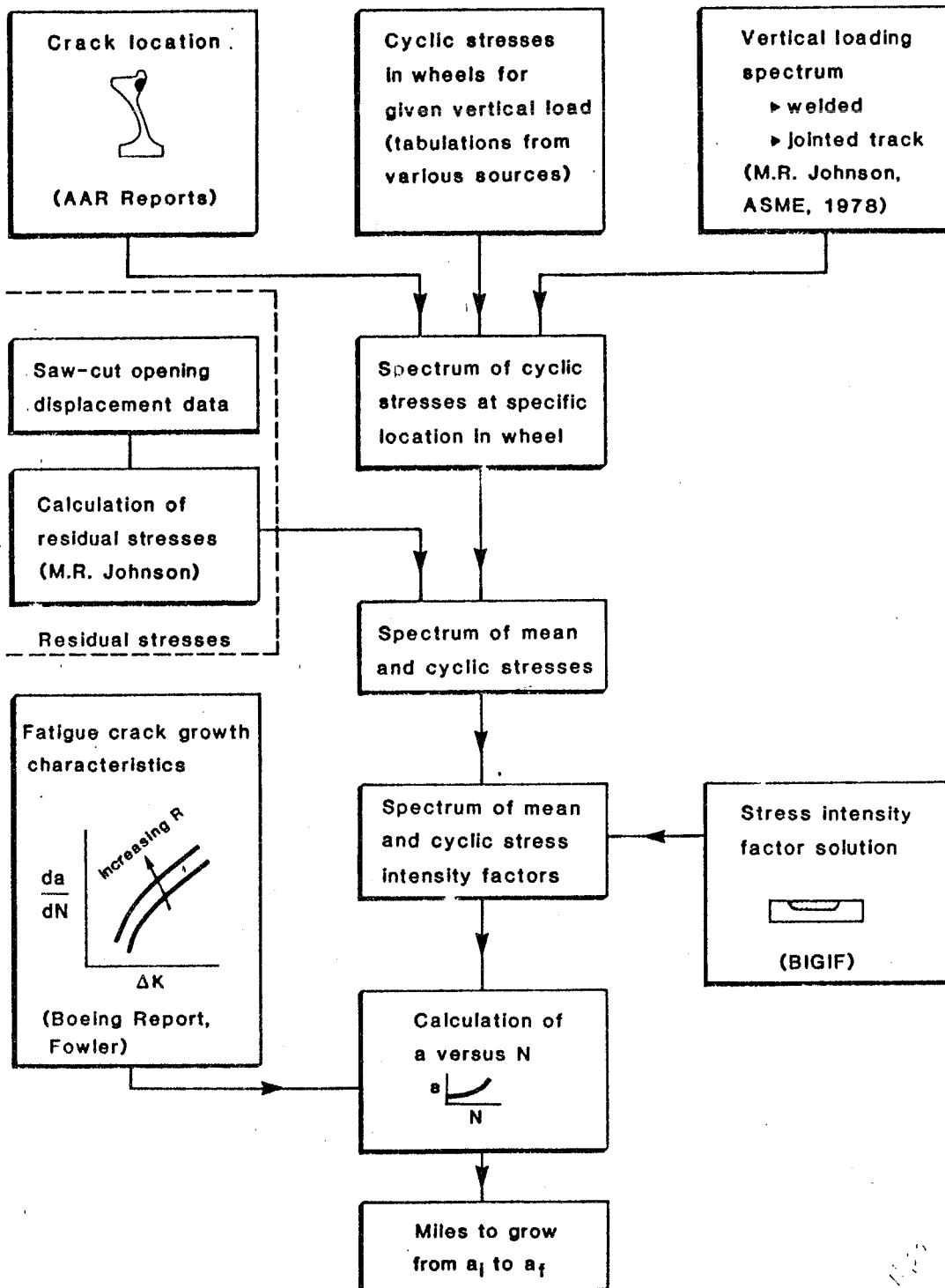
Only preliminary finite element ANSYS modeling has been attempted at this time in support of the special track and laboratory tests to estimate heat flow into the brake shoe (Task 7).

11.2.3.7 Linear Elastic Fracture Mechanics

The objective of this subtask is to predict the occurrences of wheel fracture. The interpretation of crack arrest data and derivation of associated properties is described in Task 3.

A preliminary fracture analysis has been completed. This analysis uses the residual stress fields calculated in 11.2.3.5 and cyclic mechanical stresses from various field test and theoretical sources. The entire methodology for the analysis is shown in Figure 11.17. It may be noted that the fluctuating stress estimate may not be high enough and not enough load spectra data was made available for this preliminary analysis. The results of this preliminary analysis, Figure 11.18, lead to the following conclusions:

- o Residual stresses alone are insufficient to produce a life increment less than 200,000 miles.
- o Curved and straight plate wheels are quite similar from a fatigue crack growth standpoint.
- o Periodic stress "shifts" due to braking are of lesser influence.
- o The crack aspect ratio (length/depth) at beginning of incremental life calculation is not influential.



FAA-PA-M-85-08-08

FIGURE 11.17. RESIDUAL STRESS ANALYSIS METHODOLOGY CHART.

Location	Wheel Type	Residual Stress	Applied Stress Spectrum			Initial c/a	K _{IC} , ksi-in ^{1/2}	da/dN	a _{crit} , in	a _{th} , in	Fatigue Life, miles from a _i to a _f (or a _c)			▲ a _i , in ▲ a _f , in ▼ varied ▼ K _{IC} c/a type, res loc fcg brakes more brakes jointed res. no res. brakes fcg high speed fcg no res.
			Rolling	Braking							0.75	0.75	0.50 a _c	
				freq.	σ, ksi									
A	C	I	Std	0	--	3	35	Nom	0.42	~ 0.25	3.1x10 ¹⁰	0	0	
A	C	I	Std	0	--	3	50	Nom	1.00	~ 0.25	3.2x10 ¹⁰	5.3x10 ⁸	5.9x10 ⁸	
A	C	I	Std	0	--	1	35	Nom	0.48	0.42	"	0	0	
A	S	II	Std	0	--	3	35	Nom	1.22	0.39	"	8.0x10 ⁹	8.4x10 ⁹	
D	C	I	Std	0	--	3	35	Nom	1.26	0.35	"	2.0x10 ⁷	2.1x10 ⁷	
D	C	I	Std	0	--	3	25	Worst	0.92	< 0.25	2.8x10 ⁸	2.0x10 ⁴	2.4x10 ⁴	
D	C	I	Std	1%	10	3	35	Nom	0.92	< 0.25	2.0x10 ⁷	3.2x10 ⁶	3.4x10 ⁶	
D	C	I	Std	1%	25	3	35	Nom	0.46	< 0.25	6.0x10 ⁵	0	0	
D	C	I	Jointed	0	--	3	35	Nom	1.19	~ 0.25	3.3x10 ⁸	2.7x10 ⁶	3.1x10 ⁶	
D	C	III	Jointed	0	--	3	35	Nom	> 1.19	> 1.19	"	"	"	
D	C	None	Jointed	0	--	3	35	Nom	> 0.92	0.84	"	"	"	
D	C	III	Jointed	1%	10	3	35	Nom	~ 2.0	< 0.25	1.6x10 ⁸	3.8x10 ⁷	6.0x10 ⁷	
D	C	I	Jointed	0	--	3	25	Worst	0.92	< 0.25	2.7x10 ⁶	1.5x10 ⁴	1.8x10 ⁴	
D	C	I	Hi. Sp. Jnt.	0	--	3	35	Nom	1.19	< 0.25	2.9x10 ⁷	2.6x10 ⁵	3.3x10 ⁵	
D	C	I	Hi. Sp. Jnt.	0	--	3	25	Worst	0.92	< 0.25	2.7x10 ⁵	8.0x10 ³	1.0x10 ⁴	
D	C	None	Hi. Sp. Jnt.	0	--	3	25	Worst	0.90	~ 0.50	"	1.3x10 ¹⁰	1.3x10 ¹⁰	

Location A: Back rim face
 B: Front rim face

FIGURE 11.18. SUMMARY OF ANALYSIS RESULTS.

- o High cyclic stresses due to high speed on jointed track have some influence, but less than poor fatigue crack growth properties.

11.2.4 Cumulative Fatigue Damage Model

The technical literature has been searched for candidate thermo-mechanical fatigue models that may be appropriate to treat the combination of brake thermal and rail mechanical load cycles that are important in the initiation and growth of a defect to critical size. Preliminary attempts to model the wheel failure process have been made and are described below.

11.2.4.1 Computer Simulation Approach

In the real world, very rarely are stresses measured; the quantity that is measured is strain. Hence a computer simulation of fatigue should be developed with strain as the controlling variable. This has been done at the University of Illinois by Martin [1].

In his development of the simulation, Martin breaks the stress-strain curve into small elements that are approximated by straight line segments. These segments are based mainly on a constant stress change across each element; the corresponding strains are calculated at the beginning and end of each element. To apply this segmented stress-strain curve to the computer simulation, Martin introduces the concept of availability coefficients. By availability coefficients, he controls how much of each element is used, in sequence,

to simulate the stress behavior of a strain excursion. He also states, somewhat mysteriously, that the use of availability coefficients leads to results that are equivalent to rainflow counting, which is the accepted method for obtaining complete cycles from a complex strain history.

The effort to date has been confined to learning the basic concepts. A small strain history was rainflow counted by hand before it was used in the learning phase.

The history was first examined by merely breaking the strain range into a series of increments; that is, each "element" obtained had exactly the same amount of strain in it as any other. The computer printout of availability coefficients for each strain reversal could be interpreted to correspond exactly with the rainflow count.

In the next phase, an elemental stress-strain curve was constructed, mainly as suggested by Martin. In other words, most of the elements were constructed with a constant stress range of 2 ksi. As the stress-strain curve bends over at higher stresses, the strain increment becomes larger across the element. This stress-strain behavior has the unfortunate effect of compressing the availability coefficients data, and the computer printout of the availability coefficients for each strain reversal was much harder to follow than the one obtained in the first exercise. It is believed that a strain-based elemental stress-strain curve (rather than one based mainly on stress) will solve the current problem and allow the next step in

the development of the computer simulation, which is the introduction of the fatigue behavior.

Difficulties are expected with the introduction of mean stress behavior into the fatigue damage calculation. Another approach is to use the correction suggested by Morrow [2], although it is not in closed form. A third approach is to follow that of Landgraf, which is to ignore the mean stress correction entirely [3]. While this may work in the automotive field, the main application here would be to wheels with high tensile residual stress in them, and it would appear that a mean stress correction is necessary.

11.2.4.2 Other Candidate Fatigue Models

11.2.4.2.1 Thermomechanical Fatigue Survey and Recommendation

One of the efforts undertaken in support of the assigned task of "develop(ing) a cumulative damage low-cycle fatigue model for calculating crack initiation" was to survey the current state of the art. A report of such a survey is included as Appendix 11.1.

This report presents an overview of current life prediction methods for potential application to the analysis of railroad wheel failures originating in the hot tread and rim region of the tread braked wheel. Six groups or classes of theories are reviewed.

1. Simple Time Independent Fatigue Approaches
2. Strain Range Partitioning (SRP)

3. Frequency Modified and Frequency Separation (FM)
4. Energy Based
5. Damage Rate
6. Continuum Damage

Several papers that report recent design applications of some of these methods to diesel and turbine engine components are also summarized. Recommendations for applications in railroad wheel research include: (1) additional cyclic flow behavior testing under thermomechanical fatigue simulation situations; (2) initial trials of the simple time independent elevated temperature fatigue methods (Universal Slope with and without 10% life rule) in wheel life analysis; (3) further critical evaluation and wheel applications of the SRP (Manson, et al.), FM (Coffin) and damage or crack rate (Sehitoglu) methods.

In addition, recent analyses of the propagation of tread thermal cracks reported at the 8th International Wheelset Congress in April 1985 by Meizoso and Sevillano have been reviewed. Their analysis treats the thermal braking cycle only indirectly through its effect on changing the residual stress system that the "elastic" rail contact stresses are superimposed upon.

AAR work sponsored at the University of Illinois by H. Sehitoglu is considering the interaction of thermomechanical strains and surface oxide formation in wheel steel and its effect on short crack development and propagation. This research is being followed especially

for potential application to assess the "damage" contribution of braking cycles to the wheel rim.

11.2.4.2.2 Preliminary Evaluation of Back Face Rim Failures

A preliminary attempt has been made to predict the conditions of residual stress and superimposed rail load induced stresses required for crack initiation as well as propagation in one region of the wheel rim not directly subjected to rail contact stresses - the rim back face. This fatigue evaluation considers the range of stresses caused by rail load cycles, the effect of residual stress on crack initiation and propagation, and the possible range of pertinent fatigue properties. A summary of these conditions follows.

For the normal unworn wheel profile, the quasi-static variation in stresses on the back rim caused by rail loading (even that component of load which is most influential - lateral load) is relatively small. From elastic analysis and tests reported by Wetenkamp and Kipp in a 1977 ASME paper, the hoop stress variation at the B1 location for a 20,000 pound lateral load was plotted in Figure 11.19. Note that this stress range is less than 5 ksi.

Detrimental residual stresses such as those induced in the back face rim by very severe braking cycles can reduce the expected wheel life due to crack initiation and/or increase the crack propagation rate. These effects are illustrated in Figure 11.20 for crack initiation based on Manson's mean stress correction and in Figure 11.21 for crack propagation based on data from Fowler in 1976.

LOW BACK RIM HOOP STRESS for 20 KIP LAT.

33-In. Wheel from WETENKAMP & KIPP 1977

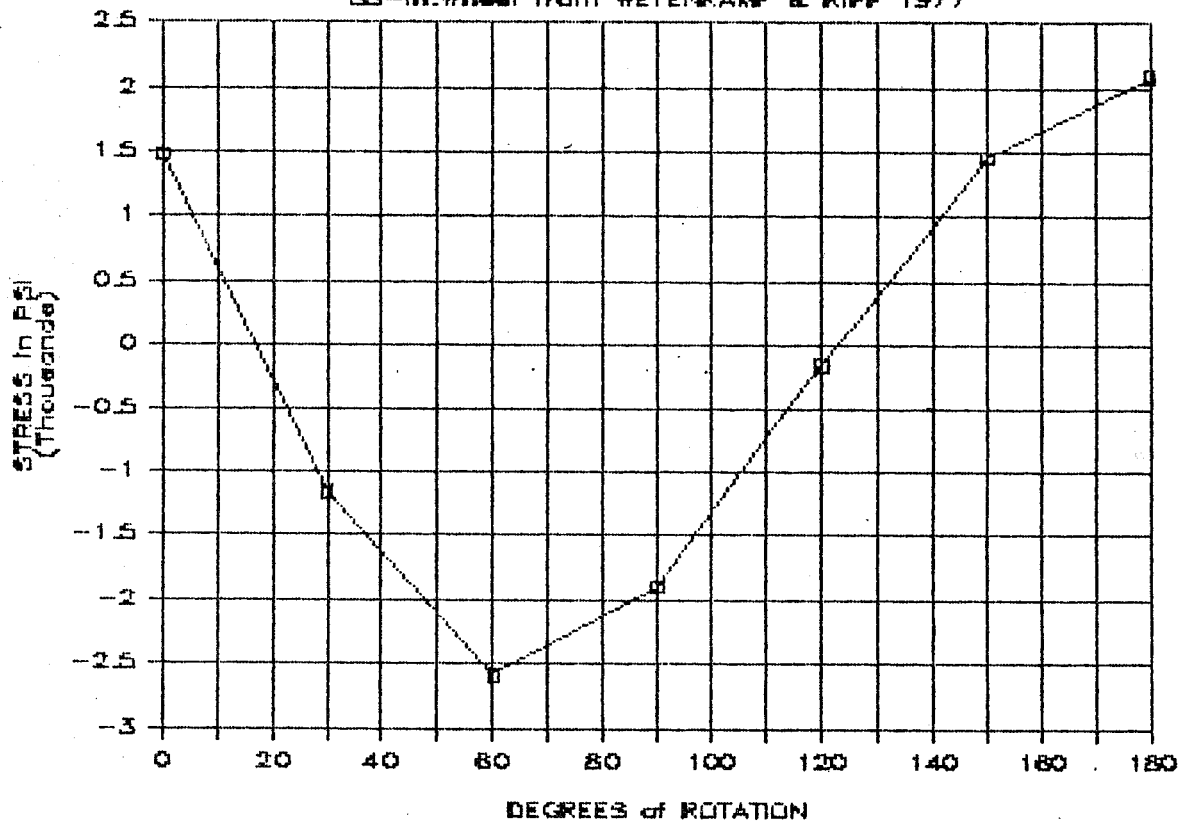
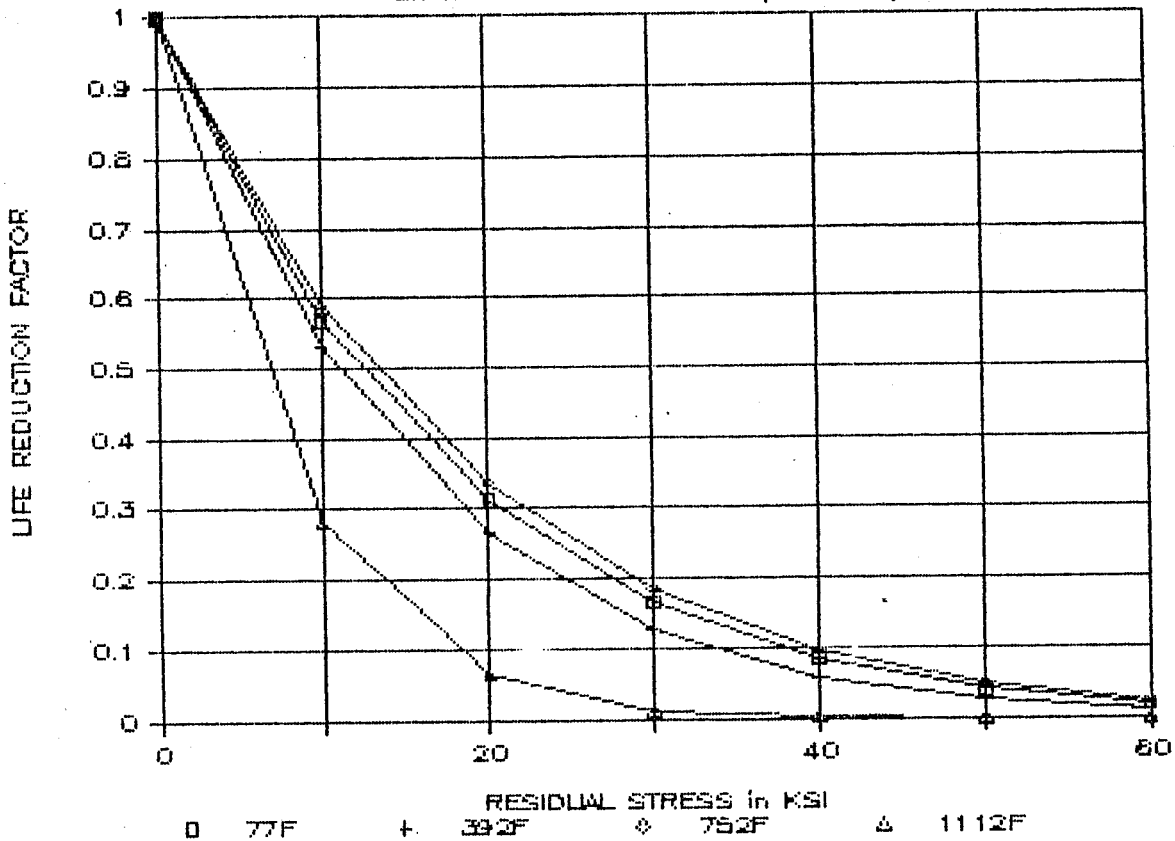


FIGURE 11.19. LOW BACK RIM HOOP STRESS FOR 20 KIP LATERAL LOAD (WETENKAMP AND KIPP).

EFFECT of RESIDUAL (MEAN) STRESS on CRACK INITIATION LIFE (CLASS U)



$$L.R.F. = \left[1 - \frac{\sigma_0}{\sigma_f'} \right]^{-1/b}$$

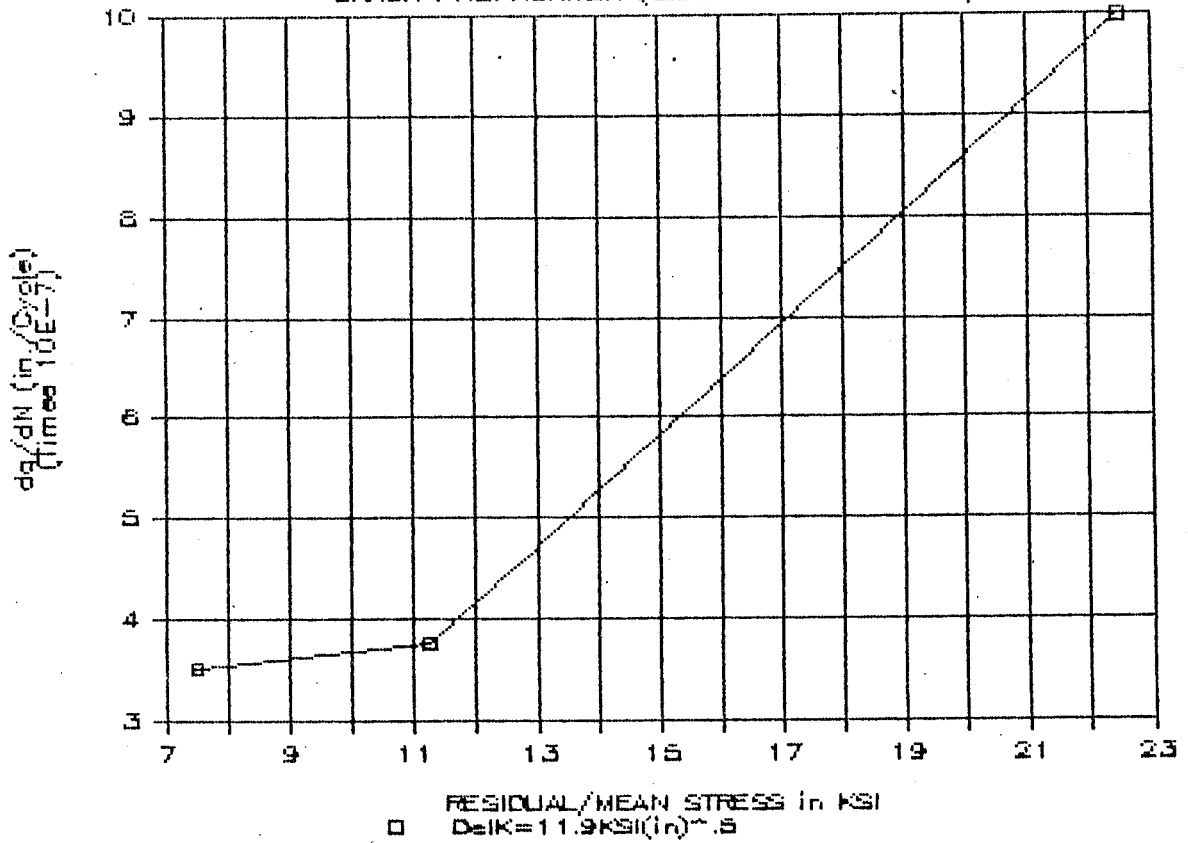
b = FATIGUE STRENGTH EXPONENT
 σ_0 = SUSTAINED MEAN STRESS
 σ_f' = FATIGUE STRENGTH COEFFICIENT

FROM S.S. MANSON, "HONORING AND UPDATING - MORROW'S
MEAN STRESS CORRECTION FOR METAL FATIGUE"
JOMO'84

FATIGUE PROPERTIES FROM M.C. FEC, "ELEVATED TEMPERATURE
FATIGUE BEHAVIOR OF CLASS B, C + U WHEEL STEELS"
ASME 1984

FIGURE 11.20. EFFECT OF RESIDUAL (MEAN) STRESS ON CRACK INITIATION (S.S. MANSON).

EFFECT of RESIDUAL STRESS on
CRACK PROPAGATION (CLASS B from FOWLER)



ASSUME 0.2" CRACK
STRESS RANGE = 15 KSI

$$\Delta K \approx \Delta \sigma \sqrt{\pi a}$$

FIGURE 11.21. EFFECT OF RESIDUAL STRESS ON CRACK PROPAGATION (FOWLER).

The value of hoop residual stress at the B1 location of a class U, CJ33 wheel after a severe 1-hour drag braking at about 44 BHP may be expected in the 22 to 33 ksi range. This level of residual stress is consistent with hole drilling measurements reported in this FRA program as well as analysis described in a later section of this report. From Figure 11.20 it may be seen that a 30 ksi residual or mean stress could be expected to reduce crack initiation life by a factor of 0.17 even for room temperature conditions. Also from Figure 11.21, the crack propagation rate for a 0.2-inch crack subjected to a stress range of 15 ksi might be expected to be increased by a factor of 3 for a residual increase from about 7 ksi to 23 ksi.

The effect of actual fabrication material surface condition (as opposed to laboratory specimen) must be accounted for as Pellini has emphasized ("Guidelines for Establishing Defect Quality Criteria in Fatigue Design," report to AAR, 1979). His " K_f " adjustment (like the notch stress concentration factor) recommended for normal production castings, for example, would be 1.5 for reliable life prediction. Perhaps a value as low as 2.0 (or a fatigue strength reduction factor of 0.5) might be appropriate for some wheels in service.

The combined effect of residual stress and reduced surface quality on crack initiation is illustrated in Figure 11.22 for room temperature Class U steel. The fatigue properties are taken from laboratory tests conducted as part of this FRA sponsored program and reported under Task T3. Note that the horizontal axis is given both in terms of reversals ($2 \times$ cycles) and miles on 33-inch diameter

STRAIN AMPLITUDE/REVERSALS for CRACKING

CLASS II at ROOM TEMPERATURE

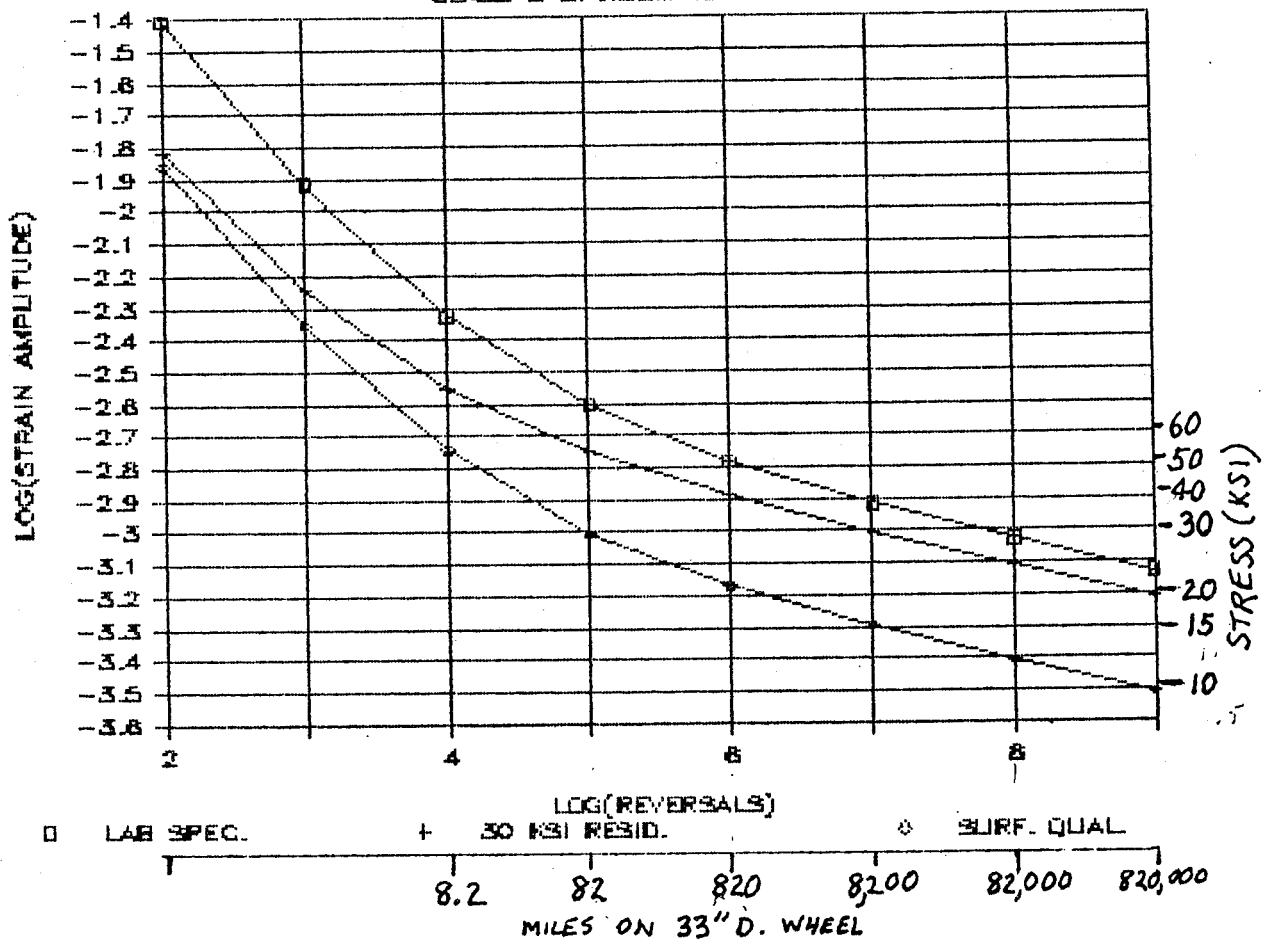


FIGURE 11.22. STRAIN AMPLITUDE/REVERSALS FOR CRACKING.

wheels. Even with these "adjustments" for residual stress and surface quality, an applied stress amplitude as high as 10 ksi would be required to initiate lower back face cracking in less than a million miles. In view of the relatively lower rail stress amplitudes in this region of the wheel predicted from earlier analyses, it appears that other detrimental loading, geometry, environment or material conditions must be considered in order to predict crack initiation here. These observations are generally consistent with comments made by Wetenkamp in 1977 and by Johnson et al, in AAR Report #R-560 dated November 1983.

11.2.5 Cyclic Path Dependence of Stress Change

Preliminary experimental inferences and material plasticity simulations of residual stress changes due to repetition of braking cycles have been made, primarily for the recently completed RDU tests. These efforts are described below.

11.2.5.1 Successive Hole Drilling

Measurement of residual stresses by the successive hole drilling method has been successfully tried and perfected during various facets of the program. Most of the test wheels during Tasks 4 and 5 have been analyzed using this method. Several rail car wheels prior to radial saw-cutting were also analyzed by this method. Careful consideration was given to avoid any source of errors that may arise from operational practices and data reduction procedures.

In order to measure residual stress with standard sensors, the locked-in stress must be relieved in some fashion (with the sensor present) so that the sensors can register the change in strain caused by removal of the stress. This was usually done destructively in the past by cutting and sectioning the part, by removal of successive surface layers, or by trepanning and coring. With strain sensors judiciously placed before dissecting the part, the sensors measure the relaxed strains, from which the initial residual stresses can be inferred by conventional methods.

The most widely used modern technique for measuring residual stresses is the hole drilling strain-gaging method. With this method, after installing strain sensors on the part surface, a small shallow hole is drilled in the surface. After drilling, the change in strain in the immediate vicinity of the hole is measured, and the relaxed residual stresses are computed from these data. The hole drilling method can be described as "semidestructive," since the small hole will not, in many cases, noticeably impair the structural integrity of the part being tested [the hole is typically 1/16 to 1/8 inch (about 1.5 or 3.0 mm) in both diameter and depth].

When a hole of small diameter is drilled in a region initially containing residual stresses, the magnitudes of strain relieved at any point P are functions of the local principal stresses σ_x and σ_y , and of the geometric relationships between the point and the hole, and the point and the principal axes.

The description of residual stress determination by the Hole Drilling strain-gaging method is already presented in Section 4.2.6.1.

Once σ_x and σ_y are determined, σ_1 and σ_2 (which can be hoop or radial stresses, depending on the orientation of gage #1 on the wheel) can be calculated from the Mohr Circle relationships:

$$\sigma_{1, 2} = \frac{\sigma_x + \sigma_y}{2} \pm \frac{(\sigma_x - \sigma_y)}{2} \cos 2\beta \quad \text{if } \beta = \beta_x$$

$$\text{and } \sigma_{1, 2} = \frac{\sigma_x + \sigma_y}{2} \pm \frac{(\sigma_y - \sigma_x)}{2} \cos 2\beta \quad \text{if } \beta = \beta_y$$

The analysis of residual stresses on the back face of the rim (B1 location) revealed that the stress components in the hoop and radial directions were of the same order of magnitude resulting in a bi-axial state of stress.

After the evaluation of residual stress at B1 location, the hole drilling strain-gaging method is applied at B2 location in the rim fillet region about 5.5 inches radially down from the flange tip. The third (B3) location is in the hub fillet region about 10 inches radially down from the flange tip.

The development of residual stresses in a typical test wheel (Wheel No. 8) at B1, B2 and B3 locations during drag braking simulation testing on RDU are presented in Figures 11.23, 11.24, and 11.25.

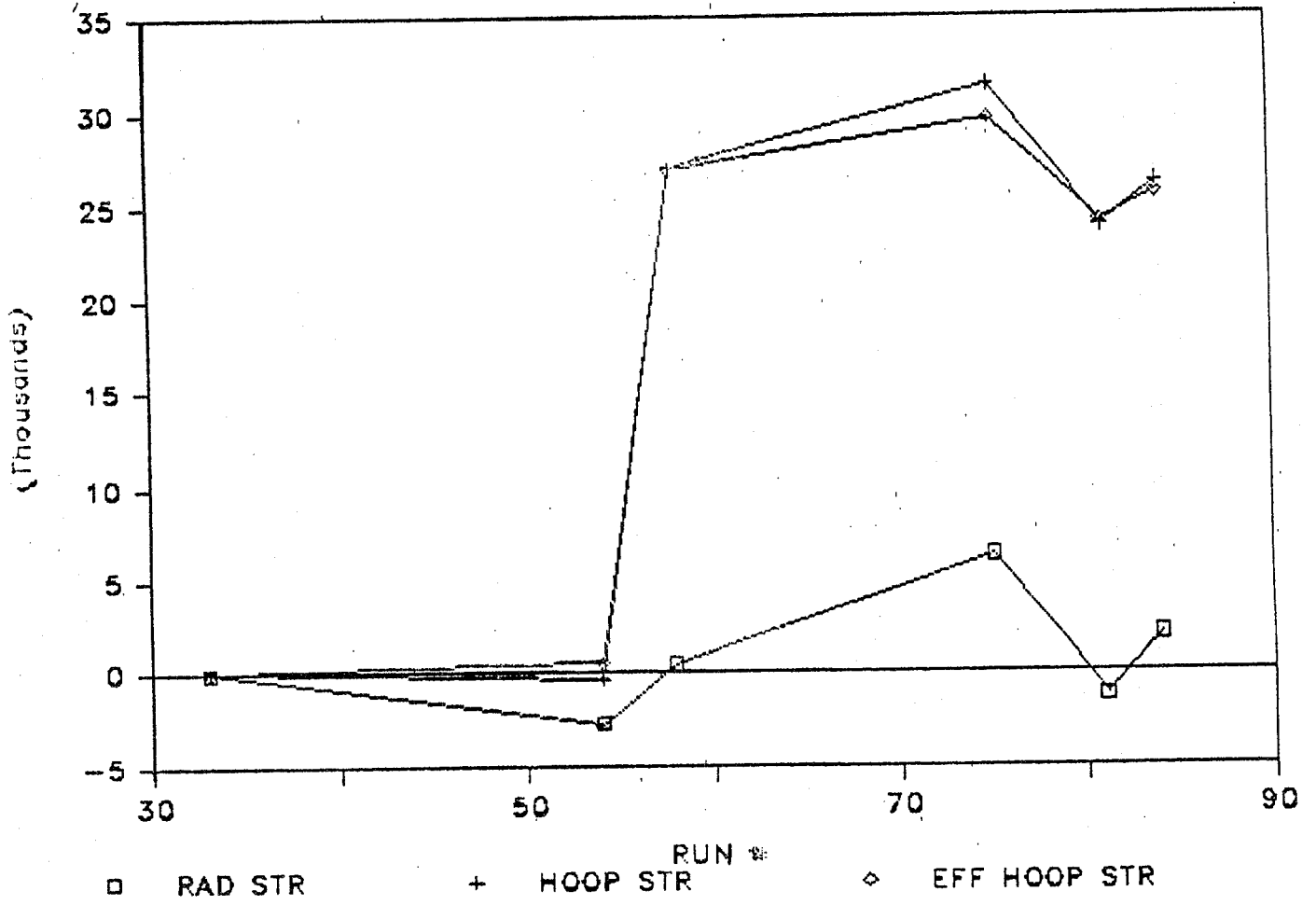


FIGURE 11.23. HOOP STRESS AT B1 LOCATION, WHEEL #8.

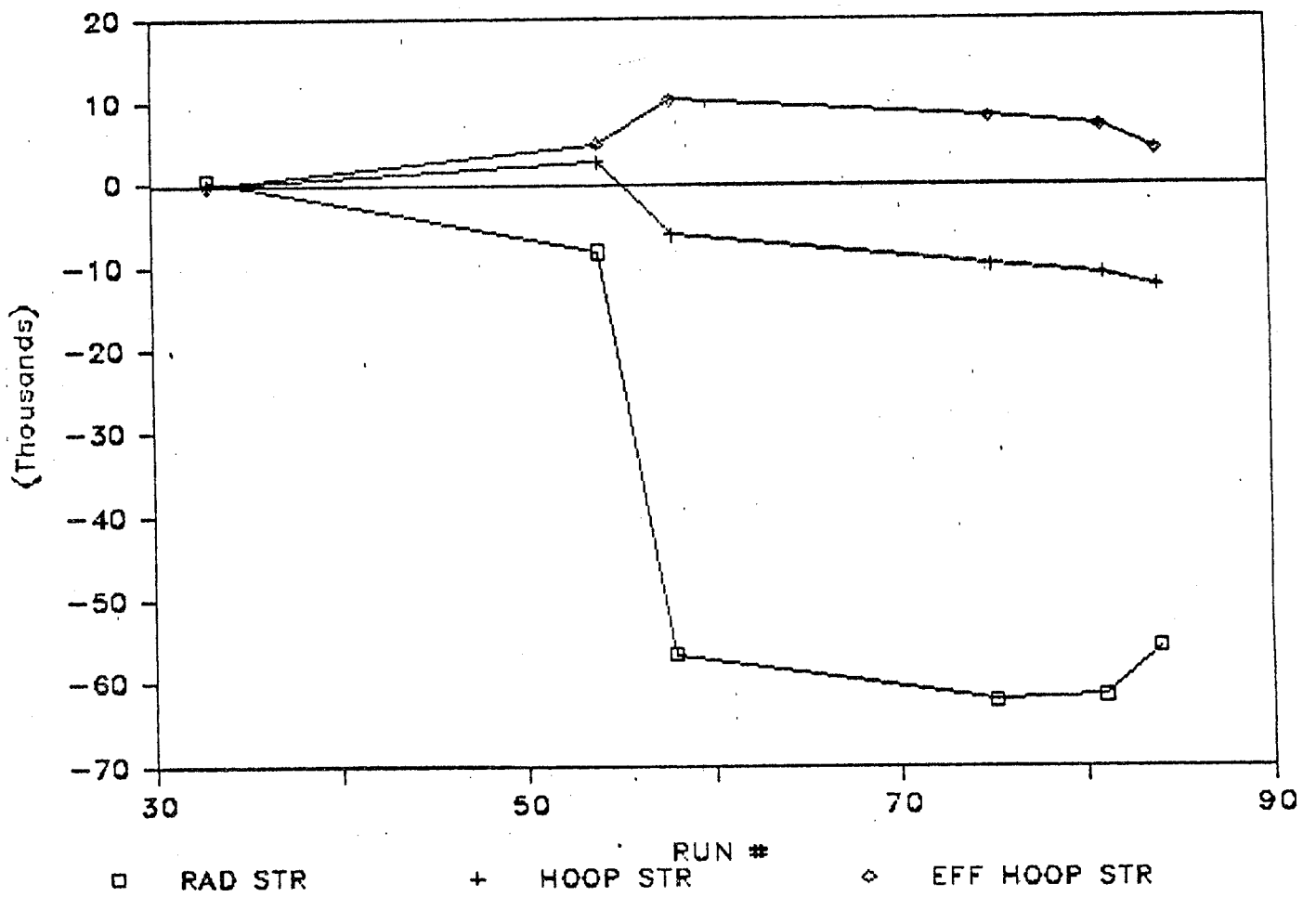


FIGURE 11.24. HOOP STRESS AT B2 LOCATION, WHEEL #8.

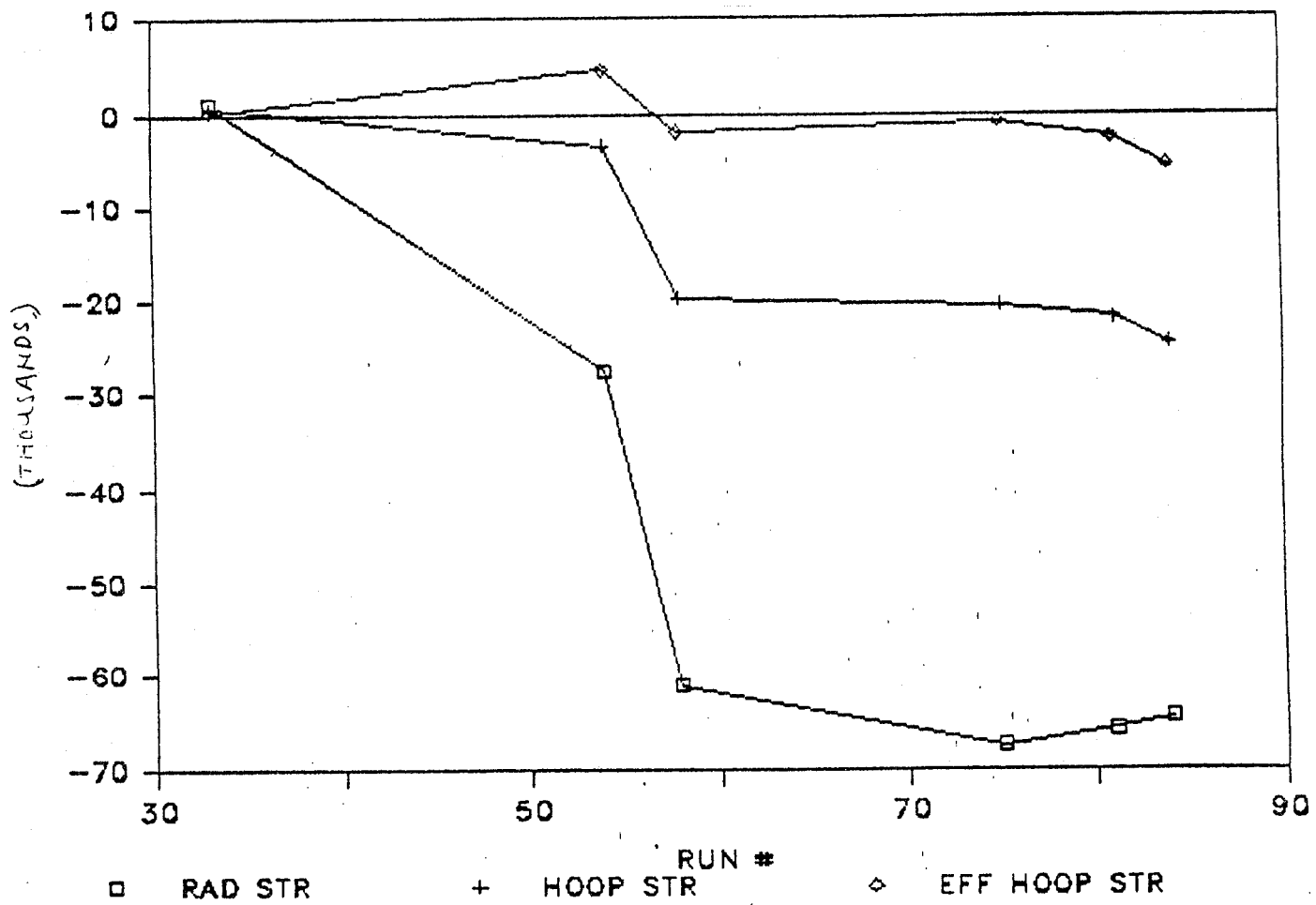


FIGURE 11.25. HOOP STRESS AT B3 LOCATION, WHEEL #8.

11.2.5.2 Computer Simulation Approach

A semi-empirical approach to the prediction of stress changes due to braking cycles is based on a material constitutive representation or computer simulation of the stress response for measured surface strains and temperatures. An initial application of the method based on the most elementary "flow model", (that is, perfect plasticity with a temperature dependent yield stress) is described in this section. The flow properties assumed in these analyses are illustrated in 11.26. A best fit straight line temperature relationship is given for the conventional (fast rate) 0.2% and 0.02% plastic strain offset yield strengths for Class U steel. For the higher temperature and slower strain rates, lower flow stress values may be expected as discussed under Task 3.

11.2.5.2.1 Uniaxial Model

This method may be illustrated in the most straightforward manner by use of a uniaxial model based on hoop strain measurements made at the back face, B1, location for the wheel induction heating experiment and the most severe braking cycles experienced on the Roll Dynamics Unit (RDU).

The brake horsepower input histories for the Induction heating and RDU tests selected for analysis are shown in Figures 11.27 and 11.28 respectively. The measured temperature histories at the B1 location for these tests are given by Figures 11.29 and 11.30.

ASSUMED EFFECT of TEMP. on YIELD

CLASS U STEEL at NOMINAL 0.002/SEC RATE

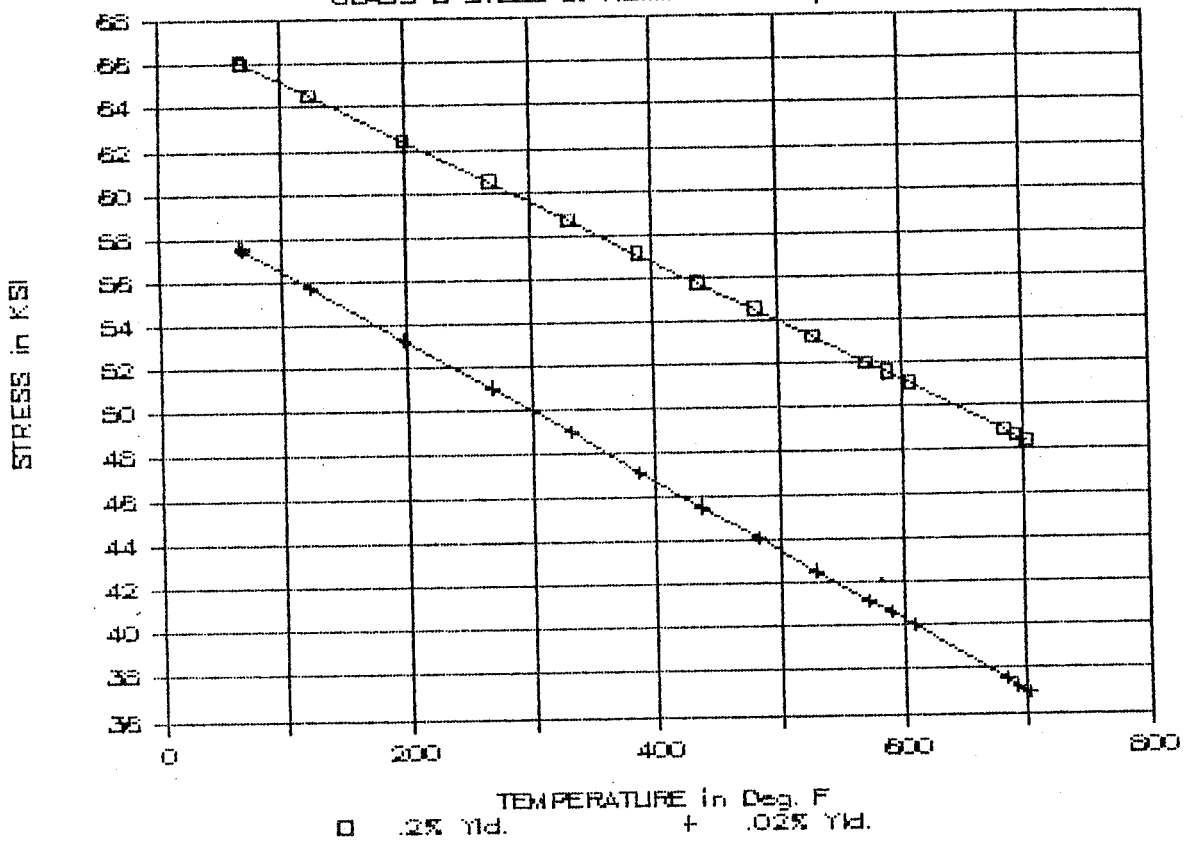


FIGURE 11.26. ASSUMED EFFECT OF TEMPERATURE ON YIELD.

HORSEPOWER HISTORY IND.HT. TESTS CP1-CP5

12, 15, 25, 30 & 30 MIN. DURATION

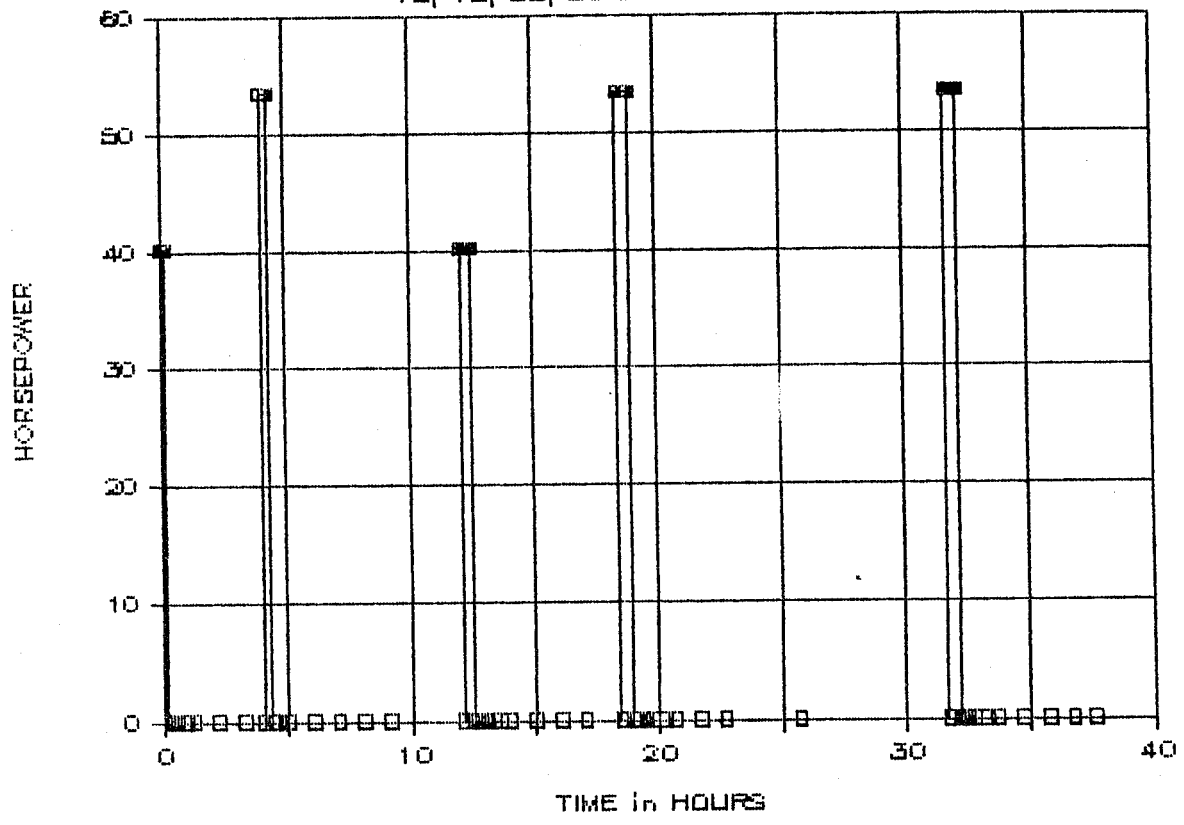
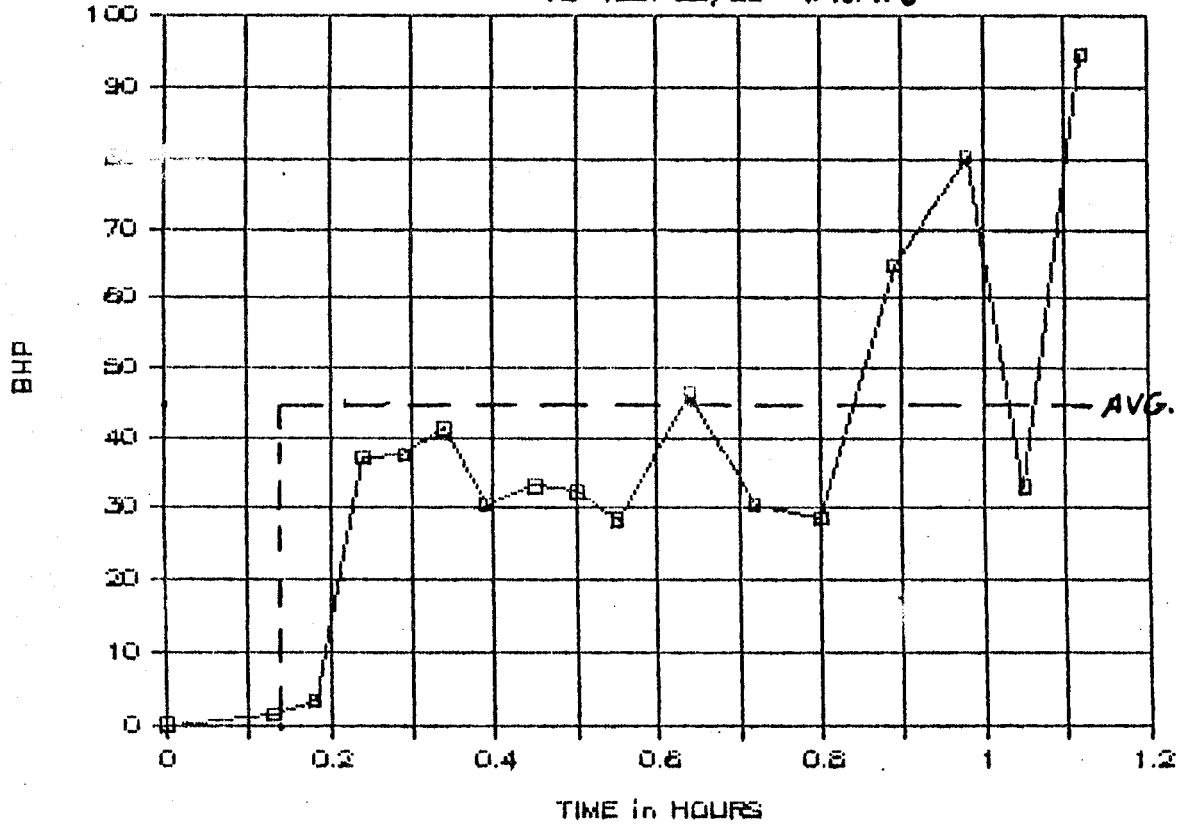


FIGURE 11.27. HORSEPOWER HISTORY, INDUCTION HEATING TESTS CP1-CP5.

BHP HISTORY

for TEST 55/56 WHL. #8



TEST	BRAKE CYC PRESS. (PSI)	SPEED (MPH)	DURATION (MINS.)	TARGET BHP	ACTUAL AVG BHP	NOTE
TEST 55/56	45/60	42/50	60	50	43.8*	SHOE BURNED
TEST 57/58	45	42	30			NOT MEAS. AT WHL. #8
			+30 OF FIXED PRESS + SPEED.			

* INCLUDES POWER LOSS TO ENVIRONMENT + ROLLER

FIGURE 11.28. BRAKE HORSEPOWER HISTORY, WHEEL #8.

IND. HT. TEMPERATURE HISTORY at B1
 TESTS CP1, CP2, CP3, CP4, CP5

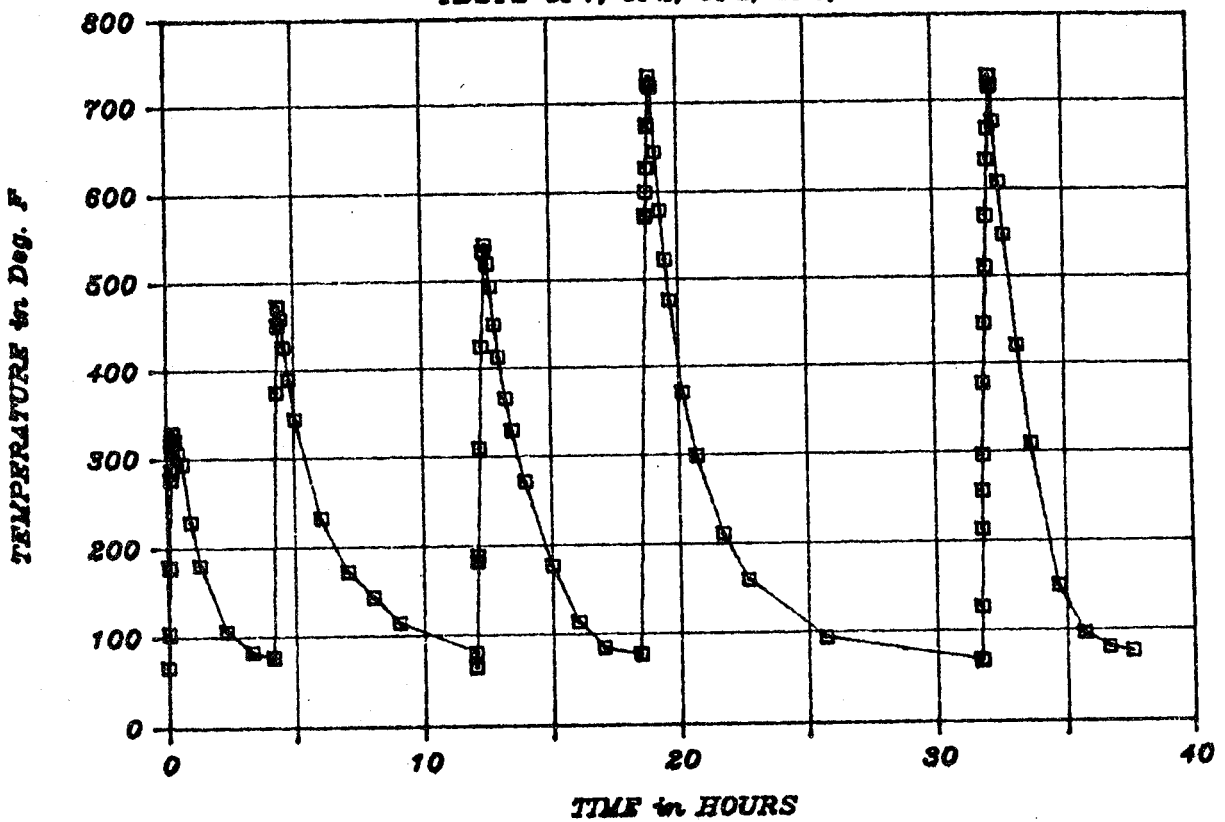


FIGURE 11.29. INDUCTION HEATING TEMPERATURE HISTORY AT B1, TESTS CP1-CP5.

RDU TEMPERATURE HISTORY

at B1 for TESTS 55-58

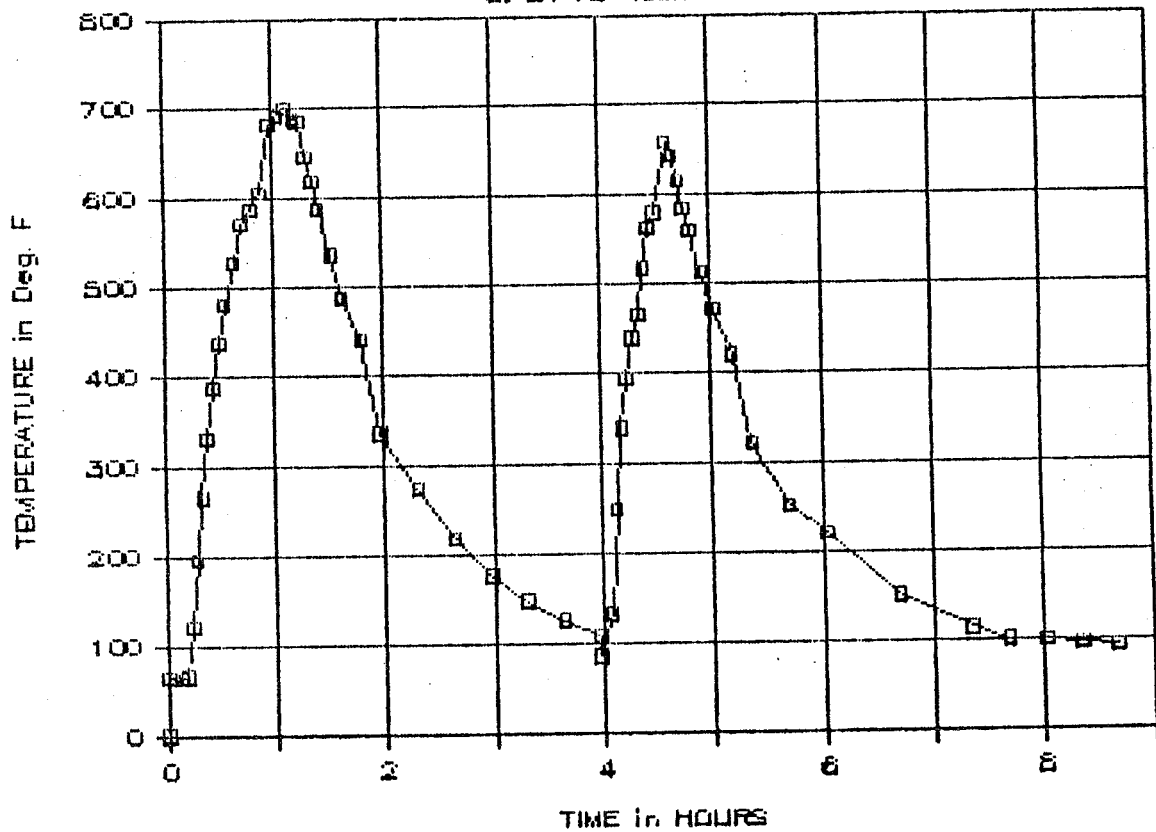


FIGURE 11.30. RDU TEMPERATURE HISTORY.

The corresponding hoop mechanical strain histories are provided by Figures 11.31 and 11.32.

Estimates of the associated stress histories were made by a typical computer spread-sheet analysis, assuming elastic response to the imposed strain until the current value of yield stress is reached at any temperature. Beyond initial yield the stress remains at the value of yield stress corresponding to current temperature as long as straining continues in the same direction. When "unloading" occurs the stress response is elastic for the change in strain. The results of following such a program for stress history are demonstrated in Figures 11.33 and 11.34. The corresponding stress-strain "loops" are shown in Figures 11.35 and 11.36.

The value of about 22 ksi for hoop residual stress predicted for the RDU test is generally consistent with the value of 27 ksi predicted from hole drilling measurements after cycle #57/58. It is also interesting to compare the results of this simple uniaxial model to an inelastic finite element analysis reported by Johnson, et al., in AAR Report R-580 in 1983. Their results for "hot" and "cold" (or residual) hoop stresses at the B1 location are plotted in Figure 11.37 for various 1-hour drag braking input BHP intensities. At 44 BHP the residual hoop stress would be interpolated at about 32 ksi. Considering the many material and loading history uncertainties this "theoretical" spread of 22 to 32 ksi is relatively encouraging, especially in view of the intermediate hole drilling result at 27 ksi.

IND. HT. STRAIN HISTORY at B1

TESTS CP1, CP2, CP3, CP4, CP5

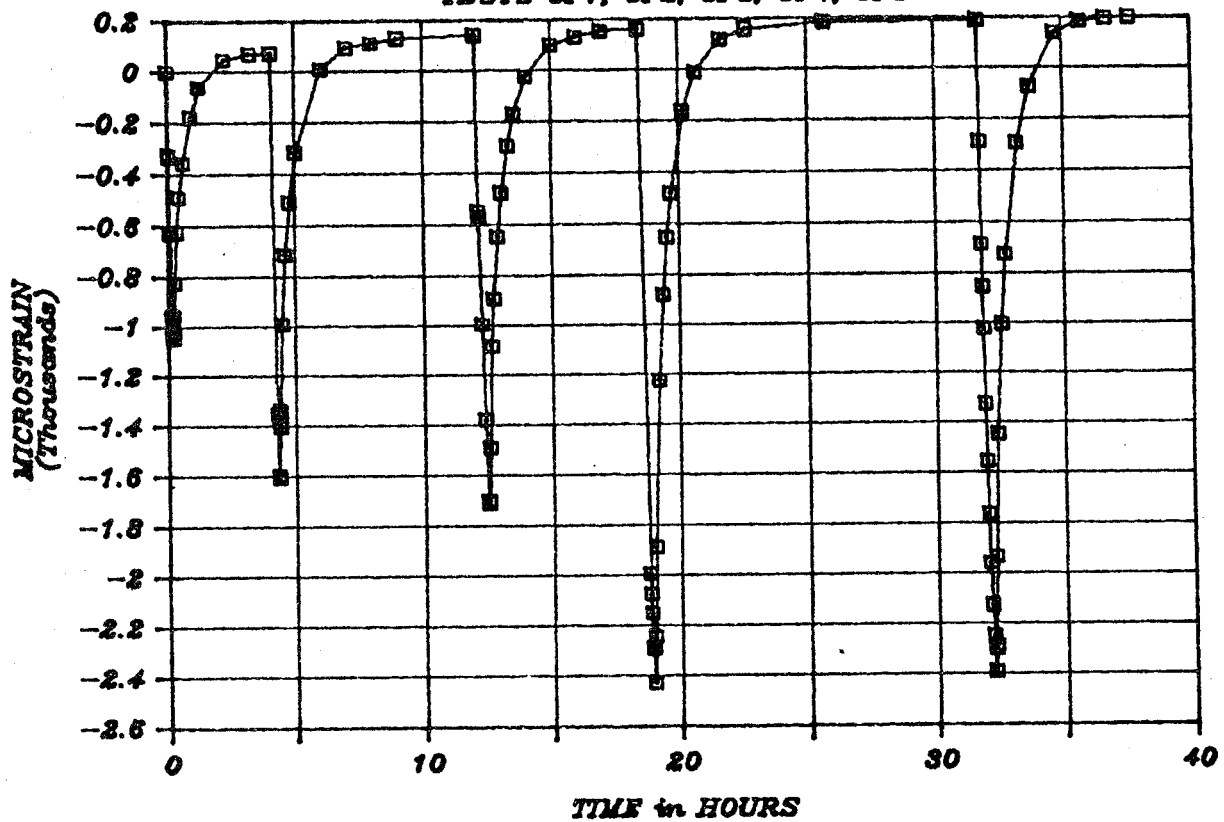


FIGURE 11.31. INDUCTION HEATING STRAIN HISTORY AT B1, TESTS CP1-CP5.

RDU STRAIN HISTORY

at B1 LOCATION for TESTS 55-58

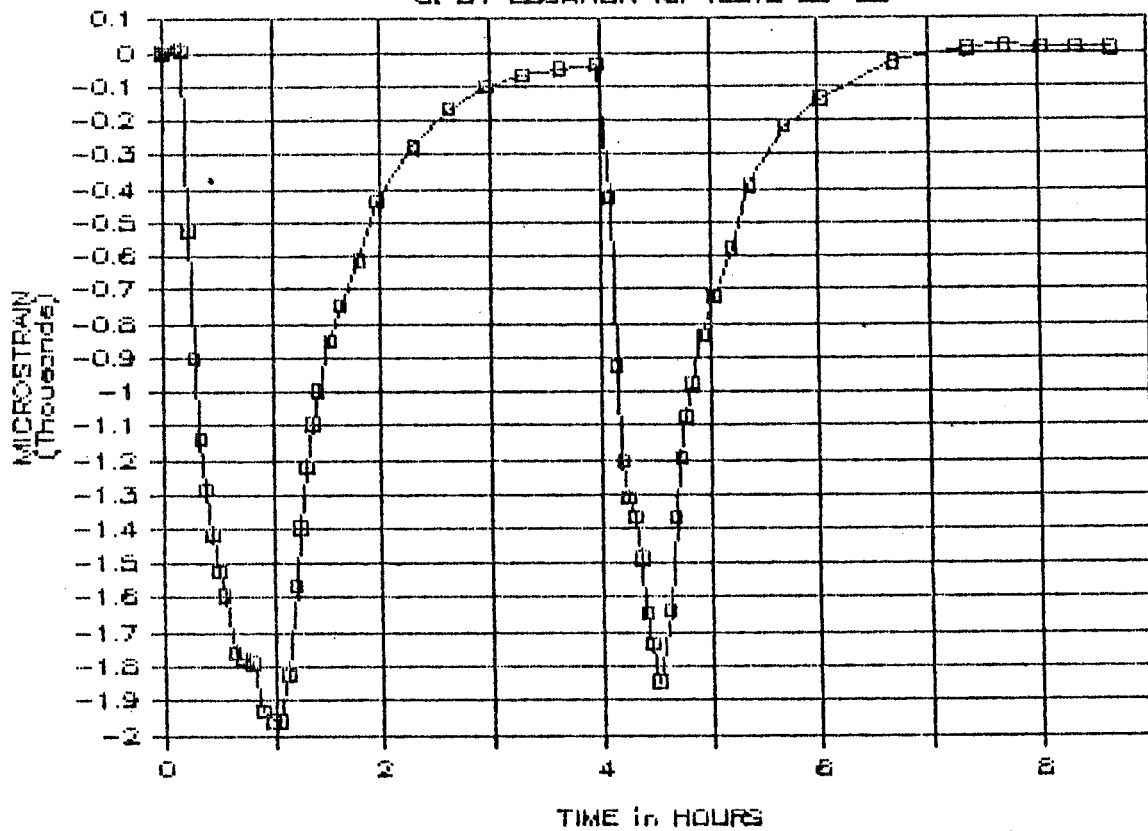


FIGURE 32. RDU STRAIN HISTORY.

IND. HT. CALCULATED STRESS HISTORY
 at B1 for TESTS CP1, CP2, CP3, CP4, CP6

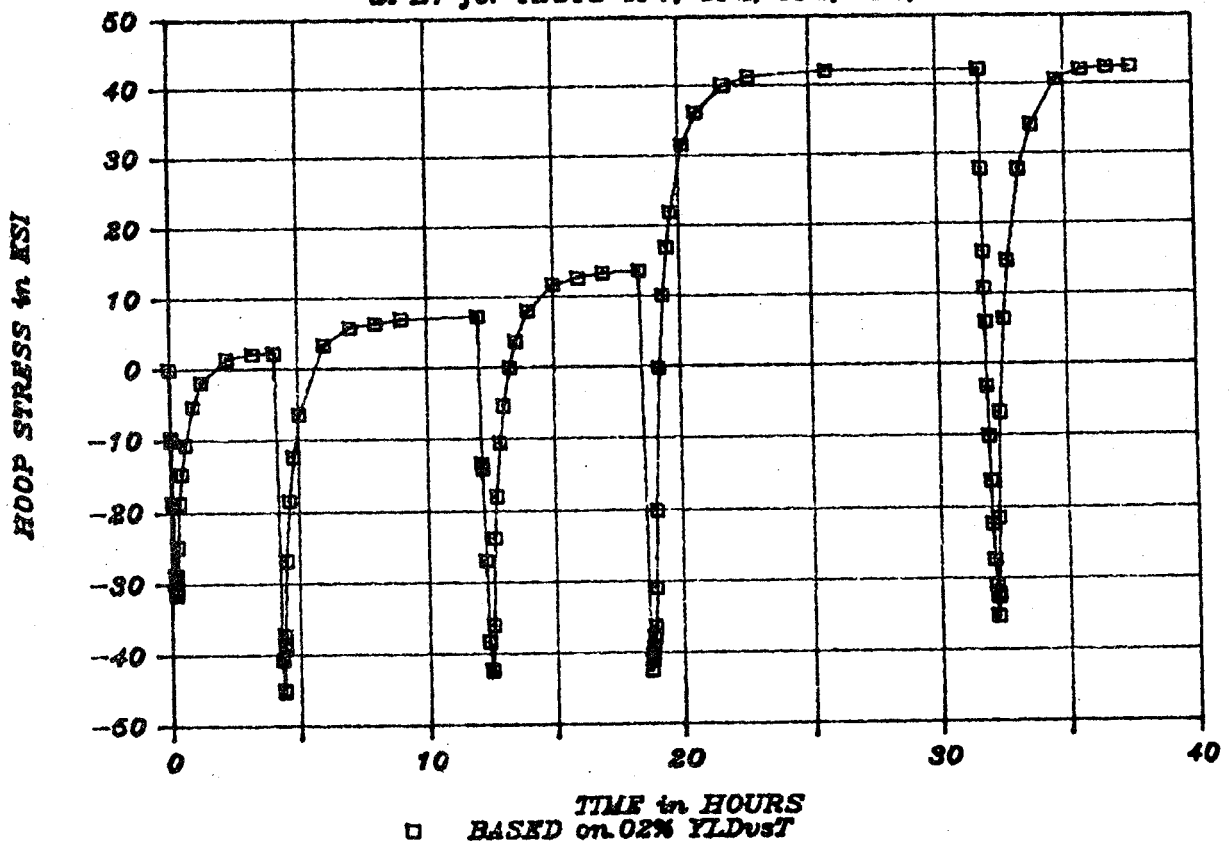


FIGURE 11.33. INDUCTION HEATING CALCULATED STRESS HISTORY.

RDU CALCULATED STRESS HISTORY

at B1 LOCATION for TESTS 55-58

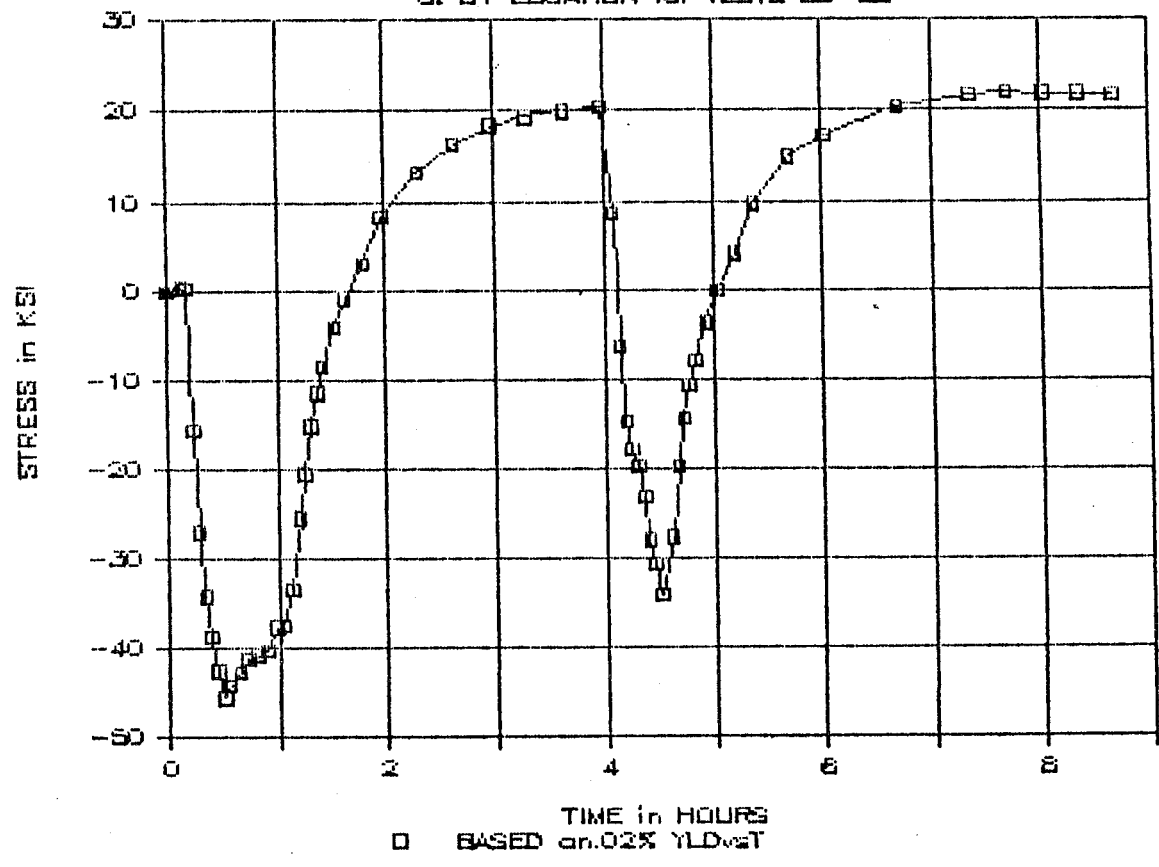


FIGURE 11.34. RDU CALCULATED STRESS HISTORY.

STRESS/STRAIN LOOPS at B1 RIM LOCATION

for IND. HT. TESTS CP1 to CP6 (.02MYld)

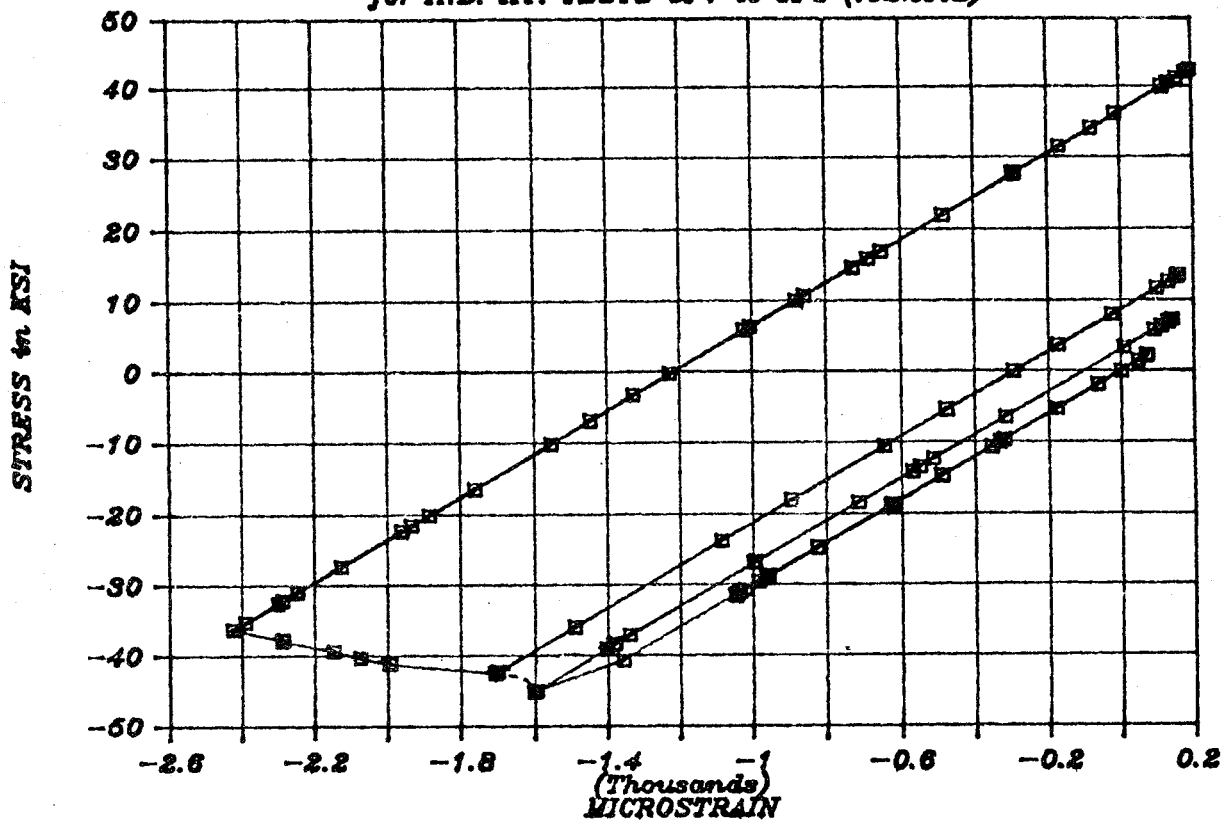


FIGURE 11.35. STRESS/STRAIN LOOPS AT B1 RIM LOCATION.

RDU STRESS/STRAIN LOOPS

at B1 for TESTS 55-58

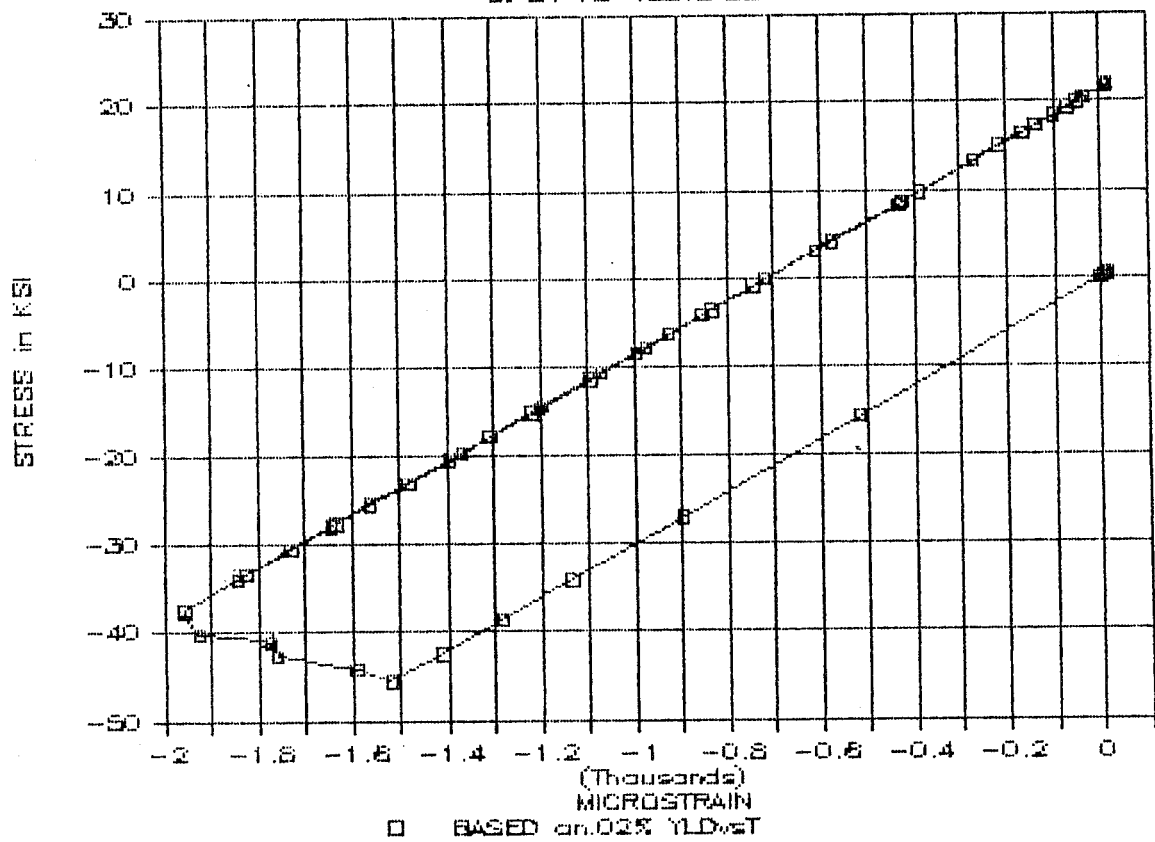


FIGURE 11.36. RDU STRESS/STRAIN LOOPS.

F.E.A. INELASTIC STRESS CALCULATIONS

at B1 for 1 HR. DRAG (AAR R-560 1953)

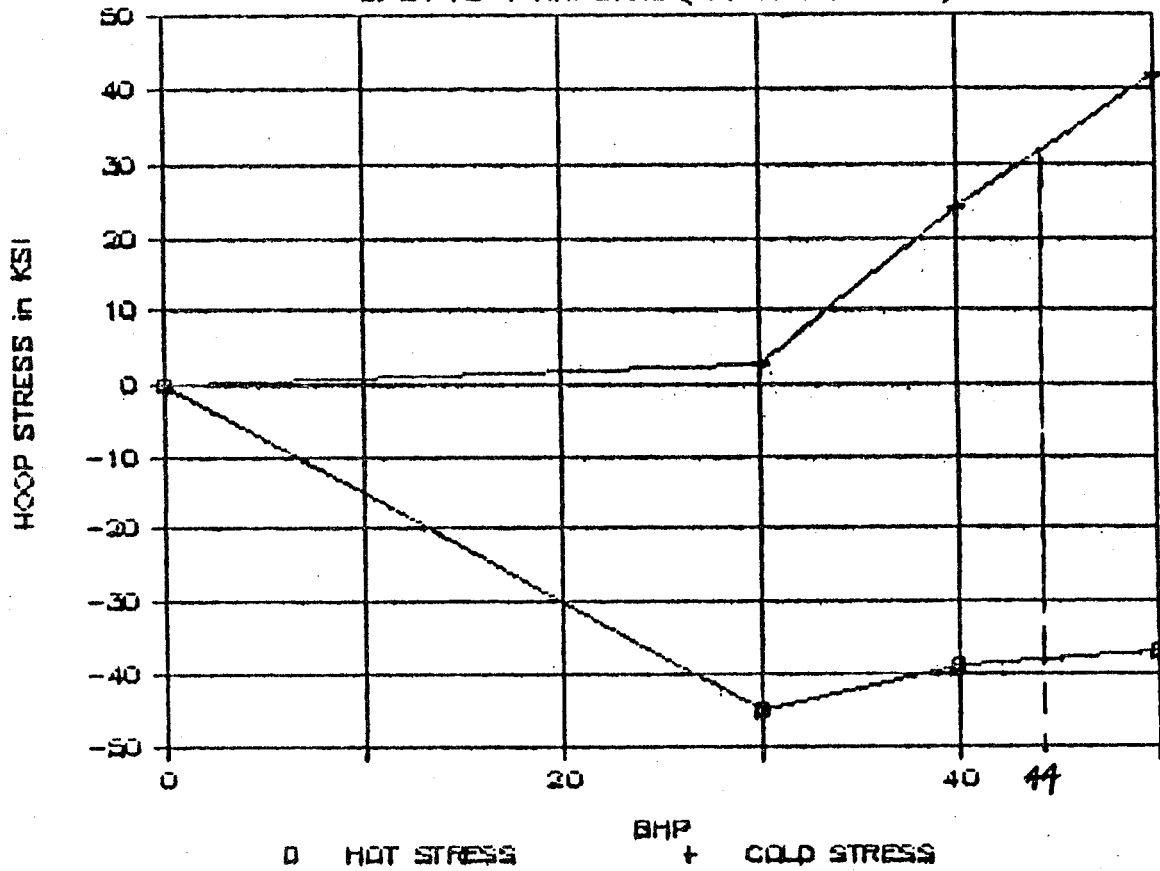


FIGURE 11.37. FINITE ELEMENT ANALYSIS INELASTIC STRESS CALCULATIONS.

11.2.5.2.2 Biaxial Plasticity Model

During wheel braking tests (such as those conducted on the RDU and on track at TTC), the surface biaxial strains and temperatures were measured to estimate the associated stress state. For this estimation, it is necessary to have a satisfactory biaxial stress-strain constitutive relationship which should be able to account for straining beyond the elastic regime, the incremental nonproportional character of the strain state (nonconstant strain component ratios) as well as the effect of temperature on the current value of material yield or flow stress.

The most elementary theory that satisfies these minimum requirements is an extension of the uniaxial perfect plasticity model described above in Section 11.2.5.2.1.

In the biaxial (rotationally symmetric) case the stress components must satisfy both the yield condition as well as the incremental plastic flow rule. The yield condition is taken as the Von Mises relationship, which may be expressed in nondimensional form as the parabola.

$$x^2 + y^2 - xy = 1$$

where

x is the ratio of radial stress to the current value of yield,
and y is the corresponding ratio of circumferential stress.

The associated plastic flow rule requires that the increments in plastic strain be such that the vector formed by these strain compo-

nents is normal to the yield surface. This condition leads to another second degree equation, a hyperbola in this case, that must be solved simultaneously with the parabolic yield condition for each time increment for which strains and temperatures change. Account must also be taken of the possibility of elastic unloading at some time after yielding has occurred.

This calculational scheme for taking the actual mechanical strain components and temperature histories (B1, B2, and B3) and predicting the stress components is described in Appendix 11.2. Provision is made in these computations for a yield or flow stress that decreases with increases in temperature. As in the simple uniaxial model no account is taken directly of strain hardening or inherent cycle or rate dependency. Nevertheless, it is believed that this method provides an efficient and relatively simple but logical method of estimating the biaxial stress (applied and residual) as well as the plastic strain components which will differ from the measured residual strain components in most cases.

This method is now being applied to the RDU data and only preliminary results are available at this time. However, some appreciation of the form of results for selected data may be gained by reference to Figures 11.38 and 11.39.

They illustrate the complex radial and circumferential stress-strain loop calculated from the reduced strain and temperature data taken at wheel plate location B2 for most severe RDU braking cycle (55/56) on Wheel #5.

RADIAL STRAIN AGAINST STRESS
WHEEL : 5 LOCATION B2 RUN 5556

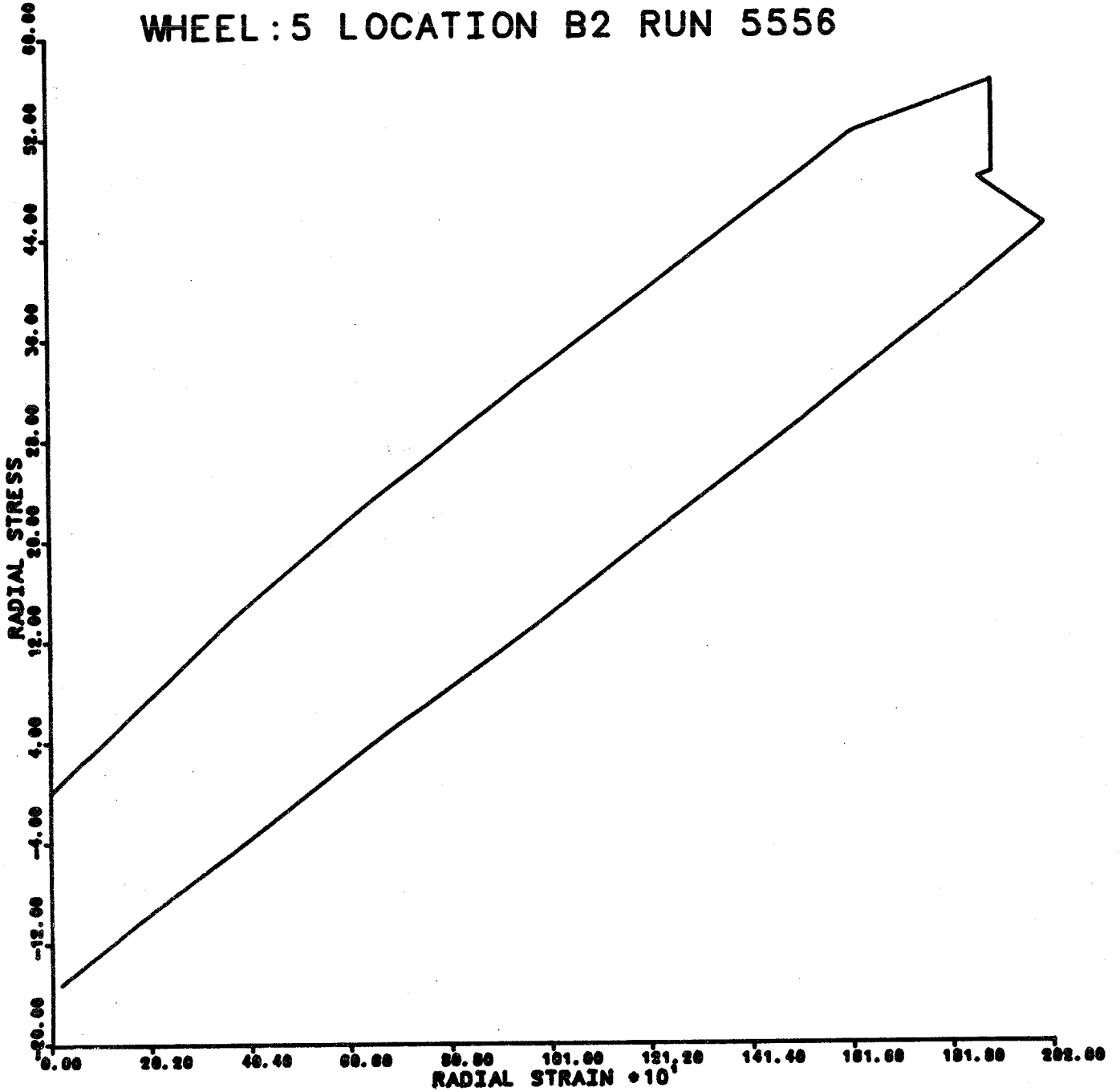


FIGURE 11.38. RADIAL STRESS-STRAIN LOOP CALCULATED AT B2
IN RDU TEST #55/56.

TANGENTIAL STRAIN AGAINST STRESS
WHEEL:5 LOCATION B2 RUN 5556

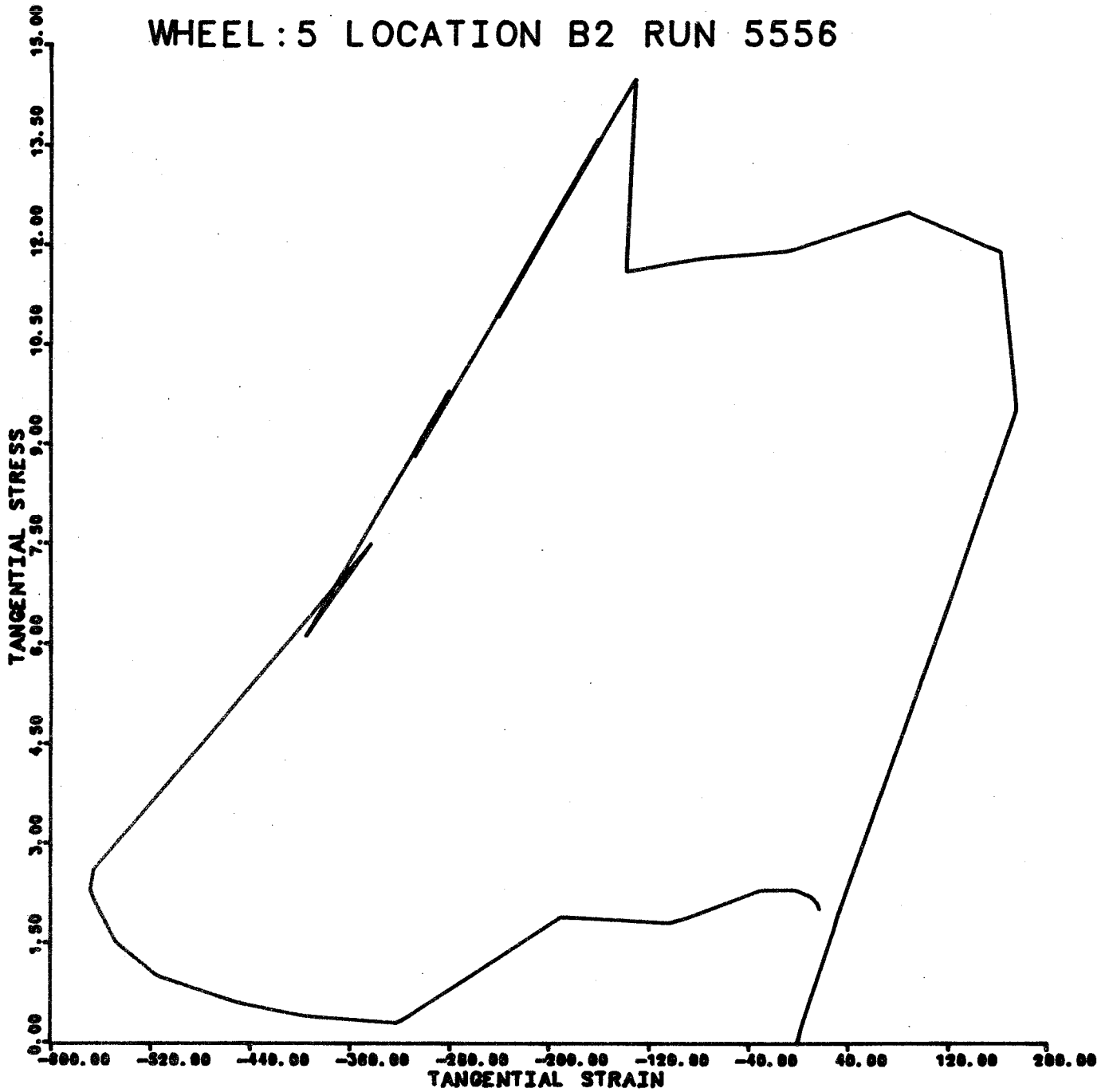


FIGURE 11.39. CIRCUMFERENTIAL STRESS-STRAIN LOOP CALCULATED AT B2 IN RDU TEST #55/56.

An obvious limitation of the "perfect" plasticity material model described above is the inability to treat the known inherent material cycle and rate dependence of wheel steel. In order to gain some insight into the effect of repeated braking cycles on residual stress changes, ratchet effects and plastic "damage" accumulation, more realistic constitutive material models are required. The ANSYS finite element program includes a wide range of material options in addition to the special kinematic hardening selected for the wheel induction heating analysis attempt described in Section 11.2.3.1 above.

Some exploratory studies of uniaxial cyclic material response with ANSYS special non-linear material options have been conducted for certain hypothetical input total strain and temperature cycles. These examples have permitted comparison to, and qualification by, closed form independent solutions described in Appendix 11.3. By way of illustration, Figure 11.40 are the ANSYS produced stress-strain loops in temperature peaks to 800 degrees K (980 degrees F). The material behavior in this case features a second degree power creep law and classical kinematic plasticity with temperature dependent properties selected to roughly approximate Class U steel thermo-mechanical properties published by Sehitoglu in 1982. It is sufficient here to simply note the salient feature of such a stress-strain loop in contrast to the elastic unloading behavior predicted with the simple, perfectly plastic models. Reversed plastic strain and creep effects are apparent with this relatively simple non-linear model. Closer simulation of actual uniaxial cyclic and

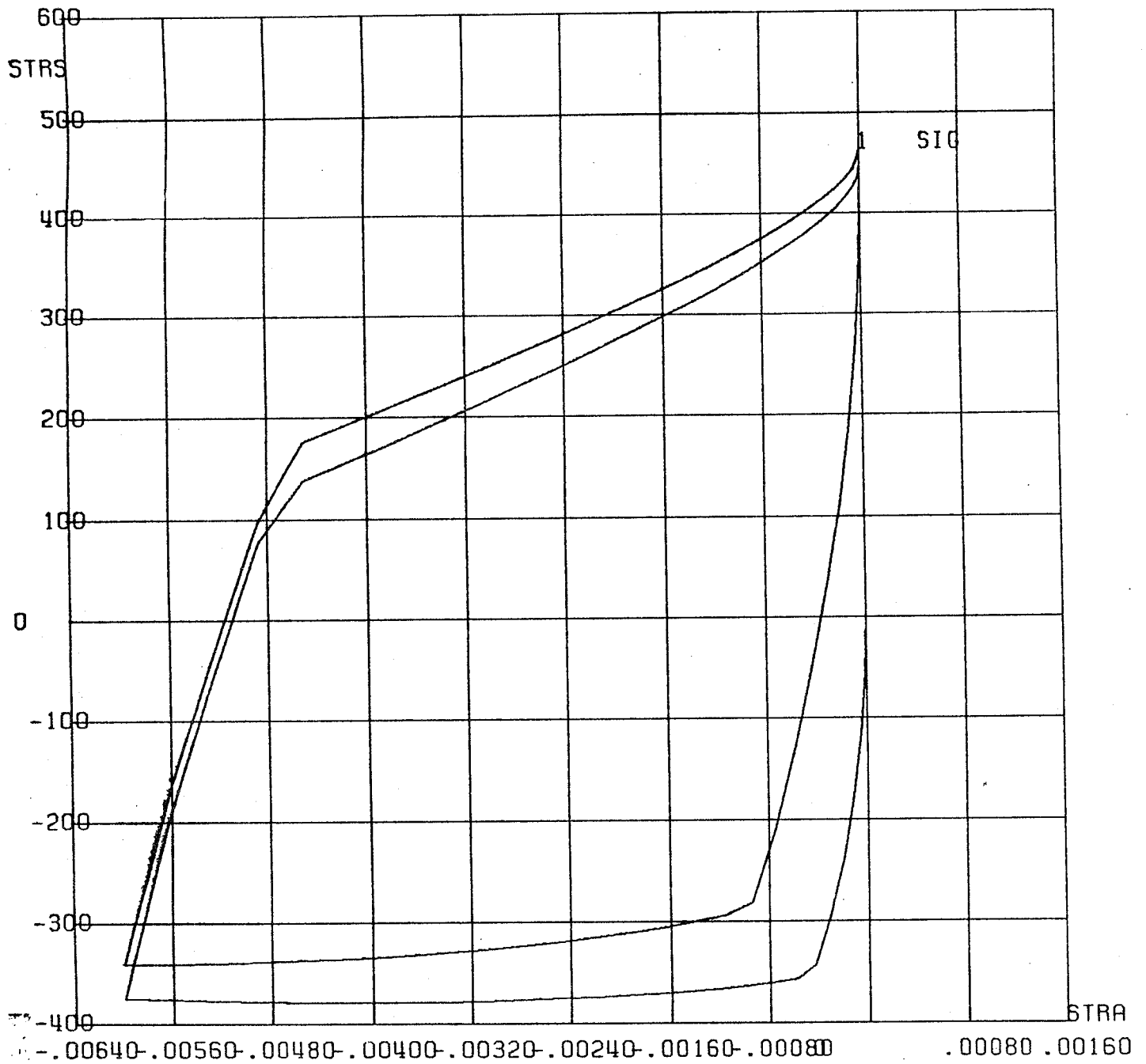


FIGURE 11.40. ANSYS STRESS-STRAIN LOOPS TO 800°K.

variable rate behavior under way in Task 3 is possible. Even if full finite element wheel model analysis with such properties do not prove to be cost effective, such ANSYS material options will be helpful in predicting stress states associated with measured uniaxial and biaxial strain and temperature cycles.

11.2.6 Tread Cracking Analysis

Experimental work has just begun on the wheel thermal tread cracking rig. Supporting analytical effort to date has consisted in further refinement of plans as summarized below.

11.2.6.1 Martensite Cracking

The objective of the tests with the thermal cracking rig is to evaluate the relative susceptibility of Class B, C and U wheels to develop thermal cracks in a martensitic tread surface layer. To date, the rig has been designed and constructed and preliminary trials have been conducted on a thermocoupled Class U wheel to determine the test conditions necessary to produce cracking. Infrared thermography and hardness tests, as well as observations of cracking, were used in this effort.

11.2.6.2 Hot Spot Thermal Fatigue

Finite element analysis work to estimate hot spot strain/stress cycles has not yet begun.

11.3 WORK REMAINING

Highlights of the significant work remaining are given below in the same subtask format previously introduced.

11.3.1. General Data Correlation

Initial predictions of residual stress levels in one of the wheels tested in the RDU and one after induction heating wheels gave excellent correlation with measured values. Therefore, as wheels are tested on the dynamometer and on track, further stress predictions will be made and correlated with test results. The centralized data base at TTC will provide necessary information for statistical analysis such that nondimensional parameters can be developed to indicate the severity of wheel damage.

11.3.2 Wheel Stress Analysis Programs

While elastic stress analysis programs are being used, work must be completed on the following elastoplastic analysis: (1) predictions and comparisons of strain history from the Induction Heating Test and (2) introduction of time-temperature dependent material properties and analysis of several cycles to simulate laboratory tests.

11.3.3 Applications

The work remaining for the application of analytical effort under each subtask is given below.

11.3.3.1 Induction Heating Analysis

Complete predictions of plastic strains will be performed when exact strain gage locations are measured.

11.3.3.2 Detailed Residual Stress

One wheel has been started and three additional wheels have to be analyzed.

11.3.3.3 Tread Crack Rig Design

Work has been completed on the rig, the system has been demonstrated, and analysis is expected to be completed by February 1986.

11.3.3.4 Wheel/Rail Heat Transfer

Work has been completed.

11.3.3.5 Saw-Cut Analysis

Data have been gathered on 347 wheels and 127 wheels are available for cutting.

11.3.3.6 Thermal Analysis of Brake Shoes

Work has not yet begun.

11.3.3.7 LEFM (Linear Elastic Fracture Mechanics)

A preliminary analysis has been made, and where a complete compilation of available mechanical load data has been assembled into an analysis spectra in January 1985, a final analysis will be made.

11.3.4 Cumulative Fatigue Damage Model

Candidate theories on models which have been identified must now be applied using information being developed on wheel strains and stresses due to distributions of braking and rail load spectra.

11.3.5 Cyclic Path Dependence of Stress Change

The several analytical and experimental methods developed and partially qualified for predicting stress changes for measured strain temperature cycles must be applied to the data base being developed from the RDU Induction Heating and Truck Tests.

A Fortran program has been developed at TTC to compute the hoop radial and effective stresses during the heating cycle (drag braking) including material yield and plastic strains. This analysis will be further tuned and verified for various tests undertaken on RDU as well as track.

The results of hole drilling strain gaging analysis being conducted at TTC will be verified by Mr. Gil Blake of Wiss, Janney, Elstner, and Associates for the validity of equations and analysis procedures.

11.3.6 Tread Cracking Analysis

11.3.6.1 Hot Spot Analysis

The refinement of a previously published method based on finite element analysis using elevated temperature cyclic and fatigue properties remains to be done.

11.3.6.2 Tread Cracking Rig Data Analysis

Twelve wheels (4 each, Class B, C, and U) will be tested on the thermal cracking rig to evaluate their relative susceptibility to "martensite" thermal cracking under the conditions established in the preliminary trials. Infrared thermography and hardness tests will be used to assure that all of the wheels are tested under the same conditions. Inasmuch as four wheels of each class are being tested, statistical techniques will be used to assess the repeatability of the test results. Further, an attempt will be made to correlate these results with other thermal crack related tasks.

11.4 SCHEDULE

This comprehensive analytical task involves an ongoing effort to correlate theory and experimental results from most of the other program tasks. Hence its completion in terms of a final program evaluation will follow the last experimental task completion by approximately 3 months.



12.0 DETERMINE RESIDUAL STRESS AND METALLURGICAL
CHANGE IN TEST WHEELS (TASK 11)

12.1 CURRENT TASK 11 STATEMENT OF WORK

The AAR shall determine stress and metallurgical changes in test wheels by saw-cutting and mapping for residual stress determination and macrostructure evaluation using techniques developed in T3. In consultation with the FRA COTR, AAR will select six wheels from the four pairs listed below:

- a. One pair of wheels in as-received (newly annealed) condition; analysis will establish baseline stresses.
- b. Two pairs of straight plate wheels, each pair with a different thermal history.
- c. One pair of parabolic plate wheels.

The wheel will be sliced, drilled and strain-gaged to map the residual stresses in the test wheel. Required data acquisition and processing procedures will be applied to produce elaborate analyses of the triaxial residual stresses which shall be correlated with the known thermal and mechanical loading histories of the wheels to increase the amount of confidence in the proposed wheel failure mechanisms during the course of research.

12.2 MAJOR FINDINGS/CURRENT STATUS

Current status of the three subtasks included in the T11 Statement of Work follow.

12.2.1 Residual Stress Estimation from Saw-Cutting Results

Greater experimental emphasis has been placed on the wheel saw-cut opening and strain release measurements than originally planned in order to take advantage of the method of estimating internal residual stresses described above in Section 11.2.3.5. Front face as well as back face saw-cut opening displacements have been measured in a total of 9 wheels to date. In addition, certain wheels to support the analysis mentioned above have been extensively strain gaged around the wheel surface on either side of the saw-cut path in order to help confirm the assumptions of saw-cut displacement behavior.

In addition to extended efforts mentioned above which are performed before, during and after saw-cutting, hole drilling strain-gaging was performed on 14 selected wheels at 3 critical locations in each wheel before saw-cutting.

The residual stresses evaluated at these critical locations were correlated with the flange tip displacement (in the hoop direction) to saw-cutting at various depths of cut. It was seen that the flange tip displacement at a given depth of cut exhibited a certain

relationship with the bi-axial state of stress at the selected critical locations. Figures 12.1 through 12.5 show these linear relationships between the biaxial state of stress at a given location and the flange tip displacement (in hoop direction) at selected depths of cut. The stress used to correlate this displacement is an "equivalent" uniaxial stress that would produce the same hoop strain as the measured biaxial stress components.

This general correlation suggests that a measure of the residual stress intensity, at least for the lower back rim location, B1 may be estimated from the flange tip saw-cut opening response.

12.2.2 Associated Metallurgical/Macrostructural Evaluation

Slices have been taken from the saw-cut wheels, and they will be etched to reveal any alteration of metallurgical structure due to brake shoe heating.

12.2.3 Detailed (Triaxial) Residual Stress Tests Results

The purpose of this subtask is to develop an experimental/analytical method to determine the residual stresses within the rims of wheels and to determine such stresses in wheels that have been exposed to severe braking. The method to be developed involves an analytical combination of strains determined by dissection and hole drilling strain-gaging techniques.

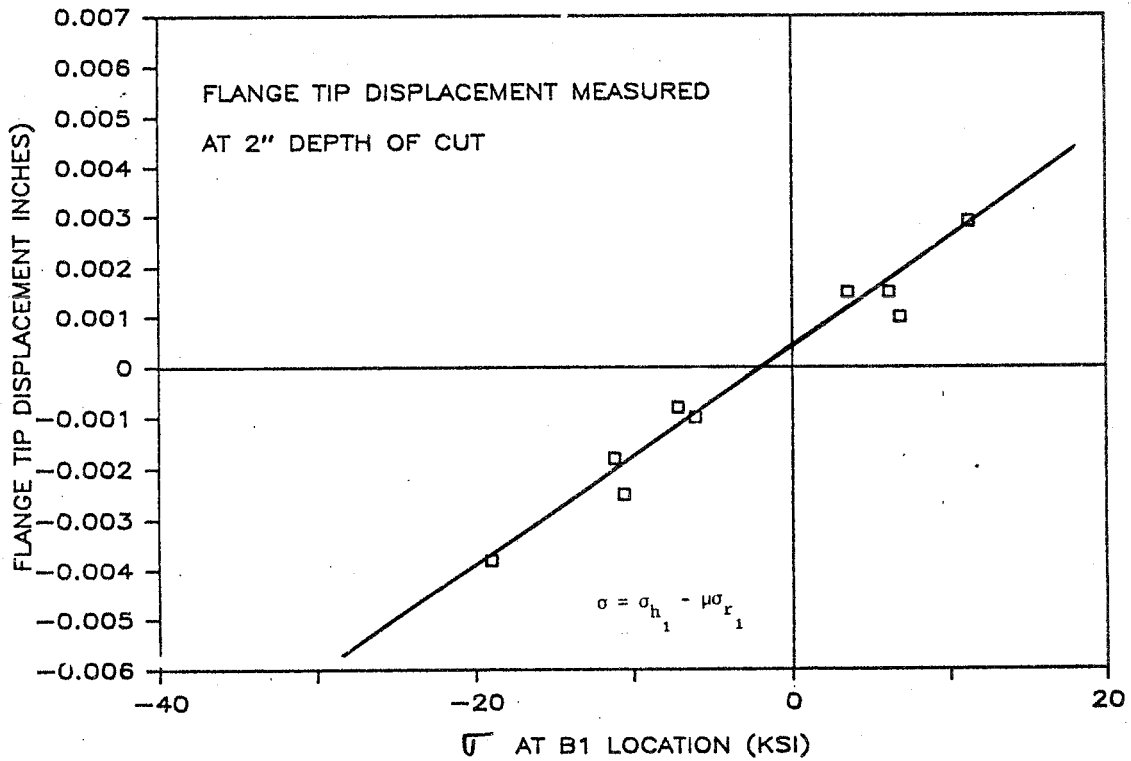


FIGURE 12.1. FLANGE TIP DISPLACEMENT AT 2 INCHES DEPTH OF CUT VS σ AT B1 LOCATION ($\sigma = \sigma_{h1} - \mu\sigma_{r1}$).

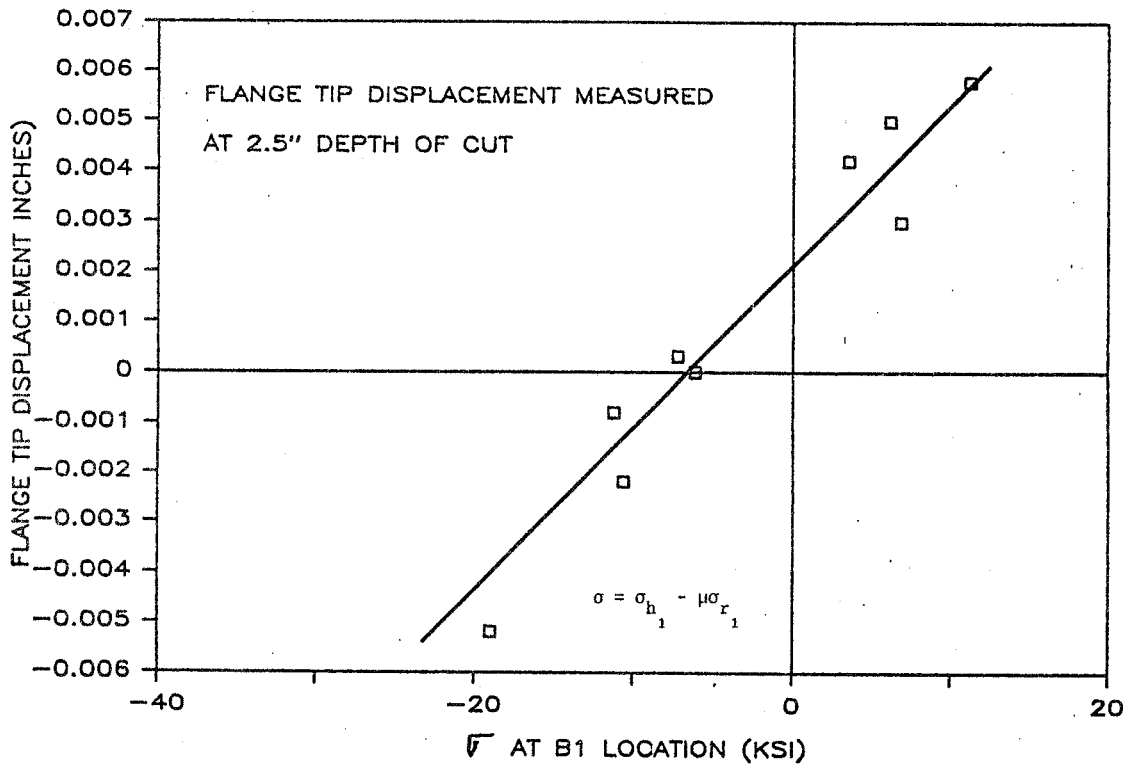


FIGURE 12.2. FLANGE TIP DISPLACEMENT AT 2.5 INCHES DEPTH OF CUT VS σ AT B1 LOCATION ($\sigma = \sigma_{h1} - \mu\sigma_{r1}$).

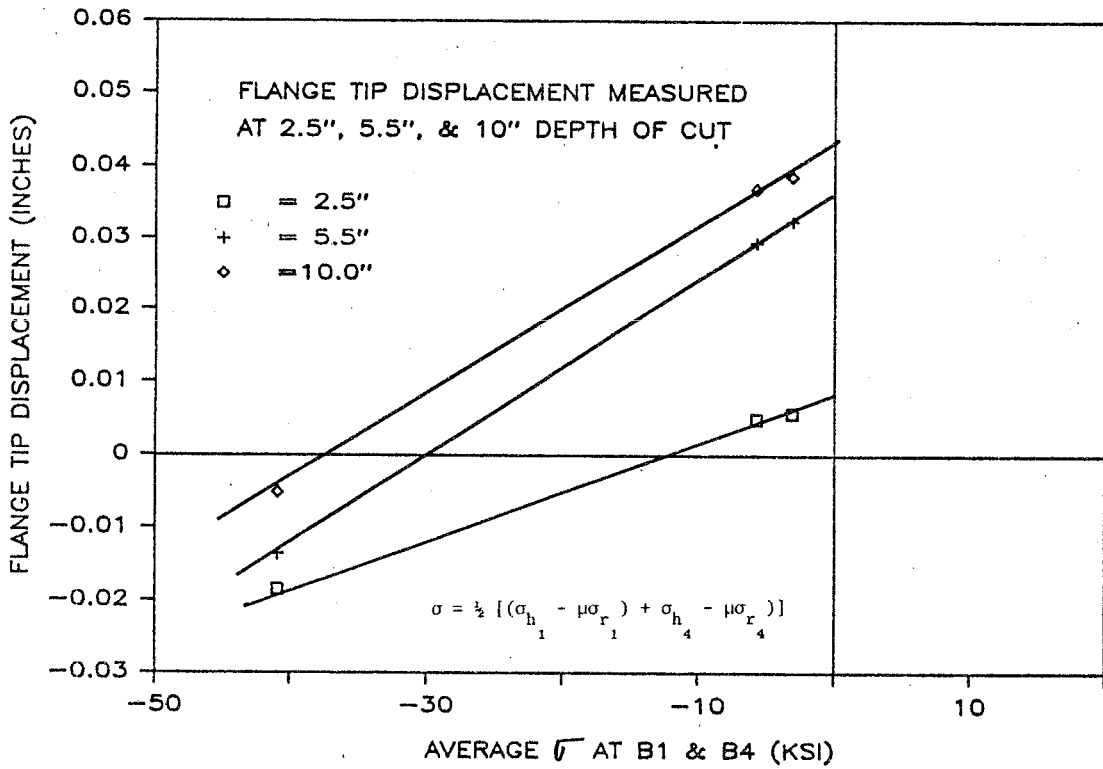


FIGURE 12.3. FLANGE TIP DISPLACEMENT AT 2.5, 5.5, AND 10 INCHES DEPTH OF CUT VS AVERAGE OF σ AT B1 AND B4 LOCATIONS.

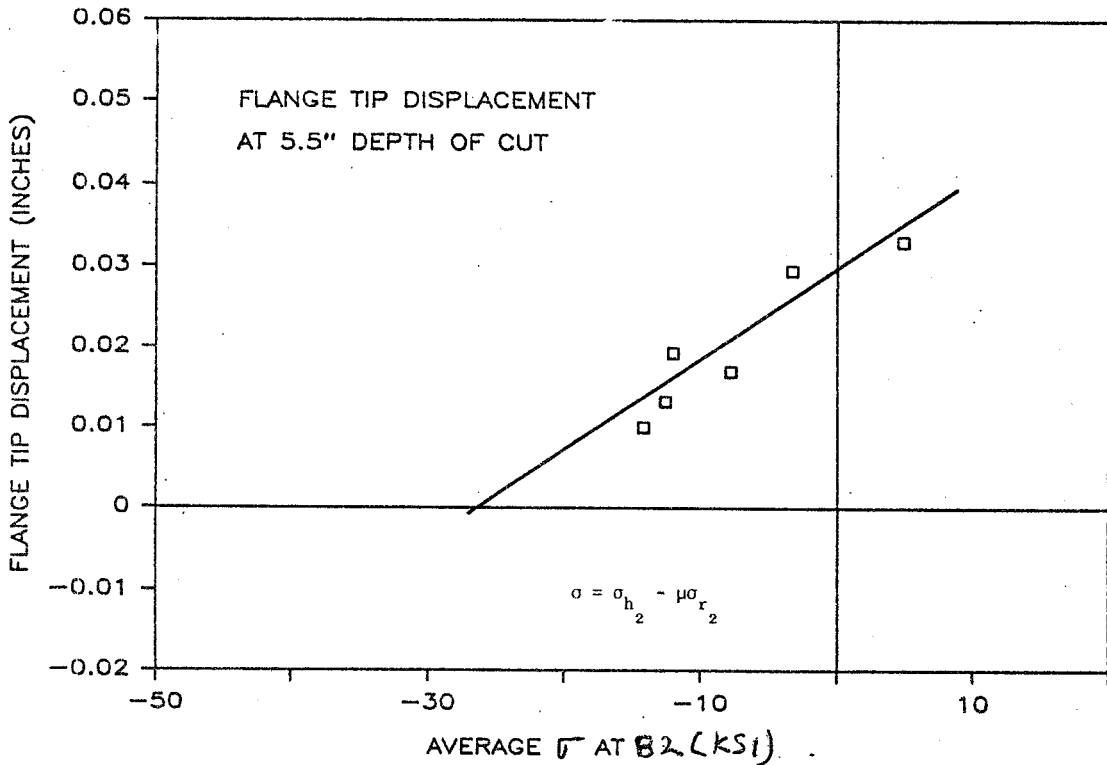


FIGURE 12.4. FLANGE TIP DISPLACEMENT AT 5.5 INCHES DEPTH OF CUT VS σ AT B2 LOCATION ($\sigma = \sigma_{h_2} - \mu\sigma_{r_2}$).

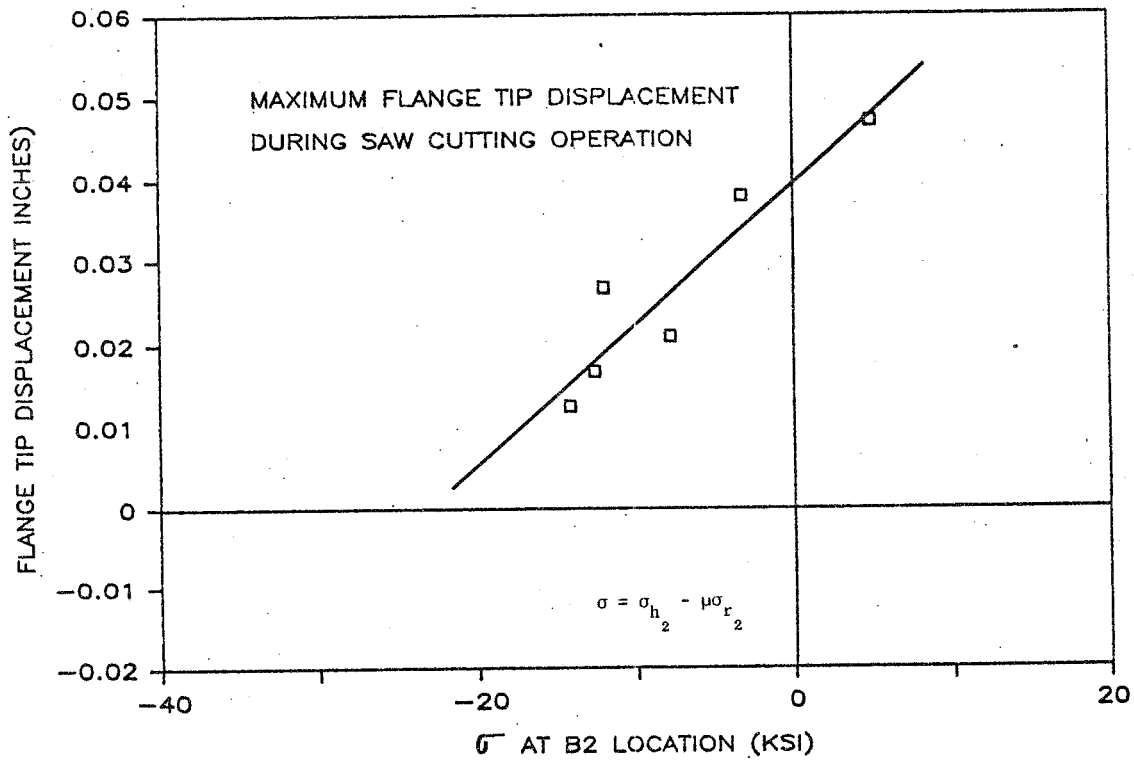


FIGURE 12.5. MAXIMUM FLANGE TIP DISPLACEMENT DURING SAW-CUTTING OPERATION VS $\bar{\sigma}$ AT B2 LOCATION ($\sigma = \sigma_{h2} - \mu\sigma_{r2}$).

With the help of our consultant, Wiss, Janney, Elstner, and Associates, the experimental and analytical plans have been developed. Strain-gaging of the first wheel has started at the Technical Center.

12.3 WORK REMAINING IN TASK T11

12.3.1 Saw-Cutting Work Remaining

BN wheel distribution. [Britto to provide.]

12.3.2 Macrostructural Work Remaining

Specimens are being prepared to do all macrostructural testing in one period.

12.3.3 Detailed Residual Stress Work Remaining

The program calls for determination of residual stresses in six wheels. Therefore, completion of the experimental work on the first wheel, all of the experimental work on the five remaining wheels, and the analytical work on six wheels remains to be done.

At the September 4, 1985 FRA/AAR project review meeting in Pueblo, it was agreed that test and analysis of fewer than 6 wheels may be justified in view of:

1. the possibility that the reliability of the method of estimating internal residual stress from saw-cutting analysis will be satisfactorily substantiated after as few as two wheels.
2. the redirection of greater than planned resources into the expanded technical scope of detailed saw-cutting subtask, which has greater potential for practical and economical application to a larger number of wheels.

12.4 SCHEDULE FOR COMPLETION OF TASK T11

12.4.1 Saw-Cutting Schedule

The first test wheel will be sliced as per the proposed plan during November/December 1985.

12.4.2 Macrostructural Evaluation Schedule

This test is planned for February 1986.

12.4.3 Detailed Residual Stress Schedule

The experimental part of this program got off to a slow start because of manpower availability problems. However, it is expected that by reducing the number of test wheels as suggested in Section 12.3.3, this program can be completed by the end of the contract period.

13.0 FURNISH SUITABLE BRAKE DYNAMOMETER (TASK 12)

13.1 CURRENT TASK STATEMENT OF WORK

The AAR shall furnish a dynamometer capable of exerting brake shoe loads and wheel-rail mechanical loads. The shaft and housing of the dynamometer must be capable of sustaining a wheel failure without damage. A brake dynamometer facility with the above features shall be installed at the AAR Chicago Technical Center and shall be available for this program.

13.2 MAJOR FINDING/CURRENT STATUS

An Adamson-United dynamometer was purchased from United States Steel Corporation and installed at the AAR Technical Center in Chicago. Operation began in October 1984. This dynamometer, shown in Figure 13.1, is capable of testing railroad wheels measuring 28 to 42 inches in diameter at speeds up to 1500 rpm with a 400 HP D.C. motor. Inertia loads of up to 68 million ft-lbs at top speed are available in increments through the use of removable fly wheels. The brake system is capable of exerting up to 45,000 pounds on each brake shoe in either a single or clasp arrangement. In addition, vertical loads of up to 70,000 pounds and lateral loads of up to 15,000 pounds can be applied to the tread of the wheel by reaction with the 110-inch diameter track wheel. Wheels can be tested also without rail contact. The types of wheel tests that can be conducted with this dynamometer include stop tests and grade or drag-

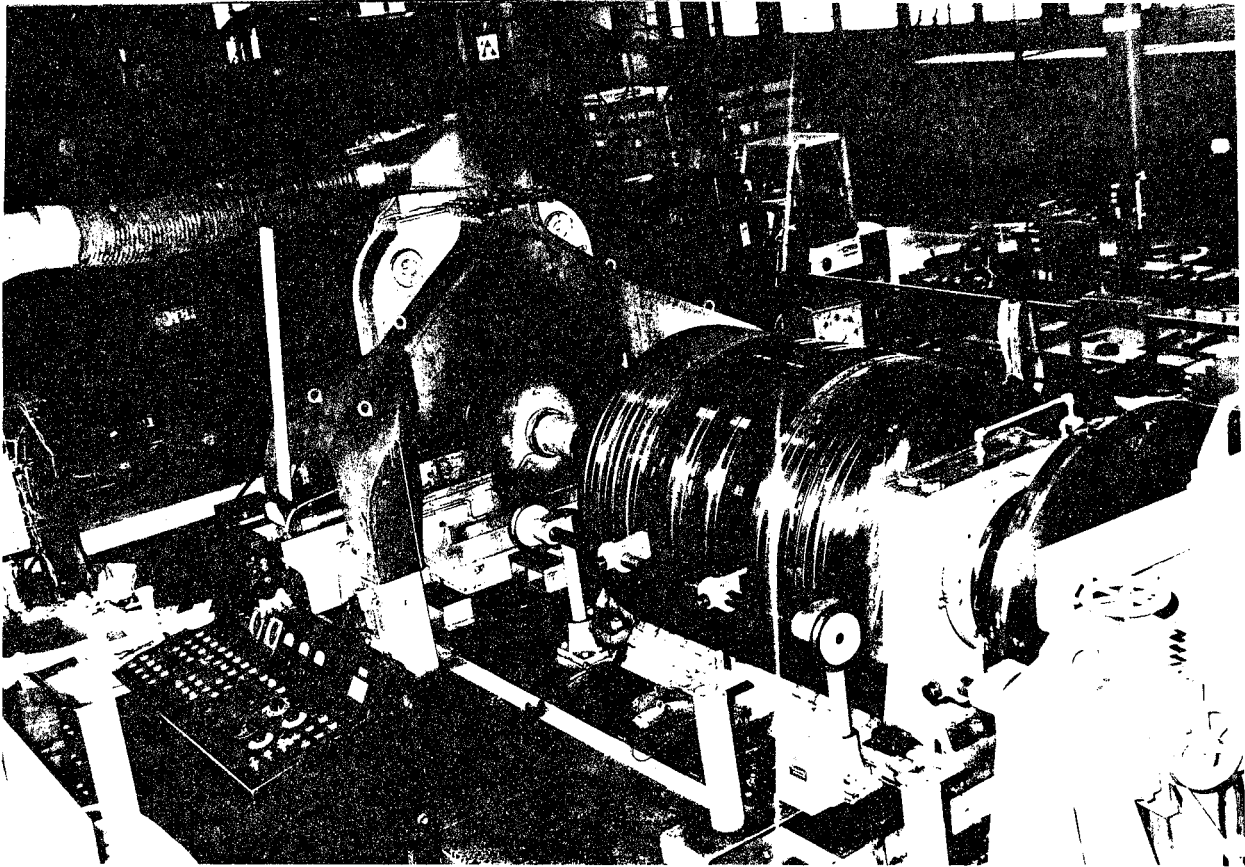


FIGURE 13.2. DYNAMOMETER AT AAR CHICAGO.

braking tests. In addition, the dynamometer can be used for testing brake shoes with static tests, as well as stop tests and grade tests. Futhermore, this machine can also be used to test full-size axles as rotating cantilever beams.

13.3 WORK REMAINING

This item is complete; the dynamometer has been in operation for one year. However, plans are being made to update the controls, instrumentation, data acquisition, and data presentation systems of the dynamometer. This is not part of this task order.

13.4 SCHEDULE

Update of the dynamometer should be completed in 6-8 months. Installation and training time of about four weeks may have an effect on dynamometer work associated with other tasks.

14.0 MODIFY TTC ROLL DYNAMICS UNIT (TASK 13)

14.1 CURRENT TASK STATEMENT OF WORK

Necessary modifications shall be performed at the RDU of the TTC for the provision of a longitudinal restraint system and vertical loading system with the test truck supported on the Roll Module Unit. Braking loads shall be applied with a suitable pneumatic system. Data shall be acquired and processed with the available facilities.

14.2 MAJOR FINDINGS/CURRENT STATUS

With the test truck mounted on the Roller Module Unit (RMU) of the RDU, brake testing was performed by actuating the brake cylinders according to the schematic described in Figure 14.1. The shop compressed air was admitted into the brake cylinders of the test truck through a regulating valve (set at the required pressure), as well as through a remote-control directional valve such that test wheels were subjected to desired braking loads. The technique of brake shoe force measurement developed in the "AAR Brake Shoe Performance Test" was utilized for calibration of forces developed at the interface between the brake shoe and the tread of the wheel.

Load fixtures for the braking tests are depicted in Figure 14.2. Each vertical actuator provided a force of 54,000 pounds for simulating a 70-ton loaded car. The hydraulic power unit and the related control hardware for hollow-axle testing were utilized for operating the vertical actuators.

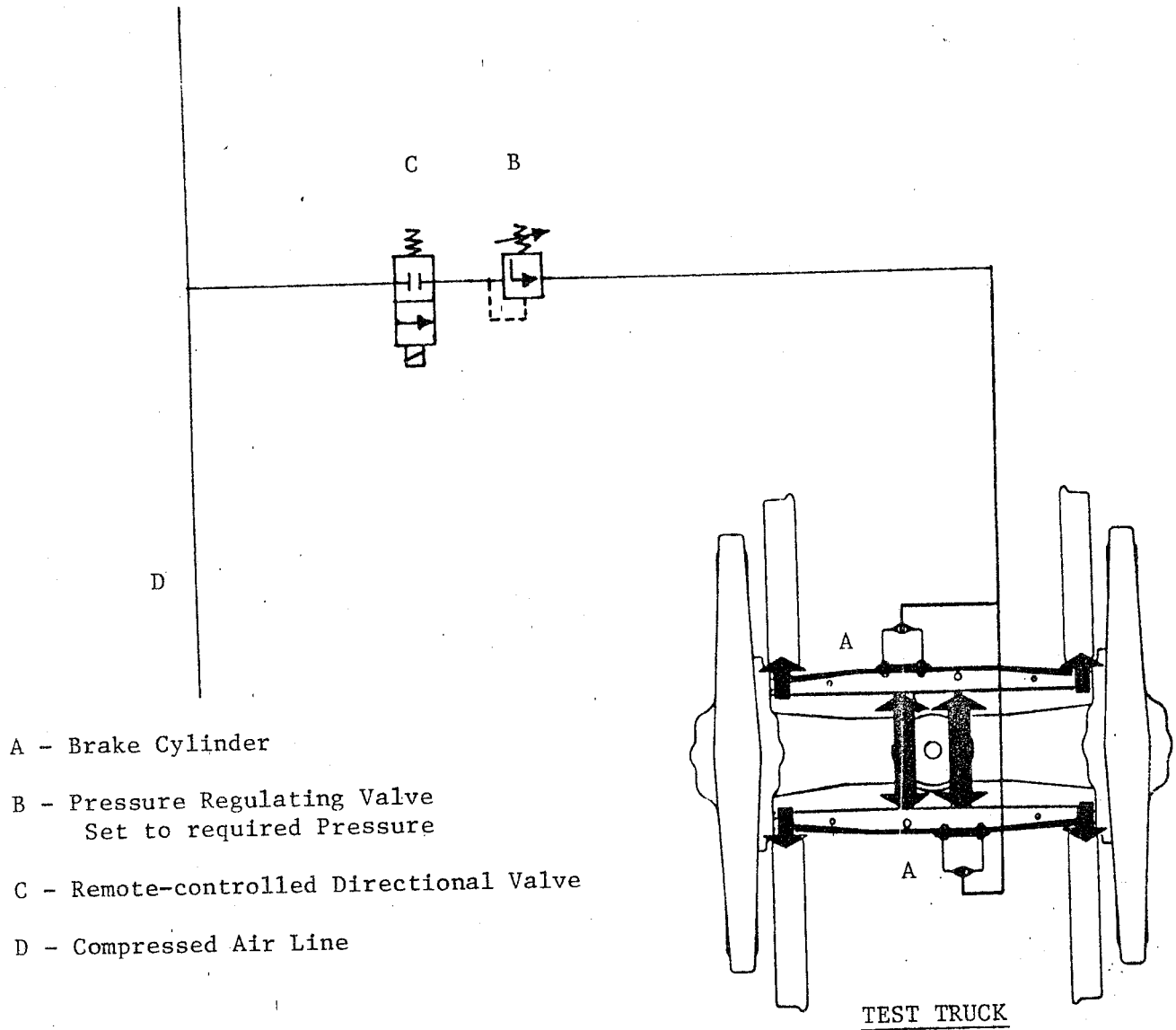


FIGURE 14.1. BRAKE FORCE APPLICATION CONTROL SYSTEM.

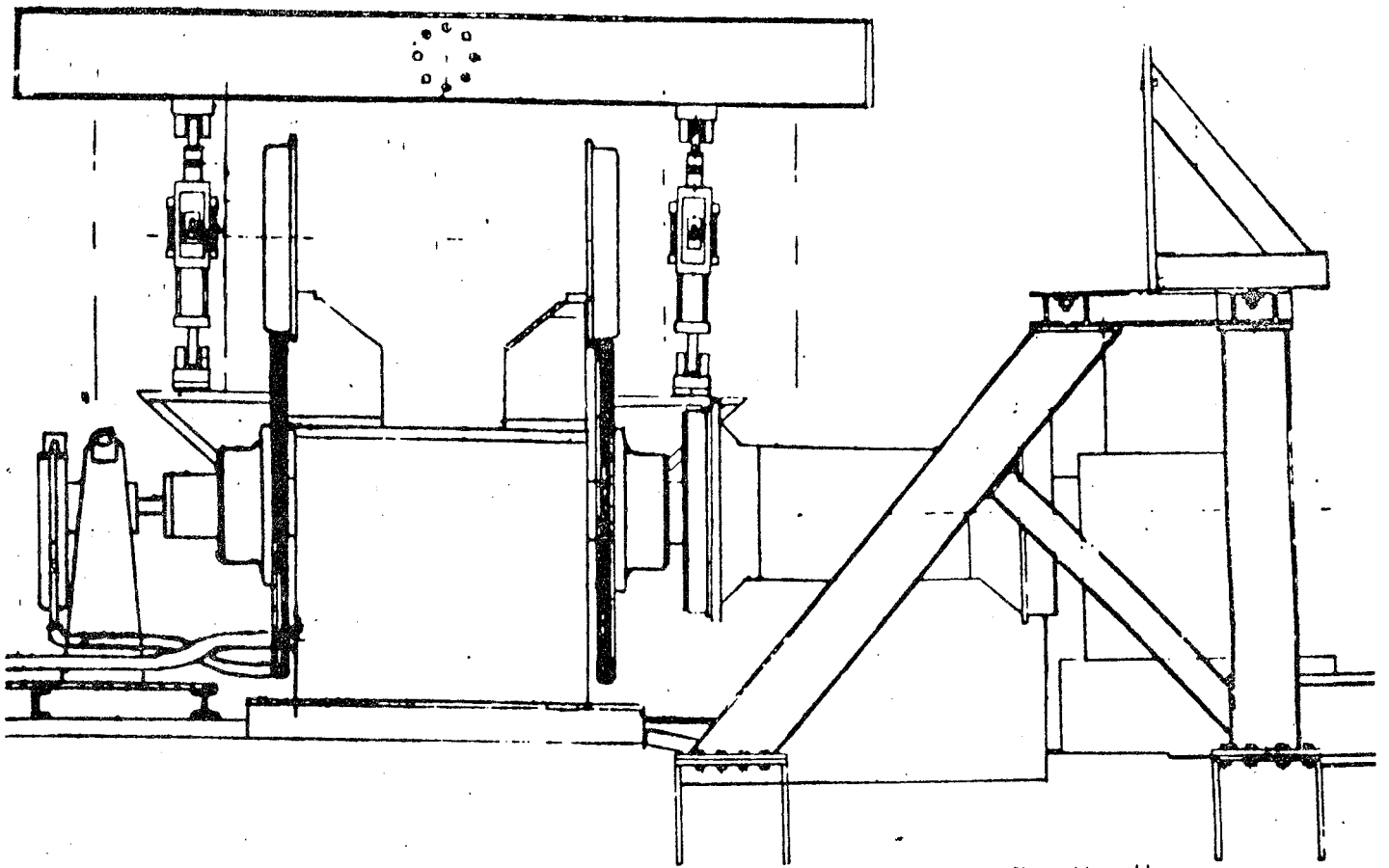


FIGURE 14.2. HOLD-DOWN DEVICE FOR RDU BRAKING TESTS.

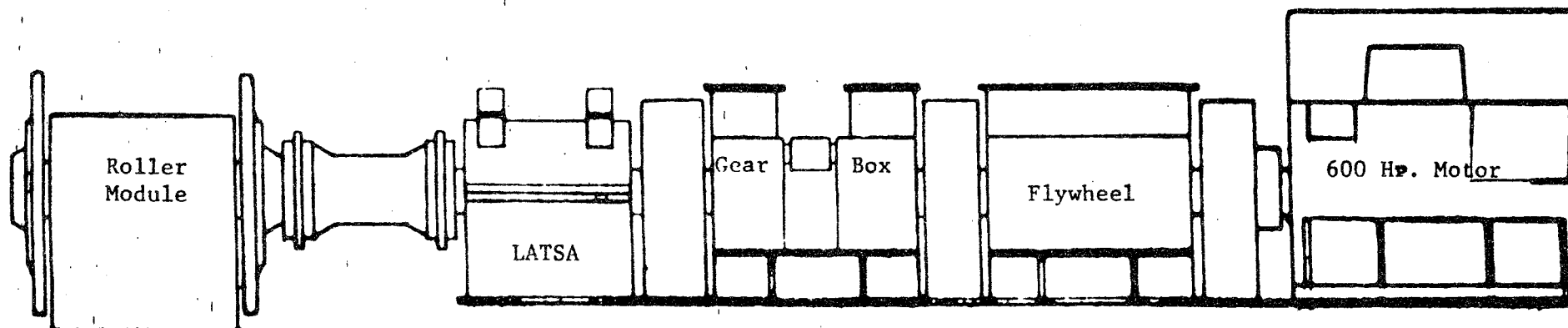
For the simulation of a 70-ton loaded car, reconfiguration of the Roll Module Units (RMU) was performed so that each RMU provided approximately 40,000 pounds of rolling inertia. Each driving train consisted of one Lateral Actuator Thrust Assembly (LATSA), one gear box, one #2 flywheel, and one 600 HP motor. The reconfiguration of the RDU is presented in Figure 14.3.

14.3 WORK REMAINING

The RDU has been modified; no further work remains to be done on this task.

14.4 SCHEDULE

Not applicable (all work completed).



#2 - Flywheel to be used for 70-ton car (fully loaded) simulation

FIGURE 14.3. RMU DRIVE TRAIN RECONFIGURATION FOR RDU BRAKING TESTS.



15.0 EVALUATE NDE TECHNIQUES

15.1 CURRENT TASK STATEMENT OF WORK

The AAR/TTC shall review and evaluate nondestructive testing techniques for isolating cracked or critically stressed wheels. The AAR shall initially investigate promising methodologies through discussions and marketing literature, followed, in the second year of the contract by a critical review and selection of one of the crack detection or residual stress measurement prototypes for test and evaluation. (As part of the review, the results of tests with the Barkhausen Residual Stress Measurement System from the Union Pacific Railroad will be correlated with AAR/TTC results.) The selection of a system for test and evaluation shall be made in consultation with the FRA COTR. Another measurement system, a hot wheel detector, shall be placed in service at TTC to monitor temperature buildup in wheels of the test consist.

15.2 MAJOR FINDINGS/CURRENT STATUS

The present test plan covered under subproject SP4 includes critical review and selection of only one NDE (either crack detection or stress measurement) prototype, followed by limited testing and evaluation of this one device in support of appropriate program tasks at TTC. (A hot wheel detector will also be placed in service at TTC in conjunction with the track testing planned at TTC.)

15.2.1 Selection Criteria

1. Since it appears that the majority of wheels which have experienced stress reversal will not have any evidence of discoloration, the inspection system should be capable of performing a roll-by inspection (as a wayside system) or at least as a repair track NDE system.
2. Either a system that can reliably isolate thermal cracks or a system that can detect a residual tensile field would be equally effective in reducing wheel caused derailments. A system capable of isolating both conditions would be ideal.
3. Any system that requires some observable physical feature for a decision to inspect would probably not be effective.

15.2.2 Review of State-of-the-Art NDE Techniques

The present state-of-the-art techniques for nondestructive inspection are unable to reliably determine either the presence of cracks or the level of residual stresses in wheels. A brief description of various NDE techniques for determining the level of residual stress and/or the presence of thermal cracks in wheels, is presented below:

15.2.2.1 Residual Stress Detection Methods

A. X-ray Diffraction. The principle of the X-ray diffraction (XRD) technique lies in the fact that the angle at which the X-ray beam is diffracted from the atomic planes of a crystal is indicative of the spacing of those planes. When a material is placed under stress, the plane spacing increases (tension) or decreases (compression) and the distance between the atomic planes in the metal changes. From the wave length of X-ray radiation and the angle between the incident and diffracted X-ray beam, the interplanar spacing of the atomic plane's reflecting the beam can be measured. Stresses are determined by measuring the strain in the atomic lattice and by relating the strains to stresses through the elastic theory. X-ray diffraction has the following limitations. 1) It is only able to measure surface stresses (~0.001 inch) and is restricted to a small surface area upon which the beam is focused. X-rays may not be able to penetrate surface rust or mill-scale which may require surface preparation; 2) the XRD process is affected by texture and cold work, and, therefore, accurate readings cannot be made on wheel treads that have been coldworked; 3) the technique requires time to analyze sufficient data for a stress determination, typically a few minutes.

B. Barkhausen Methods. The phenomenon that is the basis of this technique is the abrupt, discontinuous movement of microscopic magnetic domain boundaries that often occurs in ferromagnetic materials under the influence of an external magnetic field.

If a piece of ferromagnetic steel is magnetized, it will elongate in the direction of an applied magnetic field, and conversely, if the same piece is stretched by an applied load, it will be magnetized in the direction of the load. The same occurs with compression, except that the resulting magnetization now occurs at 90 degrees to the direction of compressive load.

To conveniently employ the magnetoelastic interaction for stress investigation, another physical phenomenon is needed. This is the Barkhausen effect, the series of abrupt changes or jumps in the magnetization of a steel when the magnetizing field is gradually altered. Combining these two phenomena leads to a qualitative stress indication so that an increasing tensile stress is accompanied by a growing "Barkhausen noise" level generated by jumps, and an increasing compressive stress by a diminishing noise level. More accurate quantitative data can be obtained through the use of calibration procedures with known loads.

The excitation field is developed by a variable field electromagnet in contact with the specimen. An induction coil between the magnet poles senses changes in specimen magnetization and translates this into an output voltage that is displayed on an oscilloscope. Cycling the external field polarity results in the output amplitude achieving a maxima that is indicative of the material stress state. To develop quantitative stress values from such information, it is necessary to construct a

calibration curve of stress versus Barkhausen noise intensity for the material of interest. Figure 15.1 shows a curve of this type for three different steels.

The Southwest Research Institute study in 1974 established that the Barkhausen phenomenon generated in railroad wheels is sufficiently stress sensitive to be used as a stress indicator. However, there were significant variations and some inconsistencies in the data from wheel to wheel and at similar locations on the same wheel.

An important factor contributing to data variability in the Barkhausen technique is the small volume of material from which the stress indication is obtained. The near surface nature of the Barkhausen effect, when combined with a coil pickup covering an area of only 0.01 inch, causes the technique to be more sensitive to short range stress gradients and shallow surface conditions than a conventional stress relaxation measurement using strain gages. Despite such characteristics, reasonable qualitative agreement was established for the Barkhausen method.

As a step toward utilizing the Barkhausen noise technique to classify wheels according to the severity of overheating, the SWRI study tentatively identified the area on the back rim surface nearest the tread as that most likely to yield consistent linear results.

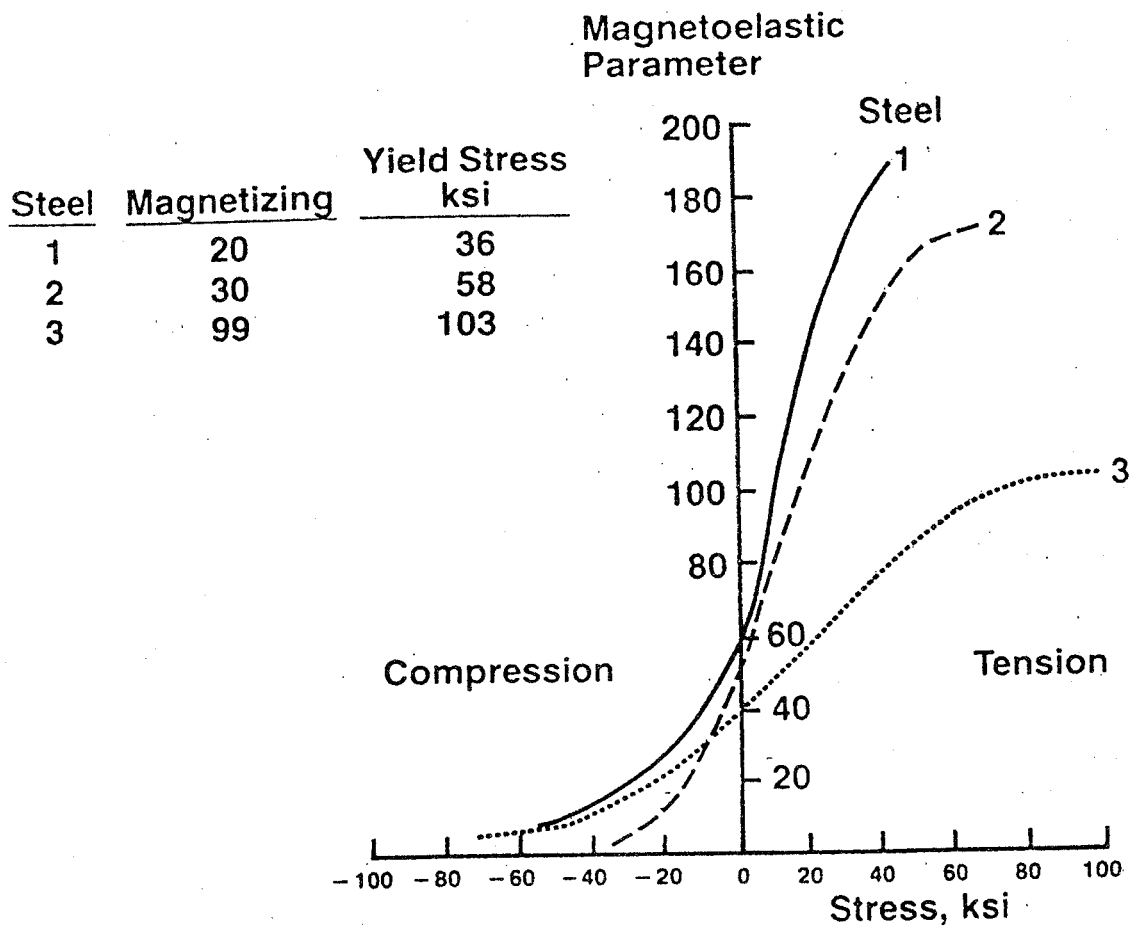


FIGURE 15.1. CALIBRATION OF CURVES FOR THREE DIFFERENT STEELS WITH INCREASING YIELD STRENGTH FROM 36 KSI TO 103 KSI.

A recent experiment of 80 wheels by SWRI for an AAR member road found some 16 percent to have high residual stresses using an improved SWRI detector. These data were verified by an independent saw-cutting program.

The results of SWRI's Barkhausen measurement system by the Union Pacific Railroad on sixty discolored wheels will be correlated with the results of an AAR/TTC saw-cutting program of the same wheels currently being conducted at TTC.

Another portable Barkhausen system currently being marketed by American Stress Technologies, Inc., promises potential for its applicability to railroad wheels.

- C. Ultrasonic Bi-Refringence. The principle behind this technique is that the state of stress in a metal influences the propagation velocity of ultrasound. Therefore, the precise measurement of transit times through a known thickness of stressed material can give an indication of the average stress level. The key to obtaining reliable results is the accurate assessment and mitigation of the material variables. Chemistry, preferred orientation, and microstructure affect the sound velocity and must be mitigated through adequate calibration.

This technique has been applied to railroad wheels. The basic procedure was to measure the transit time differential of simultaneously generated 2 MHz pulses through an unstressed

reference block and the stressed specimen. This was accomplished using a dual trace oscilloscope to display the two signals and by expanding the time base until individual pulse cycles could be seen. Since a difference in transit time appears as a phase shift in the two signals, the delay - time multiplier on the oscilloscope could be used to determine the differential by making the pulses coincident.

The actual determination of stress in steel is complicated by its anisotropic nature with respect to sound propagation. Under compression, shear waves polarized parallel to the principal stress axis will travel faster than waves polarized perpendicular to it. The difference between the transit time differentials of the two wave orientations is, thus, a better measure of the average stress than either orientation alone. As applied to the evaluation of wheel rims, the parallel and perpendicular orientations correspond to the circumferential and radial directions, respectively.

The first step in utilizing this technique is the establishment of an acoustic stress constant for wheel material that relates ultrasonic velocity changes to applied stress. This is accomplished by incrementally loading a block of rim steel to simulate the circumferential compressive stresses found in wheels and measuring the transit time differential of pulses traveling in this block and an identical reference block. At each load level, measurements are taken with wave polarization both

parallel and perpendicular to the principal stress axis. The difference in transit time differentials of these two polarizations is used, in conjunction with the path length and the value of each load level change, to establish an acoustic stress constant for a typical wheel material.

Once the acoustic stress constant is determined, the average stress across a wheel rim can be calculated by measuring the difference in the radial and circumferential transit time differentials and by knowing the sound path length. In a similar manner, stress changes can be detected by making measurements before and after the event of interest. It has been demonstrated that accurate measurement of ultrasonic velocity in stressed wheels can be used to evaluate that stress condition. However, the material variability found in wheels of different classes and manufacture would require the use of some independent technique to establish material characteristics prior to any stress measurements. The technique also requires an accurate value for the ultrasonic path length, which may necessitate the actual measurement of the rim width of each wheel tested.

- D. Magnetomechanical Acoustic Emission. The Magnetomechanical Acoustic Emission (MMAE) method is a mechanical counterpart to the magnetic Barkhausen effect.

When the level of applied magnetic field is varied, the shift in magnetic domain structures produces ultrasonic waves, which are detected as Acoustic Emission (AE) signals. The MMAE phenomenon's potential as a new nondestructive method for stress measurement was earlier tested with measurements of rail and wheel steels to assess the feasibility of developing a useful instrument for field use. However, tests on this technique on wheels have been inconclusive because it was difficult to distinguish tensile from compressive stresses.

- E. Magnetic/Ultrasonic Technique. Residual stress characterization by a magnetic/ultrasonic technique which is currently being developed at Langley Research Center, holds promise for a practical nondestructive method adaptable for rail car wheels. However, this technique is applicable under laboratory conditions and needs to be adapted for railroad wheel inspection.

In this method, the state of internal stress in steel is measured by the material magnetic domain interaction with both the stress field and the ultrasonic wave propagation. All the tests to date indicate that a sensor concept is presently available which is capable of separating tensile from compressive stress in steel.

The unique feature of this technique is the measurement of small changes in ultrasonic wave velocity by the application of external D.C. magnetic field in the material under various

stress conditions. The fractional change in the natural velocity ($\Delta W/W$) of a wave propagating along the external field direction is affected by the uniaxial stress applied in the same axis. The simultaneous measurements of magnetic induction confirmed that the stress effect on the natural velocity curve is dominant in the domain wall motion region. The slope of $\Delta W/W$ is negative under compression and positive under tension for steel specimens with different carbon contents. Results of measurements with residual stress show exactly the same tendency. Recent measurements on permanently bent specimens with different radii of curvature confirmed the possibility of quantitative stress measurement.

15.2.2.2 Crack Detection Methods

Wheel inspection for cracks begins in the manufacturer's shop with procedures defined in Association of American Railroads Specifications M107 and M208 for wrought and cast wheels, respectively. Both outline the same requirements for ultrasonic inspection of rims for inclusions and voids and wet magnetic particle inspection of plate surfaces for discontinuities. Adherence to these specifications effectively sets a minimum quality limit for all new wheels entering service.

The techniques and frequency of in-service inspection are not specified in the Association of American Railroads rules, but are determined by the experience of each performing railroad. All railroads

rely principally on visual inspection, with a modest use of magnetic particle or penetrant methods by some. The frequency of inspection is flexible at best, depending heavily on the operating schedule of the vehicle and the repair needs of other components. This lack of explicit inspection intervals, which is inherent in the mobile nature of railroading, places an increased burden on the inspection that does take place to find defects in their earliest stages.

Experience has shown that the vast majority of defective wheels are detected visually before an accident can occur. Despite this basic effectiveness, visual inspection is characterized by several factors that tend to limit its sensitivity and reliability. Primary among these is its inherent subjectivity. Any system that relies solely on people for critical decisions is subject to the inconsistencies generated by differences in individual motivation, skills, knowledge, and health. Reliable wheel inspection depends heavily on such variables as inspector job satisfaction and visual acuity. The physical condition of the inspected wheel can also influence the ability of visual examination to detect small defects. The presence of oil and dirt on plate surfaces will hide all but the largest plate cracks. Similarly, hot and cold working of the tread can obscure thermal cracks with flowed metal.

A. Ultrasonics. The science of ultrasonics is being applied to the problem of wheel evaluation in many forms. The search unit of one system fits into a special section of rail that is designed to guide the outer tread of passing wheels over a

fluid filled transducer boot. Inside the boot are two oppositely directed transducers set in a gimbaled support that allows them to maintain a constant entry angle to the wheel tread. On contact with a wheel, couplant is sprayed on the boot and an ultrasound pulse is directed circumferentially around the tread as a surface wave by one of the transducers. Initial and multiple order reflections are subsequently received by this transducer from any crack that has developed on the rim faces, tread, or flange. It is claimed that reliable detection of cracks 0.5 inch long and 0.050 inch deep can be achieved.

After full attenuation of the initial signal has occurred, in about five milliseconds, a second pulse is directed around the wheel in the opposite direction by the second transducer. This dual pulse-echo technique enhances the chances of detecting cracks that are inclined to the surface since they are anisotropic in their ability to reflect sound. The use of dual transducers also allows the analysis of the through-transmitted signal for additional information on the wheels' condition. The attenuation rate of this signal is indicative of the general wheel surface condition and is believed related to the near surface stress level. The time interval between multiple receptions of the through transmitted pulse is used to classify wheels by diameters, and details of the pulse shape can reveal a high flange condition.

A major problem with this system has been its inability to distinguish between benign surface shelling cracks and thermal cracks. It has been suggested that a system employing swept ultrasonic frequencies or dual frequencies may be able to make a distinction between minute shells and true thermal cracks. The sweep frequency ultrasonics holds promise for a viable crack detection system and is described separately in this section.

- B. Acoustic Signature Analysis. One of the earliest methods of nondestructively evaluating railroad wheels was to have car inspectors strike them with a hammer and listen to the resulting sound. In this way it was possible to detect many defective wheels because they ring differently than good wheels. A more sophisticated version of this technique, known as acoustic signature analysis, is a possible basis for an automatic, in motion, wheel inspection system.

In the acoustic signature method, a wheel is excited by either natural or artificial means into vibrating, and the radiant sound is analyzed for its characteristic spectral content or signature. The introduction of discontinuities, such as cracks, into the wheel will affect the modes of vibration and, consequently, the signature. Early results have shown that impact excitation is the most suitable means of generating sound of sufficient intensity and spectral content in the frequency range (1-5 KHz) found to be most sensitive to wheel

cracks. In addition, this form of excitation allows the use of damping rate measurements as a supplemental indicator of wheel condition. It has also been established that the best detection system is one using a trackside microphone, near the impactor, to pick up acoustic radiation.

Recent field trials of an acoustic signature system in a joint SP-AAR program have established doubts that this type of system will be able to reliably detect critical size (3/4 inch) thermal cracks.

- C. Sweep Frequency Ultrasonics (Thermal Crack Detection). The reliable, non-destructive detection of railroad wheel cracks remains an elusive task. Ultrasonic technology has been applied by several investigators, and a commercial unit was produced. However, difficulties in the separation of benign surface checking and actual thermal cracks has prevented a single frequency system from finding wide application.

The use of sweep frequency ultrasonics in a difference mode may provide the key to practical, reliable, and accurate crack detection in rail car wheels. The frequency output/input allows for very powerful articulation of signal properties in conjunction with computer storage of output that will allow, for example, signal A (wheel/transducer position 1) to be subtracted from signal B (wheel/transducer position 2). This subtraction or difference approach will readily show the signal

difference between A and B. This difference can be physically related to a crack that has in fact changed location through rotation of the wheel with respect to the fixed input/output transducer positions.

15.2.3 Screening Criteria

The screening criteria for selecting NDE techniques to detect cracked or critically stressed wheels are interpreted to be minimum performance requirements for the three categories of detection systems that are proposed for use in screening the most promising candidate prototypes for subsequent testing and evaluation.

15.2.3.1 Possible Locations for NDE System Use

The screening criteria to be used in selecting the most promising candidate NDE systems depend on the intended use or area (location) of application of the system. While it is most desirable to have a reliable system for railroad wayside deployment, there are still safety benefits associated with a system capable of use on wheels at repair tracks or even in wheel shops. Therefore, criteria appropriate to all three use scenarios are discussed.

15.2.3.2 Performance Categories

In each of the three NDE measurement system categories (stress & cracks) there are several performance regions or areas of concern. These are:

1. Accuracy of measurement or detection uncertainty range (\pm measurement units).
2. Reliability of detection of critical conditions (probability).
3. False alarm rate.
4. Maintainability.
5. Environmental compatibility.

15.2.3.3 Performance Levels

In addition, within each performance region several levels of performance will be identified. These levels are:

1. Good (possesses necessary capabilities).
2. Sufficient (possesses minimum capabilities).
3. Not Sufficient (marginally useful).

15.2.3.4 Screening Criteria for Stress & Cracks

The screening criteria, in terms of the above categories, are presented in tabular form in: Table 1, for wayside use; Table 2, for repair track use; and Table 3, for wheel shop use.

Finally, it should be noted that the criteria will be refined in the course of the proposed research.

TABLE 1. SCREENING CRITERIA FOR RAILROAD WAYSIDE NDE SYSTEMS.

Category	Performance Level	Stress	NDE System	Cracks
Accuracy	Good Sufficient Not Sufficient			
Reliability	Good Sufficient Not Sufficient			
False Alarm Rate	Minimal High Excessive			
Maintainability	Good Sufficient Not Sufficient			
Survivability	Good Sufficient Not Sufficient			
Cost	Excessive Reasonable			

TABLE 2. SCREENING CRITERIA FOR REPAIR TRACKS NDE SYSTEMS.

Category	Performance Level	Stress	NDE System Cracks
Accuracy	Good Sufficient Not Sufficient		
Reliability	Good Sufficient Not Sufficient		
False Alarm Rate	Minimal High Excessive		
Maintainability	Good Sufficient Not Sufficient		
Survivability	Good Sufficient Not Sufficient		
Cost	Excessive Reasonable		

TABLE 3. SCREENING CRITERIA FOR WHEEL SHOP NDE SYSTEMS.

Category	Performance Level	Stress	NDE System Cracks
Accuracy	Good Sufficient Not Sufficient		
Reliability	Good Sufficient Not Sufficient		
False Alarm Rate	Minimal High Excessive		
Maintainability	Good Sufficient Not Sufficient		
Survivability	Good Sufficient Not Sufficient		
Cost	Excessive Reasonable		

15.2.3.5 Screening Criteria Evaluation

The following four NDE techniques have been evaluated in order of priority, using the screening criteria developed in Tables 1 through 3.

1. Magnetic Ultrasonic Technique (Residual Stress Detection - NASA Langley)
2. Sweep Frequency Ultrasonic Technique (Thermal Crack Detection - JPL)
3. Barkhausen (Residual Stress Measurement)
4. X-ray Diffraction (Residual Stress Measurement)

The applicability of the above systems was evaluated with reference to railroad wheels, and the following NDE techniques have been tentatively selected for further development and usage under appropriate conditions.

15.2.4 Selected Techniques

1. Thermal Crack Detection - Sweep Frequency Ultrasonic Technique - JPL.

SCREENING CRITERIA EVALUATION

SCREENING CRITERIA FOR REPAIR TRACK NDE SYSTEMS
WITH POSSIBILITY OF ROLL-BY INSPECTION

TYPE OF SYSTEM: MAGNETIC/ULTRASONIC TECHNIQUE (BEING DEVELOPED AT NASA LANGLEY RESEARCH CENTER)

Category	Performance Level	Stress	NDE System Cracks
Accuracy	Good Sufficient Not Sufficient	Good	N/A
Reliability	Good Sufficient Not Sufficient	Good (Time=30 sec)	N/A
False Alarm Rate	Minimal High Excessive	Minimal	N/A
Maintainability	Good Sufficient Not Sufficient	Sufficient	N/A
Survivability	Good Sufficient Not Sufficient	Sufficient	N/A
Cost	Excessive Reasonable	Reasonable	N/A

SCREENING CRITERIA EVALUATION

SCREENING CRITERIA FOR REPAIR TRACK NDE SYSTEMS

TYPE OF SYSTEM: SWEEP FREQUENCY ULTRASONIC (THERMAL CRACK DETECTION BEING DEVELOPED BY JPL)

Category	Performance Level	Stress	NDE System Cracks
Accuracy	Good Sufficient Not Sufficient	N/A	Good
Reliability	Good Sufficient Not Sufficient	N/A	Sufficient
False Alarm Rate	Minimal High Excessive	N/A	Minimal
Maintainability	Good Sufficient Not Sufficient	N/A	Good
Survivability	Good Sufficient Not Sufficient	N/A	Sufficient
Cost	Excessive Reasonable	N/A	Reasonable

SCREENING CRITERIA EVALUATION

SCREENING CRITERIA FOR REPAIR TRACK NDE SYSTEMS

TYPE OF SYSTEM: BARKHAUSEN (RESIDUAL STRESS MEASUREMENT)

Category	Performance Level	Stress	NDE System Cracks
Accuracy	Good Sufficient Not Sufficient	Sufficient	N/A
Reliability	Good Sufficient Not Sufficient	Sufficient (being tested by saw-cutting comparison)	N/A
False Alarm Rate	Minimal High Excessive	Not applicable	N/A
Maintainability	Good Sufficient Not Sufficient	Not known being evaluated by BN & UP)	N/A
Survivability	Good Sufficient Not Sufficient	Not Sufficient (not good enough for field application)	N/A
Cost	Excessive Reasonable	Unacceptably high. Requires prescreening of wheels, which will miss a large population of wheels with high stresses	N/A

Remarks: Barkhausen technique can be considered as a reliable backup system for the evaluation of state of stress in the wheel under shop conditions.

SCREENING CRITERIA EVALUATION

SCREENING CRITERIA FOR REPAIR TRACK NDE SYSTEMS

TYPE OF SYSTEM: X-RAY DIFFRACTION (SURFACE RESIDUAL STRESS MEASUREMENT)

Category	Performance Level	NDE System Stress	Cracks
Accuracy	Good Sufficient Not Sufficient	Good (excellent for surface)	N/A
Reliability	Good Sufficient Not Sufficient	Acceptable	N/A
False Alarm Rate	Minimal High Excessive	Minimal	N/A
Maintainability	Good Sufficient Not Sufficient	Unacceptable	N/A
Survivability	Good Sufficient Not Sufficient	Unacceptable	N/A
Cost	Excessive Reasonable	Acceptable equipment, Unacceptable labor	N/A

15.2.4.1 Hot Wheel Detection

A hot wheel detector will be placed in service at TTC in conjunction with the track testing covered under Technical Task T6. The hot wheel detector is a modified version of a typical hot box detector. The temperature buildup in selected test wheels subjected to prescribed thermal loads will be monitored by the hot wheel detector. Various temperature settings will be tried between 300°F and 600°F to trigger an alarm when those temperatures are attained by the test wheels while being subjected to drag braking cycles. The operational use of the hot wheel detector will evaluate the effectiveness of hot wheel detectors and support partially the track testing effort in establishing the temperature levels attained by a selected number of test wheels undergoing drag braking cycles.

During the proposed track testing covered under FRA Task Order #6, a hot wheel detector will be installed as a wayside system to determine the wheel temperatures as they pass by, and the temperatures recorded by the detector will be compared with the instrumented wheelsets being subjected to prescribed drag braking cycles.

15.2.5 Barkhausen Technique for Residual Stress Determination

AAR will subcontract a suitable contractor for performing Barkhausen Noise Analysis on Dynamometer, RDU and track test wheels during testing and post-testing before saw-cutting (approximately 180 wheels). The calibration constants for various test wheel materials

will be established and Barkhausen noise analysis will be compared with the results of the hole-drilling as well as other NDE techniques.

In order to extend the limited approach taken in Task T14 (of Task Order #6) towards NDE development adaptable to railcar wheels, an unsolicited proposal entitled "Nondestructive Testing and Evaluation of Railroad Wheels" was submitted to FRA on July 2, 1985 for acquisition, test, and evaluation of the most promising systems.

This proposal addressed non-destructive test evaluation far more comprehensively. To be specific:

1. Both types of detection systems (crack and stress) ought to be considered appropriate for adaptation as NDE Techniques in the goal of isolating critically stressed or cracked wheels.
2. Both techniques, as appropriate, should be supported by controlled testing of the prototypes at TTC, as well as field testing, in order to develop their successful implementation as required for detection of stressed or cracked wheels.

15.3 WORK REMAINING
(Under review.)

15.4 SCHEDULE
(Under review.)



16.0 CONDUCT RDU TESTS OF THE M-2 CAR AXLE/BEARING FAILURE MODE (TASK 15)

16.1 CURRENT TASK STATEMENT OF WORK

The AAR shall conduct testing at the RDU of the TTC to determine rates of fretting wear and thermal runaway on hollow axle/bearing/wheel assemblies of commuter railcars (M-2 Fleet). Runs of 11,000 and 1,000 miles with an M-2 truck shall be performed on the RDU, and dynamic measurement of bearing temperature and torque shall be monitored. Each test run shall investigate two axle/bearing/wheel assemblies. NOTE: This work has been completed.

16.2 MAJOR FINDINGS/CURRENT STATUS

The objective of this test program was to examine the thermal properties of bearings that have service-worn grooves between the axle and roller bearing assembly, and to take static measurements of bearing cup and seal wear ring movement, and any wear which may occur between the bearing cones and the axle. The dynamic performance of a "bent" solid axle with a straight hollow axle was also compared.

All tests were completed and the data obtained were transmitted to the Transportation Systems Center for analysis.

16.3. WORK REMAINING

None.

16.4 SCHEDULE

Not applicable.